



HAL
open science

Contribution to the improvement of VRLA batteries for cycling applications

Marion Perrin

► **To cite this version:**

Marion Perrin. Contribution to the improvement of VRLA batteries for cycling applications. Chemical Sciences. Université Henri Poincaré - Nancy 1, 2001. English. NNT : 2001NAN10185 . tel-01746862

HAL Id: tel-01746862

<https://hal.univ-lorraine.fr/tel-01746862v1>

Submitted on 29 Mar 2018

HAL is a multi-disciplinary open access archive for the deposit and dissemination of scientific research documents, whether they are published or not. The documents may come from teaching and research institutions in France or abroad, or from public or private research centers.

L'archive ouverte pluridisciplinaire **HAL**, est destinée au dépôt et à la diffusion de documents scientifiques de niveau recherche, publiés ou non, émanant des établissements d'enseignement et de recherche français ou étrangers, des laboratoires publics ou privés.



AVERTISSEMENT

Ce document est le fruit d'un long travail approuvé par le jury de soutenance et mis à disposition de l'ensemble de la communauté universitaire élargie.

Il est soumis à la propriété intellectuelle de l'auteur. Ceci implique une obligation de citation et de référencement lors de l'utilisation de ce document.

D'autre part, toute contrefaçon, plagiat, reproduction illicite encourt une poursuite pénale.

Contact : ddoc-theses-contact@univ-lorraine.fr

LIENS

Code de la Propriété Intellectuelle. articles L 122. 4

Code de la Propriété Intellectuelle. articles L 335.2- L 335.10

http://www.cfcopies.com/V2/leg/leg_droi.php

<http://www.culture.gouv.fr/culture/infos-pratiques/droits/protection.htm>

U.F.R. : S.T.M.P.

Ecole Doctorale : EMMA

Formation Doctorale : Physique et Chimie de la Matière et des Matériaux

Thèse

présentée pour l'obtention du grade de

Docteur de l'Université Henri Poincaré, Nancy I

en Physique et Chimie de la Matière et des Matériaux

par **Marion PERRIN**

**Contribution à l'amélioration des batteries au plomb
fermées pour l'application au véhicule électrique**

**Contribution to the improvement of VRLA batteries
for cycling applications**

Soutenue le 09 Novembre 2001 devant la commission d'examen

Membres du jury :

Président :	M. J. STEINMETZ	Professeur, UHP Nancy I
Rapporteurs :	M. D. PAVLOV	Professeur, CLEPS, Sofia (Bulgarie)
	M. P. SPINELLI	Professeur, Politecnico di Torino, Turin (Italie)
Examineurs :	M. J. GARCHE	Professeur, Université de Ulm (Allemagne)
	M. H. DÖRING	Chargé de Recherches, ZSW, Ulm (Allemagne)
	M. P. LAILLER	Directeur du Centre de Recherches, CEAC, Gennevilliers

A Cléo, 2 ans et demi pour beaucoup trop longtemps...

A Chat...

Danksagung

Dr. Harry DÖRING. Immer kritisch denken, nah an der Säure bleiben und die Berichte rechtzeitig abgeben! Ich habe von Dir viel gelernt und deine Verantwortung in dieser Arbeit ist enorm. Vielen Dank Harry dafür, daß ich sie unter Deine Betreuung durchführen durfte.

Prof. Jürgen GARCHE. Ihr Name ist zum großen Teil für den guten Ruf des ZSWs verantwortlich. Ich danke Ihnen, mir erlaubt zu haben, in Ihrem Institut meine Doktorarbeit anzufertigen.

Sabine PILLER. Noch wichtiger als die Arbeit die man macht sind die Leute mit denen man sie macht. Danke Sabine, daß du die Lücken der Motivation, die verschiedenen Probleme und die glücklichen Stunden miterlebt hast.

Dagmar KÖSTNER. Für die chemischen Analysen, die Korrosionstests, aber auch für die Jogging-Stunden danke ich Dir Dagmar.

Bernhard SCHMIDT. Immer wenn es um Elektronik geht weischt du was zu tun ischt! Danke Bernhard, daß Du meine Batterien so gut versorgt hast.

Dr. Rainer WAGNER, Dr. Ludger LÜBBERS, Dr. Erika VOGEL, Dr. Martin SINZ und das Sonnenschein-AJS-Team. Ohne Leute "die wissen wie man eine Platte macht", aber auch eine ganze Batterie, wäre diese Arbeit nicht entstanden. Ich danke Ihnen für die gute Zusammenarbeit.

Dr. Klaus IHMELS, Dr. Anton WEISS, Dr. Werner BÖHNSTERDT, Jürgen BOESLER, Dr. Jörg DEITERS und das Daramic-AJS-Team. Dafür, daß der AJS ein gutes Produkt ist kann ich nichts. Danke, daß Sie mir erlaubt haben, als erste auf diesen Separator zu arbeiten und danke für die angenehme erfolgreiche Zusammenarbeit.

Das ZSW-team. Es war eine bereichernde Zeit bei Euch, vielen Dank an alle.

Die Ulmer Freunde. Die Nachhilfe Stunden auf Deutsch waren auch sehr nötig. Ich danke Sabine, Holger, Uta, Claudia, Thomas, Christina, Monika, Christine und alle die an diese Stelle gehören, die ich aber nicht alle erwähnen kann, für die Unterstützung.

Remerciements

Prof. Jean STEINMETZ. Pour votre responsabilité dans l'idée même d'effectuer une thèse qui a germé à l'issue de l'année de Maîtrise sous votre direction enthousiaste, pour votre accueil au laboratoire, vos corrections scrupuleuses, je vous présente mes remerciements les plus sincères.

L'équipe du laboratoire de Chimie du Solide Minéral. Ma gratitude va à Sandrine BARDAT pour les analyses en microsonde, Alain KOHLER pour les splendides photographies au MEB, Gwenaëlle pour l'accueil sur sa paillasse et l'introduction technique, Stéphane pour le soutien moral de sa rédaction en parallèle, Sébastien pour le soutien logistique des épaules, Sylvain, Jean et les autres.

Prof. Daniel MALTERRE. Bien que témoin du moment le moins glorieux de ma scolarité, vous n'avez pas jugé nécessaire de me pénaliser. Je vous en suis profondément reconnaissante.

Dr. Patrick LAILLER. Vous avez spontanément accepté d'apporter votre expérience industrielle à ce jury multiculturel. Je vous en remercie sincèrement et me réjouis de rencontrer enfin le directeur du centre de recherche CEAC Exide France de Gennevilliers.

Sylvain, ma famille et mes amis. Vous avez supporté stoïquement le pain noir, les débordements écologistes, les réponses spontanées en Allemand, me gardant amour et soutien par delà la frontière. Je vous en remercie et vous assure de mon affection.

Acknowledgements

Prof. Detchko PAVLOV. The number of times you are present in the references list of this work is not a flattery: you are the specialist on the field of the lead acid-battery and I thank you for accepting to be my referee.

Prof. Paolo SPINELLI. The way you make electrochemistry understandable is impressive. Therefore, I am very thankful for the fact that you accepted to criticise this Ph.D. work and be my referee.

Dr. Patrick MOSELEY, Dr. Alan COOPER. I know I could have done it in French! I want to express my gratitude to you for the support of the ALABC (International and European) but also for your constant availability and the way you had to solve any problem.

Dr. Ken PETERS. Thank you Ken for the discussions we had on the oxygen cycle.

The small world of the lead-acid battery. You became somewhat of a family to me and I thank you for the enriching discussions.

Foreword

If you say once, you are working for the future of the lead-acid battery, you will always get the same astonished question asked: "Does actually the lead-acid battery have more than a past?"

Indeed, its past is glorious. And its future will be glorious as well.

It must be conceded, its past is long! But even after 150 years intensive research and developments, the lead-acid battery is a country with still many regions to explore and many development possibilities.

Facing this long existence time and the high economical importance of the lead-acid battery, the amount of literature existing on the subject lead-acid battery is almost infinite. Therefore, I chose to write this document with a bibliographical part at the beginning of each chapter describing the evolution of the research and the state of the art in the concerned field. I hope that way to have produced a manuscript easier and pleasanter to read.

For getting a Ph.D. title from the University of Nancy, France, most of the experimental work took place at ZSW, in Germany, working on a European project. This arrangement gave good prerequisites for trying to get the European label for this Ph.D. And since most German people do not read French and even less French people read German, it seemed logical to write this thesis in English, also in order to allow an easier reading for the Bulgarian and the Italian referees. This mixture of nationalities and encountering of different frames of mind was much enriching and was also a main aspect of these years of Ph.D. work.

Abstract

The performances and life of the VRLA battery for cycling application were improved by applying a mechanical pressure on the electrode stack with help of a new separator (AJS).

The mechanical properties of AJS allow the transfer to the electrodes of a mechanical pressure that limits the free space throughout the cell life. Thus, while the negative active material is compacted, the positive active material develops a structure with a skeleton robust against discharge and large voids allowing a better utilisation over the whole plate thickness. The positive grid corrosion decreases and the mechanical stack stabilisation allowed by AJS reduces dramatically the effects associated with positive grid growth.

The association of phosphoric acid with AJS improves the cell performance at high discharge currents for a while provided the cells are adequately charged. With cycling, the effect of phosphoric acid disappears.

The oxygen recombination in AJS cells is slow but sufficient for cycling life over 1000 cycles. The oxygen transfer takes place across the gas space and through gas channels in the separator that are freed of their electrolyte by an oxygen overpressure.

Keywords

Valve Regulated Lead-Acid (VRLA) Battery; mechanical pressure; AJS separator; corrosion; phosphoric acid; oxygen transfer; recombination.

S.C.D. - U.M.A. NANCY 1
BIBLIOTHÈQUE DES SCIENCES
Rue du Jardin Botanique
54600 VILLERS-ÈS-NANCY

<i>Foreword</i>	5
<i>Summary</i>	11
<i>Introduction</i>	14
The drawback of energy production	14
Emissions related to transportation	16
The lead-acid battery: a competitor for the electric vehicle propulsion	16
Motivation of the work	17
1 The lead-acid battery	24
1.1 Electric energy accumulation	24
1.2 History of the lead-acid battery	25
1.3 Principle	25
1.4 The electrochemical system "lead-acid battery"	26
1.4.1 General considerations	26
1.4.2 Secondary reactions	30
1.5 Different designs of the lead-acid battery	32
1.5.1 Flooded battery	32
1.5.2 VRLA battery	35
1.5.3 Bipolar lead-acid battery	36
1.5.4 Different designs of lead-acid batteries.....	38
1.6 Life limiting factors	38
1.6.1 Drying out	38
1.6.2 Short circuits.....	39
1.6.3 Sulphation	39
1.6.4 Thermal runaway	39
1.6.5 Stratification.....	39
1.6.6 Failure of the positive electrode	40
1.6.7 Failure of the negative electrode.....	42
1.7 Different ways for the improvement of the lead-acid battery	43
1.7.1 Design.....	44
1.7.2 Composition and characteristics of the active materials	45
1.8 Conclusion about possible improvements of the lead-acid battery	47
2 Experimental techniques	49
2.1 Electrical tests on batteries	49
2.1.1 Internal resistance, open circuit voltage, peak power (IROCVP test).....	49
2.1.2 ECE 15 test.....	50
2.1.3 Cycling test.....	50
2.1.4 Dependence of the discharge capacity on the discharge current.....	50
2.2 Preparation of polished sections	50
2.3 Microscopy	51
2.3.1 Optical microscopy	51
2.3.2 Scanning Electron Microscopy	51

2.3.3	Microprobe Analysis	51
2.4	Chemical analysis and electrolyte concentration.....	51
2.5	Porosimetry	51
2.6	X-ray diffraction.....	51
2.7	IR pictures.....	51
2.8	Electrochemical techniques	51
2.8.1	Cyclic voltammetry	51
2.8.2	Potentiostatic corrosion measurement.....	52
2.8.3	Galvanostatic corrosion measurement.....	53
3	Mechanical pressure application	54
3.1	Bibliography of “compression”.....	54
3.2	Electrolyte immobilisation/separation systems	56
3.2.1	The complex influence of a passive part: the separator	56
3.2.2	Gel.....	57
3.2.3	AGM.....	57
3.2.4	The new Acid Jellying Separator (AJS).....	58
3.2.5	More than compression	60
3.3	Performance improvement through EMPA.....	60
3.3.1	Experimental conditions.....	61
3.3.2	Parameter test.....	64
3.3.3	Cycling life	68
3.3.4	Conclusion about the electrical tests	70
3.4	Mechanical pressure development during one cycle	70
3.4.1	Typical evolution of the mechanical pressure	70
3.4.2	Increase of the mechanical pressure during discharge.....	71
3.4.3	Evolution of the mechanical pressure during charge.....	79
3.4.4	Influence of the separation system.....	80
3.4.5	Influence of the initial mechanical pressure.....	84
3.4.6	Behaviour for a battery	84
3.4.7	Conclusion about the mechanical pressure evolution during one cycle.....	85
3.5	Evolution of the mechanical pressure over cycling life	86
3.5.1	Variation of mechanical pressure between beginning and end of discharge.....	86
3.5.2	Increase of mechanical pressure between the beginning and the end of one cycle.....	86
3.6	How does EMPA affect the performance of the lead-acid battery.....	88
3.6.1	Changes in the structure of the negative electrode	88
3.6.2	Post mortem analysis of the positive electrode.....	90
3.6.3	Models describing the positive active material.....	98
3.6.4	Why mechanical pressure application increases the life of the positive active material.....	100
3.7	Conclusion about mechanical pressure application on the lead-acid cell.....	101
3.7.1	Mechanical pressure variation on the cell walls	101
3.7.2	Structural changes in the negative electrode.....	102
3.7.3	Structural changes in the positive electrode.....	102
3.7.4	How does mechanical pressure application improve the life of the lead-acid battery	102
3.7.5	Importance of the separator	102

3.7.6	Perspectives	103
4	Corrosion	106
4.1	Generals about corrosion of lead and lead alloys	106
4.1.1	Definition.....	106
4.1.2	When does corrosion occur.....	107
4.1.3	The corrosion layer on the positive lead grid	107
4.1.4	Effect of the active material on the corrosion	109
4.1.5	Conclusion of the literature study on corrosion	109
4.1.6	Effect of antimony	111
4.2	Effect of mechanical pressure on corrosion	112
4.2.1	Corrosion measurement under potentiostatic conditions.....	112
4.2.2	Mechanical stabilisation of the plate stack with the AJS separator	115
4.2.3	Observation of grids after cycling.....	116
4.2.4	Conclusion about the effect of mechanical pressure on the positive grid corrosion	116
5	Phosphoric acid	118
5.1	Bibliography of the phosphoric acid	118
5.2	Results concerning the influence of phosphoric acid.....	119
5.2.1	Cyclic voltammetry on pure lead	119
5.2.2	Phosphoric acid and electrical performance.....	121
5.2.3	Mechanical pressure and the effect of phosphoric acid.....	122
5.2.4	Effect of phosphoric acid on the potential of pasted electrodes	124
5.2.5	Phosphoric acid and gas formation	125
5.2.6	Oxidative effect of phosphoric acid	126
5.2.7	Phosphoric acid and corrosion.....	127
5.2.8	Structural changes in the positive active material due to phosphoric acid.....	132
5.3	Conclusion about the effect of phosphoric acid.....	135
6	Oxygen cycle	137
6.1	Observation of the gas effects trough mechanical pressure recording.....	138
6.1.1	Mechanical pressure during one charge	138
6.1.2	Evolution over life of the gas effects	140
6.2	Recombination efficiency.....	142
6.2.1	Current repartition and recombination efficiency determination.....	142
6.2.2	Recombination efficiency of an AJS cell.....	144
6.3	Transfer of oxygen from the positive electrode to the negative electrode	147
6.3.1	IR pictures for the determination of the recombination sites	147
6.3.2	Oxygen transfer trough the AJS separator.....	148
6.4	Conclusion about the oxygen cycle	151
General conclusion.....		154
Achievements of this Ph.D. work		154
Perspectives		154
Towards sustainable development		155
References.....		158

<i>Glossary</i>	<i>161</i>
<i>Index of Figures</i>	<i>162</i>
<i>Index of Tables</i>	<i>165</i>

Summary

For defeating the treat of global warming, the world has to reduce drastically its greenhouse gases emissions. Since transportation contribute for almost 30% to the harmful emissions, the extensive use of electric vehicles could decrease drastically our emissions. For the propulsion of the electric vehicle, the lead-acid battery is a competitor with many advantages like robustness, availability, high recyclability and low cost. But its performance and life have to be improved for the lead-acid battery to be a dominant actor in cycling applications. This improvement was the target of this Ph.D. work and was achieved with the utilisation of a new separation system (AJS) for VRLA batteries.

The good mechanical properties of AJS allowed mechanical pressure application on the electrode stack and the sustaining of this pressure during the whole battery life. Therefore, improved performance and cycling life were obtained with over 1000 full cycles for AJS cells. During cycling under mechanical pressure application, the positive active material gets a “corralloid structure”. It consists of a skeleton of dense lead dioxide allowing for robustness against discharge and of cavities providing an electrolyte reserve for the further discharge. Additionally, even the innermost parts of the positive electrode are utilised at high discharge rates.

The utilisation of AJS proved to decrease the damages associated with positive grid corrosion in lead-acid batteries. Firstly, the application of mechanical pressure on a lead surface decreases its corrosion rate. But moreover, the new separation system, combined with external mechanical pressure, confere a high tightness to the electrode stack. Thus, for growing under the effect of corrosion, the positive grid must deform also the surrounding separators and negative plates. Therefore, the effects associated with positive plate growth are dramatically decreased.

We showed that addition of phosphoric acid in the electrolyte of the AJS/VRLA cells improves the performances of the cells in the beginning of life provided the charging regime allows for a high polarisation of the positive electrodes. Under these conditions, phosphoric acid is adsorbed on the positive plate thus blocking the lead dioxide precipitation sites and increasing the lead IV ions solubility. The lead dioxide precipitates in much smaller crystals and tends to precipitate in the inside of the electrode where no phosphoric acid is present, thus forming lead dioxide aggregates of high density.

The oxygen cycle proved to proceed at a much lower rate in AJS/VRLA cells than in cells with other separation systems. The transfer of oxygen from the positive to the negative electrode takes place via gas channels. These channels are formed when an oxygen pressure builds up on the positive plate that frees the largest pores of the separator. Since the life of the AJS/VRLA cells can last as long as 1000 full cycles and is not limited by drying out, the oxygen recombination rate is not a problematic question for the cells containing AJS.

As a conclusion, the construction of an improved lead acid battery was proposed consisting of a battery case of strong material, separators with good mechanical properties like AJS, negative plates pasted only on the grid thickness, positive plates with a high density paste, high evenness elements for a limited free space and 30 g/l phosphoric acid in the electrolyte. A high electrolyte saturation and a suitable charging regime would allow for full efficiency and long lasting of this battery.

The construction and testing of this battery design, a full understanding of the effect of phosphoric acid as well as an investigation of the transmission of the mechanical pressure to the positive grid and its effect on corrosion depending on the characteristics of the active material are further research ways that were opened here. There is still a lot of work to do before the optimal lead-acid battery is produced for electric vehicle applications but a small step towards this target was done in this work that may be a small contribution to sustainable development.

Résumé

Pour enrayer le processus du réchauffement planétaire, il est nécessaire de réduire nos émissions de gaz à effet de serre. Dans la mesure où les moyens de transports contribuent pour presque 30% aux émissions de dioxyde de carbone, l'utilisation intensive de véhicules électriques peut réduire sensiblement les émissions dans la mesure où la production d'énergie électrique repose pour une plus grande part sur les énergies renouvelables ou nucléaire.

Pour la propulsion du véhicule électrique, la batterie au plomb est un concurrent privilégié de par sa robustesse, sa haute recyclabilité, sa disponibilité en grande quantité, son niveau de développement et son faible coût. Mais pour une application de type véhicule électrique, ses caractéristiques en matière de performances et de durée de vie en cyclage profond doivent être améliorées. C'est cette amélioration ainsi qu'une meilleure connaissance du système plomb/acide qui ont été recherchés dans ce travail de thèse.

L'utilisation d'un nouveau séparateur (AJS) a permis d'accroître les performances mais surtout la durée de vie de batteries au plomb fermées. Cette amélioration est liée aux bonnes propriétés mécaniques du séparateur qui est capable de transférer au bloc d'électrodes une pression mécanique et de la soutenir tout au long de la vie de la batterie. L'application d'une pression mécanique sur les parois d'une cellule au plomb a permis de restreindre l'espace vide que la matière active positive peut occuper lorsque sa structure devient plus poreuse au fur et à mesure des cycles. Lorsque l'espace d'expansion est limité, d'une part un squelette de particules de dioxyde de plomb densément agglomérées se forme qui rend la matière active positive plus robuste à la décharge. D'autre part, à forts taux de décharge, une utilisation plus homogène de la matière active sur toute l'épaisseur de l'électrode est autorisée.

L'emploi du séparateur AJS a en outre permis de réduire la corrosion des grilles positives et les effets néfastes qui lui sont associés. D'une part la pression mécanique transférée aux grilles positives diminue la vitesse à laquelle elles se corrodent et d'autre part, le séparateur AJS stabilise le bloc d'électrodes en lui donnant une grande compacité. La croissance de la grille positive liée à la corrosion est ainsi limitée et par là les risques de formation de court circuit par le dessus du bloc d'électrodes.

L'addition d'acide phosphorique dans une cellule au plomb/AJS fermée a permis d'améliorer ses performances à fort courant de décharge en début de vie dans la mesure où un régime de charge approprié permettant une forte polarisation des électrodes positives était appliqué. Dans de telles conditions, l'adsorption de l'acide phosphorique sur les électrodes positives permet une fine cristallisation du dioxyde de plomb liée à une haute solubilité des espèces plomb IV qui ont tendance à précipiter là où l'acide phosphorique n'est pas adsorbé et à augmenter la compacité des agrégats de dioxyde de plomb dans l'électrode positive. L'influence de l'acide phosphorique perd toutefois en intensité au fur et à mesure que le nombre de cycles subis par la batterie augmente.

Enfin, il a été prouvé que le nouveau séparateur permet un cycle de l'oxygène limité qui a lieu grâce au transfert en voie gazeuse de l'oxygène de l'électrode positive vers l'électrode négative par le biais des plus gros pores du séparateur. L'accumulation d'oxygène sur l'électrode positive conduit à une différence de pression entre les deux côtés du séparateur qui libère ces pores de leur électrolyte. La recombinaison de l'oxygène ainsi autorisée suffit à assurer une vie des cellules plomb/AJS de plus de 1000 cycles profonds.

Au vu de ces résultats, la construction d'une batterie « améliorée » a été proposée dont les éléments seraient un bac en matériau rigide, un séparateur présentant de bonnes propriétés mécaniques tel AJS, des plaques négatives empâtées sur la seule épaisseur de la grille, des plaques positives avec une pâte de densité assez élevée, des constituants de grande régularité afin d'avoir un espace vide minimal dans chaque cellule et un électrolyte contenant 30 g/l d'acide phosphorique. Une saturation initiale en électrolyte de 100% ou légèrement supérieure et un régime de charge adéquat assureraient de pleines performances à cette batterie dont le principal avantage est d'utiliser l'expansion des électrodes positives

pour produire une « auto-compression » sans avoir à recourir à une pression mécanique extérieure difficile à réaliser techniquement.

La production de cette batterie améliorée, une étude approfondie de l'adsorption de l'acide phosphorique en fonction du potentiel de l'électrode positive ou une observation de l'effet sur la corrosion de la matière active qui transmet une pression mécanique à la grille positive sont quelques unes des pistes de recherche laissées ouvertes par cette thèse. Par conséquent, un grand travail de compréhension et de développement reste à faire avant que la batterie au plomb optimale soit produite pour des applications de type véhicule électrique. Ce travail espère avoir tout de même permis quelques progrès dans cette direction et apporté ainsi une petite contribution au développement durable.

Introduction

The drawback of energy production

Our world develops and makes rapid technological progress. But development relies on energy. As a matter of fact, the production of energy is in most of the cases a transformation of chemical energy into either electrical or mechanical energy. And since this transformation generally a combustion, combustion products like carbon dioxide or nitrogen oxides are rejected in the atmosphere. Figure 1 is an illustration of this allegation and shows the energy mix of which commercial primary energy is gained. “Globally, fossil fuels provide 87% of commercial primary energy” [1].

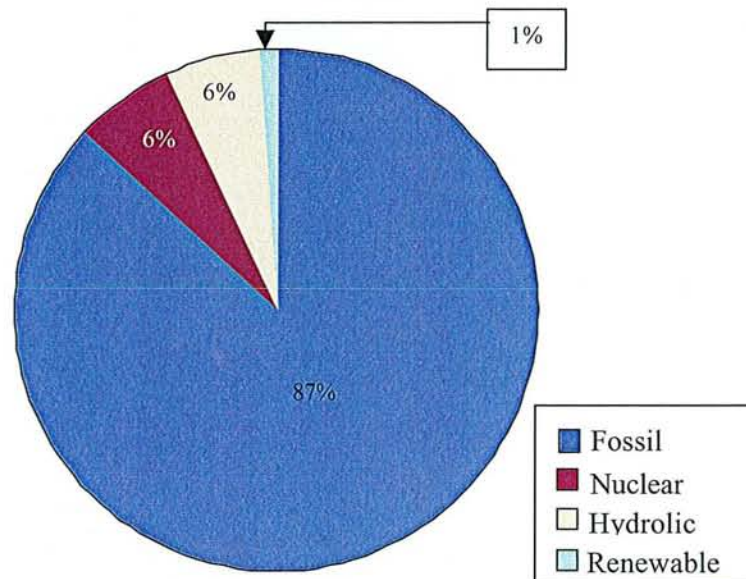


Figure 1: Energy mix for production of the commercial primary energy

Form this primary energy, one third flows in the production of electrical energy with again over 67% of fossil fuels in the mix for the electrical energy production.

The gases emitted as a result of combustion are responsible for the growth, in the atmosphere, of a layer that allows the solar rays to penetrate into the atmosphere but hinders the long wave radiation emitted by the earth surface to go out as shown in Figure 2. That way, the trapped radiation is oscillating between the earth surface and the polluting gas layer, warming the earth surface and the air between the two surfaces, just like in a greenhouse. The effect of warming the first layer of the atmosphere is known as the greenhouse effect and the gases responsible for the formation of the barrier layer in the atmosphere are called the greenhouse gases.

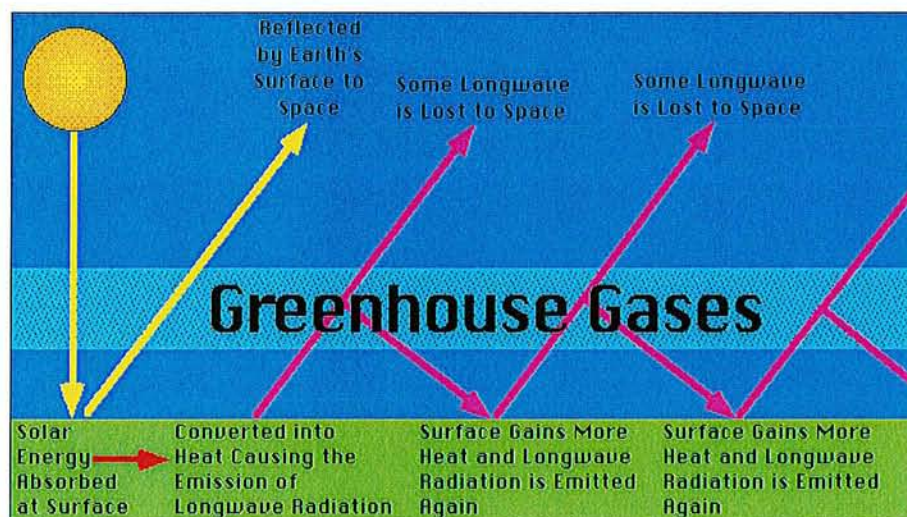


Figure 2: Schematic representation of the mechanism of the greenhouse effect [2]

Why the global warming of the earth surface is a threat for the human being is obvious. The expansion of water and melting of ice will lead to an increase of the ocean level (50 cm by the year 2100) and reduce the usable surface. In many countries, the water will become a strategic resource and many climatic disasters have to be expected. Figure 3 gives a schematic representation of the consequences of a global warming by 1°C in terms of wetter and dryer places.

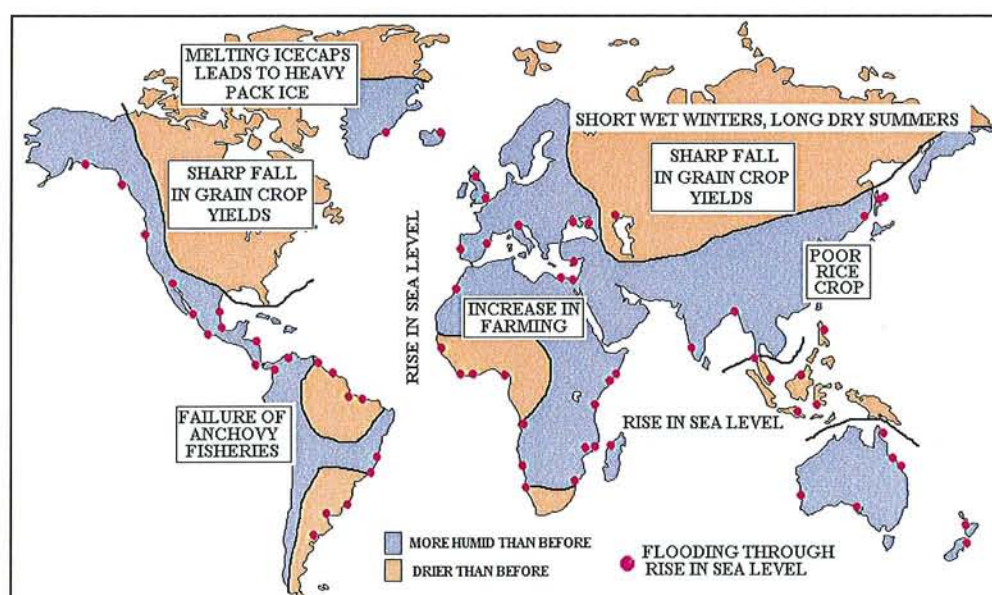


Figure 3: The consequences of a global warming by 1°C [3]

Facing the threat of global warming, in December 1997, 117 countries meeting for the United Nations global meeting on climate change in Kyoto, Japan, agreed the Kyoto protocol. This protocol saw the introduction of a set of legally binding limitations on emissions from the world's 39 industrialised countries by which the greenhouse gas emissions of these countries aggregate should be reduced by 5.2% in the year 2008-2012 when compared to their 1990 emission levels. This Kyoto protocol is much important because it is the first step on the way to a necessary global ecological regulation.

Emissions related to transportation

We showed that development needs energy and energy production implies pollution. And one of the greatest sources of greenhouse gases and in the same time, one of the most sensitive sign for development is the car. The World Health Organisation [4] found that the “pollution caused by motors could kill more people each year (in Austria, France and Switzerland) than road accidents.” Moreover, a European Commission report [5] states that "transportation accounted more than 30% of the EU total final energy demand in 1995" thus leading to the fact that "from an environmental point of view, transport accounted for 26.5% of CO₂ emission in the European Union in 1995". Facing this immense contribution, it is necessary to reduce either the number of vehicle or the quantity of emission for one vehicle in order to meet the Kyoto exigencies.

You may think that the solution for reducing of the greenhouse gas emissions made by transportation would be to find a new method for transportation and leave behind the private car. But if some people in industry countries can afford the luxury of leaving their car at home and go to work by bike or by bus, it is in many cases a step only reachable after the development has come through the obligatory phase of having possessed a car. Furthermore, the world develops, its population grows, and the number of cars that was 676.2 million in the year 1996 [6] is foreseen to reach over one billion in the year 2005 and 3.5 billions by 2050. This means that the only reduction of the production of greenhouse gas for each car will not be enough. For effectively reducing the greenhouse gas emissions by transportation, zero emission vehicles have to be produced. The development need a “more” in technology as people will not go back to less technology if not forced to [7].

For years, the only knowledge of these alarming estimations was not able to markedly push the research for the development of low emission or zero emission transportation. A political interest had to be showed that would motivate the industry to make the necessary investments in the research and development.

The lead-acid battery: a competitor for the electric vehicle propulsion

In 1994, the state of California created legislation concerning the ZEV (zero emission vehicles) and the sales of electric vehicles were projected to be 2% of all vehicles in 1998 and 10% in 2003 i.e. for example 850000 cars by 2000 [8]. Even if the environmental legislation concerning the zero-emission vehicles has been delayed and softened and has not produced the results expected, the Californian act for clean air was a great motor for the research to alternatives to the combustion engine.

In order to use an electrical engine, one need a source of electrical energy in the car and the most used electrochemical system for the conservation of electrical energy is the lead-acid battery. Besides its robustness, its low cost, its availability and its ability to be recycled at over 98% make it a successful product difficult to compete with.

Of course the image of the lead-acid battery is disappointing because most people know it as an old system used only for the starting of cars. But in fact, lead-acid batteries are present in our life even more in the “new society” of the internet age since this system is also used for telecommunications (transmission stations...), uninterrupted power supply systems and internet (PC and server backup...), energy production and distribution, military applications (submarine...), aviation (powering of the flight control system...), railway applications, accumulation of electricity gained from solar and wind energy... [9].

In spite of its many qualities, the lead-acid battery has some weak points and has to compete with many electrochemical accumulators for the propulsion of the electric vehicle. Table 1 shows a recapitulation of the advantages and drawbacks of all the possible challengers.

	Lead-acid	Ni-MH	Na-NiCl	Li
Security	+	0	0	-
Power (W/kg)	70 to 100	120 to 150	150	300
Cost (US\$/kWh)	150	>750	300	>750
Cycles (3h rate)	500	700	1000	1000
Energy (Wh/kg)	25 to 35	65 to 75	75	100
Development level	++	+	(+)	(+)
Environment	98% recycling	No heavy metal	No poison substance	
Main problems	Low energy	Self discharge	High temperature	Safety

Table 1: Advantages and drawbacks of the different competitors for the EV powering [10]

The most important parameters for the choice of an energy supplier for electric vehicles are, listed by priority:

- Security,
- Power density,
- Specific cost (If the cost of the battery is not very important for the cordless utilisation, “in the case of the electric vehicle, where the battery may account for half the total cost, it is a major factor” [11].),
- Specific energy (This factor limits the driving range).

Concerning the first three requirements, the lead-acid battery is in a quite good position. But for staying a main actor of the battery scene, in particular in the field of electric/hybrid vehicles, the lead-acid battery needs to fulfil some criteria [12]:

- High specific energy (50 Wh/kg) for a driving range of about 150 km,
- High specific power (150 W/kg),
- Low cost (<150 US\$/kWh),
- Cycle life over 500 full cycles,
- Rapid recharge.

In an attempt to drive the research in the field of VRLA batteries, lead producers, battery manufacturers, component suppliers and related industrial sectors have been pooling research and development resources to a common purpose. They founded the ALABC (Advanced Lead-acid Battery Consortium) as a counterpart to the USABC (the US Advanced Batteries Consortium that concerns all the advanced batteries systems as e.g. lithium and nickel/metal hydride). This Ph.D. thesis has for a big part been performed in the frame of a project supported by the ALABC and the European Community.

Motivation of the work

Many factors could be improved for the lead-acid battery to be a main actor in the market of the electric/hybrid vehicle. One is the energy density, another would be its charge efficiency and fast charge ability so that the drawback of the limited driving range for one charge can be overcome by often charging the batteries. Additionally, in a system containing a lead-acid battery, “the cost of battery and replacement generally far exceeds the operating costs, generally by a factor three or four” [13]. What can be a greater motivation for the improvement of the cycle life in deep cycle application? This work attempts to find a way to improve the performance and life of the lead-acid battery.

And in first line, for improving a system, it is necessary to know it. Even after over 150 years research and development on the subject, the lead-acid battery has still many mysteries. It had the chance to be allowed to make first experiments with a new separation system that proved to open wide possibilities for the lead-acid battery. Through the use of this new separation system, investigation of many processes happening inside the battery was allowed as well as better understanding of the complex influence of a passive part in the lead-acid battery: the separator.

The thesis presents an introduction to the lead-acid battery, followed by results concerning the improvement of the performance of the lead-acid battery by the application of mechanical pressure and its mechanism. The effect of mechanical pressure on the corrosion process and its interaction with phosphoric acid are then described, followed by some considerations on the oxygen cycle.

This work is meant to be a contribution on the way to a better understanding of the lead-acid battery in general and maybe it will allow an improvement of its performances in the future.

More in general, it is also an attempt to contribute in a modest way to the world's conservation. The signs are clear enough: the global warming is a reality and we must act and reduce emissions before we reach a "global thermal runaway". I feel, I will not be allowed to tell the next generation I did not know what was going on. If this work allows any little improvement of the lead-acid battery for use in an electric car or as an accumulator in photovoltaic equipment, it will already be a success.

Introduction

Les effets pervers de la production d'énergie

Notre monde se développe et fait de rapides progrès technologiques. Mais le développement repose sur l'énergie et la production d'énergie repose dans la majorité des cas sur une transformation d'énergie chimique soit en énergie électrique, soit directement en énergie mécanique. La Figure 1 représente les différentes sources d'énergie commerciale primaire. « Globalement, les combustibles fossiles fournissent 87% de l'énergie commerciale primaire » [1].

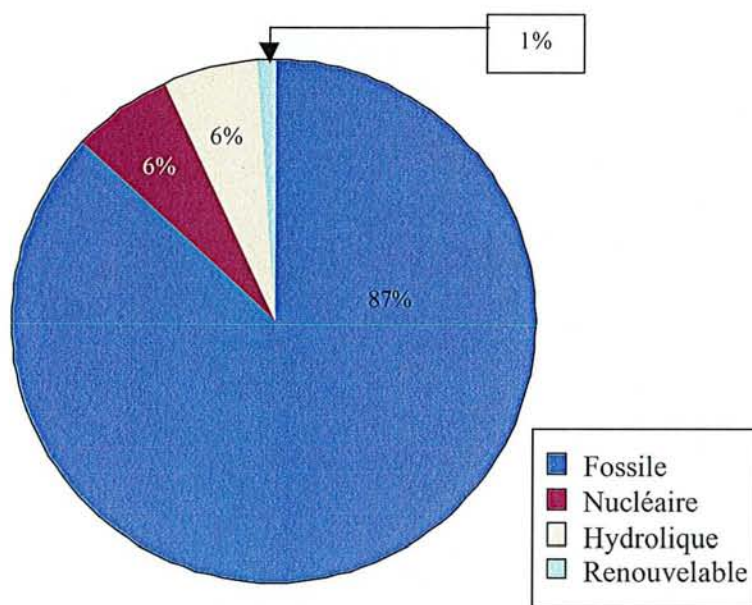


Figure 1: Les différentes sources d'énergie commerciale primaire.

Un tiers de cette énergie primaire est utilisée pour la production d'énergie électrique, ce qui conduit de nouveau à une contribution de plus de 67% des combustibles fossiles à la production d'énergie électrique. Ce passage d'une forme d'énergie à l'autre se produit donc essentiellement par combustion et les produits de combustion sont ainsi rejetés dans l'atmosphère à l'instar du dioxyde de carbone ou des oxydes d'azote. Ces gaz sont responsables de la croissance dans l'atmosphère d'une couche qui permet le passage des rayons solaires mais bloque une partie des rayonnements à grande longueur d'onde qui sont réémis par la surface de la terre. Ainsi, la radiation est indéfiniment réfléchiée entre la surface de la terre et cette couche barrière (Figure 2) et provoque un réchauffement de la surface de la terre et de l'air compris entre les deux surfaces de réflexion. Cet effet de réchauffement des couches internes de l'atmosphère, semblable à ce qui se produit dans une serre, est nommé l'effet de serre et les gaz polluants mis en jeu sont les gaz à effet de serre.

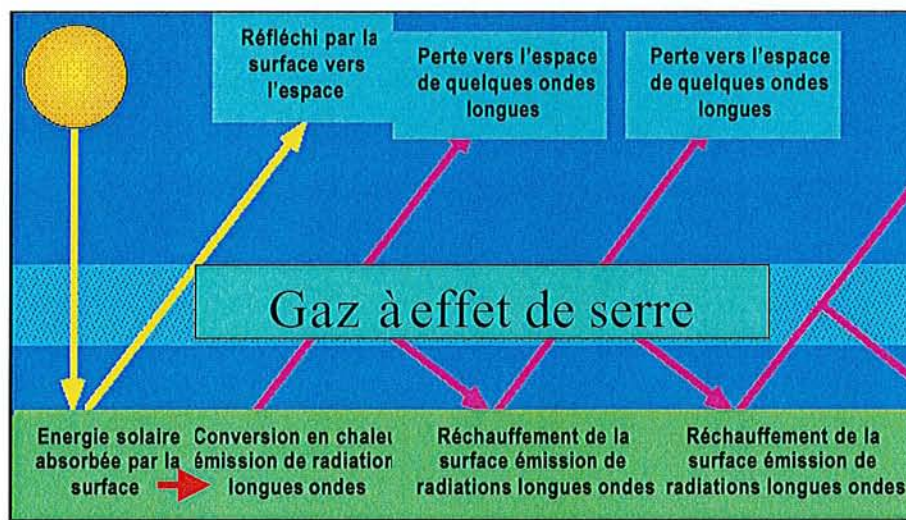


Figure 2: Représentation schématique du processus de l'effet de serre [2]

Les raisons pour lesquelles un réchauffement planétaire est une menace pour l'humanité sont évidentes. L'expansion des océans liée au réchauffement et la fonte des glaciers vont causer une élévation du niveau des océans de 50 cm avant l'an 2100 et réduire les surfaces utilisables pour l'être humain. Pour de nombreux pays, l'eau va devenir une ressource stratégique et de nombreuses catastrophes naturelles sont à prévoir. Une répartition géographique des zones qui verront une augmentation ou une diminution des précipitations dans l'hypothèse d'un réchauffement global de 1°C est proposée en Figure 3.

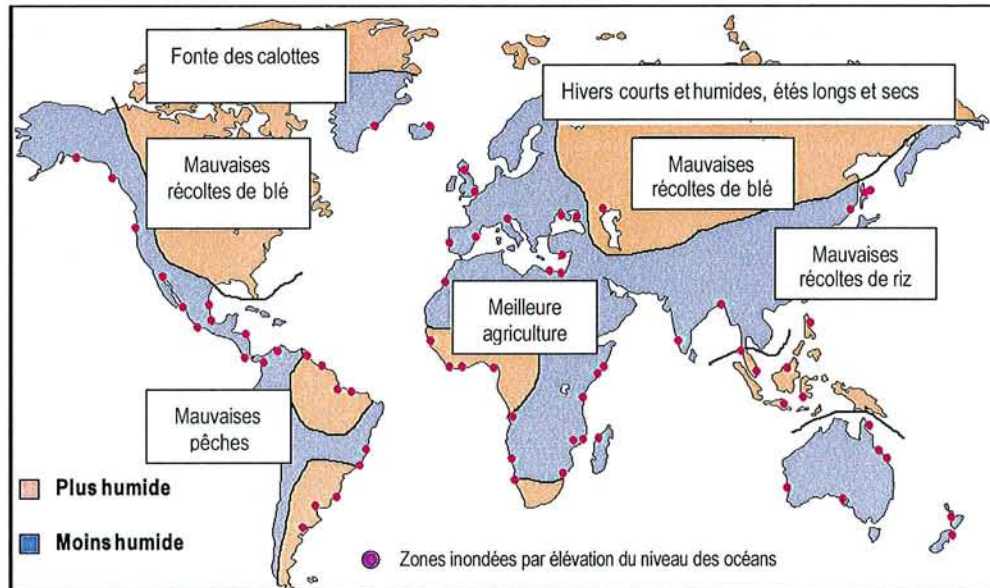


Figure 3: Variations climatiques dans le monde pour un réchauffement global de 1°C [3]

Pour faire face à la menace du réchauffement planétaire, 117 pays se sont réunis en décembre 1997 au Japon pour la conférence des Nations Unies sur le changement climatique global. Ils y ont signé le traité de Kyoto qui prévoit une limitation des émissions de gaz à effet de serre de 39 pays industrialisés. Ces pays sont contraints par une réglementation à réduire de 5,2% leurs émissions de gaz polluants par rapport aux niveaux de 1990. L'importance de ce traité réside dans le fait qu'il est le premier pas vers une régulation écologique internationale nécessaire.

Les émissions liées aux transports

Le paragraphe précédent a démontré que le développement est basé sur l'énergie et que la production d'énergie est une énorme source de pollution. Et l'une des plus importantes sources de gaz à effet de serre mais en même temps, l'un des signes les plus sensibles de développement économique, c'est la voiture !

L'Organisation Mondiale de la Santé a estimé que « la pollution causée par les moteurs pourrait tuer plus de personnes chaque année (en France, Autriche et Suisse) que les accidents de la route » [4]. En outre, un rapport final à la Commission Européenne affirme que « les transports sont responsables de plus de 30% de la dépense totale de la communauté européenne en énergie finale » et qu'ainsi, « du point de vue de l'environnement, les transports sont responsables de 26,5% des émissions de dioxyde de carbone dans la communauté européenne en 1995 » [5]. Ces chiffres alarmants prouvent qu'il est nécessaire, pour atteindre les objectifs fixés par le traité de Kyoto, d'agir soit sur la pollution dont est responsable chaque véhicule, soit sur le nombre de véhicules.

Vous allez sans doute penser que la solution pour réduire les émissions de gaz à effet de serre consisterait à trouver un nouveau moyen de déplacement qui rendrait la voiture superflue. Mais si certaines personnes dans les pays industrialisés peuvent se permettre le luxe de laisser leur véhicule chez elles et de se rendre à leur travail en bus ou en bicyclette, une telle démarche n'est souvent envisageable qu'à l'issue d'un développement qui est passé par la possession d'une voiture. En outre, la population mondiale croît de façon exponentielle, le développement économique se poursuit et le nombre de voitures, qui atteignait 676,6 millions en 1996 [6], doit selon les estimations dépasser le milliard en 2005 et 3,5 milliards en 2050. Ces chiffres signifient clairement que la seule réduction des émissions produites par chaque voiture ne sera pas une mesure suffisante pour diminuer la production de gaz à effet de serre. Pour réduire substantiellement les émissions, il sera nécessaire de produire des véhicules qui n'émettent aucun gaz polluant. Par conséquent, c'est seulement par un « plus en technologie » que le réchauffement planétaire pourra être endigué puisque les êtres humains ne s'accommoderont en aucun cas de ce qu'ils considéreraient comme une régression s'ils n'y sont pas forcés [7].

La batterie au plomb, concurrente pour la propulsion du véhicule électrique

Depuis des années, la connaissance de ces chiffres alarmants n'a pas suffi à motiver sensiblement la recherche pour le développement de véhicules à faibles émissions ou à émissions nulles. Il était nécessaire qu'une volonté politique se dessine qui pousse l'industrie à faire les investissements nécessaires dans la recherche et le développement de solutions.

En 1994, l'état de Californie a voté une loi qui contraignait les producteurs de véhicules à veiller que 2% de tous les véhicules de l'état de Californie ne produisent aucune émission dès 1998. Ce chiffre devait atteindre 10% en 2003 ce qui correspondait à 850 000 véhicules non polluants en l'an 2000 [8]. Bien que cette loi ait entre temps été assouplie, tolérant aussi des véhicules à faibles émissions et repoussant les échéances, elle a eu pour effet de propulser la recherche dans le domaine du véhicule peu ou non polluant. Nous avons vu que la transformation d'énergie chimique en énergie mécanique par combustion est en grande partie responsable des émissions polluantes. Ceci signifie que pour produire un véhicule non polluant, il faut utiliser un moyen de propulsion autre que le moteur à combustion. L'alternative idéale est alors le moteur électrique. Et pour alimenter un moteur électrique, une source d'énergie électrique doit être présente à bord du véhicule. Le système électrochimique actuellement le plus utilisé pour l'accumulation d'énergie électrique est la batterie au plomb. Outre sa robustesse, son faible coût, son aptitude à être recyclée à plus de 98% et sa disponibilité en grande quantité en font un produit difficile à concurrencer.

Il est vrai que l'image de la batterie au plomb est plutôt celle d'un produit suranné, utilisé pour le seul démarrage des voitures. Mais en fait, la batterie au plomb est un élément présent autour de nous encore plus dans la nouvelle société de l'ère multimédia qu'auparavant. En effet, ce système d'accumulation de l'énergie électrique est aussi utilisé dans les domaines des télécommunications, des systèmes d'alimentation sans interruption et de sauvegarde de données, de la production et de la distribution d'énergie, de l'aviation et l'aérospatiale, de la défense ainsi que dans les applications solaires ou éoliennes et les systèmes ferroviaires...[9]

En dépit de ses nombreuses qualités, la batterie au plomb souffre de quelques points faibles qui la handicapent vis à vis des autres systèmes électrochimiques dans la compétition pour la propulsion du véhicule électrique. Dans Tableau 1, les avantages et inconvénients de chaque système électrochimique susceptible d'alimenter le moteur d'un véhicule électrique sont répertoriés.

	Plomb/acide	Ni-MH	Na-NiCl	Li
Sécurité	+	0	0	-
Puissance (W/kg)	70 à 100	120 à 150	150	300
Coût (US\$/kWh)	150	>750	300	>750
Cycles (3h rate)	500	700	1000	1000
Energie (Wh/kg)	25 à 35	65 à 75	75	100
Niveau de développement	++	+	(+)	(+)
Environnement	Recyclage à 98%	Pas de métaux lourds	Pas de substances toxiques	
Principal problème	Faible énergie	Auto-décharge	Haute température	Sécurité

Tableau 1: Caractéristiques des différents systèmes électrochimiques pour la propulsion du véhicule électrique [10]

Les paramètres dominant le choix d'une source d'énergie pour le véhicule électrique sont par ordre de priorité:

- la sécurité,
- la puissance massique,
- le coût (Si le coût n'est pas le facteur déterminant dans le cas des appareils électroniques portables, "dans le cas du véhicule électrique, où la batterie peut être responsable de la moitié du coût, c'est un facteur primordial." [11]),
- l'énergie massique (c'est le facteur qui détermine l'autonomie du véhicule).

Pour ce qui concerne les trois premiers paramètres, la batterie au plomb est en bonne position. Mais pour rester un acteur dominant sur la scène des accumulateurs électrochimiques, en particulier dans le domaines de véhicules électriques ou hybrides, la batterie au plomb doit satisfaire à certains critères énumérés ci-après [12] :

- Energie massique élevée (50 Wh/kg) pour une autonomie d'environ 150 km,
- Puissance massique élevée (150 Wh/kg),
- Faible coût (< 150 US\$/kWh),
- Recharge rapide.

Afin de pousser la recherche dans le domaine des batteries au plomb fermées, des producteurs de plomb, des fabricants de batteries, des sous traitants et des acteurs industriels liés au secteurs de la batterie au plomb ont mis en commun leur ressource de recherche et développement. Ils ont fondé le ALABC (Advanced Lead-Acid Battery Consortium, Consortium pour la batterie plomb/acide avancée) comme pendant à l'USABC, un consortium américain destiné à la recherche sur les systèmes électrochimiques "avancés" c'est à dire par exemple le lithium ou l'hydrure de métal.

Le travail relaté dans cette thèse a été conduit pour la plus grande part dans le cadre d'un projet financé par le ALABC et la Communauté Européenne.

Motivation de ce travail de thèse

De nombreuses améliorations peuvent être apportées à la batterie au plomb afin de lui assurer un rôle dominant sur le marché du véhicule électrique ou hybride. L'une serait l'augmentation de son énergie massique, une autre serait le développement de son aptitude à la recharge rapide de telle façon que l'inconvénient lié à la faible autonomie soit pallié par les charges fréquentes et rapides de la batteries. En outre, dans un système contenant une batterie au plomb, "le coût de la batterie et de son remplacement excèdent généralement largement le coût de fonctionnement, couramment d'un facteur trois ou quatre" [13]. Quel argument pourrait motiver plus un allongement de la durée de vie en cyclage profond ?

Ce travail vise donc à l'amélioration des performances et de la durée de vie des batteries au plomb.

En premier lieu, pour améliorer un système, il est nécessaire de le bien connaître. Or, quoique comptant 150 années de recherche et développement intensif à son sujet, la batterie au plomb est encore la détentrice de nombreux secrets. J'ai eu la chance de pouvoir réaliser les premières expériences avec un nouveau système de séparation. Ce système a révélé qu'il ouvrait de larges possibilités au système plomb/acide. En outre, l'investigation de nombreux processus se déroulant dans la batterie a été rendue possible grâce à son utilisation ainsi que la meilleure compréhension du rôle que joue un composant "passif" de la batterie: le séparateur.

Ainsi dans cette thèse, une introduction de la batterie plomb/acide sera tout d'abord faite. Des résultats concernant l'amélioration des performances de la batterie au plomb par l'application d'une pression mécanique seront présentés ainsi qu'une description des mécanismes mis en jeu. L'effet de la pression mécanique sur le processus de corrosion et son interaction avec l'acide phosphorique seront ensuite décrits. En dernier lieu, l'effet du nouveau système de séparation sur le cycle de l'oxygène sera abordé.

Le but avoué de ce travail est la meilleure compréhension du système plomb/acide afin de permettre une amélioration de ses performances et de sa durée de vie. Mais dans un sens plus général, cette thèse tend à contribuer de façon modeste à la conservation de l'environnement. Notre planète nous donne des signes clairs: le réchauffement global est une réalité et nous devons agir pour réduire nos émissions. Aux questions des générations futures, je ne pourrai pas répondre que je ne savais pas. C'est pourquoi si ce travail permet quelque petite amélioration que ce soit de la batterie au plomb conduisant à son utilisation dans un véhicule électrique ou dans un équipement photovoltaïque, ce sera déjà un succès.

1 The lead-acid battery

1.1 Electric energy accumulation

Figure 4 presents all batteries and electrochemical sources of electrical energy. By opposition to the primary batteries that can be used only for one discharge, the lead-acid battery is an accumulator or secondary cell. It means that it can be discharged and recharged.

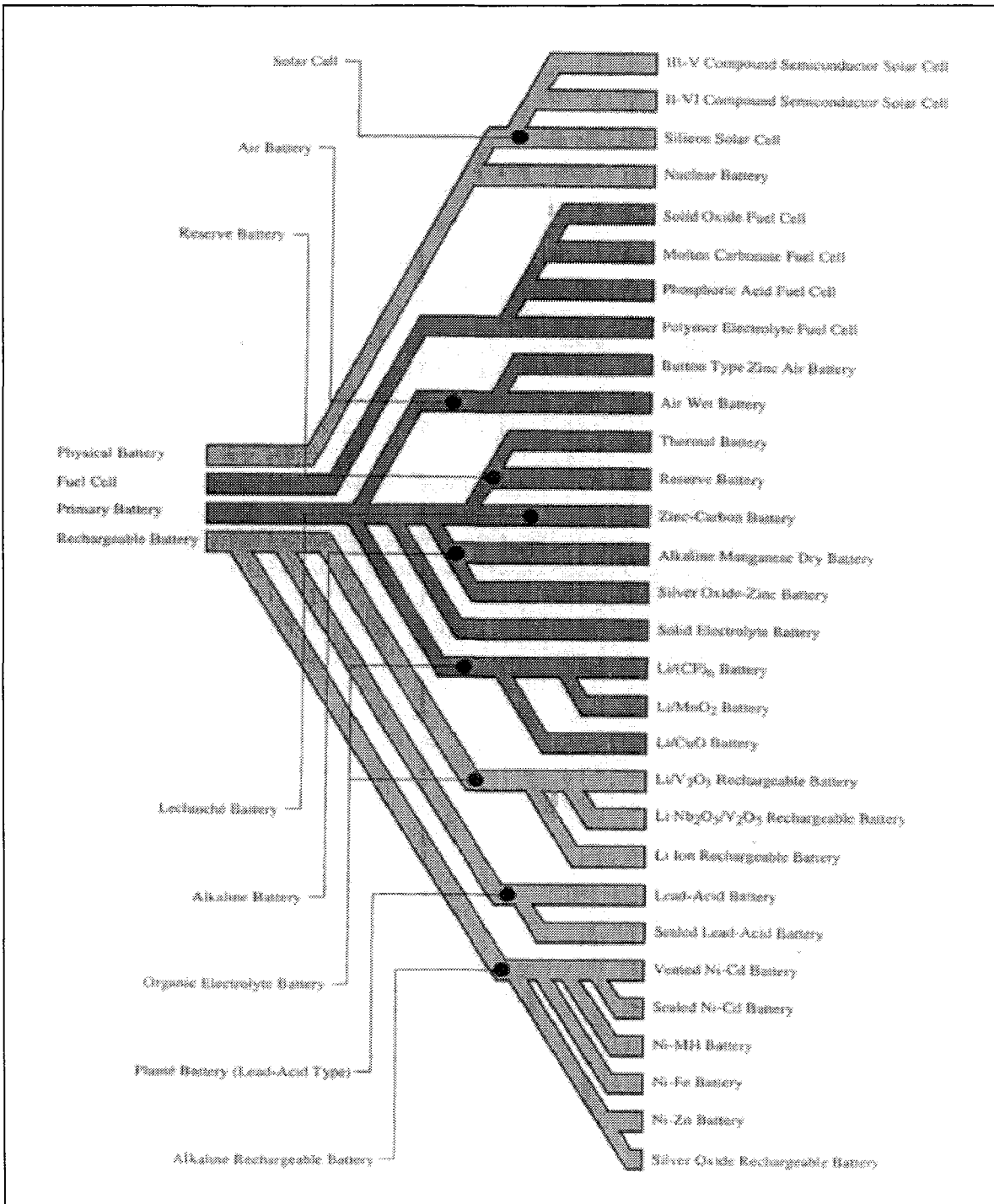


Figure 4: All types of batteries [10]

1.2 History of the lead-acid battery

Even if Sinsteden published performance data for this system in 1854, Gaston Planté was the first able to demonstrate a rechargeable lead-acid battery in 1860. A more detailed history of the lead-acid battery can be found in [14] and [15].

Since its discovery, the lead-acid battery gained gradually importance as a consequence of the industrial revolution that began in the United Kingdom for some 200 years. Used nowadays in first line for the starting of cars, the global sales of lead-acid batteries amounted between April 99 and March 2000 over 12 billion US\$. From these 12 billion US\$, the SLI (starting, lighting, ignition) market amounted over 8 billion US\$ and industry batteries about 3.2 billion US\$, the rest concerning portable rechargeable applications [10].

1.3 Principle

Principally, the denomination "*battery*" describes a connection in series of several cells. For example, the usual car battery, with a voltage of around 12V is a connection in series of 6 lead-acid cells. But the word battery is in fact used also for single cells nowadays.

As every electrochemical cell, the lead-acid cell consists of a positive electrode and a negative electrode that are immersed in an electrolyte. At each electrode, an electrochemical reaction takes place that releases electrons (oxidation) or absorbs electrons (reduction) as shown in Figure 5.

The positive electrode, that accepts electrons during discharge, consists of high fine porosity lead dioxide (PbO_2) supported by a lead current collector.

The negative electrode, that delivers electrons during discharge, consists of metallic lead of high porosity (just like a sponge) with some additives (BaSO_4 , expander) The active material is also supported by a current collector, usually of similar composition as the one of the positive electrode.

The electrolyte consists of dilute sulphuric acid (H_2SO_4). It is responsible for the ionic conduction but is also an active material since it is consumed during discharge and regenerated during charge. Therefore, during cycling, the density of the sulphuric acid changes. Densities of 1.28 g/cm^3 are usually encountered in a fully charged state. In the concentration range encountered in the lead-acid battery, i.e. between 1 mol/l in the discharged state and 5 mol/l in the charged state, the sulphuric acid is not fully dissociated and is present as H_3O^+ and HSO_4^- .

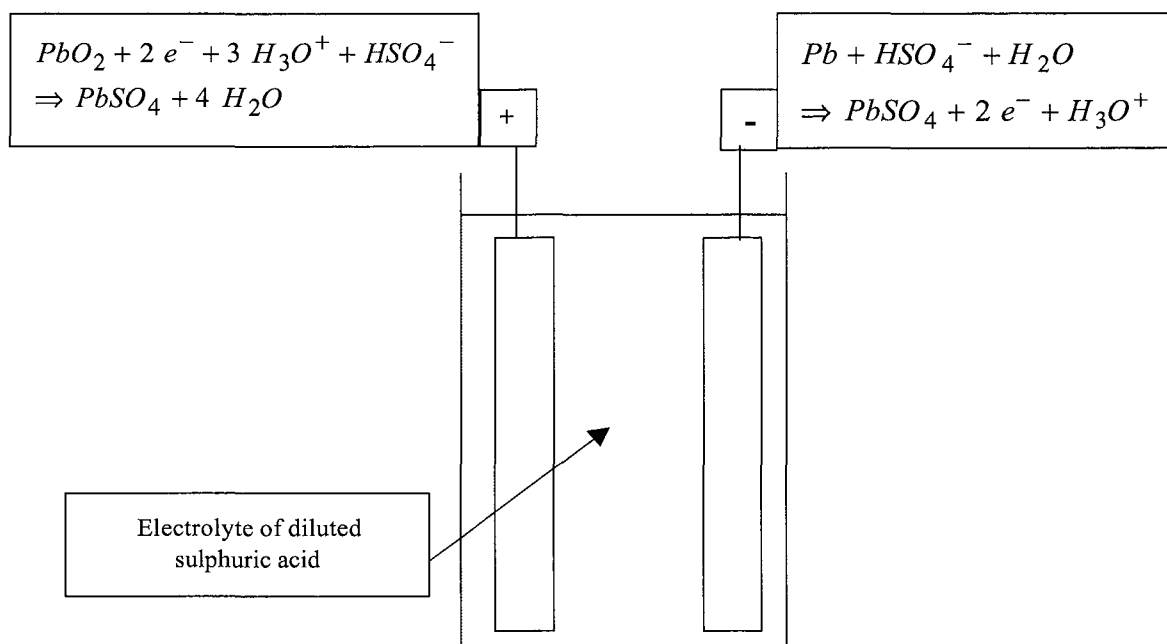
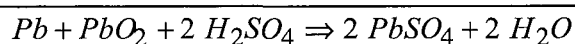
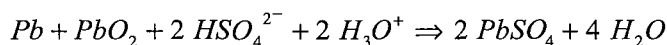


Figure 5: Electrode reactions of the lead-acid battery

The sum of both electrode reactions is the cell reaction:



Or more correctly



Equation 1

1.4 The electrochemical system "lead-acid battery"

1.4.1 General considerations

Two laws govern every chemical or electrochemical reaction: in first place thermodynamics and in second place, kinetics.

1.4.1.1 Thermodynamics of the system Pb/H₂SO₄/PbO₂

For a chemical or electrochemical reaction to happen, the first condition to fulfil is that the reaction is thermodynamically possible and favoured. Essentially, thermodynamics do not take into account the reaction path, considering only the energy of the products and the reactants. It describes therefore the maximum performance that can be expected from a system.

The thermodynamic state functions describe the energetic state of a system. Concerning an (electro-) chemical reaction, it is the difference between the initial and the final state that is of interest. The most important parameter is the one that describes the amount of energy that can be converted into work i.e. the **free enthalpy of reaction ΔG**: $\Delta G = \Delta H - T\Delta S$.

ΔG represents the maximum amount of electrical energy that can be gained during a reaction if all work is converted into electrical energy.

Equation 2 gives the electrochemical expression for the free Gibbs energy.

$\Delta G = -zFE_0$	$z = \text{number of electronic charges exchanged}$ $F = \text{Faraday constant} = 96500 \text{ As}$ $E_0 = \text{equilibrium potential of the reaction}$	Equation 2
---------------------	---	-------------------

The reaction of Equation 1 has a free enthalpy -372.6 kJ . It means a cell equilibrium potential of $E_0 = 1.931 \text{ V}$ for standard conditions (i.e. when HSO_4^{2-} and H_3O^+ are present with an activity of 1 what means at a density of the acid of about 1.065 g/cm^3 [16]). The cell equilibrium voltage at different concentrations is given by the Nernst equation (**Equation 3**).

$$E_0 = E_{0,standard} + \frac{RT}{zF} \ln\left(\frac{[Ox]}{[Red]}\right) \quad \begin{array}{l} [Ox] = \text{activity of oxydant} \\ [Red] = \text{activity of reducer} \end{array} \quad \text{Equation 3}$$

A usual approximation of it is $E = 0.84 + d$ where d is the acid density (in g/cm^3).

When different reactions are thermodynamically possible in a system, the one with the highest voltage takes place in priority. In other words, the two half reactions with the highest difference of potential happen.

From the cell voltage deduced from **Equation 3**, the thermodynamic would assume that the lead-acid battery is not viable. Namely, the electrolyte is dilute sulphuric acid and on each electrode of the lead-acid cell, the reaction of water decomposition should take place. In this case, the lead-acid battery could not be conserved in a charged state.

A small scale of the half-cell reaction potentials is represented in Figure 6.

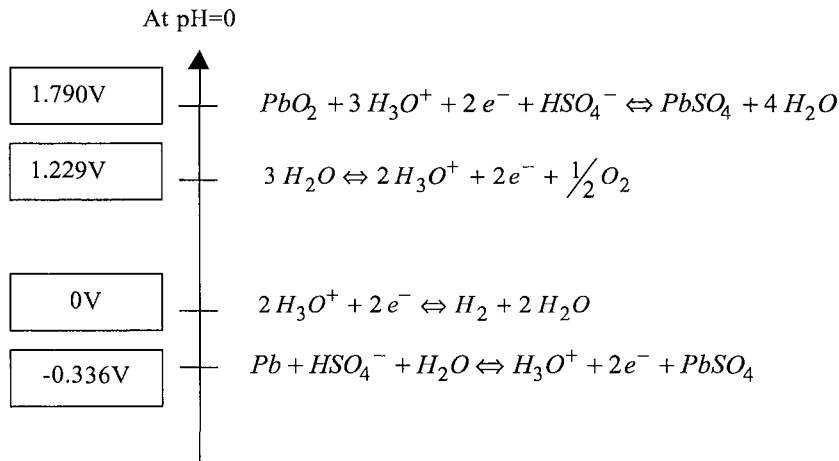
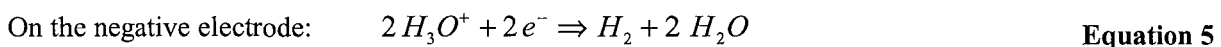
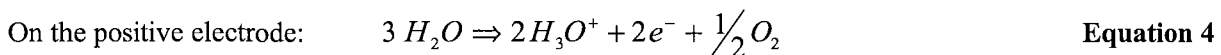


Figure 6: Schematic repartition on the voltage scale of the reactions in a lead-acid battery

From this scale, the thermodynamic says that during rest, water will decompose to oxygen on the positive electrode and to hydrogen on the negative electrode. The reactions that would take place are:



When a current flows between the electrodes, these reactions correspond to the electrolysis of water and when no current flows, the counter reaction is on the same electrode and self-discharge of the accumulator happens.

The domain of stability of the different species in the system Pb/H₂O depending on the potential and on the pH conditions are summarised in the so called Pourbaix diagram that is shown in Figure 7 for different concentrations of Pb²⁺.

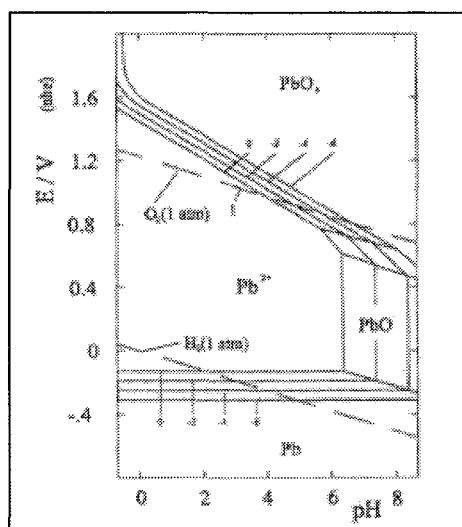


Figure 7: Pourbaix diagram of the lead/water system [17]

(0,-2,-4,-6 lines indicate Pb²⁺ concentrations of 1, 10⁻², 10⁻⁴, 10⁻⁶ mol/dm³ respectively)

From a thermodynamic point of view, not only water decomposition should take place on the electrodes of the lead-acid cell. The Pourbaix diagram also shows that lead is not stable at the potential of the positive electrode in conditions of low pH as encountered in the lead-acid battery. The detail of the reactions that are not the normal charge or discharge reactions and that take place because of thermodynamic considerations is discussed in section 1.4.2.

1.4.1.2 Kinetic of the lead-acid battery

In fact, the second law that governs an electrochemical reaction, that is to say the kinetic, allows the lead-acid battery to exist.

The kinetic takes into account the reaction path by which a reaction takes place. Namely, in order to get a flow of electrons, some resistance has to be overcome that leads to a deviation of the reaction potential from the equilibrium potential. This resistance corresponds to the sum of each reaction step that precedes or follows the actual charge transfer step and that is limited by e.g. transport or diffusion. That way, the rate at which each reaction step happens is controlled by its kinetic parameters and the kinetic of reaction is limited by the kinetic of each reaction step. Therefore, polarisation has to be applied to the electrode in order to obtain a reaction and this polarisation deviates the electrode potential from the equilibrium potential of the reaction that would be deduced from the thermodynamic data. This polarisation is the sum of e.g. the overpotentials of crystallisation, diffusion, charge transfer, pre- and post-reactions...

An electrochemical equilibrium is always composed of one reaction and its reversal. The dependence of the reaction rate on the deviation from the equilibrium potential is a **current/voltage curve** in which each reaction direction can be represented.

For example, a voltammogram of the lead dioxide/lead sulphate electrode in sulphuric acid is presented in Figure 8. It was taken during cyclic voltammetry of a disc electrode made from pure lead in the anodic region in sulphuric acid ($d=1.28 \text{ g/cm}^3$) at a potential variation rate of 5 mV/s .

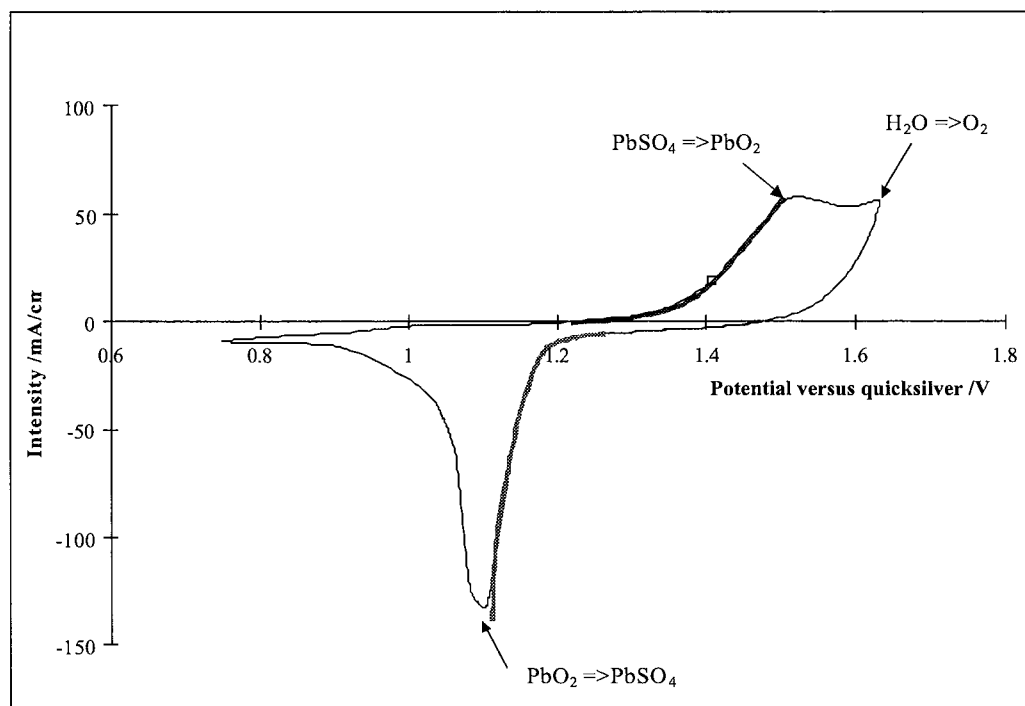


Figure 8: Cyclic voltammogram of Pb in H_2SO_4 , cycle 100

Only the part of the voltammogram drawn in thick represents the dynamic current/potential curve of the $\text{PbO}_2/\text{PbSO}_4$ pair but the reactants are available in a limited amount. Additionally, the other reactions that can happen in the system $\text{Pb}/\text{H}_2\text{SO}_4$ are also present in such a measurement (i.e. oxidation of water at high potential). The extrapolation of the only unlimited $\text{PbO}_2/\text{PbSO}_4$ reaction is shown in Figure 9. The **equilibrium potential** is reached when a reaction and its reverse are equally fast. The current at the equilibrium potential is the so called **exchange current**.

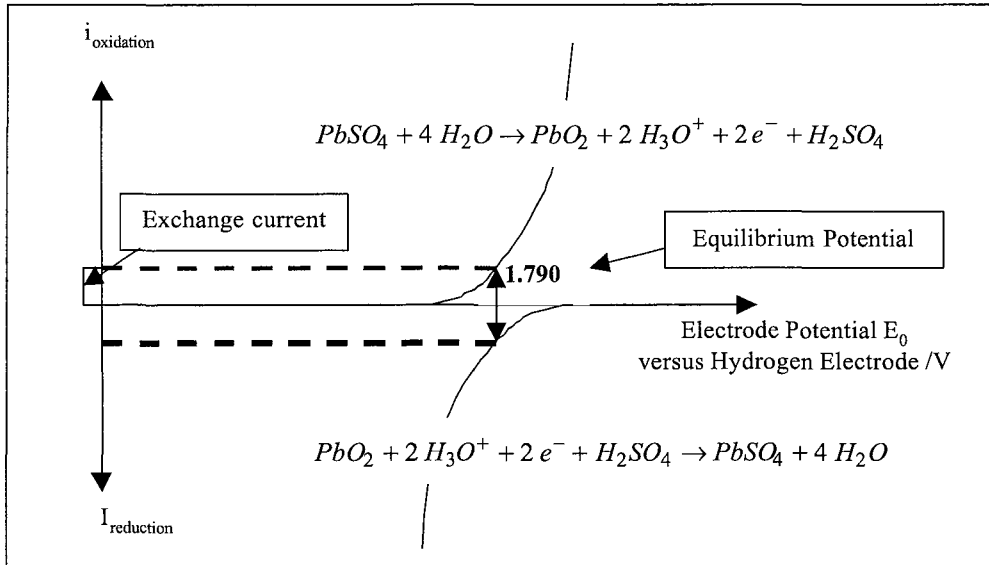


Figure 9: Extrapolated current/potential curve of the $\text{PbO}_2/\text{PbSO}_4$ pair

For each electrochemical reaction that is not limited by diffusion, the current/voltage dependence follows the Butler-Volmer equation [16].

$$i = i_0 \left\{ \exp \left[\frac{\alpha F}{RT} (E - E_0) \right] - \exp \left[-\frac{(1-\alpha)F}{RT} (E - E_0) \right] \right\}$$

i : current density

E_0 : equilibrium potential

i_0 : exchange current density

α : transfer factor describing the efficacy of the over-voltage on forward and backward reactions

E : actual electrode potential

In the range where the reversal equation can be neglected (potential range far from the equilibrium), the second term of the Butler-Volmer equation can be neglected and the equation becomes a simple exponential law. It is then convenient to represent the logarithm of the current as a function of the voltage. One obtains that way the so-called Tafel lines. A schematic representation of the Tafel lines of the water dissociation reactions on lead is shown in Figure 11 in the next section (the reduction current is also represented as positive).

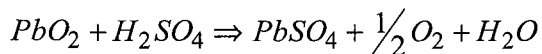
1.4.2 Secondary reactions

The secondary reactions (or parasite reactions) are the ones that are not wanted but that have an equilibrium potential lying within the cell operation voltage. Therefore, they are inherent in the system and unavoidable. Not only the water dissociation is a parasite reaction in the lead-acid battery but also the corrosion of lead.

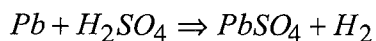
Secondary reactions during rest.

The potential of the negative electrode is more negative than the reaction potential of Equation 5 and on the positive, the potential is higher than the reaction potential of Equation 4.

Since there is by definition no outer current flow between the electrodes during rest, the counter reaction that delivers or accepts electrons takes place on the same electrode. This is the discharge reaction of each electrode and the global reactions are given in Equation 6 for the positive electrode and in Equation 7 for the negative electrode.



Equation 6



Equation 7

When such a reaction takes place on an electrode, the electrode is at a mixed potential that is determined by the kinetic parameters of the oxidation and the reduction just as illustrated for the positive electrode in Figure 10.

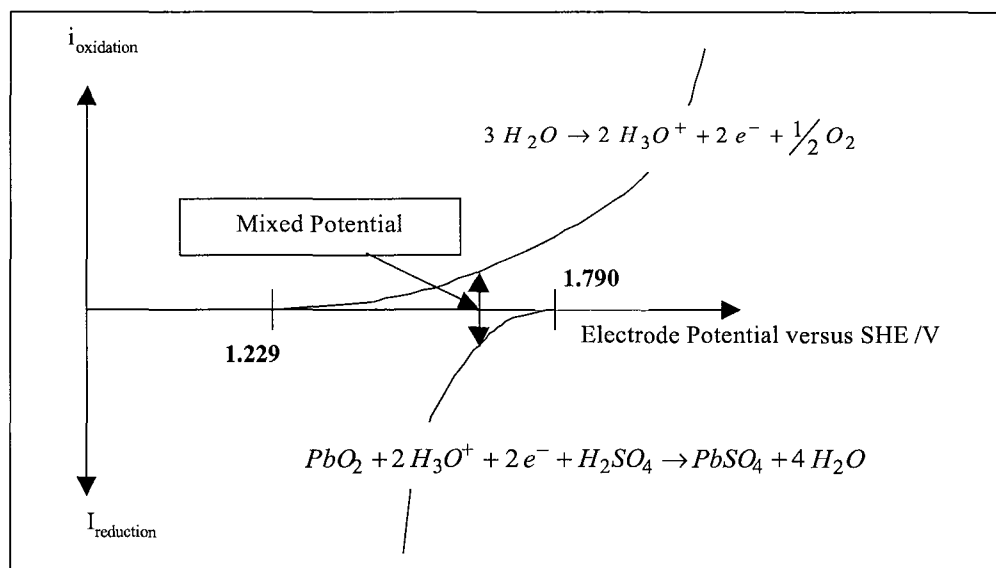


Figure 10: Mixed potential of the positive electrode during self discharge

Therefore, the rest potential of the lead-acid cell is not equivalent to the equilibrium potential calculated from the Gibbs energy and the Nernst equation. Each electrode is at a mixed potential because water dissociation takes place on it and the rest potential of the cell is the difference between the mixed potentials of the two electrodes. But due to the low kinetic of the water decomposition on both the positive and the negative electrode, the deviation of the cell open circuit voltage from the equilibrium potential is quite negligible.

During rest, another secondary reaction takes place, this is the rest corrosion of the positive electrode. Namely, lead cannot be in equilibrium with lead dioxide. When these two materials are in contact, a lead oxide layer builds up between them. And since the lead oxide is not stable in sulphuric acid, it reacts with the electrolyte and forms lead sulphate. During rest, the lead oxide layer is transformed to lead sulphate.

Secondary reactions during charge.

During charge, both the positive and the negative electrodes are polarised. It means that the current flow leads to a deviation from the open circuit potential at each electrode and the whole cell potential increases. Depending on the current density, the charge reaction of both electrodes takes place already when the polarisation of the electrodes is low. When recharge proceeds, the polarisation of the electrodes increases as a result of the lower amount of available uncharged material and of the higher concentration of sulphuric acid in the pores. Due to the higher polarisation of the electrodes, the secondary reactions are concurring with the charge reaction. The different kinetics of the oxygen and the hydrogen evolutions lead to different evolution rates of the gases for the same polarisation of the positive and negative

electrode respectively. Therefore, "positive electrodes typically begin gassing at about 70% state-of-charge, while negative electrodes commence at about 90%" ([18] and references therein).

The representation of the Tafel lines of the oxygen evolution on the positive electrode and of the hydrogen evolution on the negative electrode depending on the electrode potential is made in Figure 11.

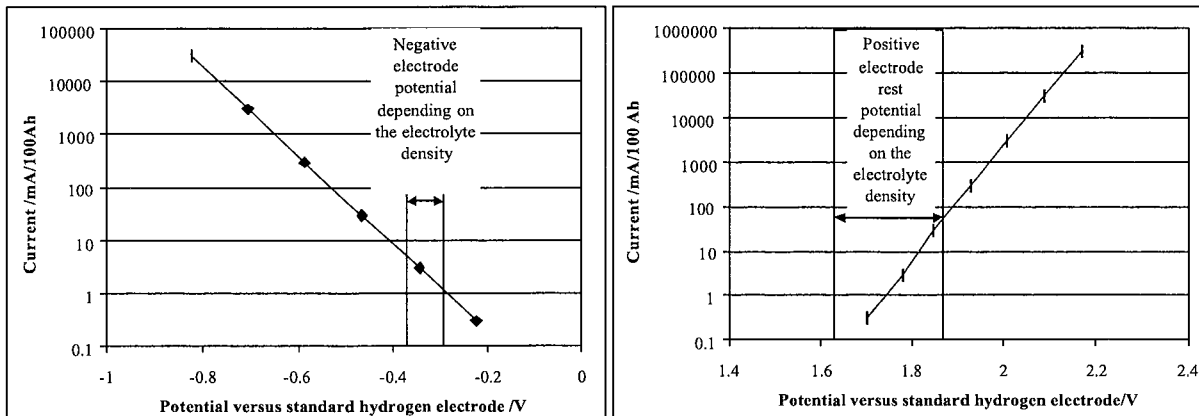


Figure 11: Tafel lines of the hydrogen and oxygen evolutions on lead [16].

One can easily deduce from these curves that during rest, the water dissociation is unavoidable but that the reactions described in Equation 4 and Equation 5 are in fact extremely slow on lead. They need a high deviation from the equilibrium voltage in order to proceed at a noticeable rate.

The other secondary reaction that happens during charge and overcharge is the corrosion of the positive lead grid. The corrosion process is detailed in section 4.

1.5 Different designs of the lead-acid battery

There are many lead-acid battery designs. They can be classified on the base of the state of their electrolyte (liquid or immobilised) and depending on the design of their electrodes. In the different categories of lead-acid batteries, diverse features can differentiate a battery from another and make it more suitable for one or another application. For example, thicker grids are more resistant against corrosion but only suitable for a stationary design because of their weight.

1.5.1 Flooded battery

The first lead-acid battery consisted of lead sheets that were cycled in sulphuric acid so that a layer of active material could form on the electrodes as a corrosion product. These were the Planté electrodes. In 1881, Fauré had the idea to cover lead foils with a paste of lead oxide that is then charged and thus oxidised or reduced to active material. That way, the capacity of the batteries was increased.

The "usual" lead-acid battery may be described as the "car battery" or the SLI battery (for starting, lighting, ignition) and has a prismatic flooded Fauré design. A schematic representation of the "typical" lead-acid battery is presented in Figure 12.

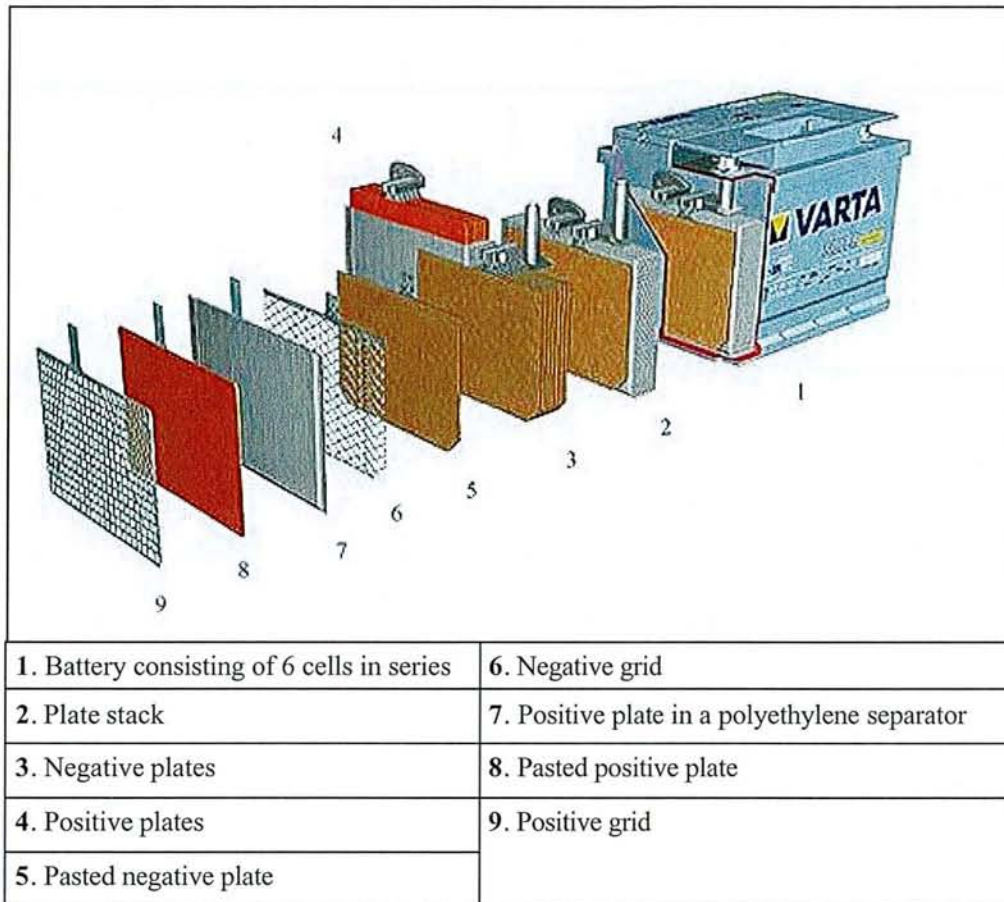


Figure 12: Schematic representation of a flooded lead-acid battery [19]

The electrodes consist of pasted grids and in order to hinder the formation of short circuits, a separator is placed between the positive and the negative electrode. The separator must have the following properties:

- Electronic isolation,
- Ionic conduction by providing open pores that are filled with acid. The ionic transfer between both electrodes has to be easy so that the internal resistance of the lead-acid cell is minimised,
- Stability in 40 wt% sulphuric acid,
- High porosity for a good ionic conductivity but also a low displacement of acid.

There are modified designs of the typical prismatic flooded cells. While the negative electrode always has a Fauré design, the positive electrodes can have two designs other than the usual pasted grid, the most encountered one being the tubular plate. In this variation, the positive electrode is a connection of kind of tubes consisting of a lead spine surrounded with positive active material and contained in a gauntlet.

Figure 13 shows what a tubular plate looks like. This design allows the contention of the positive active material in a tight envelope and is characterised by a prolonged cycling life.

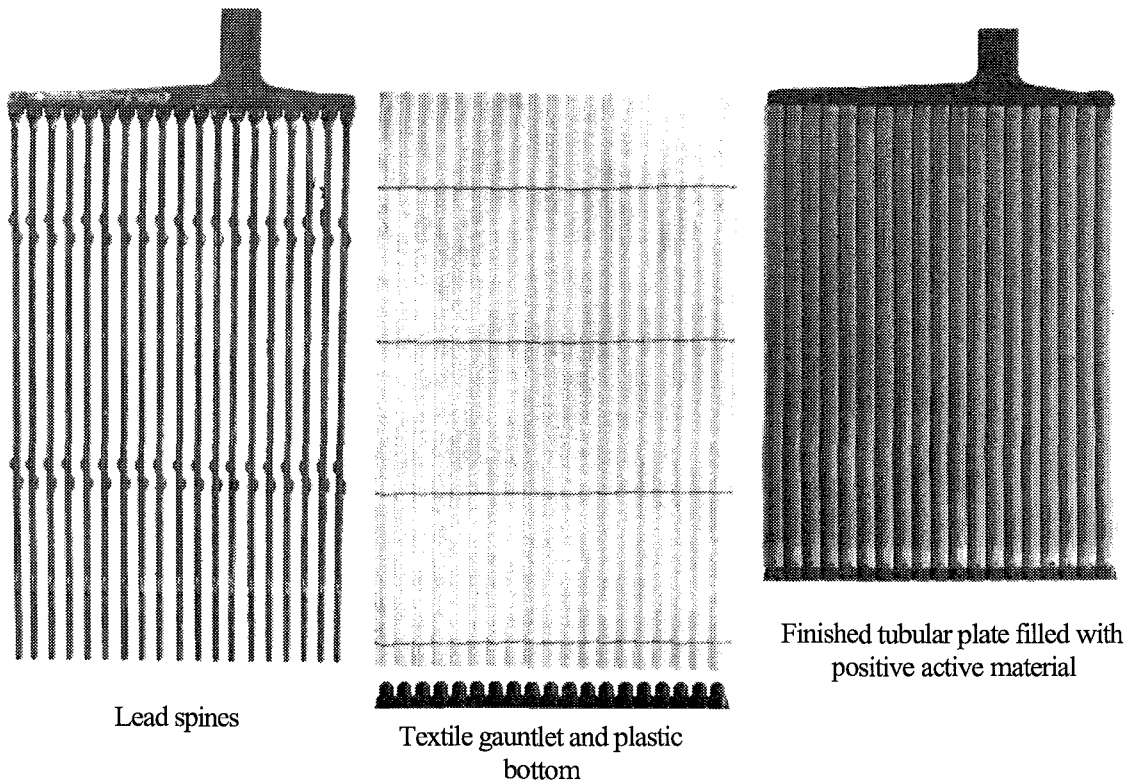
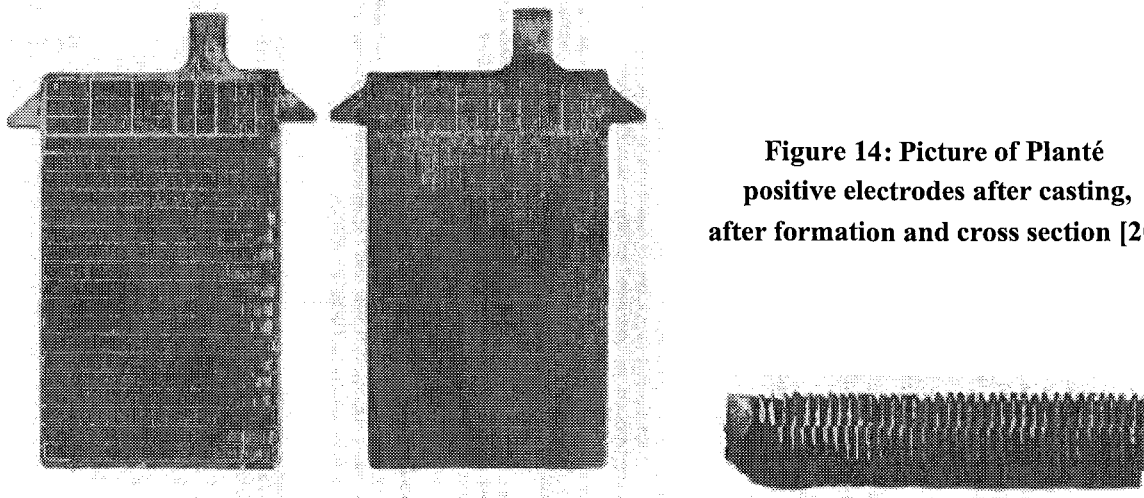


Figure 13: Picture of a tubular plate and its components [20]

The last variant of the positive electrode for flooded battery is the Planté design. "The Planté version of positive plates is made from a casting of pure lead that has numerous thin vertical grooves, strengthened by a series of horizontal cross-ribs, in order to increase the surface area. The active material (PbO_2) is formed electrochemically from the lead itself by carrying out a series of charge/discharge cycles" [21].



The flooded lead-acid battery needs a periodical maintenance by refilling water that has escaped as a result of the electrolysis of water from the electrolyte (self discharge or overcharge reactions). Additionally, a flooded battery is not tight because openings for the water filling are provided and since it contains liquid electrolyte, the battery cannot be tilted or used top side down for security reasons but also because the electrolyte supply of the electrodes would be modified. Furthermore, spilling of the

electrolyte and escaping of acid aerosols happen especially during overcharge and create a very corrosive atmosphere around the battery leading to corrosion of the terminals and possibly also of the surrounding metal parts (wires etc...).

1.5.2 VRLA battery

Since every market is moving towards more security and less maintenance, it was necessary to develop a new product that would overcome the drawbacks of the flooded design of lead-acid batteries quoted above. The first step for this development was the immobilisation of the electrolyte by addition of silicon dioxide to make a spill proof battery.

The result of the development towards a closed battery is the valve regulated lead-acid battery (VRLA battery). Why valve regulated? Because a fully closed battery design, as is for example existing for the nickel/cadmium system, is not possible. Namely, as was shown in section 1.4.2, secondary reactions are inherent for the lead-acid battery:

- On the positive electrode, oxygen evolution and grid corrosion happen,
- On the negative electrode, hydrogen evolution takes place.

In a VRLA battery, the electrolyte is immobilised and also starved so that some voids are present that allow the oxygen produced on the positive plate to reach the surface of the negative plate. At the rest potential of the negative plate, and even more at its charge potential, oxygen is reduced to water and this reduction is the thermodynamically most favoured one. As long as oxygen is present and as long as a free lead surface is provided, the oxygen reduction takes place in priority. That way, the electrolyte loss (or more precisely, the water loss) is avoided. A precise description of the processes involved in the oxygen cycle and of its limitation is given in section 6.

But even if the oxygen cycle is fully efficient, the unavoidable secondary reactions that are grid corrosion and hydrogen evolution happen. Even more, in the case of a fully efficient oxygen cycle, the current balance imposes that the corrosion current on the positive electrode equals the oxygen reduction current on the negative electrode during overcharge or float charge (see section 6 for more details).

As a result of the hydrogen production, an overpressure would build up in a closed design, leading to possible damages. For that reason, in order to allow the release of the hydrogen, the VRLA battery is provided with a valve. This valve has on opening pressure in the range of some hundred Pascal overpressure (i.e. ≈ 10 kPa).

The summary of the reactions that can be encountered in a VRLA battery is presented in Figure 15.

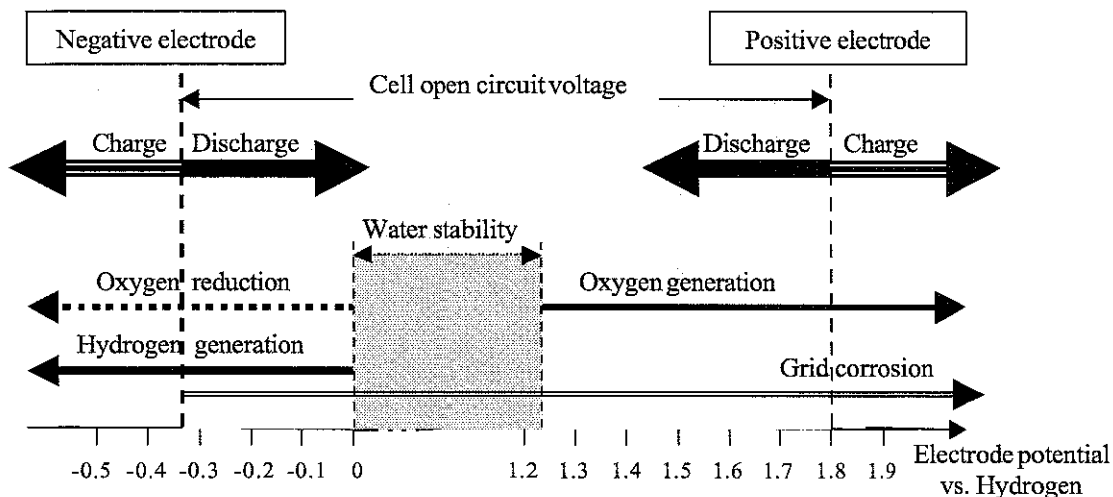


Figure 15: Reactions in a valve regulated lead-acid battery [22]

There are two techniques for immobilising the electrolyte in a VRLA battery. One can either adsorb it in a separator consisting of glass fibres that retain the electrolyte by capillary forces, or form a gel that fixes the electrolyte by mixing silica dioxide with the electrolyte. A better description of the two immobilisation/separation systems is made in section 3.2.

The transfer of oxygen in a gas is about 10^4 times faster than in a liquid [23]. Therefore, in a system with immobilised electrolyte, in order to get the required oxygen transfer, some free room in the pores of the separator or in the gel is necessary. Thus, additionally to the characteristics cited above for the separators of the flooded design, an AGM separator for VRLA application has to have a large surface for adsorption and a high fine porosity. For the gel system, additionally to the gel, a separator of high thin porosity provides electrical isolation and at the same time, good oxygen transfer.

In the same way as for the flooded design, the VRLA battery exists in a prismatic design with either pasted grids as positive electrode or with tubular positive plates. Another variation of the VRLA battery is the spiral wound design as presented in Figure 16. This is the design that is currently in development or already proposed by many producers. The basic idea of the spiral wound design is the utilisation of grid alloys with high lead content in order to get the best corrosion resistance and no negative electrode poisoning (see section 4). But pure lead grids have low mechanical properties. Therefore, the spiral wound design is used for providing a mechanical stabilisation of the plate stacks.

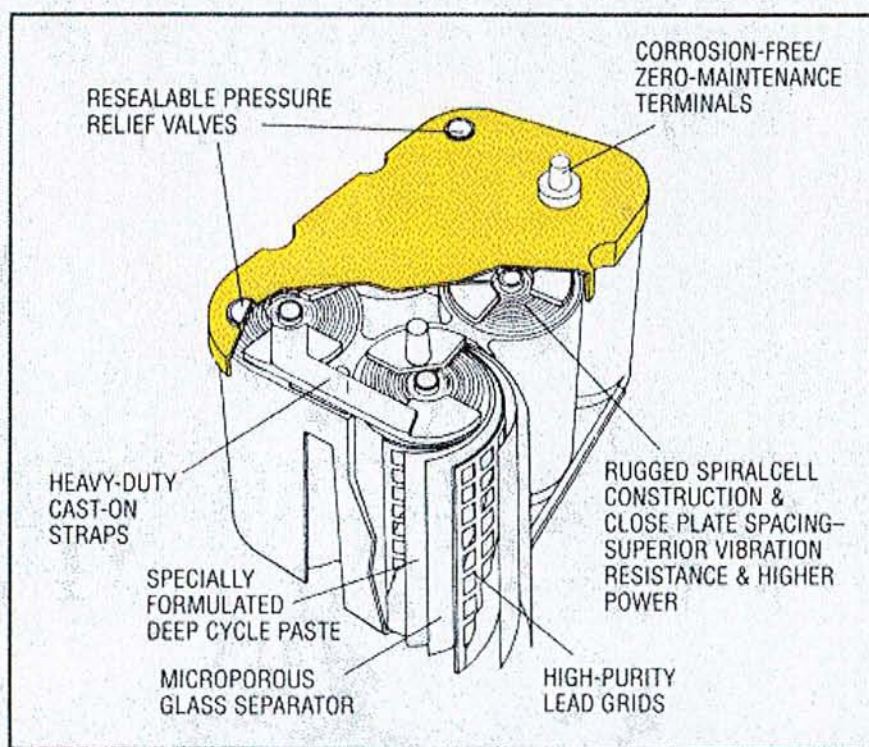


Figure 16: VRLA battery in spiral wound design. Yellow Top by Optima

1.5.3 Bipolar lead-acid battery

A very attractive solution to overcome the problem of the limited power of the lead-acid battery is to reduce drastically the internal resistance by using a bipolar design. In a bipolar battery, the inter-cell wall makes the connection between two cells and acts as a current collector and mechanical support for the

positive electrode of the first cell and the negative electrode of the second cell. A schematic representation of the bipolar design comparatively to a monopolar design is presented in Figure 17.

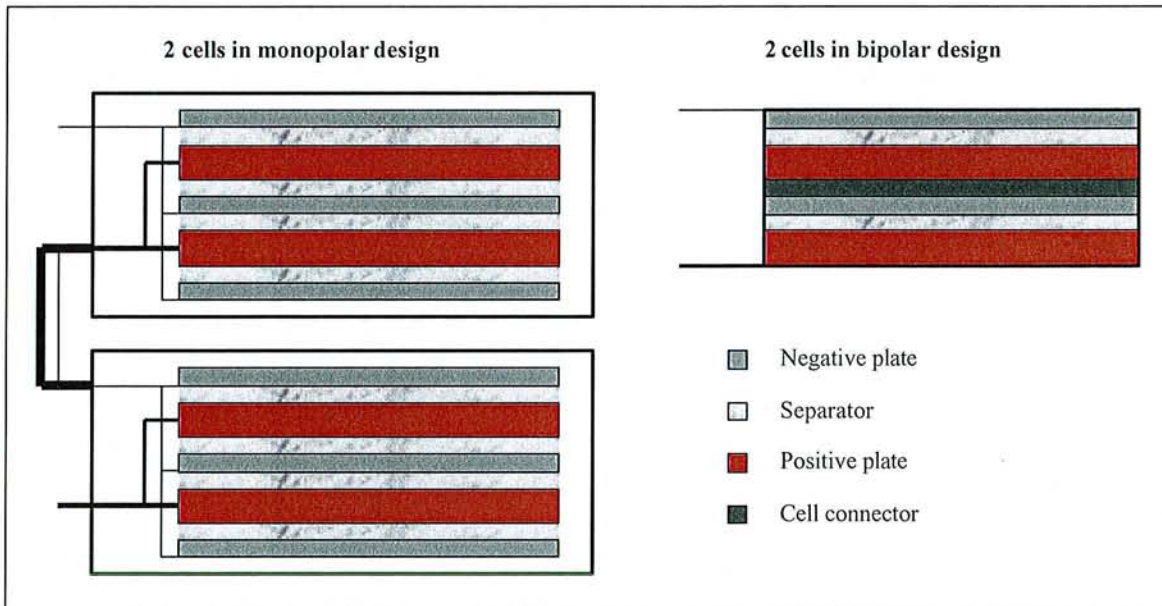


Figure 17: Two cells in monopolar and in bipolar design.

The problem of the bipolar plate is that the active material carrier is in the same time the current collector and has to be electronically conductive but ionically isolating. Additionally, the material of the bipolar plate must be resistant against corrosion in an environment of concentrated sulphuric acid and high anodic potentials on the positive side. Noble metals cannot be used because they present too low hydrogen and oxygen overpotentials and they are expensive. Therefore, only corrosion resistant lead alloys are suitable and in this case the life of the cell is limited by the corrosion rate of the alloy and the thickness of the plate. More sophisticated materials could also be used (like conductive polymers) but they are expensive. A “side by side bipolar design” could overcome the problem of the bipolar plate material. In this design, the connection between the positive and the negative electrode is realised by a common edge of the current collector.

In her paper of 1994 [8], Bullock reviews the state of the art of the bipolar design as well as the advantages and limitations that are associated with the bipolar technology. These advantages and drawbacks are summarised in Table 2.

Advantages	Drawbacks and limitation
<ul style="list-style-type: none"> • High power (less passive parts, low internal resistance) • Homogeneous voltage and current distribution • High voltage design easy to build 	<ul style="list-style-type: none"> • Low capacity (one positive one negative plate per cell and thin films) • Higher rate of side reactions (more current collector surface) • Increased heat effects in the stack • Difficulty to find a stable substrate material

Table 2: Advantages, drawbacks and limitations of the bipolar design for the lead-acid battery.

Prototypes of bipolar lead-acid batteries were realised by Arias Research Associates, Inc. and Bipolar Technologies, Inc. [24] and the development of the bipolar design reached the commercial ripeness for e.g. Electrosource HORIZON [25]. But the realisation of a bipolar battery is a technological challenge that no battery manufacturer was able to meet until now for a large scale production.

1.5.4 Different designs of lead-acid batteries

Table 3 shows the most commonly encountered lead-acid battery designs. Principally, for all different designs, the flooded or the valve-regulated variant is possible. But in fact, some designs are only produced in one or the other variant.

No bipolar lead-acid battery has currently reached the level of development that would allow a commercialisation. This is the reason why the bipolar design is not present in Table 3. But principally, flooded as well as VRLA batteries could be produced in bipolar design and both the pasted or the Planté technology would be suitable for the bipolar plate production.

Positive electrode	Grid/pasted			Spines/Tubular		Thin film/Pasted	Planté
	Spiral	Prismatic		Prismatic			
Usual design	Spiral	Prismatic		Prismatic		Spiral	Prismatic
Usual type	VRLA AGM	VRLA Gel/AGM	Flooded	VRLA Gel/AGM	Flooded	VRLA AGM	Flooded

Table 3: Different usual designs of the lead-acid battery

1.6 Life limiting factors

The cycling life of lead-acid batteries, in their flooded or valve regulated version, can be limited by many processes [21] and [26]. The major life limiting factors are listed in this section.

1.6.1 Drying out

This is the result of overcharge or self-discharge. In flooded batteries, drying out happens only if maintenance is not carefully carried out. The electrolyte level decreases and only the lower part of the electrodes participate to the charge and discharge. In such a case, a concomitant increase of the acid concentration takes place.

In VRLA batteries, this failure mode is more critical. It "is mostly connected with a too severe charging regime, often in combination with high cell temperature" [26].

Another factor influencing greatly the water loss of the battery is the so-called poisoning. It happens when a metal, on which hydrogen evolution happens at a lower overpotential than on lead, deposits on the negative plate. Or when a metal on which oxygen evolution happens at a lower overpotential than on lead is present on the positive plate.

In the case of the "negative electrode plating", the poisoning happens e.g. when the concerned metal dissolves from the positive grid and is reduced on the negative. This metal can be present in the positive grid as an alloying agent for lead. In that case, it gives desired mechanical properties to the alloy (as is the case for antimony). The "poisoning metal" can also be present in the alloy or in the paste if the raw materials are of low purity. This could happen when recycled lead is used and this problem of poisoning could be a limiting factor for the use of recycled lead as a primary material for lead-acid batteries.

The poisoning metal can also be present as an impurity in the sulphuric acid or in the water as well as in other components.

1.6.2 Short circuits

When a contact builds up between a positive and a negative electrode, the current flows through the short circuit and is lost for the user outside of the battery. A self-discharge of the accumulator takes place and also a warming of the spot where the short circuit happens. Such a short circuit can form through the separator, either by puncture or by formation of conducting bridges in the pores of the separator. Therefore, the separation system used is of great importance regarding this failure mode.

The short circuit can also build up around the separator with help of shed material or across the corrosion product from the top lead (see illustration of top lead corrosion in section 4)

1.6.3 Sulphation

This name designates the process of irreversible formation of large lead sulphate crystals on both electrodes. Sulphation happens preferentially when a battery is left in a state of too low state of charge (SOC) for a long time. Because big lead sulphates minimise their surface energy in comparison to smaller crystals and are thermodynamically more stable, lead sulphates undergo a dissolution/precipitation mechanism during rest periods. As a result, small lead sulphate crystals dissolve and big lead sulphates grow. When the battery is discharged, sulphuric acid is consumed and the density of the electrolyte decreases (see Equation 1). Since the solubility of lead sulphate is depending on the sulphate concentration of the electrolyte, the lower the electrolyte density, the higher the solubility of lead sulphate. Consequently, at low SOC of the battery, the dissolution/precipitation is easier.

Lead sulphate is an insulator and its discharge happens through a dissolution/precipitation mechanism. The formation of big lead sulphates causes a decrease of the specific lead sulphate surface and thus a decrease of the dissolution kinetic in the following charge as well as an increase of the diffusion path between the dissolution sites on the lead sulphate crystals and the precipitation sites on the lead electrode [27]. That way, the lead sulphate crystals are not totally converted to either lead or lead dioxide. Additionally, they cover a part of the electrodes and passivate the active material that lies under them. Both the active material that is stored in the crystals and the active material that lie under them are lost for the electrochemical processes, thus leading to a reduced capacity of the accumulator. This sulphation is a phenomenon that concerns both the positive and the negative electrodes. It happens on the whole surface of the electrodes. High temperatures, low current deep discharges and rest periods in a discharged state favour this homogeneous sulphation.

1.6.4 Thermal runaway

This failure mode is specific for the valve regulated design and more particularly, it concerns the VRLA batteries in which the oxygen cycle is very efficient. In fact, the oxygen production is catalysed by an increase in temperature. In parallel, the oxygen reduction on the negative plate is an exothermic reaction. That way, in designs where the oxygen transfer between both electrodes is easy and where the temperature is not managed, a process of "catalyse of the oxygen production by the oxygen reduction" happens (see reference [28]). If the heat exchange with the surrounding medium is insufficient, a dramatic increase of the temperature happens, leading to damages in the battery.

1.6.5 Stratification

The sulphuric acid is an active material in the battery. It is consumed during discharge and produced during charge. Since the sulphuric acid is denser, when coming out of the pores during charge, it tends to fall under the effect of gravity. This is the process of *stratification* in which the electrolyte on the bottom of a cell tends to be more concentrated than on the top. It is a process where diffusion and gravity fight against each other but with repeated cycling, gravity dominates.

In such a case, the current flow in the cell becomes inhomogeneous. Namely, the Nernst equation shows that the potential is depending on the concentration of the electrolyte. As an approximation, the value generally accepted for the rest potential of a cell depending on the density (d) of the acid expressed in g/cm^3 is:

$$E_0 = 0.84 + d \quad [16]$$

With the resistance of the current collector being very low, when current flows in the cell, it tends to flow preferentially in the places of low potential. It means that the top of the cell suffering stratification is preferentially charged while the bottom is still in a discharged state. This leads to a sulphation of the bottom of the electrodes.

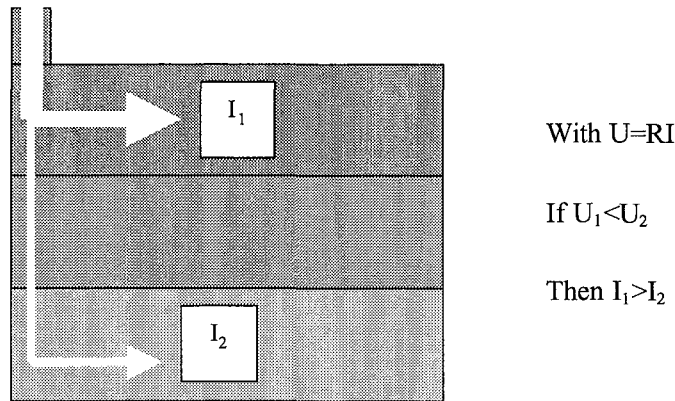


Figure 18: Schematic representation of the current flow in a stratified cell

Additionally, during charge and overcharge, because of the voltage repartition, small exchange currents flow between the top and the bottom of the plate that have the same consequence of sulphating the bottom of the plates.

When a battery where the electrolyte is in a liquid form is overcharged, the gas formed at the end of charge allows convection movements of the electrolyte that mixes up. For this reason, flooded batteries need a certain amount of overcharge. Otherwise, they will suffer stratification and therefore, inhomogeneous sulphate passivation while in the systems where the electrolyte is strongly immobilised, the stratification of the acid is hindered.

The process of "stratified sulphation" can also be associated with the natural repartition of the current in a conductor. Due to the resistance of the conductor, the charge current at the top of the electrodes is higher than at the bottom [29]. Therefore, a "natural sulphate stratification" of the batteries must be expected that is not present if the positive and negative poles are in opposite direction or if there is a top-bottom contact.

1.6.6 Failure of the positive electrode

1.6.6.1 Corrosion

"The corrosion of the positive grid represents a restriction of the lead-acid battery that finally limits the useful life, if no other reasons cause failure before"[16]. As a consequence, a well-designed battery should always fail because of corrosion. But this corrosion is not allowed to be premature and in order to delay it, corrosion resistant alloys have been developed. In the case of VRLA batteries, the hydrogen evolution and the corrosion rate are in balance and unavoidable. The consequences of positive grid corrosion are a loss of mechanical stability of the plate, a loss of conductivity of the current collector and a grid growth that can lead to short circuits around the edges of the separators.

1.6.6.2 Premature failure modes for the positive plate

If the failure mode is not the corrosion or if corrosion happens too early in the battery life, we are in presence of a premature failure of the positive electrode. Voss [30] proposed the very useful hierarchy of the premature positive electrode failure modes shown in Figure 19.

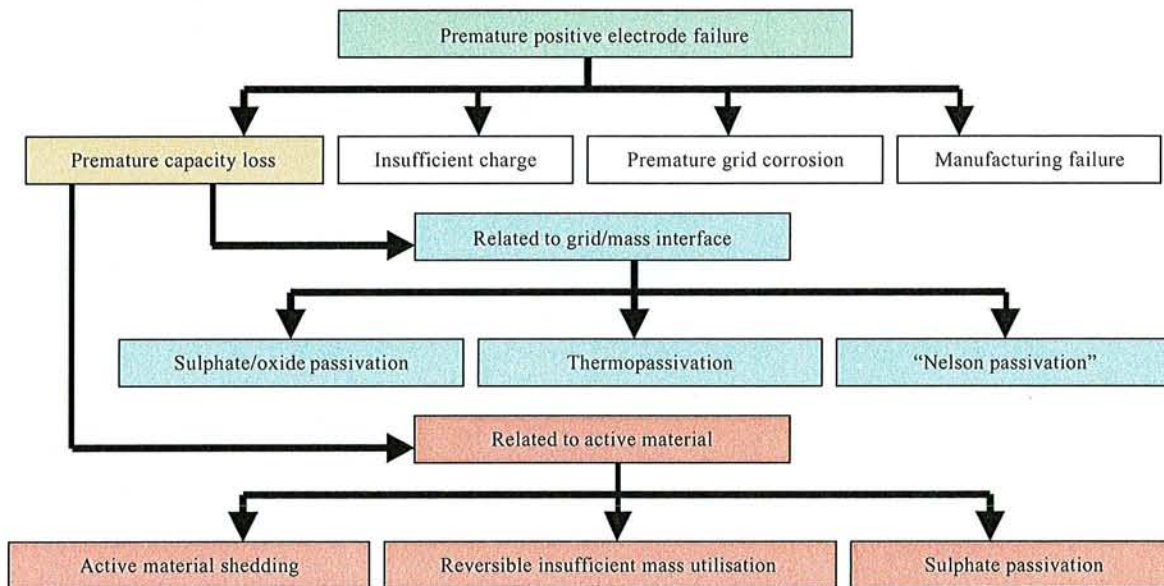


Figure 19: Premature positive electrode failure modes[30]

The premature capacity loss (PCL) of the positive plate is the most encountered failure mode for both flooded and VRLA batteries. The PCL was imputed by different authors either to the shedding of the positive active material, or to a loss in the electrochemical activity of the positive active material (PAM) due to the increased amount of electrochemically inactive material [31] or to a loss of conductivity of the PAM. It was proved by the use of a model that the conductivity decrease of the positive active material is the actual reason for the capacity loss of the positive plate [32]. Later on, this process was called the conductivity limited capacity loss [33]. The region of reduced conductivity can be the interface between the grid and the active material and in this case, the loss of capacity happens early in the cycling life. This phenomenon was called PCL1 [34]. When the region of reduced conductivity is the bulk of the positive active material itself, the capacity loss process happens more gradually and is called PCL2. The following lines describe shortly the processes summarised in Figure 19.

- *Sulphate/oxide passivation*. Happens at the grid/PAM interface. It is the formation of a layer of reduced conductivity that consists of lead sulphate or lead monoxide. This can happen during rest and was described in section 1.4.2. as rest corrosion
- *Thermopassivation*. This concerns the formation of a passivation layer at the interface between the grid and the positive active material that is due to the high temperature used for drying the plates. Namely, the high temperatures favour the solid state corrosion reaction as well as the reactions in the liquid phase. That way, full dried plates are covered with an insulating layer and thus inactive in further cycling [35].
- *Nelson Passivation*. This effect concerns only the positive grids consisting of pure lead. An α -PbO₂ layer builds up due to the absence of corrodable grain boundaries and acts as a resistor since it cuts off much of the positive active mass during discharge but if the discharge is pursued to lower voltages than usual, the normal positive active mass utilisation can be observed [36].

- *Active material shedding.* This is the phenomenon by which some active material is leaving the bulk and either falling on the bottom of the cell (mudding in flooded cells) or penetrating in the large pores of the separators (as can be the case for large porosity AGM in VRLA cells). This phenomenon happens after the particles lost mechanic contact with the rest of the active material (CLCL) and is strongly influenced by the oxygen formation in which oxygen bubbles push the particles that lost contact out of the matrix. Shedding happens at the end of charge [17] and the material from the sludge consists of almost pure lead dioxide [37].
- *Sulphate passivation.* It is either the homogeneous sulphation (section 1.6.3) or the inhomogeneous sulphate passivation associated with stratification (section 1.6.5)

1.6.7 Failure of the negative electrode

With the progress made on the positive electrode, negative plate failure is proved to be now the main failure mode of the VRLA battery [26]. Just in the same way as for the positive electrode, one can draw a figure of the different premature negative electrode failure modes (Figure 20).

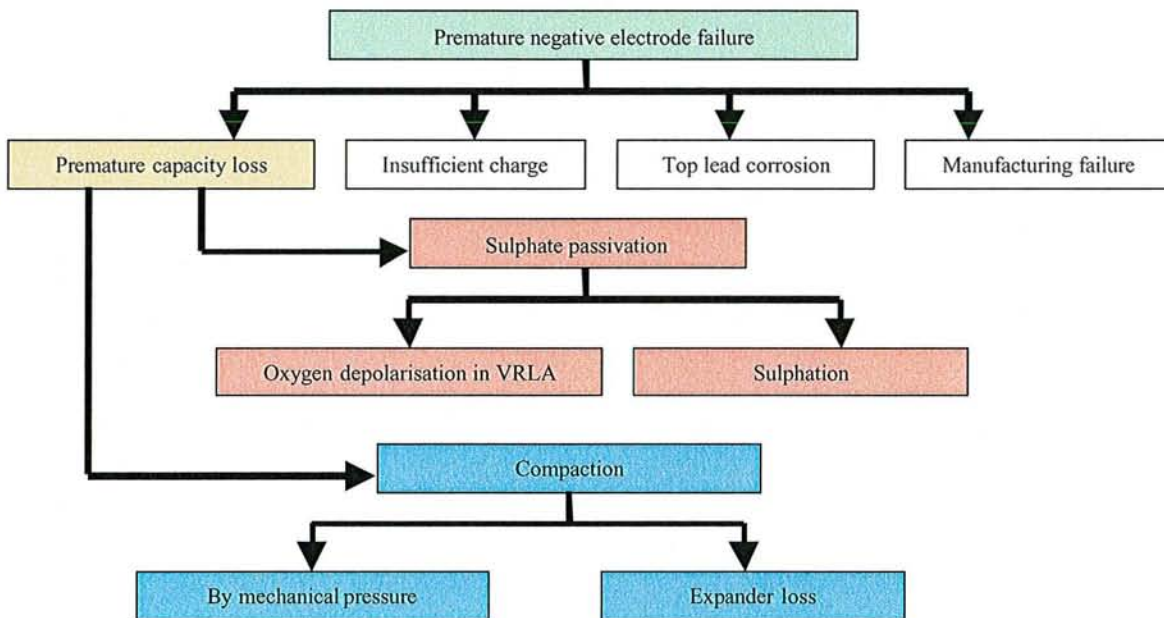


Figure 20: Premature negative electrode failure modes

- *Top lead corrosion.* This type of corrosion only concerns the VRLA batteries [16] and can lead to a rupture of the negative grid/top bar connection [26]. The corrosion reaction is the discharge reaction of the lead electrode. It starts in principle at the equilibrium potential of the lead electrode and happens only if the potential is more positive than the equilibrium potential. In flooded batteries, during rest or float charge, concentrate sulphuric acid is always in contact with the lead and the potential of the negative electrode stays low. But an increase of the electrode potential happens in VRLA batteries in areas where oxygen reduction occurs, producing water and leading to a depolarisation of the concerned area. Subsequently the pH of these areas increases. Because the conductivity of the thin electrolyte film leading to the concerned areas is reduced (increased pH), an additional voltage drop occurs that keeps these areas in a discharged state, not allowing for the reduction of the formed sulphates.
- *Sulphate passivation by oxygen depolarisation.* This sulphation of the negative electrode happens only in the VRLA batteries and is related to the basic principle of the VRLA battery, namely the

oxygen cycle. When oxygen reaches the negative electrode, it is reduced. During charge, the current that flows in the oxygen reduction is lost for the charge reaction. If the oxygen transfer from the positive plate to the negative is too easy, the very efficient oxygen cycle can lead to a chronic insufficient recharge of the negative electrode [38]. Additionally, if the VRLA battery is untight, oxygen from the outside comes in contact with the negative plate and reacts with the lead to form lead sulphate. This leads also to a sulphate passivation of the negative electrode.

- *Compaction.* The loss of porosity of the negative electrode with increasing cycling number is a well-known phenomenon both in flooded and valve regulated lead-acid battery designs. This loss of porosity decreases the specific surface of the negative active material and therefore, the number of available reaction sites is decreasing. Subsequently, the negative material utilisation decreases. There are two processes by which the negative material loses its porosity.

The first one is chemical. It is the leakage of the additives that are adsorbed at the negative plate surface and promote the formation of the spongy structure of lead by disturbing the growth of the lead crystals. These additives called expander, were discovered as rubber separators supplanted the cellulose separators. One then discovered that this replacement had a bad effect on the cycling life. The reason for that was the absence of the lignin coming from the cellulose separator. After that, expanders were added to the negative plate. But the expanders progressively dissolve in the solution and leave the negative plate. And since they are mostly of organic nature, in contact with the positive plate, they are oxidised to e.g. carbon dioxide and leave the battery. Thus the restoration of the spongy structure of the negative plate during charge is not possible any more.

The second reason for compaction is of mechanical nature (see section 3.6.1). Namely, the fact of applying a mechanical pressure on the positive plate of the battery proved to increase its performance and the battery assembly nowadays is very tight. As a result, a progressive compaction of the soft negative active material occurs.

1.7 Different ways for the improvement of the lead-acid battery

One general drawback of the lead-acid system is that the electrolyte is an active material. The sulphate ions SO_4^{2-} take part to the reactions and must move to the reaction place and their big size hinders a quick movement. By opposition, in the concurring systems like the lithium systems or the nickel systems, the ions that have to move during charge and discharge are very small and thus very mobile. In the alkaline systems, OH^- and H^+ are available in a sufficient amount from the water. In the lithium systems, the lithium ions intercalated during discharge in the positive electrode are delivered as the discharge product at the negative electrode ($\text{Li} \Rightarrow \text{Li}^+$). Therefore, the conductivity of the electrolyte is almost unchanged in alkaline and lithium systems. Their quantity of ions and the number of diffusion paths do not have to be oversized. While in the lead-acid system, the conductivity of the electrolyte decreases during discharge and thus, the power capability. Therefore, electrolyte must be present in excess in the lead-acid battery.

In order to improve the performance of the lead-acid battery, in particular for assuring to the lead-acid battery a place in the market of electric vehicles, both its life and its energy density have to be improved. While the life limiting factors were listed in the former section, Figure 21 shows where efforts have to be made in order to increase the specific energy of the lead-acid battery [39].

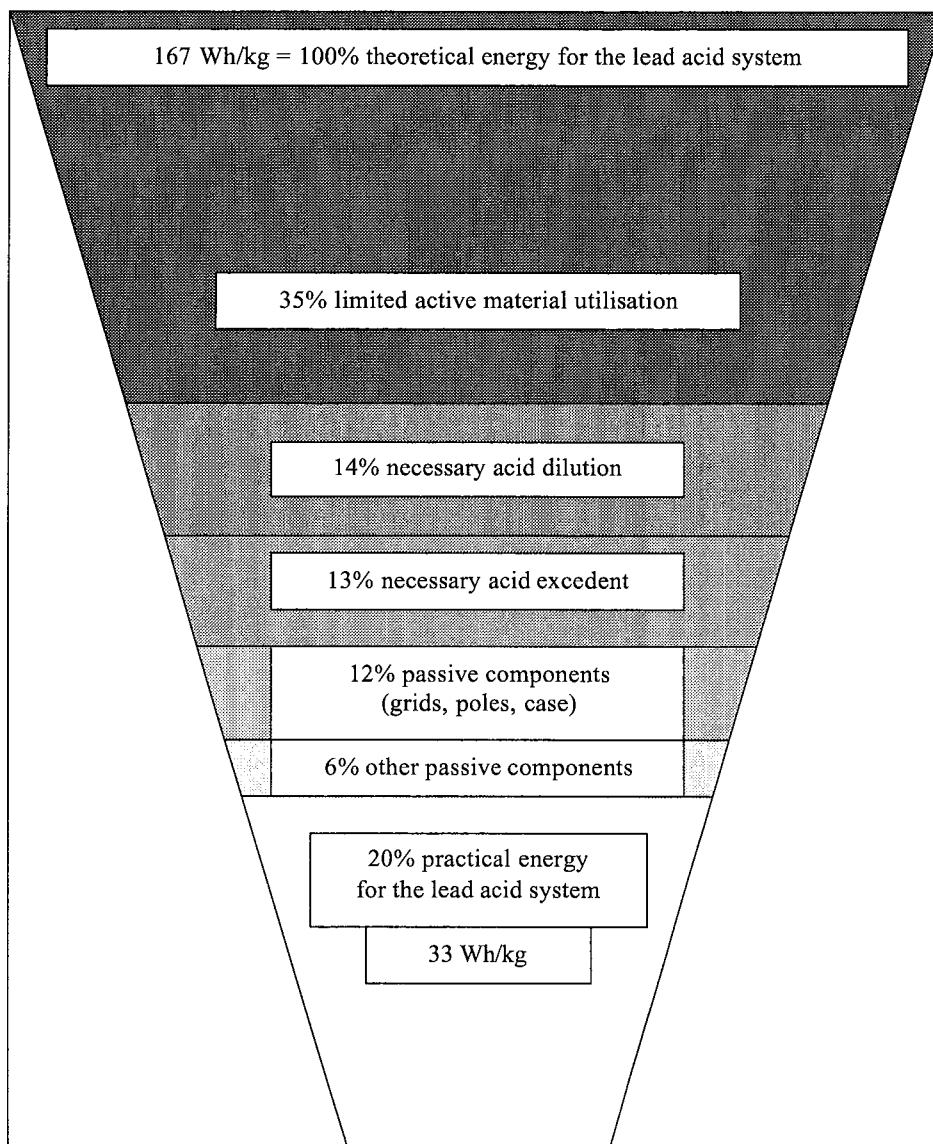


Figure 21: Specific energy loss in a flooded the lead-acid battery at high discharge rate (about 1h)

The highest cost in energy is related to the low active mass utilisation, to the electrolyte excess and to the passive components. In the following lines, we will summarise which parameters can be influenced in order to improve these two points and to overcome failure, focusing on the electric vehicle applications.

1.7.1 Design

- **VRLA design.** These batteries have less excess electrolyte and a tighter assembly and therefore a higher specific energy. The additional weight due to the separation/immobilisation system does not compensate this gain in specific energy
- **Strong immobilisation of the electrolyte.** Such a design allows no stratification and associated inhomogeneous sulphate passivation.
- **Thin plates.** The active material utilisation depends on the distance from the active material to the current collector. An illustration of this phenomenon is made in Figure 22.

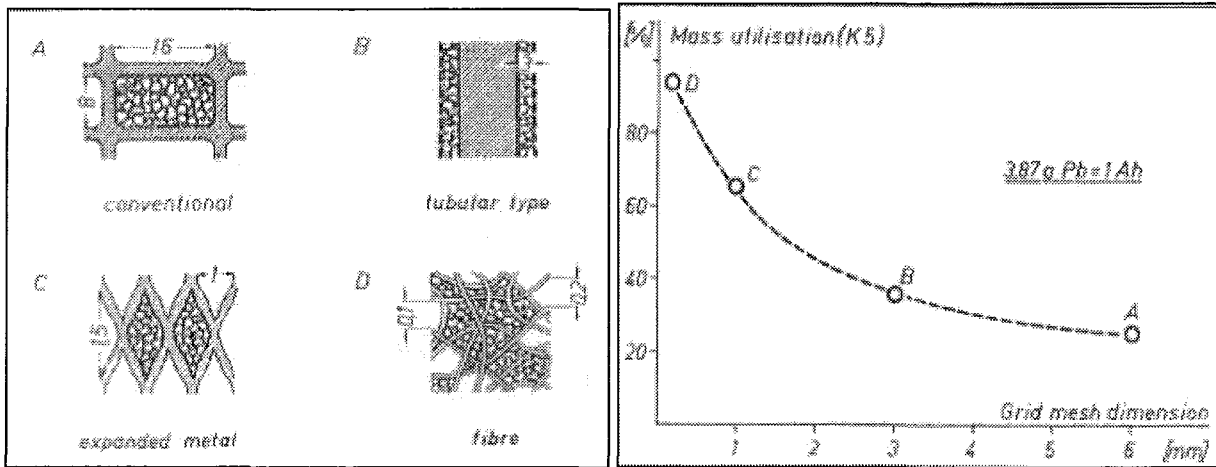


Figure 22: Active material utilisation depending on average distance to the current collector [40]

A thin plate design allows a higher active material utilisation and less passive parts. The thin plate design is possible in a prismatic or a spiral wound form but the distance between the electrodes is reduced and that way, the risk of short circuits formation increases. Additionally, a thin plate is less resistant against corrosion.

- **Mechanical pressure.** It is claimed to improve the performance of the battery when applied on the plate stack. For the application of mechanical pressure to be durable, a separator with adequate mechanical properties is required.
- **Oxygen cycle.** While a very efficient oxygen cycle may decrease the water loss, a too efficient oxygen cycle may lead to thermal runaway and to a chronic insufficient recharge of the negative plate. Thus, the oxygen recombination process has to be clearly understood and a compromise between water loss and thermal runaway must be found. The oxygen cycle can be influenced by the design of the battery, in first line by the immobilisation system used (gelled batteries are known to recombine less than the AGM designs) and by the saturation of the separator in electrolyte, i.e. the amount of paths that are left free for the oxygen transfer from the beginning of life of the battery.
- **Separator.** The choice of the separation system is very important since it determines the short circuit formation, the oxygen transfer as described above, and the mechanical pressure. Additionally, the choice of the separator and the immobilisation system influence the characteristics of liquid drainage and acid stratification in the battery.

In this work, especially these design factors are addressed.

1.7.2 Composition and characteristics of the active materials

The elaboration process of a Fauré type plate for a lead-acid battery is summarised in Figure 23

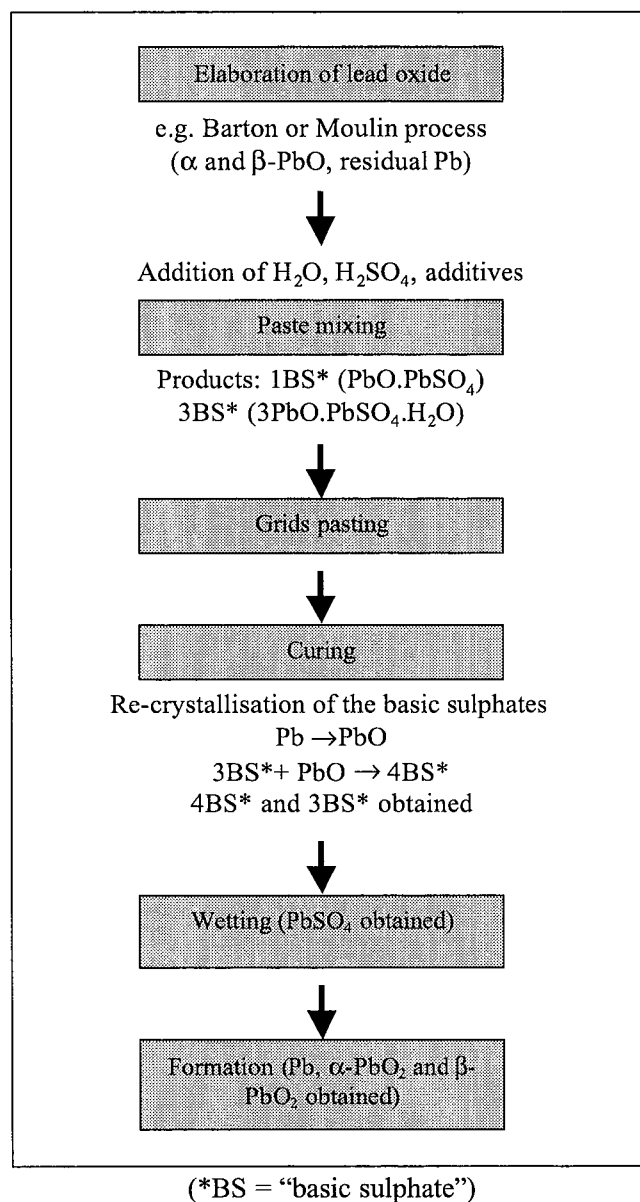


Figure 23: Elaboration process of the plates for a lead-acid battery [41]

1.7.2.1 Composition variation

The composition of the paste prior to formation influences the characteristics of the final active material. Some of the characteristics of the active material that can be modified are listed below

- *Composition of the positive and negative active materials.* The electrodes are sensitive to the composition of the original paste prior to formation (i.e. previous to the first original charge). It is commonly accepted that electrodes with $3\text{PbO} \cdot \text{PbSO}_4$ (3BS) show better capacity while electrodes with $4\text{PbO} \cdot \text{PbSO}_4$ (4BS) show better cycling life. Laruelle et al. [42] observed that the electrodes show better performances if the paste consists of $4\text{PbO} \cdot \text{PbSO}_4$ (4BS). Even more, they showed that the shape of the 4BS is influencing the future performance of the positive plate (crystals with a needle shape lead to a better positive active material utilisation).
- *Porosity.* The density and porosity of the active material have a dramatic effect on the performance of a battery. An active material with high porosity will deliver more capacity in the beginning of cycling because its specific surface is larger but it will also fail earlier than a paste of lower porosity. This earlier failure results in the fact that the porosity increases with cycling to a point where the

conductivity is affected and this point is reached later for pastes of lower initial porosity. Changing the amount of sulphuric acid and water that are added to the paste can vary these characteristics of porosity and density.

- *Additives.* Almost all possible materials have been added to the lead-acid battery in order to improve the performance of the battery. The patents concerning additives are reviewed in [43]. The additives can be sorted depending of their mode of addition to the lead-acid battery, i.e. either in the active material or in the electrolyte. Or they can be sorted on the base of their mode of action.
 - *Stabilising the active material mechanically.* Polymer fibres are commonly added to the positive paste for a mechanical stabilisation of it.
 - *Influencing the solubility of the lead sulphate.* The problem of sulphation at low SOC could be overcome by decreasing the solubility of the lead sulphate [44]. Since this solubility is depending on the sulphate ions concentration in the electrolyte, the addition of sulphate salts to the electrolyte could modify the size of the lead sulphate crystals. For deep cycling application, e.g. NaSO_4 is added to the electrolyte in order to increase the SO_4^- concentration and thus the electrolyte conductivity at low SOC.
 - *Influencing the crystallisation of lead sulphate.* For example, barium sulphate has crystal parameters that are similar to the one of lead sulphate. Therefore, barium sulphate is added in the negative paste because it acts as a germ for the lead sulphate crystals and lead to a fine precipitation of the sulphates.
 - *Influencing the crystal growth of the lead dioxide.* For example, phosphoric acid adsorbs on the positive plate and modifies the crystal growth of the lead dioxide, thus hindering the premature capacity loss (both PCL1 and PCL2)
 - *Influencing the crystal growth of lead.* These additives are the so-called expanders that are adsorbed on the lead surface and disturb the growth of the lead crystals so that it has a spongy structure.

This work will only focus on one aspect of the active material composition: it is the addition of small amounts of phosphoric acid in the electrolyte(section 5).

1.7.2.2 Process variation

The process of curing and formation of the paste is very important for controlling its composition. It is beyond the frame of this work to deal with the modification of these processes.

1.8 Conclusion about possible improvements of the lead-acid battery

The lead-acid battery is a much complex system with many interactions that are not all well understood yet. Improving one characteristic of the system may deteriorate another. Therefore, compromises have to be permanently accepted. And because some improvements are incompatible, the market of the lead-acid battery tends more and more to a specialisation. For example, batteries for PV application do not need a high specific energy by opposition to the ones for EV applications, the battery for UPS in a hospital needs a higher reliability than the one for other applications.

The announced objective of this work was the improvement of the lead-acid battery, in particular of the VRLA design for electric vehicle applications. The different ways followed in order to get an improvement were the application of mechanical pressure and the utilisation of an additive to the electrolyte. In parallel, the effect of the mechanical pressure on corrosion was studied. And since for applying a mechanical pressure, a new kind of separator was used, the particular effect of this separator on the oxygen cycle was also investigated.

Conclusion sur les généralités concernant la batterie au plomb

Dans ce chapitre, le fonctionnement du système électrochimique $\text{Pb}/\text{H}_2\text{SO}_4/\text{PbO}_2$ a été décrit en termes de thermodynamique et de cinétique et les facteurs qui affectent sa durée de vie et ses performances ont été détaillés.

Il en ressort que le système plomb/acide est fort complexe et de nombreuses interactions ne sont pas encore parfaitement comprises. L'amélioration d'une caractéristique risquant de porter préjudice à une autre, des compromis doivent être en permanence acceptés dans la réalisation d'une batterie au plomb. Et puisque certaines caractéristiques sont incompatibles avec d'autres, le marché de l'accumulateur au plomb tend à se spécialiser. Ainsi, par exemple une batterie destinée à une application photovoltaïque aura une faible énergie massique par comparaison avec une batterie pour un véhicule électrique.

Le but déclaré de cette thèse était l'amélioration de la batterie plomb/acide, en particulier dans sa version fermée, pour l'utilisation dans les véhicules électriques. Par conséquent, puisqu'un utilisateur va rouler avec son véhicule jusqu'à ce que son "réservoir" soit vide, il était nécessaire de développer un accumulateur ayant de bonnes performances en cyclage profond.

La principale direction suivie pour l'amélioration du système plomb/acide fut l'application d'une pression mécanique par le biais d'un nouveau système de séparation dont on a étudié l'effet sur les performances et la durée de vie de batteries ainsi que sur la corrosion.

La seconde modification apportée au système fut l'utilisation, en interaction avec le nouveau séparateur et la pression mécanique, d'un additif à l'électrolyte dont les conséquences sur les performances et l'état de la batterie en fin de vie furent observées. En dernier lieu, l'influence du nouveau séparateur sur le cycle de l'oxygène a été déterminée.

2 Experimental techniques

The standard techniques of observation and analyse used all along the work will be explained in the present section. Other techniques were implemented for the purpose of the work and are not listed here. For better readability, they will be detailed in the paragraph in which the results concerning the technique are also reported.

2.1 Electrical tests on batteries

Cells and batteries were first evaluated concerning their performance under dynamic conditions and under cyclic conditions with different separation systems and electrolyte formulations. All tests were performed at ZSW (Ulm, Germany). They characterise the electric performance of a battery. Delivering electrical energy is finally the actual purpose of a battery, therefore the electrical tests are the ones that unquestionably assess the relevance of an improvement.

2.1.1 Internal resistance, open circuit voltage, peak power (IROCVP test)

The IROCVP test is taken from the EV battery test procedure adopted by the EUCAR traction battery group [45]. This test was performed on a Digatron bench that can provide 300A at 300V. The software associated with the bench is a Digatron BTS 600.

Within this single test, the internal resistance, the open circuit voltage and the peak power can be determined versus depth of discharge. First, the open circuit voltage is determined after a rest period of 3 hours (or less if the voltage changes less than 1% over a 30 minutes period). Then, a high discharge current of 300A is applied during 30s followed by a rest period of 3 minutes. The high current internal resistance is deduced from the ratio between the voltage difference (rest voltage after 3 minutes U_2 – voltage at the end of the high current discharge peak U_1) and the discharge current. At the end of the 3 minutes rest, the battery is discharged at the C/5 rate until 10% of the rated capacity is removed. The same procedure is then applied again at the next state of charge (SOC). When the discharge voltage limit is reached during the high current discharge or during the following C/5 discharge, the test is completed. A short recapitulation of the procedure is made for one SOC in Figure 24.

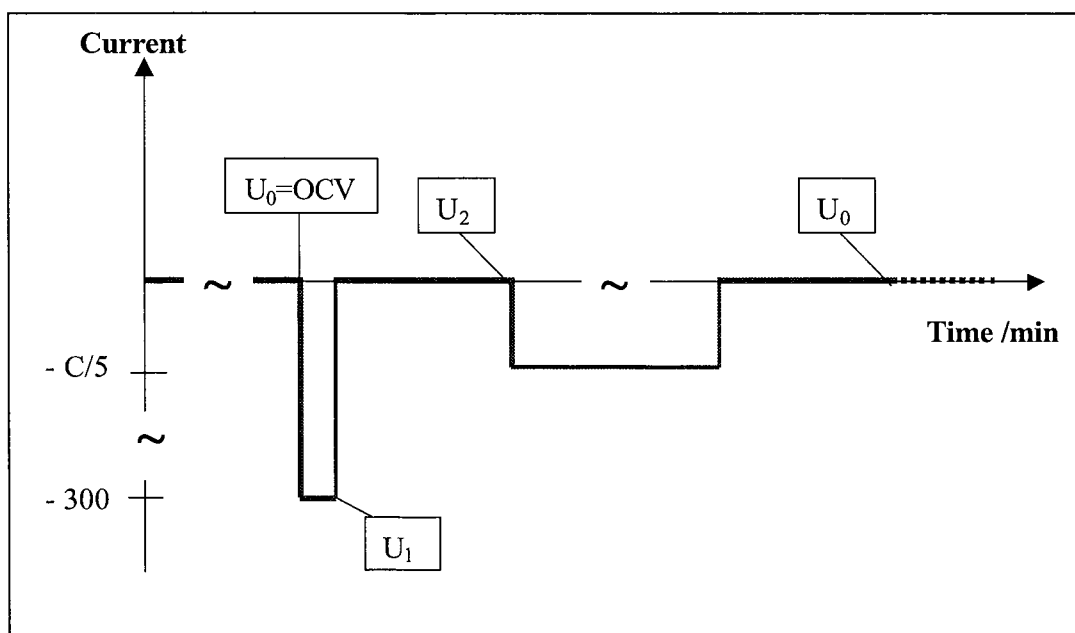


Figure 24: Summary of the IROCVP procedure for one SOC

2.1.2 ECE 15 test

The ECE 15 test was performed on the same bench as the IROCV test. The ECE 15 procedure is also taken from the EV battery test procedure of the Traction Battery Working Group [46]. The ECE 15 test is derived from the speed-time profile (standardised for vehicles with combustion engines). It gives the specific power-time profile necessary to drive a reference electric vehicle (the parameter for this vehicle are fixed) and include regenerative braking periods. Since the power profile is given in specific values (W/kg), the test can be applied to any battery with any size and weight

The driving cycle simulates urban and suburban driving periods. The sequence of 4 urban /1 suburban driving periods is repeated until the battery is not able to deliver a required minimum power. The driving range is determined by reading equivalence tables that correlate the driving time and regime (urban or suburban) with the simulated driving distance.

2.1.3 Cycling test

A cycling test was performed on both cells and batteries with different separation systems and initial external mechanical pressure. For the cells, the test took place on a 6-channels bench with 20A and 5V. For the batteries, a channel with 160A, 150V was used. In both cases, the benches were of the mark Digatron and controlled with the BTS 600 software edited by Digatron. The cycling regime of the cells was adapted as we gained experience in the new separation system. The changes in the cycling regime in these special cases are reviewed later in this work (see section . In this section, only the optimum charging regime for each cell/battery is described (Table 4)

	Type of charge	Charging current	Charging voltage	Time	I phase
AJS and gel cells	IU	14.4A	2.45V	10h	
AGM cells	IU	14.4A	2.4V	10h	
AJS and gel batteries	IUI	14.4A	2.45V	8h	400mA, 2h
AGM batteries	IUI	14.4A	2.4V	8h	400mA, 2h

Table 4: Typical charging regime of the batteries and cells

The discharge takes always place at a constant current of either 20 A (about C/2 rate until 1.6V) or 9.6 A (C/5 rate until 1.75V).

2.1.4 Dependence of the discharge capacity on the discharge current

With the same charging regime as in the cycling test, a determination of the cell/battery capacity depending on the discharge current was carried out. The equipment used was a Digatron channel controlled by a PC with the BTS 600 software. The tests were carried out at room temperature and at -18°C.

2.2 Preparation of polished sections

At the end of the cycling test, cross sections from the electrodes were made. The samples were embedded in epoxy resin. Then the sections were polished with SiC paper with the granulometry 80, 320, 500, 1200, 2400 and 4000. The final polish was made on a special tissue with a suspension of colloidal SiO₂.

2.3 Microscopy

2.3.1 Optical microscopy

The first observation of the polished sections was made with help of an optical microscope OLYMPUS of the type VANOX AHMT. Pictures of the sections were taken with help of a digital camera connected to a personal computer using the software Analysis.

2.3.2 Scanning Electron Microscopy

SEM pictures were taken at ZSW (scanning electron microscope DSM 940, ZEISS and at the University Nancy (SEM HITACHI 2500, back scattered primary electrons micrographs).

2.3.3 Microprobe Analysis

This technique provides very accurate quantitative analyses. The equipment at the University Nancy was produced by CAMECA and was of the type CAMEBAX SX 50.

2.4 Chemical analysis and electrolyte concentration

The electrolyte concentration is determined by titration. The content of lead, lead dioxide and lead sulphate in active materials from lead-acid batteries were measured with help of chemical analysis. This proved to be the most accurate technique. The procedures are standardised at ZSW in the frame of the ISO 9000 certification [47] [48] [49] and [50].

2.5 Porosimetry

The porosity of some samples of active materials was determined by Sonnenschein by weighting the samples in a dry state and then in a wet state after diving of the sample in water. The porosity is deduced from the difference between the weight in the dry state and the weight in the wet state.

2.6 X-ray diffraction

The identification by XRD of the compounds present in a powder obtained after cycling a lead grid in a solution of sulphuric acid and phosphoric acid (see section 2.8.3) was performed using a D 5000 produced by SIEMENS.

2.7 IR pictures

In order to find out regions in which high temperatures develop, IR pictures of cells were taken that were meant to show either where short circuit occurred or where preferential oxygen recombination happens. The camera was of the type PM525 of AGEMA FliR Systems and the pictures were visualised and corrected using the software IR-win.

2.8 Electrochemical techniques

2.8.1 Cyclic voltammetry

A GS PV3 variator associated with a GS PS4 potentiostat were used. They were connected to a Servogor X-Y recording device that could be controlled using the Servosoft software. The reference electrode was a Hg/Hg₂SO₄/H₂SO₄ electrode with sulphuric acid at the same concentration as the electrolyte used. The potential of such an electrode against the hydrogen electrode is depending on the concentration of the sulphuric acid (0.616V electrode potential versus SHE in standard conditions [51]). The working electrode consisted of a pure lead cylinder embedded Teflon. The surface of 0.785 cm² was polished

before each measurement until a granulometry of 1200. The counter electrode was a pure lead foil. A schematic representation of the set-up is given in Figure 25.

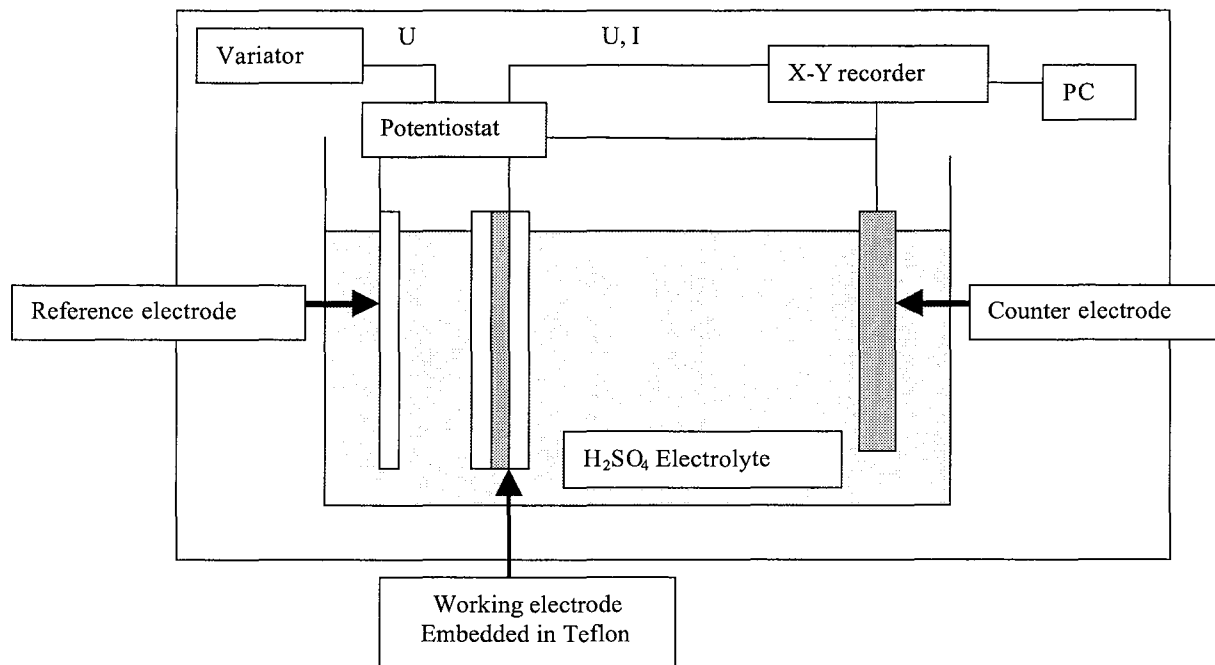
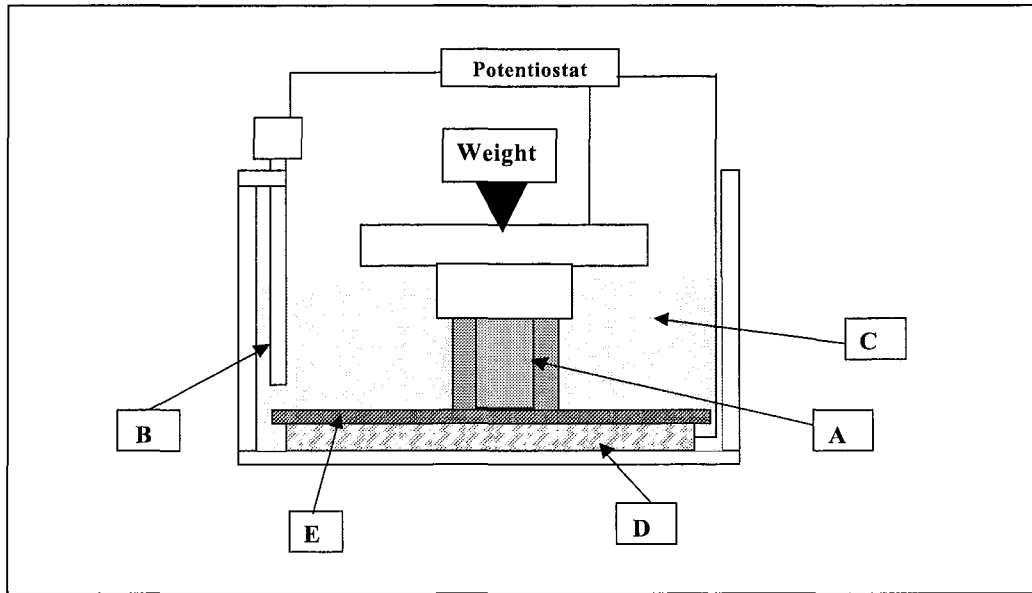


Figure 25: Set-up for the cyclic voltammetry

2.8.2 Potentiostatic corrosion measurement

In the potentiostatic corrosion measurements, the set-up was similar to the one used for the cyclic voltammetry but the variator was replaced by a frequency generator delivering a square signal between the reference electrode and the working electrode. The output between the working electrode and the counter electrode was recorded and the discharge capacity was calculated by integrating the discharge current over time. The set-up is schematically represented in Figure 26.

Figure 26: Schematic representation of the potentiostatic corrosion measurement setup.



- A: Pure lead rod in Teflon
 B: Reference electrode ($\text{Hg}/\text{Hg}_2\text{SO}_4/\text{H}_2\text{SO}_4$)
 C: Electrolyte of sulphuric acid ($d=1.28 \text{ g/cm}^3$)
 D: Counter electrode (pasted negative of 1 Ah)
 E: Separator AJS (thickness 1.45mm)

Figure 26: Principle scheme for the measurement of the effect of mechanical pressure on the corrosion behaviour of pure lead.

The corrosion regime consisted of cycles with 30 s charge at 1400 mV followed by 30s discharge at 900 mV (potentials noted versus mercury electrode).

2.8.3 Galvanostatic corrosion measurement

The test equipment consisted of the BEATE hardware ($\pm 12\text{V}$, 2.5 A) and the BASYTEC software. In this experiment, the cell potential was controlled and not the positive electrode potential. In order to minimise the variations of the negative electrode potential, the grid that acted as working electrode was inserted between two pasted negative electrodes. Their capacity is extremely large compared to the capacity of a bare grid. That way, it is certain that the negative electrode is always in a charged state and that its potential does not vary too much. In this measurement, the charge/discharge took place at constant current under end point voltage control.

3 Mechanical pressure application

3.1 Bibliography of “compression”

On his way to a battery with fast charge abilities, Alzieu [52] was the first to think about applying a mechanical pressure vertically to the plane of the electrodes of a prismatic cell in order to prevent the shedding of the positive active material. For this purpose, a multi-layer separator was used, what also was a première. In 1984 [53], Alzieu reports on compressed batteries loaded with a rapid charge regime. In the specified design, the compression/cycle life curve shows a maximum around 1 bar. At this pressure, the battery which reached 600 cycles uncompressed lasts for over 2000 cycles (cycles: 30 min IU charge, I at $3 \cdot C_5$, U at 2.65V, discharge at $(C/5)/1.7$ until the cell voltage reaches 1.5V). At higher pressure, the cells failed because the separators collapsed or because the separators design causes damages to the negative grid. In order to increase the cycle life more, Alzieu tried to prevent the shedding of the positive active material from the edges of the plates by melting the separators to form a kind of envelop around the positive electrode. At 0.75 bar compression, the battery performed up to 3000 cycles. Later on, the same team [54] separated the "heat effect" and the "expansion effect". These two effects lead to opposite expansion and contraction of the active materials during charge and discharge. The work of this team is the really first reference to an **active** application of mechanical pressure on the walls of a cell or battery.

E. J. Ritchie [43] made another early reference to the utilisation of external mechanical pressure. In 1980, he wrote that " A mechanical solution to the problem ...[of shedding positive material]... calls for sealing each positive plate in its own porous envelope, and using a tight assembly. Thus, when active material sheds, it will still be held in place and not be entirely lost from service".

It is important to differentiate the **active** mechanical pressure application from the **passive** contention of the active material that was already performed in some types of batteries.

From a wide point of view, one could say that the first "compression battery" was the first battery with tubular plates. Namely in this design, the active material is contained in a gauntlet and is therefore not allowed to expand in any direction. The first who had the idea of gauntlets was Boriolo in 1959 [55], but the first tubular design was produced even earlier (1910) with tubes of rubber material containing the lead spine and active material.

Secondly, another attempt to contain the positive active material was made with the development of the pocketing of the positive plate in a separator. That way, the positive active material is not allowed to shed easily from the positive grid and cause short circuits. Such a sealing of the electrodes in their porous envelope was made possible by the introduction of polyethylene separators around 1975. They are now the most widely used separators (70% of all automotive batteries world-wide [56]). But in fact, no real pressure is applied on the active material that way because the separators are not robust enough to constraint the active material expansion, only mudding is hindered.

A further paper concerning “active” compression was published in 1983 [57]. In a conventional AGM design, batteries compressed in a dry state at 20, 40, 100 and 300 kPa were cycled (discharge at 30°C for 3h with $1.25 \cdot I_5$, charge at 20°C for 5h with $0.9 \cdot I_5$). The cycle life was doubled by the increase of pressure from 0.2 to 0.4 bar. But a higher pressure did not lead to further improvement. The authors pointed out that the compression applied in a dry design decreased dramatically after the filling due to the shrinkage of the absorptive glass mat separators. They also measured that the force applied by the active material on the cell walls increases during discharge and decreases during charge.

In 1984, Chang showed the constraining of a plate stack to improve the cycling life but "with some sacrifice in capacity"[58]. In 1990 [37], the application of 14 kPa on a flooded battery with 5 mm glass frits as separators lead to a four times higher cycle life in comparison with a cell with electrodes hanging free in the electrolyte and in 1991, "A slight but equal pressure on the battery plates" was proved to increase cycling life [59]. One study also compared the cycle performance of AGM VRLA cells with the side walls of the container reinforced with metal frame or not [60]. The cell with a container that was allowed to freely deform under the associated effects of the cell stack expansion and of the temperature increase had a much shorter cycle life. In 1992, Paul Rüetschi reports on capacity measurements of electrodes prepared of α - or β lead dioxide [61] and points out the necessity of using "defined conditions of mechanical compression, which is essential for reproducible results". Therefore, he uses pellet electrodes with micro-fibre glass separators compressed to 40% of their initial thickness.

In 1994, J. Landfords [62] compares diverse separators and shows that, for a given compression design, the cycle life of the batteries depends much on the separator system used. While the uncompressed cells perform 90 cycles, those with 100 kPa last 750 to 1150 cycles depending on the separator used. The conclusion of Landfords is that every separator has its own specific optimal working pressure and some key points have to be taken into account for the choice of a separator:

- A high diffusion resistance of the separator increases grid corrosion
- A micro-porous separator close to the negative electrode would avoid dendrites growth
- The whole structure has to allow a good acid and oxygen transfer
- The separator close to the positive electrode has to have a structure with thin pores to avoid shedding of the positive active material.

Later on between 1995 and 1997, the research team of CSIRO (Commonwealth Scientific and Industrial Research Organisation, Division of Minerals, Melbourne, Australia) worked intensively on compression. Firstly [63], they found that the restraining of plate expansion maintains a high density of the positive active material in the battery. This density is the limiting factor in the cycle life of a battery, since the decrease in capacity becomes rapid once the material density falls under a critical value. 1996, Hollenkamp [33] used the fact that both compression and limitation of plate group expansion increase cycle life to explain premature capacity loss (PCL). What has previously been described as PCL is in fact a continuous process of conductivity limiting capacity loss (CLCL) related to preferential discharge, expansion of the PAM with subsequent increase of porosity and decrease of conductivity of the active material near to the current collector in the worst case (PCL 1). In the case of a more progressive capacity loss (PCL 2), the loss of conductivity is related to a redistribution of PAM from the region near the grid to the outside of the bulk.

Limitation of the electrode expansion and conservation of compression in the battery through the use of a separator having "spring" characteristics determine the rate at which porosity increases. In 1997, Hollenkamp and Newnham [64] found that the composition and characteristics of the PAM have a lower influence on the cycling life of a battery than the plate group compression. AGM separators have the drawback not to have the ideally required "spring" characteristics which means that the pressure in the battery is not lasting as long as battery life. It leads to a possible shedding of PAM as well as to a bad acid supply of the electrodes. CSIRO proposed several methods to allow compression to be maintained along the cycle life of AGM or gel batteries and a new design for a "compression-resistant" separator. This separator has no "spring characteristics" but can withstand up to 200 kPa pressure.

In 1995, Bashtavelova and Winsel [65] investigated the evolution of the force applied by a lead rod on the positive and negative paste during cycling. They found that during discharge, the force on the rod decreased and it increased during charge. They explained this surprising phenomenon by the fact that

“during discharge, the generated lead sulphate is deposited within the free-pore space without stretching of the PbO_2 network”.

Up to 1997, this literature study could be summarised as follows.

The most important result to point out is that for a given battery, any application of pressure on its plate group perpendicularly to the grid plane leads to a longer cycle life of the battery. This is due to a restriction of the possibility for positive active material expansion. The PAM keeps then the original low porosity and the associated high conductivity.

The separator design is becoming a critical point for the application of compression. In order to adapt to the expansions and contractions of the active material, separators have to show “spring characteristics”. The system of separation of the electrodes also has to maintain the initial compression during the whole battery life. A third point is that the optimum of compression to apply to a given battery depends on the separator used. And in the actual state of the art in the field of separators, no compression over 100 kPa could be applied to the battery because the separators crushed. In summary, a separator has to be developed that does neither shrink when wetted nor crush when compressed.

In 1997, the problem of “how to realise high compression” was not solved. It was difficult to put highly compressed plates stack in cases and strong case materials were then necessary.

As a last comment, one can point out that the mechanism by which the application of mechanical pressure improves the performance of lead-acid batteries was not comprehensively explained yet. In the same way, the evolution of the forces in the battery during cycling was a subject to controversy since the results of Takahashi and al. or Alzieu are in opposition with those of Bashtavelova et al.

Since 1998, the time at which the work for this thesis began, quite many teams have been working on “compression” for example in Australia, in Germany or in the Check Republic.

3.2 Electrolyte immobilisation/separation systems

3.2.1 *The complex influence of a passive part: the separator*

The importance of the separator has been increasing as the performance of the lead-acid batteries progressed and as the development of the VRLA battery proceeded. Namely, the requirements of immobilising the electrolyte and of leaving free gas channels for the transfer of the oxygen were added to the initial necessary features of separator, i.e. electronic isolation and ionic conductivity. Since then, the separator was not any more an inert part in the battery but more a participator. It has a strong influence on:

- *The performance of the battery.* The separator determines the internal resistance of the battery by fixing the distance between the electrodes as well as the electrolyte diffusion rate.
- *The life of the battery.* By influencing the rate of mechanical pressure that is kept on the stack, by determining short circuits will appear or not and by fixing the rate of oxygen transfer between both electrodes.
- *The manufacturing.* Different separation systems need different assembling and filling procedures and thus imply different costs.

As late as 1990 [66], the effect of the separator design on the discharge performance of a starved lead-acid cell was discussed concerning only its thickness, porosity and tortuosity, i.e. the mechanical properties of the separator were not of central interest.

Later on, due to the arising importance of pressure against the active mass (see section 3.1), the mechanical properties of the separator came under increased examination.

There are two types of VRLA batteries, with two different systems of immobilisation of the electrolyte. The first system for electrolyte immobilisation is a silica gel. The most used system is an adsorptive glass mat (AGM). Electrolyte soaks the AGM separator and is retained by capillary forces.

3.2.2 Gel

By using silica gel (SiO_2), a spill proof battery was designed as early as 1936 [67]. The Rulac cell produced in Sonnenberg was a sealed lead acid battery with a gelled electrolyte but no valve. One supposes that the hydrogen overpressure could be accommodated by hydrogen diffusion through the cell walls. The Rulac cell was the first to use the gel technology even if some authors report that the first spill proof battery basing on this technology was built in 1958 [16]. And already in 1965, “the only viable battery product appeared to be the Sonnenschein Dryfit battery, a gelled-acid product. It employed a soft rubber check valve...” [68]

When 5-8% pyrogenic silica is added to an electrolyte of dilute sulphuric acid, the molecules of electrolyte are fixed on the big surface area of SiO_2 (200 to 300 m^2/g) by Van der Waals forces and a gel with thixotropic properties is formed. In order to fix the distance between the electrodes and to hinder the formation of short circuits, a separator is used that has typically some 70% porosity and a mean pore size of 0.5 μm [72]. The separator has a typical backweb thickness of 0.3 mm and is ribbed in order to leave some free room between the plates. That way, the gel can fill the space between the plates and provide electrolyte homogeneously.

At the beginning of its life, a gel VRLA battery behaves more like a flooded battery: only a limited oxygen transfer is possible trough the fresh gel. After some cycles, some water has dried out and cracks have formed in the gel constituting a network of free channels for the oxygen transfer in the gas space. It means that the oxygen recombination efficiency is low at the beginning of life but increases with operating time. Table 5 summarises the advantages of using a gelled electrolyte VRLA battery.

Advantages	Drawbacks
No stratification or drainage	Difficult filling procedure
Good cycling stability	Higher internal resistance (lower peak power)
	Higher cost
	No mechanical pressure application possible via the gel
	Limited oxygen transfer in the beginning of life
	Heavy (low specific energy)

Table 5: Advantages and drawbacks of gel for VRLA batteries.

3.2.3 AGM

Originally, AGM is a mat of glass fibres. The first AGM battery basing on oxygen recombination (with spiral wound design and associated high compression) was produced in series in 1971 [68]. In the meantime, this type of separation system consisting of fibres retaining the electrolyte by capillary forces is called recombinant battery separation mat (RBSM) [69] and can consist of glass fibres of different diameter as well as some organic fibres.

In his paper of 1996, K. Peters describes the influence of compression (or more precisely, its absence) as a main factor in the limitation of the battery life in AGM VRLA batteries [13]. He also comments the

poor knowledge we had of the way the mechanical properties of the separator change during service. The limit of compression for AGM separators beyond which fibre breakage occurs is around 45% (i.e. by 55% of original thickness).

In 1997 [69] and [70], G. Zguris reports on the mechanical properties of recombinant battery separation mat (RBSM) separators, and particularly on the advantages of 100% micro-glass separators with fine fibres. The addition of fine fibres in a conventional adsorptive glass mat (AGM) allows for less compression loss at wetting, better resiliency, better puncture strength and better spring characteristics.

In 1998, K. McGregor et al. [71] publish a recapitulation of the effects of compression on the RBSM. These separators accept some crush during the first application of pressure in the dry state. Additionally, when wetted while under compression, the RBSM shrink. At least, separators after cycling show a similar spring constant but a much reduced initial thickness.

The different advantages and drawbacks of RBSM are summarised in Table 6.

Advantages	Drawbacks
Low cost	Electrolyte stratification and drainage (depending on the fine fibres content)
Good stability of glass in sulphuric acid	Shrinks when wetted
Easy filling process of the battery	Lower cycling performances
Easy oxygen transfer during the whole life (because high porosity and large pore size)	Risk of thermal runaway (if the oxygen transfer is too easy)
Low internal resistance (= good high power capability)	Crushes when compressed (depending on the fine fibres content)
	Large pores leading to easier short circuits
	Limitation in the mat thickness (thin mats difficult to handle)
	Optimum saturation level difficult to determine

Table 6: Advantages and drawbacks of AGM as separation system for VRLA batteries.

3.2.4 The new Acid Jellying Separator (AJS)

Both existing immobilisation/separation systems for VRLA batteries show advantages and drawbacks. They also have both poor mechanical properties and cannot withstand a mechanical pressure. RBSM separators are introduced in the plate stack in a dry state. They shrink when the electrolyte is filled and they crush if a mechanical pressure is applied on the plate stack. Concerning gel, the space between the plates is filled with it and if any mechanical pressure is applied on the stack, the gel creeps or flows and the separator can only apply pressure via its ribs.

In order to combine the advantages of both systems and additionally allow the durable application of mechanical pressure on the plate stack, a new immobilisation system has been developed by Daramic [72]. It is called Acid Jellying Separator (AJS) and is produced by extrusion of a mixture consisting of silica, polyethylene and oil, with subsequent extraction of the major part of the oil to generate the porosity of the separator. The result is a flexible homogeneous separator that can be easily handled. Produced for the first time in 1997 [73], AJS was first evaluated outside of the battery. Its mechanical properties as

well as the physico-chemical properties have been determined and are summarised in Figure 27 for a sample with 1.45mm thickness. The same figure shows a picture of the separator after use in a cell. Prints of the negative plate are visible on its surface. The separator of this specification was the standard AJS for our work and was the type used in all our tests if not mentioned otherwise.

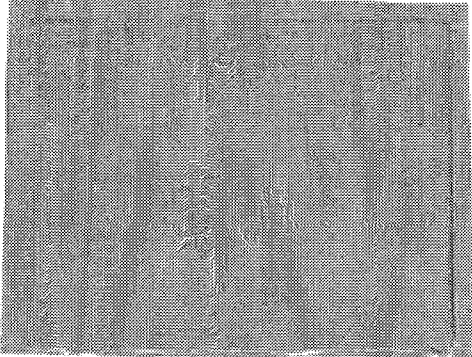
	Area weight	500 g/m ²
	Oil content	5%
	Porosity	81%
	Acid absorption (with and without vacuum)	1650 g/m ²
	Electrical resistance	136 mΩ.cm ²
	Deformation by acid wetting (isotrope)	1%
	Elongation (in machine direction)	116%
	Elongation (cross machine direction)	123%
	Tensile strength (isotrope)	0.7N/mm ²

Figure 27: Picture and properties of an AJS separator with 1.45 mm thickness

We can compare the general properties of AJS with those of the concurring systems.

In fact, the gel system is optimal for cycling application, allowing no stratification, but it is difficult to handle and it allows no application of mechanical pressure. The AGM system is easy to handle and leaves from the beginning free space for the oxygen transport but it has poor mechanical properties and is subject to stratification and drainage. AJS aims at combining the advantages of these two systems. Additionally, its good mechanical properties and small pore diameter should make it suitable for thin plate designs. Table 7 shows the properties of AJS in comparison with an AGM separator of standard specification, i.e. containing 25% fine fibres.

	AJS	AGM
<i>Thickness</i>	1.2 mm	1.85 mm (1 kPa)
<i>Electrical resistance</i>	110 mΩ.cm ²	68 mΩ.cm ²
<i>Acid absorption (1mm thickness)</i>	980 g/m ²	1100 g/m ²
<i>Porosity</i>	81 %	92 %
<i>Pore size</i>	0.2 μm	13 μm
<i>Elongation</i>	70 %	3- 4 %
<i>Thickness decrease (100 kPa)</i>	< 1 %	45 %
<i>Acid shrinkage</i>	+ 1 %	- 0.5 %
<i>Acid stratification</i>	very slow	6 times faster
<i>Drainage</i>	no drainage within 7 days	high drainage after 7 days

Table 7: Comparison of the properties of AGM and AJS

In Figure 28, the comparison is made between the mechanical properties of the standard AJS and a standard AGM with 25% fine fibres.

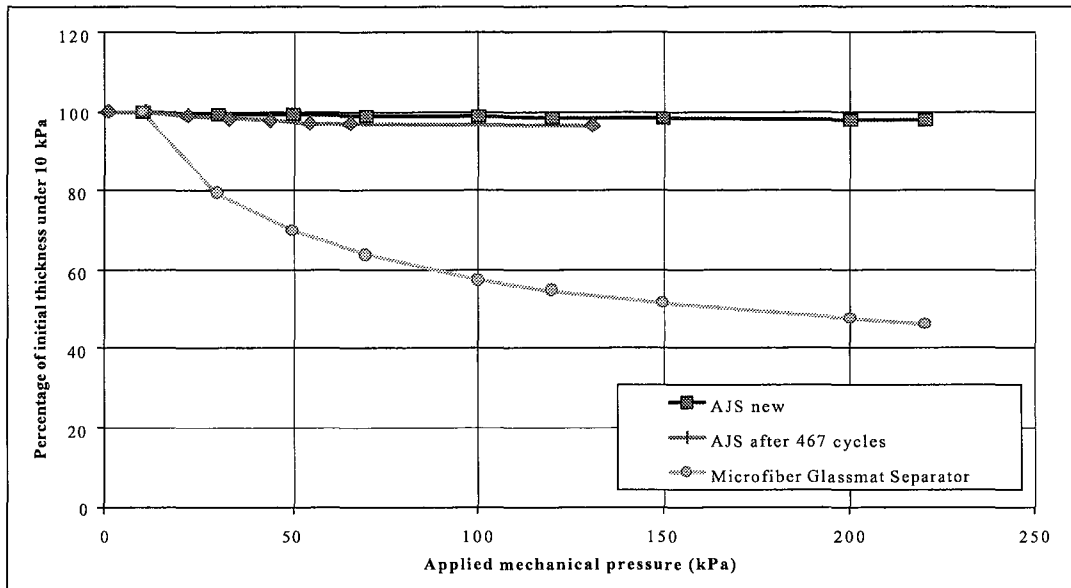


Figure 28: Relative deformation versus applied pressure for AJS and AGM

The optimum of mechanical pressure to be applied on a lead-acid cell is not clearly defined but values over 40 kPa and around 100 kPa are currently proposed.

At 100 kPa, while a typical micro-fibres glass mat has lost over 40% of its thickness, the AJS separator shrinks of only 1%: Furthermore, this mechanical stability proves to be retained over cycling. A separator that was inserted in a cell and underwent 467 cycles with full C/2 discharge is deformed of less than 3.5% when set under 100 kPa mechanical pressure.

3.2.5 More than compression

In the previous works dealing with the application of mechanical pressure on a plate stack, reference was always made to compression. Initially, with this appellation, the degree of compression of the AGM separator used was meant. But later on, “compression” meant “any application of mechanical pressure”. The word compression is only adapted in the case of a spring or when the material on which a pressure is applied shrinks. In fact, the target for the lead-acid battery is to apply a certain amount of mechanical pressure on the active material. Not the degree of thickness loss is important but the effective force that is applied on 1 cm² of surface of the electrode.

With the new AJS, it is not correct any more to speak about compression, with respect to its mechanical properties (see Figure 28). Therefore, in this work, we will not refer to compression but to External Mechanical Pressure Application (EMPA)

3.3 Performance improvement through EMPA

The application of external mechanical pressure on a cell should lead to an improvement of its performance and a new separation system seems to promise the possibility of durable application of mechanical pressure on the electrodes of a cell. In order to first find out if the new AJS separation system was suitable at all for VRLA batteries and for determining its performances in the lead-acid battery, cells then batteries were built with the new AJS separator as well as with the concurring separation systems. For comparison purpose, all cells and batteries had exactly the same design except for the separation

system. The target was firstly to prove the suitability of the AJS separator for VRLA application, secondly to see how it behaves with respect to the mechanical pressure.

3.3.1 Experimental conditions

All measurements were performed at room temperature, except the determination at low temperature of the capacity dependence on the discharge rate. The cells and batteries were submitted to two series of tests. The first one determines the parameters of the concerned cell/battery, i.e. for example its peak power, internal resistance, capacity versus discharge rate. The second is the cycling life test. The first test is necessary for a rapid characterisation of a battery and gives important results about its performance. The cycling life test costs a lot of time and money but delivers the only reliable data on the actual life of a battery.

3.3.1.1 Characteristics of the cells and batteries

The cells and batteries to which this work will refer, both in this section and in the next sections are described in Table 8, as well as the conditions of external mechanical pressure to which they are submitted.

Nature	Designation	Separation/electrolyte	IEMP**	Fixation of the EMP
cell	Gel	Darak 2000/gel + PA*	≈ 30 kPa	Thickness fixed at nominal thickness
cell	AGM	Standard AGM/ no PA	≈ 30 kPa	Thickness fixed at nominal thickness
cell	AJS 30 kPa	Standard AJS/ no PA	≈ 30 kPa	Thickness fixed after EMP adjustment
cell	AJS 60 kPa springs	Standard AJS/ no PA	≈ 60 kPa	EMP fixed through springs
cell	AJS 80 kPa	Standard AJS/ no PA	≈ 80 kPa	Thickness fixed after EMP adjustment
cell	AJS PA 30 kPa	Standard AJS/ + PA	≈ 30 kPa	Thickness fixed after EMP adjustment
cell	AJS PA 80 kPa	Standard AJS/ + PA	≈ 80 kPa	Thickness fixed after EMP adjustment
battery	AJS PA 80 kPa	Standard AJS/ + PA	≈ 80 kPa	Thickness fixed after EMP adjustment
battery	AJS PA springs	Standard AJS/ + PA	≈ 60 kPa	EMP fixed through springs
battery	AGM springs	Standard AGM/ no PA	≈ 60 kPa	EMP fixed through springs
battery	AGM free	Standard AGM/ no PA	-	-
battery	Gel	Darak 2000/gel + PA*	≈ 30 kPa	Thickness fixed at nominal value
battery	Gel free	Darak 2000/gel + PA	-	-

*PA = phosphoric acid

**IEMP = initial external mechanical pressure

Table 8: Conditions of the cells and batteries tested

The plates used in all our cells and batteries are issued from the production line of Sonnenschein in Buedingen,(Germany) and the cells/batteries were assembled by Sonnenschein. The plates were weighted before selection and only plates with the same weight were used for the cells and batteries built for this work. The separators inserted in the cells and batteries were provided by Daramic for the AJS and for the Darak 2000 while AGM was provided by H&V.

The following lines describe the detailed constituents of the cells. The batteries are built with the same plates number and the same design as the cells.

Gel cell

- Separator: Darak 2000, 153.5 mm*127.0 mm, thickness: 1.45 mm with glass mat, 10 separators / cell
- Negative plates: 6 negative dry charged plates/cell, 148 mm*123 mm, thickness = 1.90 mm
- Positive plates: 5 positive dry charged plates/cell, 148 mm*123 mm, thickness = 2.85 mm
- Electrolyte Sulphuric acid ($d= 1.30 \text{ g/cm}^3$)+silica with addition of phosphoric acid, 820 g/cell

The gel cell with addition of phosphoric acid has a design appropriate for EV application with a nominal capacity of 48 Ah (5 hours rate).

The plate groups are cast on strap. An U-shape fleece around the plate group was used to prevent short circuits around the edges of the plates. This fleece was not covering the external negative plates but only the sides of the stack as shown on the picture of Figure 29.

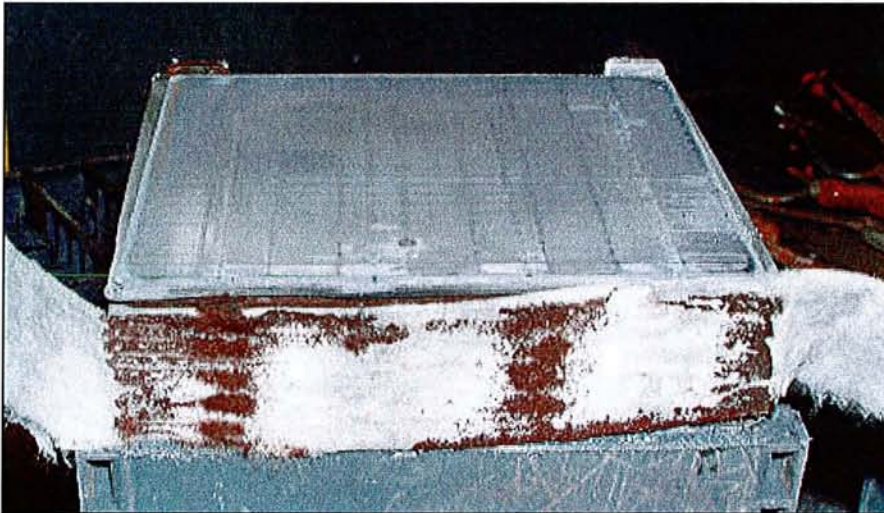


**Figure 29: Picture illustrating how the bottom fleece is placed in the gel and AJS cells and batteries.
(Here an AJS battery after some 650 cycle)**

AGM cell

- Plates: same type and number of plates as gel cells
- Separator: standard glass mat (Hollingsworth & Vose Co. Ltd) with 25% fine fibres, 156 mm *130 mm, thickness = 1.53 mm (20 kPa), separator of U shape around the positive plate.
- Electrolyte: Sulphuric acid ($d=1.30 \text{ g / cm}^3$) without addition of phosphoric acid, 589 g/cell

No additional U-shape fleece or bottom fleece was used.

AJS cell

- Plates: same type and number of plates as gel cells
- Separator: standard AJS, 160 mm*130 mm, thickness = 1.45 mm
- Electrolyte: Sulphuric acid ($d=1.30 \text{ g / cm}^3$) with/without addition of phosphoric acid (=PA).
637 g/cell without PA, 640 g/cell with PA

Bottom fleece is used only in the same way as for the Gel design

Special remark about the saturation in electrolyte of the cells and batteries.

The saturation of a VRLA cell is an important issue since it determines partially its ability to have an efficient oxygen cycle. But if a low saturation allows a good oxygen cycle and an associated smaller electrolyte loss, in the same time, a lack of electrolyte can decrease the performance of the cell.

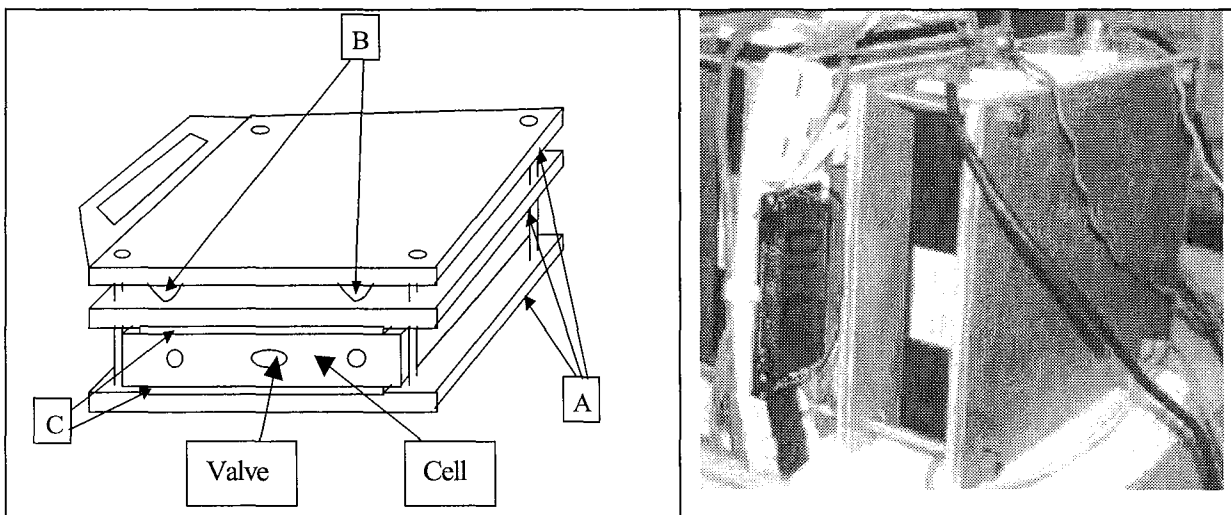
In the case of this work, the gel cells had an excess of electrolyte, the AJS cells were 100% saturated, it means that the excess electrolyte was removed. For the AGM cells, they were filled to 95% of the practical saturation. One may argue that the lower amount of electrolyte in the AGM cells is responsible for the lower performance of the AGM system. But all cells had a similar capacity at the begin of service and moreover, AGM batteries were built with a higher saturation but their performance decreased very rapidly compared to the other systems even if they were similar at the beginning of life.

The electrical tests were performed on cells and batteries with the same plate design, only the separation system and the amount and nature of the electrolyte did differ. This seemed to be the best solution for an objective comparison of the separation systems. It must be considered that the active material and plate design are optimised for the gel system, therefore, the direct comparison of the performance may not be the most relevant criterion since the optimum conditions for AJS and AGM may be different. But this work constitutes a first evaluation and must be considered as such. It delivers a lot of information and further optimisation are always possible.

The AJS cells and batteries showed no sensitivity towards electrolyte saturation provided more than 92% of the total porosity is filled. Under this value, a steep decrease of the capacity is observed. And the saturation can also be somewhat higher than 100% without any influence on the capacity.

3.3.1.2 Experimental arrangement

After having determined the characteristics of the new AJS separation system outside of the battery, it was necessary to test it in the lead-acid battery. And for getting simultaneous information on the electrical behaviour and on the development of forces in the cells and batteries, the experimental arrangement shown in Figure 30 was built.



A: Aluminium plates

B: Force sensors

C: Plastic spacers for the transmission of the force on the only electrodes surface

Figure 30: Principle scheme and picture of the realisation of an online mechanical pressure recording device.

The cells to be tested were inserted between the aluminium plates and the initial mechanical pressure was set with help of screws. That way, the thickness of the stack was fixed and kept constant for the whole cycling.

The principle of the set-up is easy: when no compressible parts are present in the cell, any force coming from the electrodes is transferred to the cell walls. The deformation of the case material is neglected and it is possible that way to measure the development of the force coming from the plate group or set from

outside on the plate group. The continuous observation of the force development is thus allowed even if the contributions of the positive and the negative plates cannot be differentiated.

For the cells whose mechanical pressure had to be kept constant and not the thickness, a design with springs was adopted as shown in Figure 31.

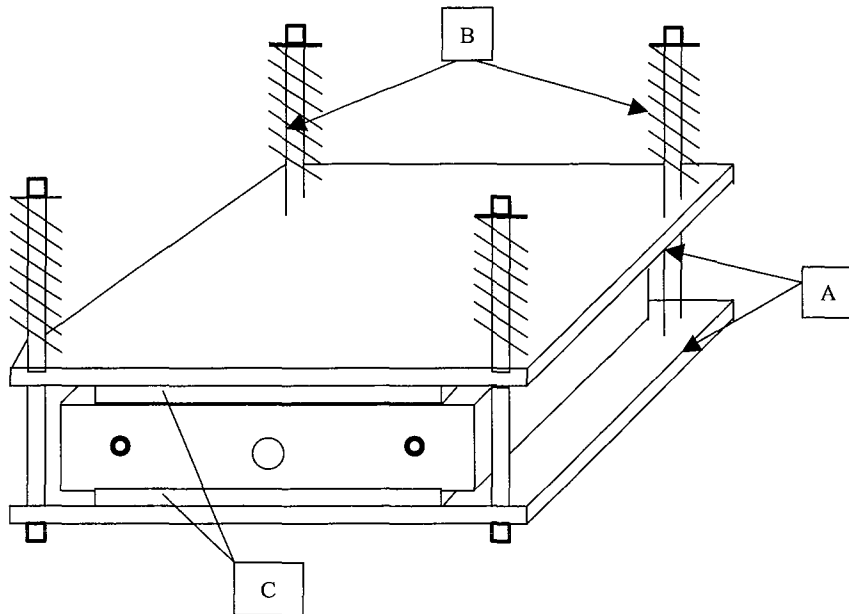


Figure 31: Design for the application of a constant mechanical pressure on a lead-acid cell.

A: Aluminium plates

B: Springs

C: Plastic spacer of the same surface as the electrodes

The constancy of the pressure applied on the cells walls in this design was verified by adding a force measurement device during one cycle additionally to the springs. The pressure variation proved to stay under 6 kPa.

3.3.1.3 Mechanical pressure recording device

The device for recording the mechanical pressure was consisting of four force sensors basing on the deformation of metallic strips (Tefal). The original properties of the force sensor equipment were modified so that the automatic cut off and the automatic reset were cancelled.

The time and temperature stability of the force recording device were checked and proved to be satisfying.

The force is applied via a plastic spacer of the exact surface of the electrodes (i.e. 182 cm²), the mechanical pressure was calculated. The corresponding value of the mass in kg is read on the display.

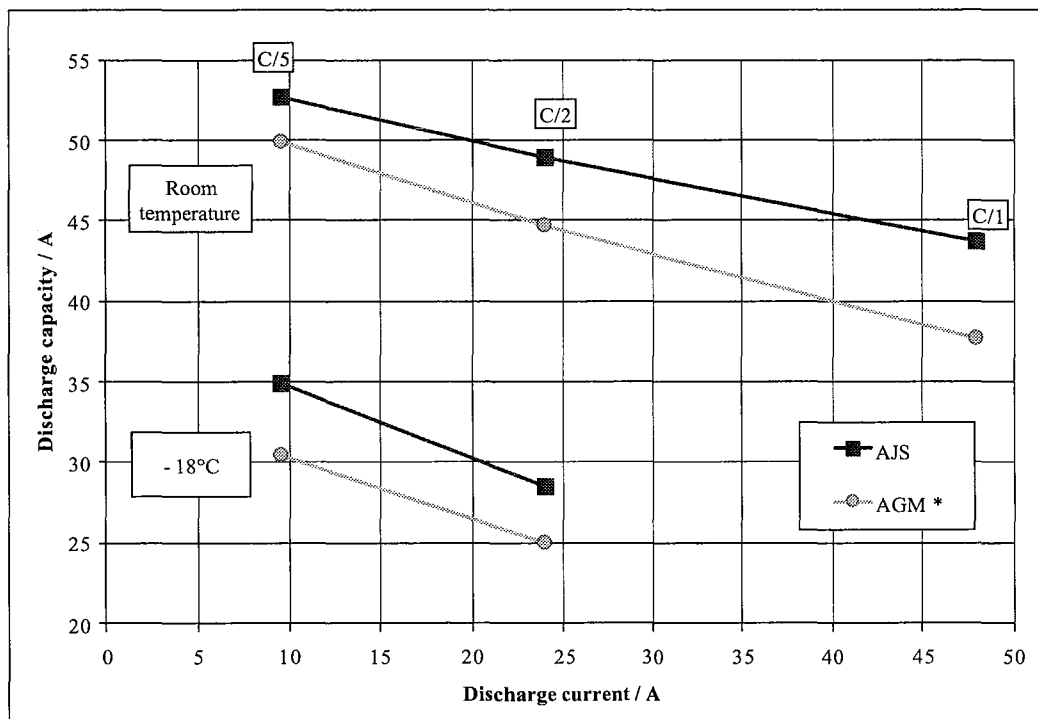
The maximum of the scale was about 150 kg, corresponding to mechanical pressures over 80 kPa. A reset was performed at about 75 kg before increasing the force via the screw to the initial desired value of the external mechanical pressure. That way, the measurement range was shifted from 0-150 kg (i.e. 0 – 80 kPa) to 75-225 kg (i.e. 40 – 125 kPa)

3.3.2 Parameter test

The parameter test allows a rapid comparison of all the systems and was supposed to show clearly if the AJS system was suitable at all for VRLA batteries in comparison with the other concurring systems. With

respect to the wide spectrum of parameters tested, an unsuitability of the AJS system would have shown out clearly during these tests. The parameter test was performed on two batches of cells and on one batch of batteries. The results were similar for all test series. For this determination, all cells were inserted between two aluminium plates and kept at the nominal thickness during the test. The batteries were in the same state of mechanical pressure as during the cycling test.

The discharge capacity versus discharge rate at different temperatures is a primordial characteristic for the user and is called the Peukert dependence. It determines the time a cell/battery will supply energy in a given utilisation. In fact, the discharge capacity for a cell/battery is strongly dependent on both the current of discharge and the temperature of discharge. The reason for that is the limitation of the diffusion process (i.e. the supply of acid at the reaction site) with increasing discharge current and with decreasing temperature. For EV applications, it is important that a battery has a good behaviour at high discharge rates and also, at low temperatures since these characteristics will determine the ability of a car to sustain high speed and also its ability to function at low temperatures.



* determination made on two different cells, the average value of both tests is represented

Figure 32: Discharge capacity versus current of discharge for cells with AGM and AJS

Figure 32 shows that the capacity dependence on the discharge current of the AJS system is very satisfying. Nevertheless, since both systems are not in their optimised conditions, the absolute values are not very relevant. But the evolution of the discharge capacity with increasing discharge current is even better for the AJS system, even at low temperature. It means that no acid supply limitation occurs in the system even if the separator has a lower and a thinner porosity. This result is very encouraging.

The ECE 15 driving test characterises the dynamic behaviour of a battery for EV applications. This test can be used for life testing but in our case, it was performed only once in order to give an estimation of the driving range for one charge of each cell tested.

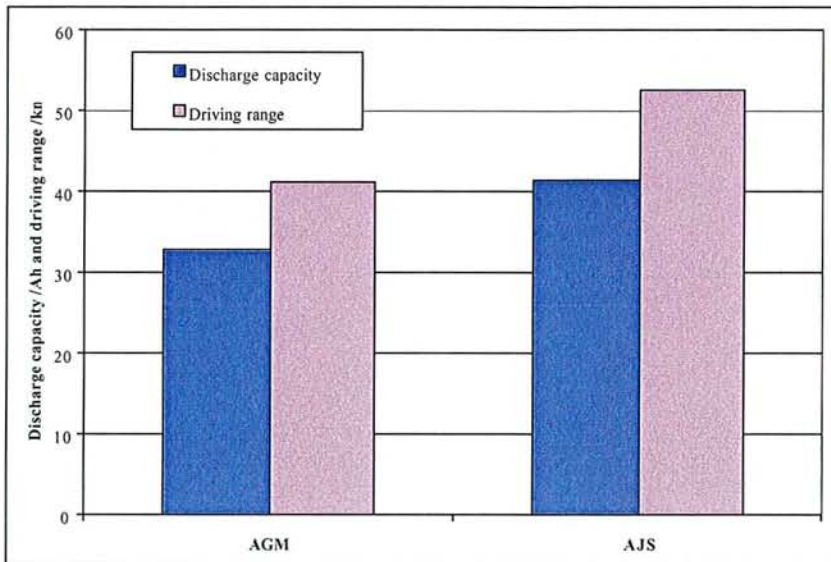


Figure 33: Discharge capacity and driving range for one ECE 15 cycle

Once again, the results delivered by the AJS cell are very satisfying with a driving range over 50 km. Within this test, the specific energy can easily be calculated and in our conditions, the batteries showed an energy of less than 25 Wh/kg. This result is quite representative of the current state of the art.

The IR-OCV-P test (internal resistance-open circuit voltage-peak power) allows the measurement of the open circuit voltage, the internal resistance and the peak power at different depth of discharge. These characteristics allow a comparison of the different systems.

Figure 34 presents the open circuit voltage versus depth of discharge for an AGM cell and two AJS cells with or without phosphoric acid

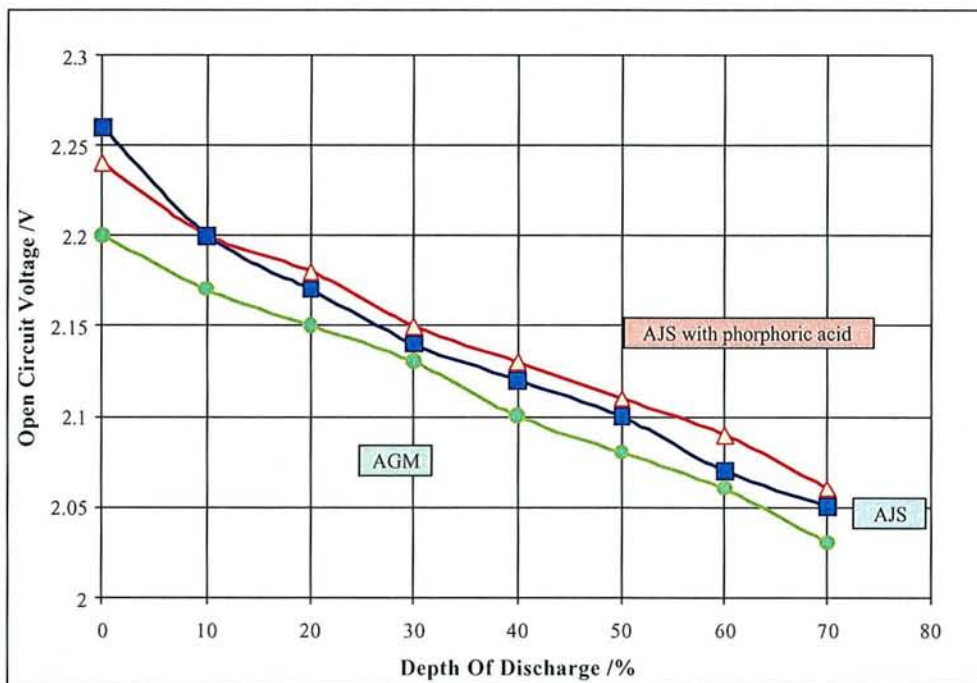


Figure 34: Open circuit voltage versus depth of discharge for different cells.

The AGM cells has the lowest open circuit voltage. This higher value found for the AJS system may be imputable to a possible slower electrolyte diffusion in the AJS cells. After charge, more time is needed for the concentrated acid present in the pores of the electrode to diffuse towards the separator and a gradient of concentration is present between the electrolyte of the pores and the electrolyte in the separator.

Figure 35 shows the high current internal resistance of the cells depending of their state of charge.

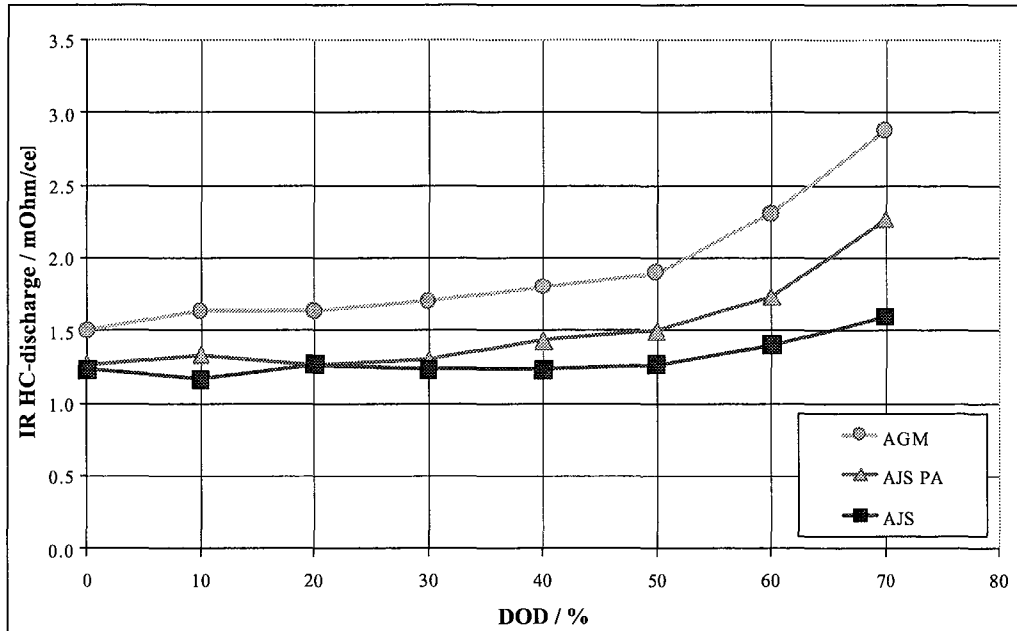


Figure 35: Internal resistance at high current of discharge versus depth of discharge for different cells.

While the lowest internal resistance is expected for the AGM cell, we measured the highest value for this cell. It can be related to either the lower saturation of the cell in electrolyte or to the fact that the contact between the plates and the separator is better in the AJS cells.

The lower internal resistance at high discharge current and the higher OCV measured for the AJS cells resulted in a higher peak power as confirmed by the results presented in Figure 36.

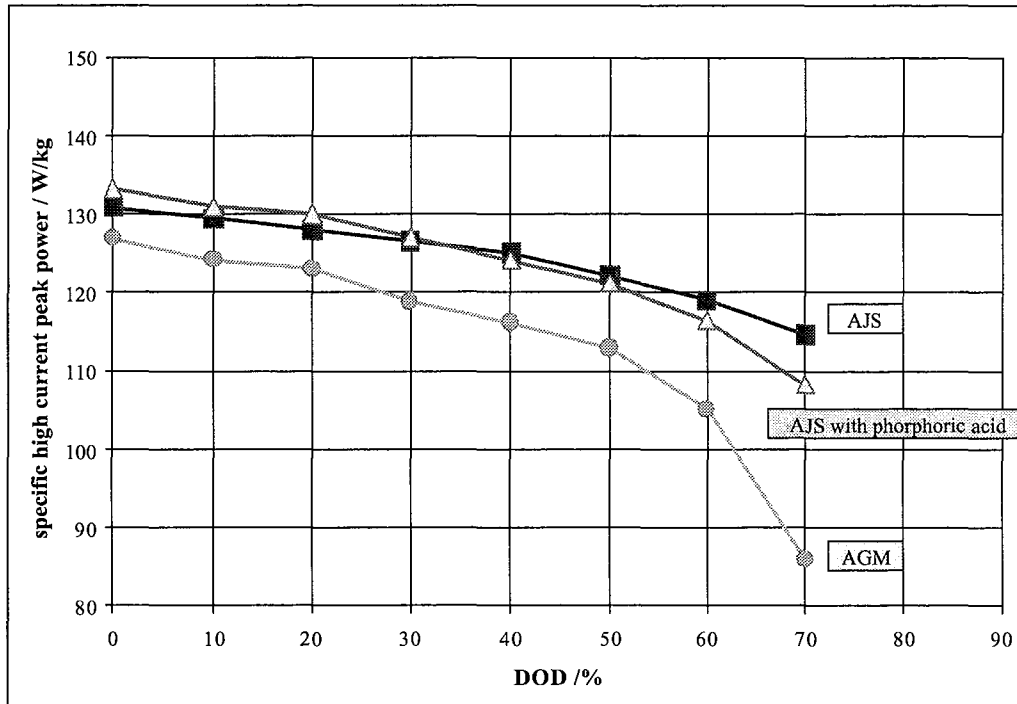


Figure 36: Specific high current peak power versus depth of discharge for different cells.

The AJS cells have a better high current peak power that is the counterpart of the lower internal resistance.

The totality of the results obtained with the parameter test are very encouraging and even surprising for the AJS separator since a higher electrical resistance of the AJS separator was measured outside of the cell by Daramic.

3.3.3 Cycling life

For the cycling life test, the cycling regime consisted of 25 cycles at 20A current of discharge (approximately 2 hours rate until 1.6 V) followed by two cycles at 9.6A (5 hours rate until 1.75 V). In the first series of experiment, the charging regime of the cells was varied depending on the nature of the separation system used (see Table 9) in order to get a satisfying charging factor for each separation and electrolyte system and also in order to get experience concerning the AJS system.

Cycle	AGM	AJS PA 30 kPa	AJS 80 kPa	AJS 30 kPa	AJS 60 kPa springs	Gel
1		14.4 A/2.4 V/10 h				14.4 A/2.45 V/10 h
47						14.4 A/2.45 V/6 h
102		14.4 A/2.45 V/10 h				400 mA/4 h
167						14.4 A/2.4 V/10 h
220	14.4 A/2.35 V/10 h					
232		14.4 A/2.4 V/10 h				
313						14.4 A/2.45 V/10 h
316	14.4 A/2.4 V/10 h					

Table 9: Charging regime of the cells

The experience gained with the cycling of cells helped choosing a suitable charging regime for the batteries described in section 2.1.3.

Figure 37 shows the evolution of the C/2 capacity of three cells versus cycle number.

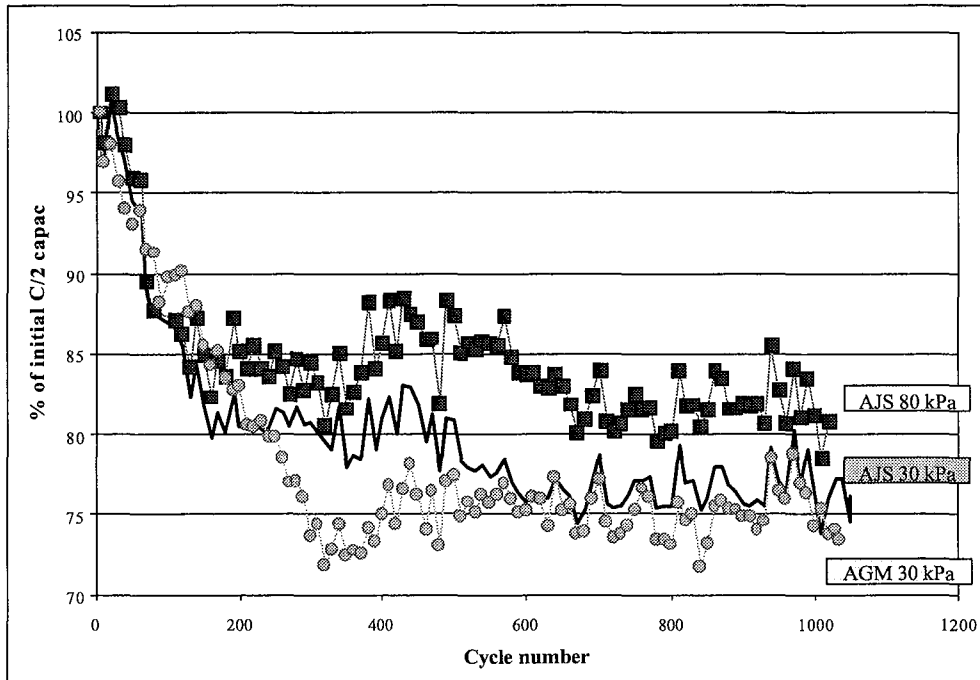


Figure 37: Evolution of relative C/2 capacity versus cycle number

The first encouraging result was the good behaviour of the AJS cell in comparison with the AGM system with the same design. But the very astonishing result was the improvement of the cycling life until reaching the end of life criterion, i.e. 80% of the initial capacity that is summarised in Figure 38.

Cell	AGM 30 kPa	AJS 30 kPa	AJS 80 kPa
Cycles until under 80% of initial capacity	≈ 250	≈ 500	≈ 1010

Figure 38: Cycle life of the cells of Figure 37

While the life is doubled with AJS in comparison to AGM with the same initial mechanical pressure of 30 kPa, this showing the ability of AJS to sustain the mechanical pressure, the life can be increased by a factor four by applying a higher initial mechanical pressure of 80 kPa. Since the cells used for this test were the first produced with AJS, this result was extremely promising. The good results were confirmed when batteries were also manufactured with different separation systems and cycled. The results of the cycling test for the batteries are shown in Figure 39.

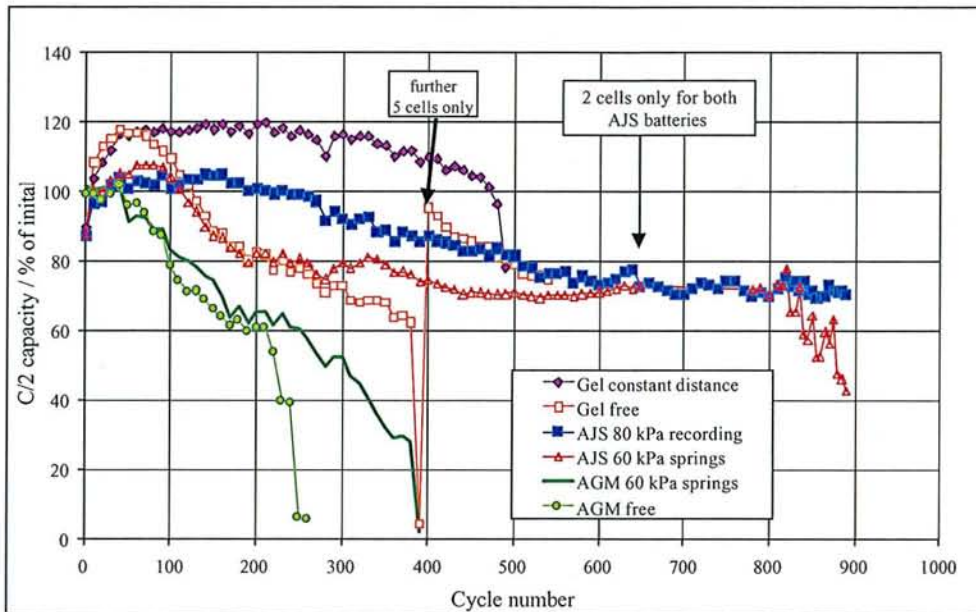


Figure 39: C/2 discharge capacity versus cycle number for batteries with different separation systems and under different initial mechanical pressures

The batteries with the AGM separator had a very short life and proved to suffer strong corrosion and extreme positive active material softening. These batteries were filled with more electrolyte than the cells in the former batch and this higher saturation seems to have led to rapid capacity loss. The gel batteries underwent strong top grid corrosion and failed after some 480 cycles for the variant with the highest mechanical pressure. And the AJS battery under high mechanical pressure lasted for over 500 cycles. Both AJS batteries showed a very stable capacity until over 1000 cycles. The last 650 cycles were performed by only 2 cells for each battery since the other cells were removed in order to check the components after a number of cycles similar to the one of the other systems.

3.3.4 Conclusion about the electrical tests

The new separation system gave very promising results in the parameter test as well as in the cycling life test. The very important point of the suitability of the new separation system for the VRLA system demonstrated and the improvement of the cell/battery life by application of mechanical pressure on the external walls was proved.

3.4 Mechanical pressure development during one cycle

The evolution of the mechanical pressure on the walls of a cell constraint at a constant thickness is still a question of controversy. The first papers reporting about this evolution ([54] and [57]) show that the mechanical pressure on the cell walls increases during discharge and decreases during charge. But later on, another team found an opposite evolution of the forces [65].

In order to find out which is the real evolution of the mechanical pressure, it was recorded by the means of the design shown in section 3.3.1.2.

3.4.1 Typical evolution of the mechanical pressure

The typical curve for the evolution of the mechanical pressure on the walls of an AJS cell during one C/5 cycle is represented in Figure 40. These values have been recorded after the cell had already performed 100 full C/2 cycles.

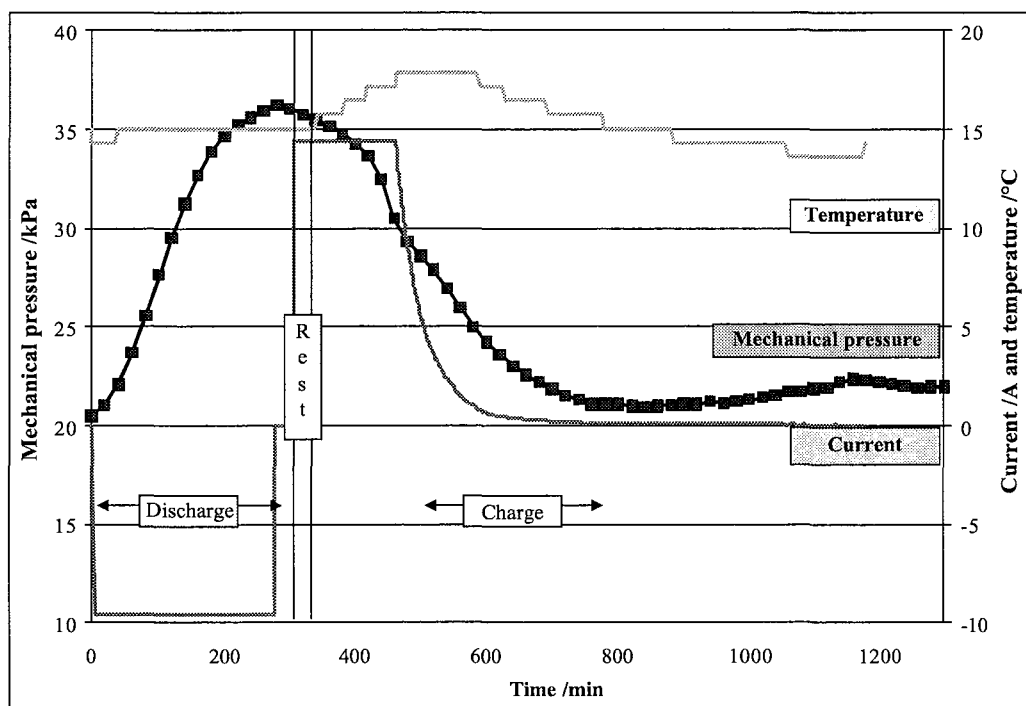
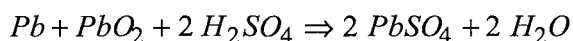


Figure 40: Evolution of the mechanical pressure on the walls of an AJS cell during one cycle

For all separation systems, a similar evolution is obtained (see section 3.4.4). In all cases, an increase of the mechanical pressure on the cell walls can be observed during discharge, followed by a decrease during charge.

3.4.2 Increase of the mechanical pressure during discharge

During discharge, the double sulphation reaction takes place. If one compares the specific volumes of the products and reactants, the volume on the positive electrode is increased by a factor 1.92 and the volume of the negative electrode is increased by a factor 2.62 if all material is transformed to lead sulphate. That way, the total volume of the active materials increases by a factor 2.27.



$$EF = \frac{V_{Products}}{V_{Reactants}} = 2.27$$

$$(V_{Pb} = 18.3 \text{ cm}^3 / \text{mol}, V_{PbO_2} = 25 \text{ cm}^3 / \text{mol}, V_{PbSO_4} = 48 \text{ cm}^3 / \text{mol})$$

3.4.2.1 Dissolution/precipitation reaction

On the positive as well as on the negative electrode, the sulphation reaction is claimed to be a dissolution/precipitation process [74]. And it is generally accepted that a precipitation reaction is not able to develop forces. The crystallisation takes place where there is free room and is not associated with a deformation of the structure. In reference [65], Bashtavelova and Winsel published results that would support this idea. They found that only at the end of discharge the mechanical pressure on the positive plate does increase after having decreased drastically during the first part of the discharge.

It is possible to calculate the variation of the porosity P_f of an electrode depending on its initial porosity P_0 (as a the ratio of the pore volume on the total volume of the electrode), on the expanding factor EF

associated with the conversion of its active material to lead sulphate during discharge and of the utilisation rate of the active material U (as a ratio of the active material part that reacted to the initial amount of active material).

The final pores volume is the difference between the initial pores volume and the additional volume the lead sulphate occupies compared to the active material.

$$V_{P_f} = V_{P_0} - (EF - 1) * U * V_{AM_0} \quad \text{Equation 8}$$

$$P_f = P_0 - [(EF - 1) * U * (1 - P_0)] \quad \text{Equation 9}$$

$$\text{With } P_f / V_{P_f} = P_0 / V_{P_0} \text{ and } V_{AM_0} = V_{P_0} * (1 - P_0) / P_0$$

The typical porosity of the active material is bigger than 54% for a new positive plate and bigger than 60% for a new negative. The evolution of the porosity of the positive and negative plate versus active material utilisation is presented in Figure 41 for new electrodes.

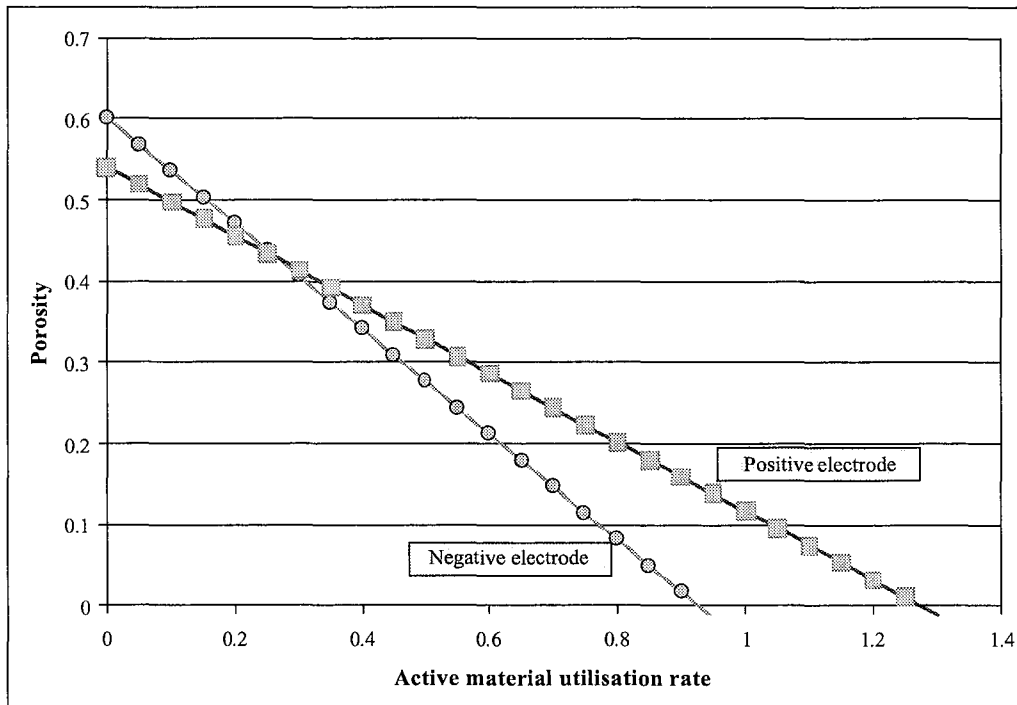


Figure 41: Porosity versus active material utilisation for new electrodes

If the free room for expansion is limited to the only porosity, it means that the crystallisation of the lead sulphate leads to no deformation of the structure, the maximum utilisation rate is obtained when all the porosity is filled ($P_f=0$, see Equation 10).

$$U_{\max} = \frac{P_0}{(EF - 1)(1 - P_0)} \quad \text{Equation 10}$$

Considering the free room associated with the porosity of new plates, the maximum utilisation rates of the positive and the negative active material would be respectively 128% for the PAM and 93% for the NAM in the beginning of life if the structure would not be affected. These results are summarised in Table 10.

active material	porosity after formation /%	expansion factor	utilisation rate
positive	54	1.92	1.28
negative	60	2.62	0.93

Table 10: Maximum active material utilisation rate basing on volume consideration

The maximum utilisation rate obtained by this calculation for positive active material is over 100%. It means that the positive electrode has enough porosity to accommodate all the lead sulphate in its structure even if all the lead dioxide is converted to lead sulphate. Thus, the discharge of the positive plate is never limited because of a room restriction, even if the battery is constraint so that the structure of the positive plate is not allowed to expand. Of course, this result implies that the dissolution/precipitation processes are not localised and apply therefore no constraint on the structure.

The effective positive active material utilisation rate (PAMU) is dependent on the discharge regime the battery is submitted to and is much less than the utilisation rate calculated here because the utilisation is limited by acid diffusion. Values in the range of 50% are commonly encountered. Under simulated electric-vehicle service, the PAMU is less than 45% [75].

While Pavlov and Bashtavelova [76] found a linear dependence between the total porosity and the actual discharge capacity of the positive active material in a lead acid cell, our calculation gives an hyperbolic dependence between the maximum active material utilisation rate without structure deformation and the porosity as shown in Figure 42 but can be approximated with a straight line in the range that concerns the effective porosity encountered in the lead-acid battery.

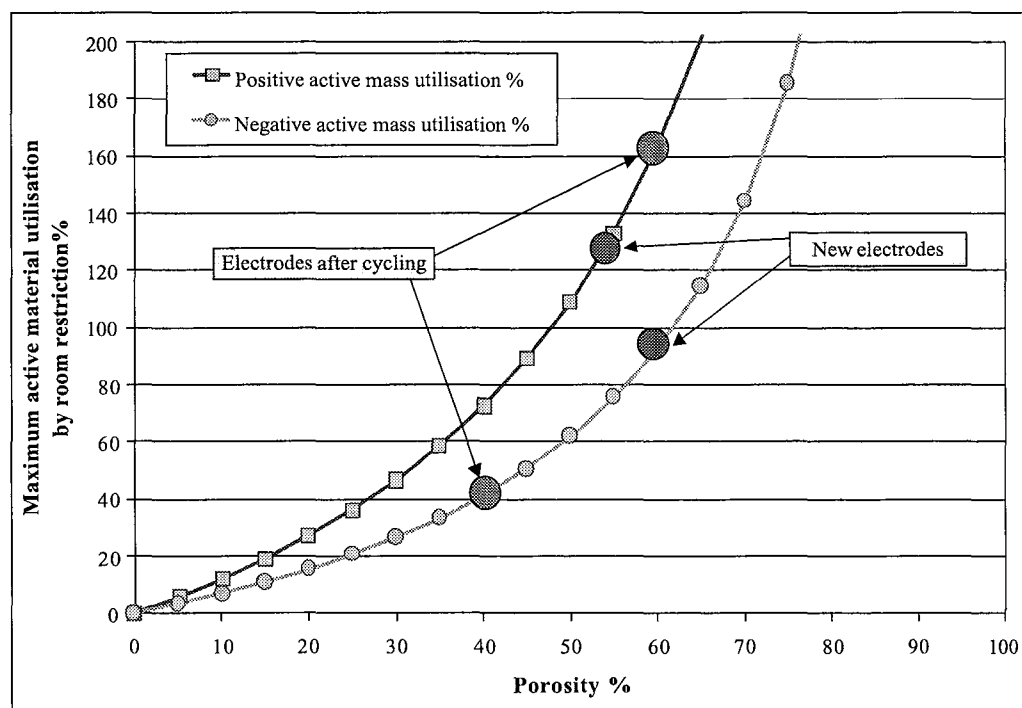


Figure 42: Maximum active material utilisation achievable if the room for expansion is limited to the only porosity.

For the new negative active material, a maximum of 93% utilisation can be achieved. Unfortunately, since the negative electrode was not the limiting one until now, no data could be found in the literature about the actual active mass utilisation of the negative plate.

The negative plates of the cells used here are pasted with 115g active material. The capacity associated with this quantity of active mass is 178.5 Ah for a 100% utilisation of the active material.

If one takes also into account that the porosity of the negative electrode decreases with cycling, the maximum possible active material utilisation decreases over life. At the end of life, a porosity in the range of 40% was measured for negative plates of an AJS cell after 465 cycles (see section 3.6.1). At this porosity, the maximum utilisation without expansion of the structure is 41%. It means that it is well possible that the restricted room available for the active material conversion to lead sulphate is responsible for the limited active material utilisation if the plate stack thickness is constraint. But in our case, a utilisation of 41% of the negative active material would lead to a discharge capacity of about 71 Ah, what is still far above the capacity the cell delivered at the opening. It means that the utilisation is also limited by another process like diffusion.

The calculation of the maximum active material utilisation without expansion allows three conclusions.

- It is possible for the positive active material to be totally converted into lead sulphate over discharge without deformation of the original structure of the plate, assuming that the dissolution/precipitation processes are not localised. It is therefore not possible to explain the force development we measured during discharge by the room limitation for the positive plate.
- The negative active material utilisation can possibly be restricted by the limited room available for the precipitation of lead sulphates. In the beginning of life, a maximum utilisation of 93% is calculated but since the porosity of the negative plate decreases over life (see section 1.6.7) to values even smaller than 40% (see section 3.6.1), the subsequent utilisation is then less than 41% basing on the only room consideration. The over-dimensioning of the negative plates allows never to reach the limits caused by this mechanism.
- It is not possible to prove that the utilisation rates observed in batteries are higher than the maximum utilisation rates calculated considering the only free room available for crystallisation. Such an observation would unquestionably induce a deformation of the plate structure and an associated evolution of the mechanical pressure on the cell walls during discharge.

In spite of these calculations, the mechanical pressure during discharge increases in our results and this increase was also observed by many other teams. It means either that a precipitation reaction can be associated with the development of forces, or the discharge reaction is not purely a dissolution/precipitation reaction. In fact, the discharge but even more the charge processes are well known to be localised, e.g. the precipitation of the lead dioxide taking place as near as possible from the lead sulphate crystal from which the lead II ions are dissolved. For example, Takehara proved that the precipitation of the charge reaction products takes place at the interface between the lead sulphates and the active material on which they grew [77]. Another argument in favour of a localised precipitation process is the fact that the sulphate ions have to diffuse to the precipitation place and are hindered in this by their big size.

3.4.2.2 Force associated with crystallisation

In the chemistry of concrete, reference is often made to crystallisation processes that lead to a destruction of the structure and to the fracture of masonry, leading to damages in buildings of historical importance (e.g. [78]). Even if the $\text{Pb/PbSO}_4/\text{H}_2\text{SO}_4/\text{PbO}_2$ system is totally different from the chemical system of a concrete, following this idea, a useful paper could be found in the literature of concrete dealing with crystallisation in pores [79]. Basing on this paper, the following argumentation for the lead-acid battery is proposed.

The driving force for crystallisation is the difference in chemical potential between the solution and the crystal. The maximum of the crystallisation pressure can be deduced from this difference in chemical potential, it means that it is dependent on the concentration of the solution and on the equilibrium concentration (if the activity coefficients are ignored).

$$\Delta\mu = RT \ln(C/C_0)$$

$$\Delta\mu = \mu_{crystal} - \mu_{liquid}$$

$$R = \text{ideal gas constant}$$

$$C = \text{concentration of solute}$$

$$C_0 = \text{equilibrium concentration}$$

Equation 11

$$P_c = P_l + \frac{RT}{V_c} \ln(C/C_0)$$

$$P_c = \text{crystallisation pressure}$$

$$P_l = \text{liquid pressure}$$

$$V_c = \text{crystal volume}$$

Equation 12

For the case of the lead-acid battery, the supersaturation of lead ions during discharge in the pores is a well known phenomenon, especially at the beginning of discharge of a fully charged cell, explaining the phenomenon known as the “coup de fouet” [80]. In a recent paper [74], Takehara measured the reaction rate of the discharge of PbO_2 in sulphuric acid (0.5 M H_2SO_4) with a rotating ring-disk electrode and could measure Pb^{2+} concentrations of $2.65 \cdot 10^2$ M on the disk while the solubility of PbSO_4 in 0.5 M H_2SO_4 is $1.88 \cdot 10^{-5}$ M. It means a supersaturation (C/C_0) around 1400. With $V_{\text{PbSO}_4} = 48 \text{ cm}^3/\text{mol}$, in such a disposition, the hydrostatic pressure that would have to be applied on a PbSO_4 crystal to suppress its growth at 25°C would have to be in the range of 3700 atm (373 MPa!).

This calculation gives the maximum of the crystallisation pressure. Of course in the battery, supersaturation in this range is not encountered. In addition, a crystal has also an internal capillary pressure that results from its surface energy following the Laplace equation, so that small crystals of spherical shape can be in equilibrium with a high crystallisation pressure depending on their surface energy.

$$P_{cap} = P_l + \gamma_{cl} \kappa_{cl}$$

$$P_{cap} = \text{capillary pressure}$$

$$\gamma_{cl} = \text{interfacial energy crystal / liquid}$$

$$\kappa_{cl} = \text{curvature of the interface crystal / liquid}$$

Equation 13

Using the same method as Edwards and Schmitz [17], we can estimate the surface tension of lead sulphate with use of data about PbSO_4 in the anglesite form from reference [81].

The melting point of PbSO_4 is $1170^\circ\text{C} = 1443.15 \text{ K}$

The approximate volume at melting temperature of PbSO_4 is $49.91 \text{ cm}^3/\text{mol} = 49.91 \cdot 10^{-6} \text{ m}^3/\text{mol}$

The deduced approximation of the surface tension of PbSO_4 is 0.179 J/m^2 .

At atmospheric pressure, a lead sulphate crystal of spherical shape with a radius of 60 nm is then in equilibrium with a crystallisation pressure of about 60 MPa.

After germination, the lead sulphate crystal has to grow into a pore and the pore walls have to exert a radial stress on the crystal in order to balance the differences in capillary pressure that appear in a crystal as a result of the growth of its different faces. The radial stress depends on the contact angle between the pore wall and the crystals face and it is most probably the origin of the force that is transferred to the cells walls in our mechanical pressure measurements. This radial stress is expressed in Figure 43.

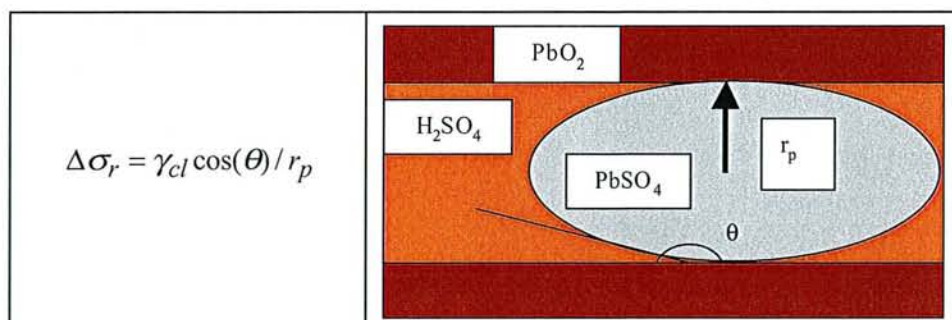


Figure 43: Expression of the radial stress on the pore wall

The bigger the pores, the smaller the mechanical stress.

In the most extreme case, i.e. when the bulk has small pores and the angle between the crystal and the pore is 180° , one finds a hoop tension in the wall of the pore that accompanies the radial stress of about **half the capillary pressure in the crystal**. This hoop tension is the one that can lead to deformations of the active material structure.

The dependence of the hoop tension on the pore size can partially explain the mechanical pressure evolution as discharge proceeds. With increasing discharge time, more and more lead dioxide is converted to lead sulphate and that way, the size of the pores in which the lead sulphate crystals grow is increasing. Thus, the mechanical pressure applied by the lead sulphate crystals to the pore wall should decrease with proceeding discharge. But of course this effect is compensated by the growth of the lead sulphate crystals that occupy almost twice the volume of the lead dioxide, before its dissolution.

In summary, a mechanical pressure can develop during discharge as a result of the lead sulphate crystal growth. The maximum value of this pressure is determined by the crystallisation pressure. Its actual value is determined by the shape and size of the lead sulphate crystals and the shape and size of the pores in the active material.

3.4.2.3 Discharge capacity and mechanical pressure increase

Disappointingly, no linear relationship could be found between the increase of the mechanical pressure during discharge and the discharge capacity. It means that the increase of mechanical pressure is not directly related to the ratio of active material conversion U . The reason for that is probably to be found in the shape of the mechanical pressure evolution in the beginning and at the end of the discharge. Namely, in these states of low and high depth of discharge (DOD), the mechanical pressure evolution is much flatter.

Logically, in the beginning of discharge, the supersaturation has to build up and the germination has to take place before the crystal growth can cause a stress development on the pore walls. Additionally, the structure of the electrodes and of the whole battery system is probably able to deform a bit and therefore to accommodate a small increase of the mechanical pressure.

At the end of discharge, the supersaturation decreases progressively. In the low charging states, the sulphuric acid concentration is decreased and the solubility of lead sulphate is consequently increased. The dependence between sulphuric acid concentration and lead sulphate solubility is shown in Figure 44 from reference [82].

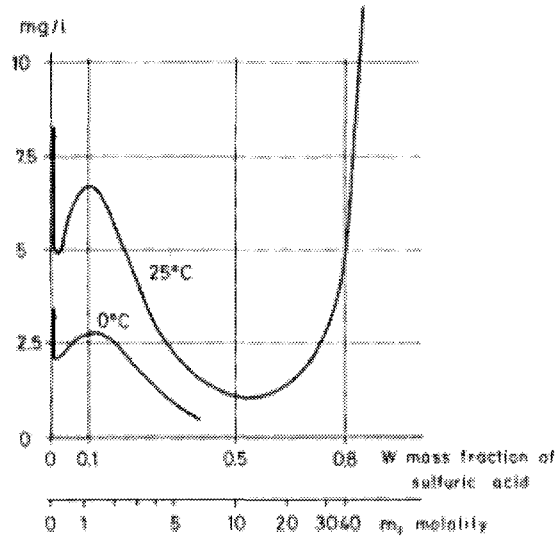


Figure 44: Solubility of lead sulphate in sulphuric acid of different concentrations

With increasing solubility of the lead sulphate, the super saturation decreases and thus the crystallisation pressure also decreases. The equation of the discharge reaction shows that for each 2 moles of electrons flowing between the electrodes, 2 moles of sulphuric acid are transformed to water. It means that there is a direct relation between the number of ampere-hours discharged from a cell and the content in sulphuric acid of its electrolyte. For each ampere-hour, 3.659g H_2SO_4 are consumed, producing 0.672 g water [16]. Taking the AJS cell for example, it contains in the original fully charged state 637 g diluted sulphuric acid at the density 1.3 g/cm^3 i.e. at ambient temperature some 252.8 g H_2SO_4 . With these parameters the mass fraction of sulphuric acid in the electrolyte (x) was calculated depending on the discharged ampere hours (y). The equation of the curve obtained is $y = -169.08x^2 - 105.07x + 68.778$ and a graphical representation of it is shown in Figure 45.

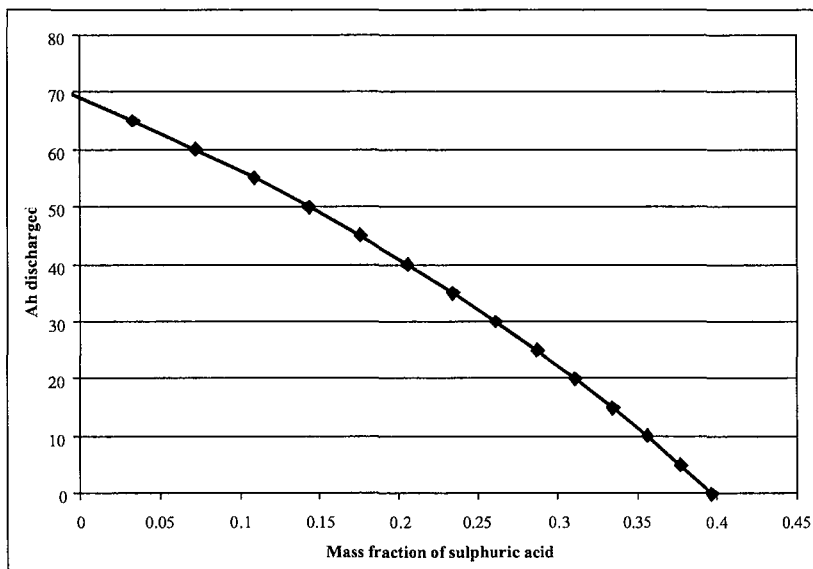


Figure 45: Dependence of the ampere hours discharged on the mass fraction of sulphuric acid in the electrolyte for an AJS cell without phosphoric acid

The association of Figure 44 and Figure 45 gives the dependence of the solubility of lead sulphate versus the capacity discharged from an AJS cell as shown in Figure 46.

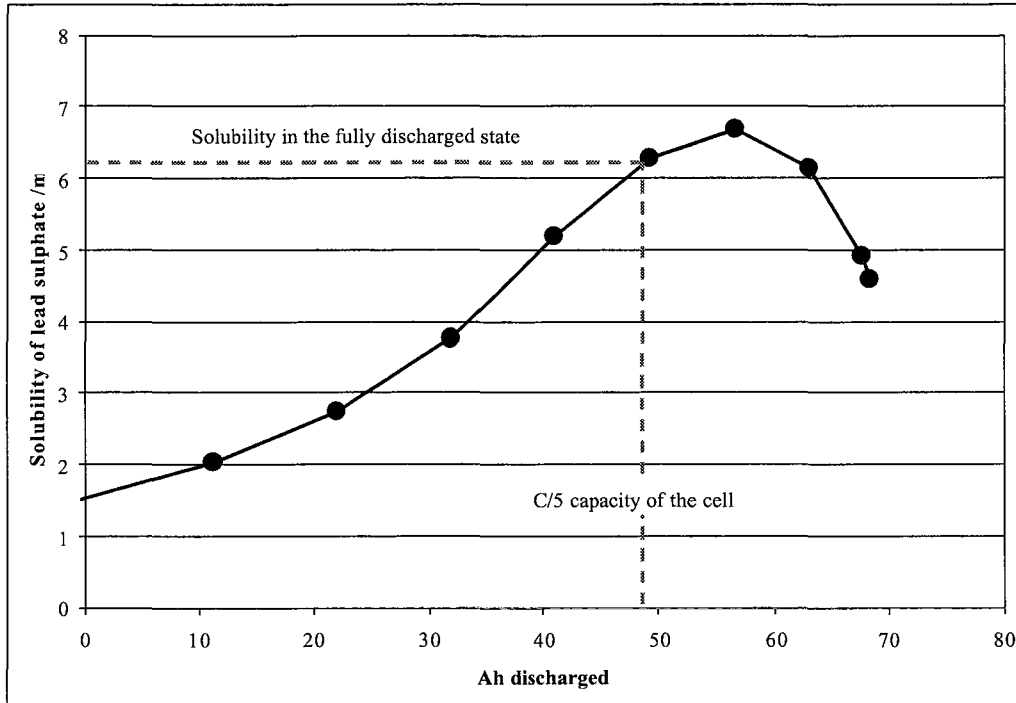


Figure 46: Solubility of lead sulphate versus discharged capacity of an AJS cell

According to these results, the solubility of lead sulphate increases all along the discharge but particularly at the end of the discharge. It is one reason for the slower increase of the mechanical pressure at the end of discharge. Additionally, the number of places where crystal growth can take place is high.

3.4.2.4 Influence of the current of discharge

The evolution of the mechanical pressure on the cell walls is presented in Figure 47 for two different discharge rates. The scale of the X axis is the number of ampere-hours discharged. For better readability, the values of the mechanical pressure at the beginning of discharge have been superimposed.

The difference in discharge capacity (41 Ah for the C/2 rate and 46.4 Ah for the C/5 rate) is not the reason for the differences in behaviour during discharge. In the former section, no linear correlation could be found between the increase of mechanical pressure during discharge and the discharge capacity. This is also confirmed by the results shown in Figure 47. For a same number of amperehours discharged from an AJS cell, the variation of mechanical pressure depends a lot on the discharge rate.

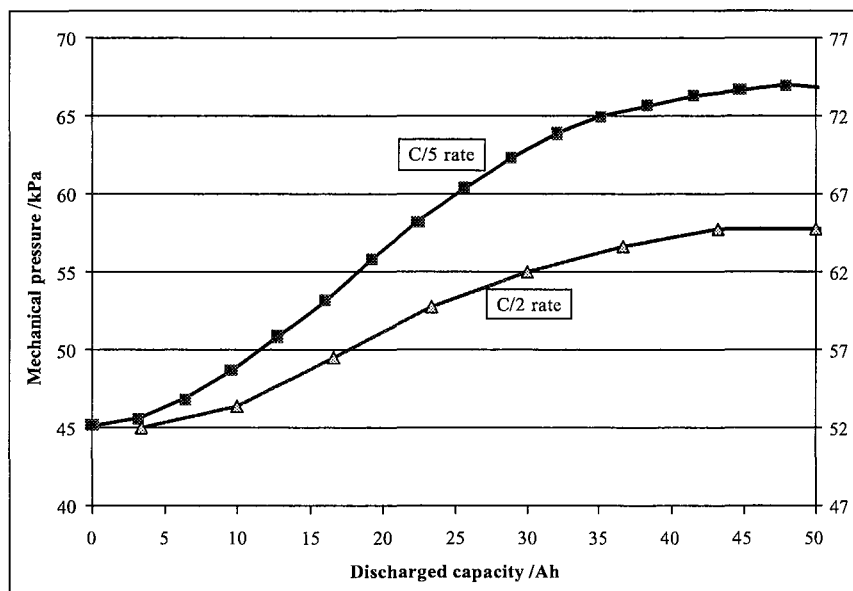


Figure 47: Evolution of the mechanical pressure versus discharged Ah at two different discharge rates for a same cell

For a similar discharge capacity, the mechanical pressure transferred to the cells walls increases much more at lower discharge rates. This is related with the fact that:

- The supersaturation is not increasing linearly with the discharge current. As a consequence, the driving force for crystallisation is not double at a double discharge current what would be necessary to develop twice the force in the same time.
- At high supersaturation, the germination process is preponderant on the crystal growth. Even if the super saturation is increased by an increased discharge current, there will be less crystal growth developing constraints in the structure and more precipitation of germs which shape allows them to be in equilibrium with higher crystallisation pressures. Therefore, the different behaviour of the mechanical pressure is related with the different crystal sizes.

3.4.2.5 Conclusion about the mechanical pressure increase during discharge

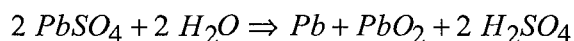
The double sulphation process is accompanied by a development of mechanical pressure. The upper limit of this pressure is the crystallisation pressure that is associated with the supersaturation in lead (II) species. The lower limit is depending on the form and interfacial energy of the lead sulphate crystals as well as on the pore size and on the contact angle between the crystal and the pore walls.

When the thickness of the plate stack is fixed and in the case of a non-compressible separator, the possibility for expansion of the active material is reduced and in such a case, the calculation of the maximum utilisation rate of the active material as a function of its initial porosity and of the expansion factor between the products and the reactants is possible. It shows that the discharge capacity can be limited by the negative plate when its porosity decreases with increasing number of cycles.

3.4.3 Evolution of the mechanical pressure during charge

During charge, there are two conflicting contributions to the mechanical pressure on the cells walls.

- Firstly, the charge reaction of the active material. It is the reverse reaction of the discharge.



Logically, if the reaction of dissolution/precipitation does not allow the formation of forces, the dissolution of the species formed during discharge would lead to no relaxation of the mechanical pressure.

We observe a decrease of the mechanical pressure during charge. In the beginning of the charge, i.e. in the first half of it, the evolution of the mechanical pressure is almost the perfect reflection of the pressure evolution during discharge, especially in the AJS cells. It comes from the relaxation of the forces evolved in the material during discharge. The shape of the “relaxation curve” speaks in favour of the idea that the growth of lead sulphate crystals during discharge puts the structures of the positive and negative electrodes under stress and that this stress is relaxed when the formed lead sulphates are back-transformed. The beginning of the charge is responsible for the transformation of most of the lead sulphate because the lead-acid battery accepts the majority of its charge in a short time. Afterwards, in order to get the remaining few percent of the active material in a charged state, it takes a long time. Therefore, the evolution of the mechanical pressure during the first half of the charge is logical as a result of the relaxation of the mechanical stress created in the structure during discharge.

- Secondly, the oxygen and hydrogen evolution. This is a positive contribution to the mechanical pressure at the end of the constant current charge period and is characterised by the apparition of a shoulder in the relaxation curve. This contribution is described more in detail in section 3.4.4.1.

Of course, relaxation can only take place where stress was present. Therefore, the relaxation curve during charge is also dependant on the current of the preceding discharge.

3.4.4 Influence of the separation system

For all the separation systems, the general tendency of the mechanical pressure is to increase during discharge and to decrease during charge. Tests were also performed on cells of a second production series and with modified separators. These cells show the same general behaviour. But depending on the separation system used, even if the general tendency is the same during one cycle, some small differences in the evolution of the mechanical pressure are observed when looking closer at the curves.

3.4.4.1 AGM

Figure 48 shows the evolution of the mechanical pressure during one C/5 discharge and the following charge. This cycle was performed after some 200 C/2 cycles for an AJS cell and an AGM cell.

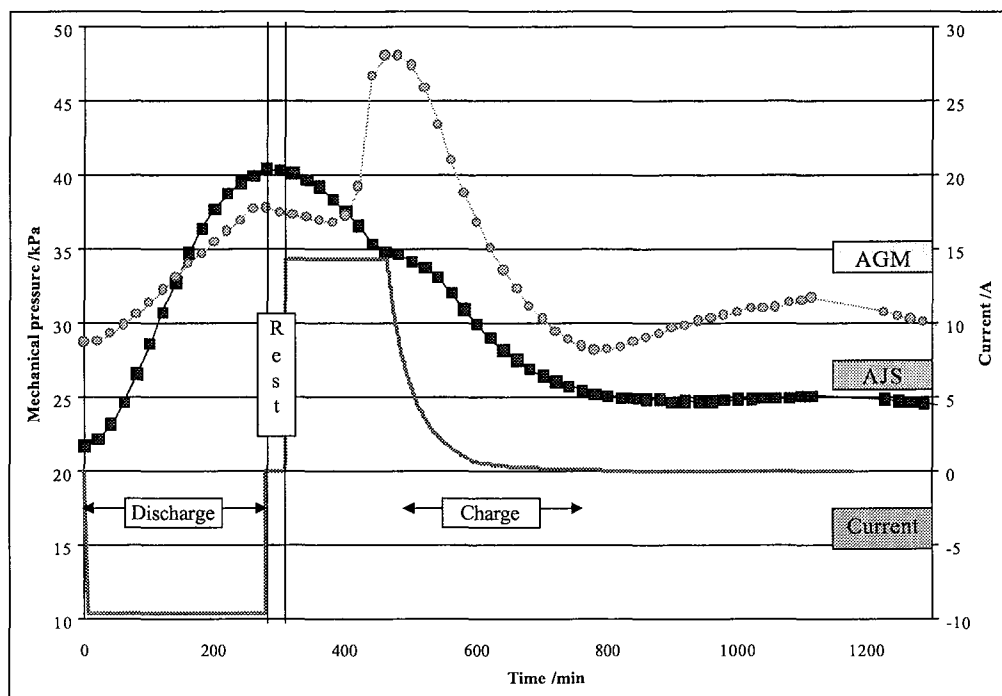


Figure 48: Evolution of the mechanical pressure during one cycle for an AJS and an AGM cell after some 200 C/2 cycles.

Since the plates of both cells are exactly the same and that only the separation system differs, the differences in behaviour have to be related with the separator.

- During discharge, the increase of the mechanical pressure with time is almost linear for the AGM cell and it is much slower than for the AJS cell. In this case, while the total increase between the beginning and the end of discharge is 18.68 kPa for the AJS cell, it is less than the half (9.06 kPa) for the AGM cell. This is due to the fact that the AGM separator is less stiff than AJS. AGM is compressed by the increasing mechanical pressure so that not all the pressure is transmitted to the cells wall. Some of the force gets lost in the compression of AGM and allows the active mass to expand. If one takes the values of the deformation of an AGM separator depending on the mechanical pressure that is applied on it (Figure 28), it is possible to calculate the expansion of the positive active material. In the region between 10 and 100 kPa, the deformation of the separator follows almost perfectly the equation $y = -18.587 \ln(x) + 142.71$ where x is the mechanical pressure applied on the separator and y is its thickness relatively to its original thickness at 10 kPa.

The initial thickness under 20 kPa of the AGM separator in our cells is 1.53 mm. If one considers that there is no variation of the thickness of the negative plate, the evolution of the positive plate thickness during discharge was calculated from the pressure evolution (Figure 48) and the separator behaviour (Figure 28) and is shown in Figure 49. The original thickness of the positive plate was 2.85 mm.

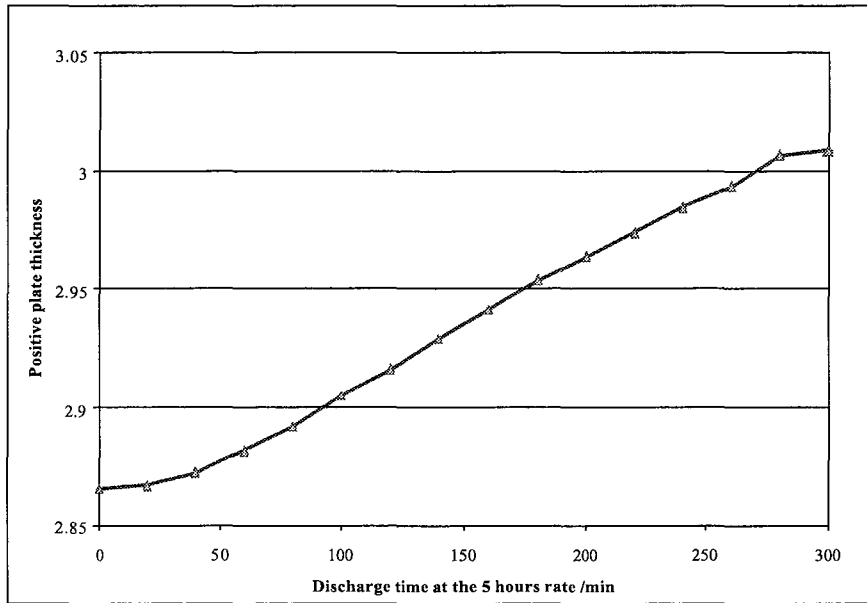


Figure 49: Evaluated thickness of the positive plate in an AGM cell during discharge

- During charge, one observes an increase of the mechanical pressure at the end of the constant current charge period. This increase is due to the oxygen evolution. Figure 50 shows the amount of gas measured downstream of the valve during charge.

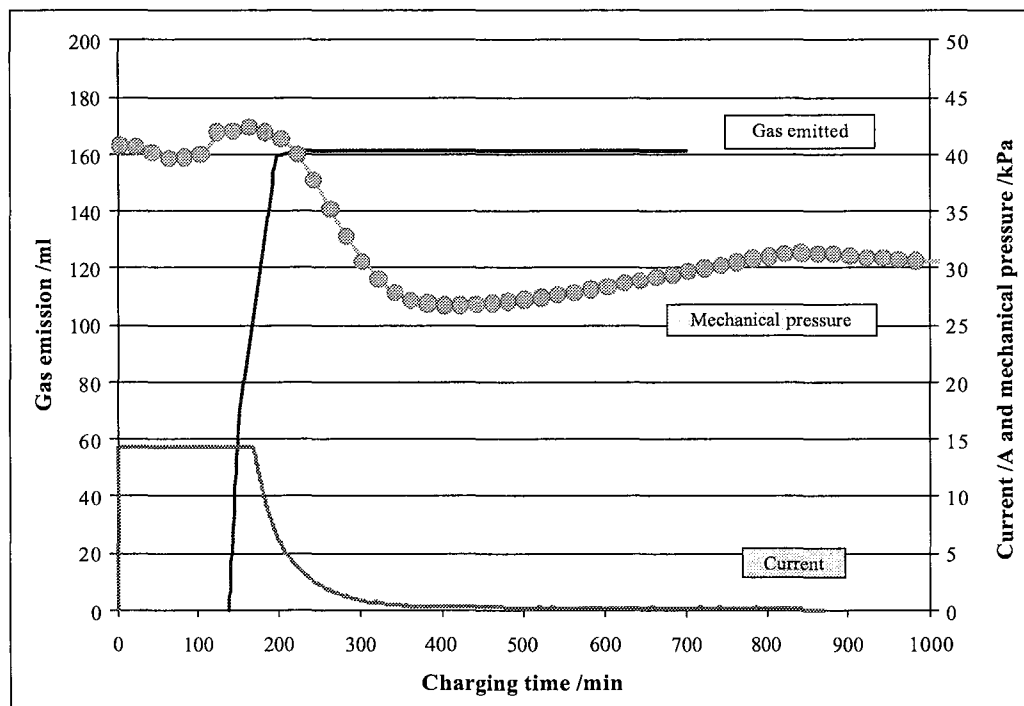


Figure 50: Evolution of released gas amount and mechanical pressure during charging of an AGM cell

Before the gas is released, the overpressure builds up in the battery until reaching the opening pressure of the valve. Since the valve opens at an overpressure around 13 kPa, a gas pressure builds

up in the free space of the cell from the value at the end of discharge (that is related to the hydrogen partial pressure and the oxygen recombination that took place during rest) to 13 kPa at the time when the valve opens up. The increase in pressure related with the gas formation cannot be smoothed by the separator since we are in presence of an hydrostatic pressure and the separator has a high and broad porosity, so that the gas can enter it very easily.

The evolution of the mechanical pressure in the AGM cell after the oxygen formation peak is complex and the behaviour is worth to be analysed in detail since many influences can be observed. The more detailed observation of the evolution of the mechanical pressure during charge and after switching out of the current will be done in section 6.

3.4.4.2 Gel

The evolution of the mechanical pressure during one C/5 cycle in a Gel cell is shown in Figure 51 in comparison with the behaviour of the AGM cell as discussed before.

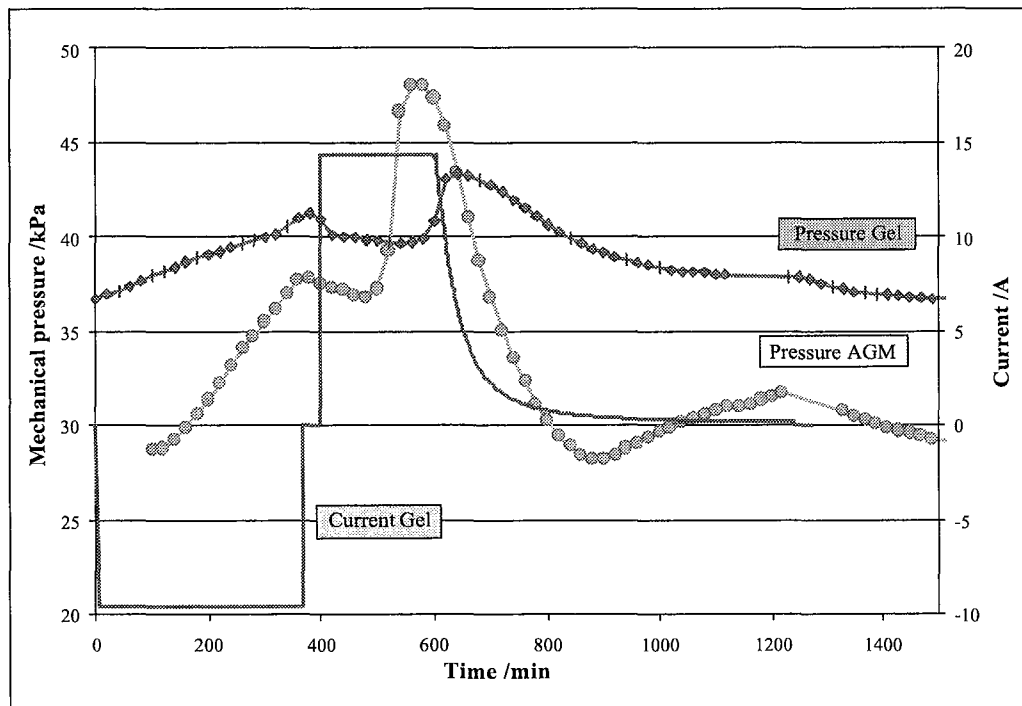


Figure 51: Evolution of the mechanical pressure during one cycle for a Gel cell and an AGM cell

- The cells had different capacities after 200 C/2 cycles. The discharge capacity of the gel cell is higher and the subsequent active material utilisation is also higher, but still the increase in mechanical pressure is smaller between the beginning and the end of discharge. It is related to the very poor mechanical properties of gel that cannot withstand mechanical pressure. The pressure is transmitted to the cell walls by the only ribs of the separator and is therefore much lower than in the AGM cell. The active material is allowed to expand in the gel without causing any pressure increase on the cell walls.
- For the behaviour during charge, the peak associated with the gas formation at the end of the constant current period can also be observed.

3.4.5 Influence of the initial mechanical pressure

Figure 52 shows the evolution of mechanical pressure during one cycle for two AJS cells subjected to different initial external mechanical pressures. Both cells had exactly the same C/5 capacity during cycle 109 (the current evolution curves are superimposed).

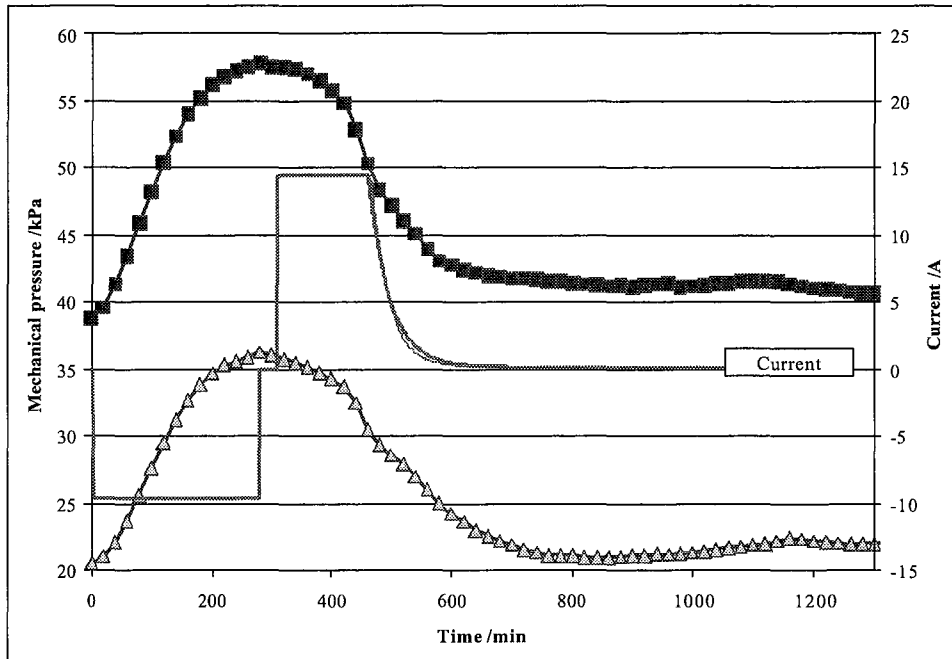


Figure 52: Evolution of the mechanical pressure during one cycle for two identical cells set at different initial external mechanical pressures

One can conclude that two identical cells with different initial external mechanical pressure have a very similar behaviour concerning the evolution of mechanical pressure during one cycle. The only differences are that:

- There is a slightly bigger increase of the mechanical pressure during discharge (about 4 kPa more) for the cell set under higher initial pressure in this cycle. This will be explained in section 3.5.1.
- The shoulder corresponding to the gas formation at the end of the constant current charge is less pronounced for the cell with the highest initial mechanical pressure. This feature will be discussed in the chapter dealing with oxygen recombination (section 6)
- The force generated during discharge cannot be influenced or suppressed by the application of an external mechanical pressure.

3.4.6 Behaviour for a battery

The evolution of the mechanical pressure for a cell and a battery consisting of 6 cells in series is shown in Figure 53. Since section 3.4.5 showed that the initial external mechanical pressure applied has only very few influence on the evolution of the pressure during one cycle, the scales in the diagram have been adapted so that the comparison is easier.

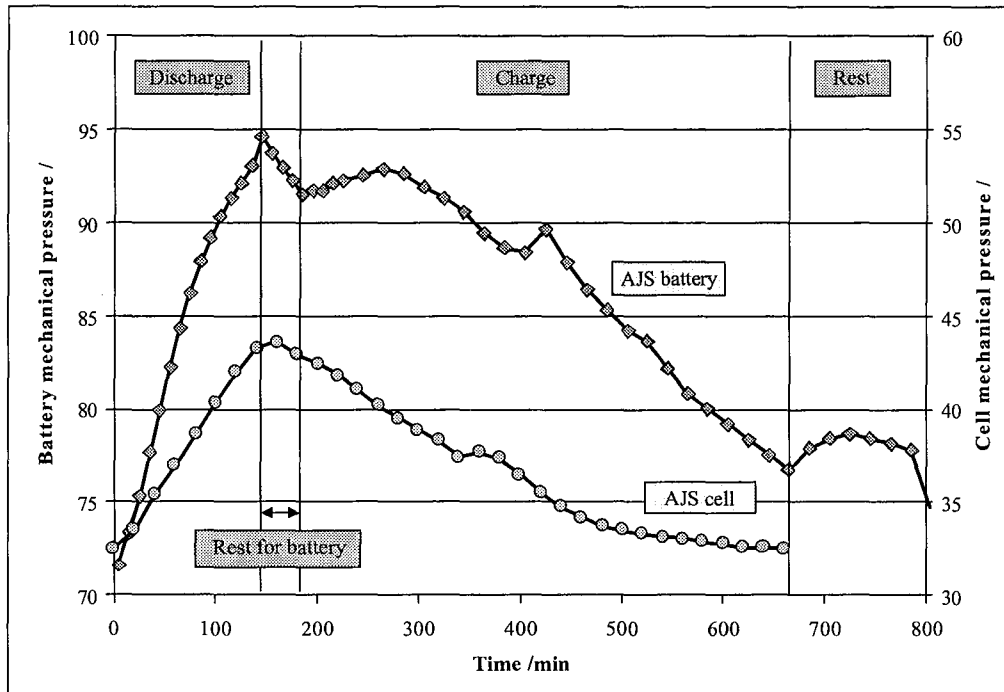


Figure 53: Evolution of the mechanical pressure during one C/2 cycle for a cell and a battery with AJS and phosphoric acid in the electrolyte

- The increase in mechanical pressure on the walls of the battery between the beginning and the end of discharge is twice as much as on the walls of a cell. It means that only the contributions of the external cells have been transmitted to the force recording device: on the inner cells walls, the principle of action and reaction applies and there is no transfer of forces from one cell to another. This result is very interesting from a practical point of view. It means that the utilisation of a moderately hard material is sufficient for the cell separation. Only the external case has to constraint the external cells and must be stiff.
- One observes a relaxation of the stress during rest. This was also observable for one cell but in a much lower extent and can be associated to reorganisation processes in the cells during rest.

3.4.7 Conclusion about the mechanical pressure evolution during one cycle

The shape of the curves representing the evolution of mechanical pressure during one cycle is constant. Independently from the separation system used, the batch of cells or the number of cells connected in series, the mechanical pressure transmitted to the walls increases during discharge and decreases during charge.

For the separation systems that can be deformed easily, the variations of mechanical pressure are smoothed by the separator and allow the positive active material to expand.

The increase of mechanical pressure during discharge is imputable to the growth of lead sulphate crystals on both electrodes. This reaction product has a much larger volume than the reactants. Its precipitation is a localised phenomenon and its growth into the pores of the electrodes exerts a pressure on the pore walls which maximum is determined by the over-saturation of lead II ions.

The recording of the mechanical pressure of the cell/battery walls allows also a visualisation of the “gas process” in the lead-acid cell/battery. This subject will be developed in section 6

3.5 Evolution of the mechanical pressure over cycling life

After having observed the evolution of the mechanical pressure during one cycle, it is now of interest to follow the evolution with increasing cycle number and find out if the ageing/failure process of a lead-acid cell/battery can be related with the evolution of the mechanical pressure on its walls.

3.5.1 Variation of mechanical pressure between beginning and end of discharge

During one discharge, the mechanical pressure increases. This increase is reported versus cycle number in Figure 54 for the AJS and the AGM cells.

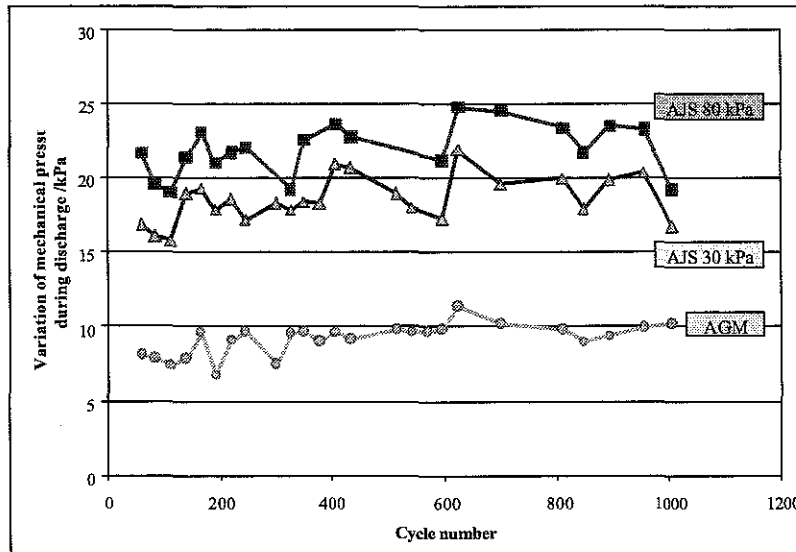


Figure 54: Increase of mechanical pressure during discharge versus cycle number

The variation of the mechanical pressure during one discharge is almost constant with increasing cycle number and is not linearly related to the discharge capacity of the cell as shown in Figure 52.

For the AJS cells with the same designs but different initial external mechanical pressure, the more pressurised cell shows a bigger increase of the mechanical pressure between the beginning and the end of one discharge. The difference is constantly about 4 kPa while the discharge capacity of the less pressurised cell is lower. Since the accommodation room is even less for the more pressurised cell, for a same minimal deformation or tendency to deformation, a higher force is necessary.

For the AGM cell, the small continuous increase of the mechanical pressure variation during one discharge can be associated with the non linear mechanical behaviour of the separator. With increasing cycle number, the initial pressure on the cells walls increases as will be shown in the next section. And for a same deformation of the separator that has to accommodate a same deformation of the active material, a higher mechanical pressure is required.

3.5.2 Increase of mechanical pressure between the beginning and the end of one cycle

Even after a rest time long enough to assure no superimposition of gas pressure, the mechanical pressure on the cells walls is slightly higher at the end of charge than at the beginning of the former discharge. This is particularly true for the non-compressible separation system.

In order to confirm this small increase of the mechanical pressure between the beginning and the end of one cycle, the value of the mechanical pressure on the cells walls was observed over cycling life for a same state of charge. In order to avoid any superimposition of gas, the value recorded at the end of discharge was chosen for this observation and is shown in Figure 55.

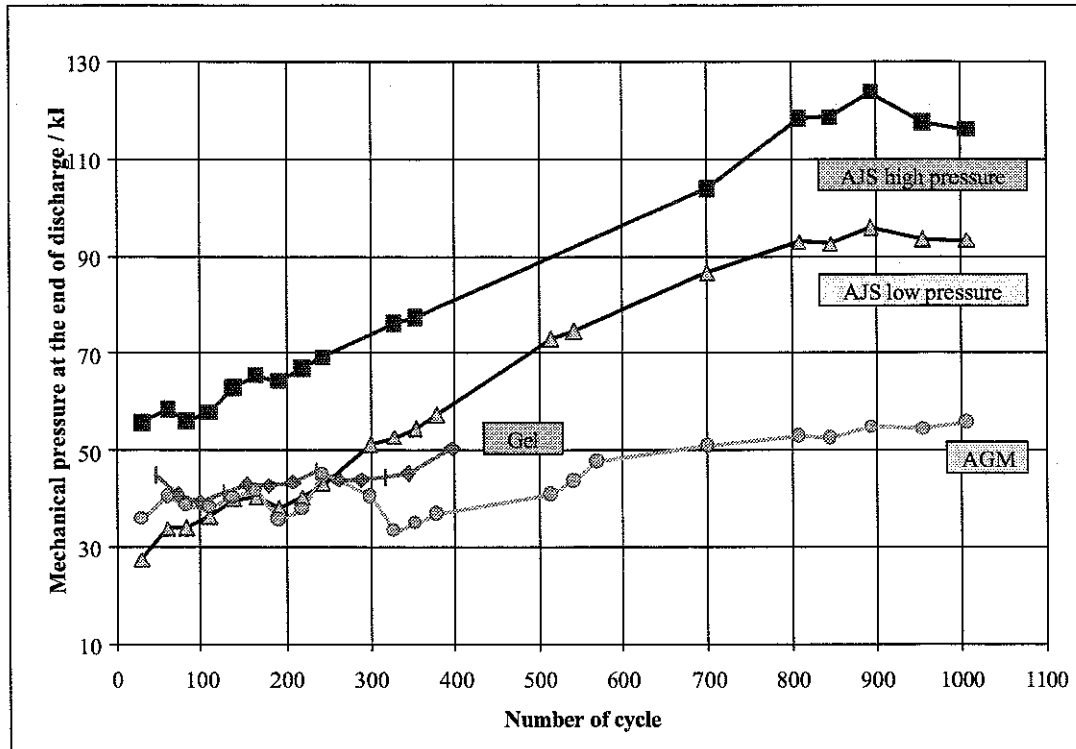


Figure 55: Evolution of mechanical pressure at the end of discharge

The increase of mechanical pressure at each cycle is related to the ageing of the cell/battery caused by the positive electrode expansion.

For the compressible systems, AGM and gel, the mechanical pressure at the end of discharge does not change much over cycling life. Once again, the increase in mechanical pressure associated with the ageing processes is accommodated by the deformation of the separation/immobilisation system: the electrodes expands and the distance between the electrodes decreases. Therefore, it is very difficult to make any conclusion about the ageing of a cell basing on the only observation of the mechanical pressure in compressible systems. For the AGM separation system, in the beginning of life, the mechanical pressure at a given state of charge does not change but from cycle 350 on, a small increasing tendency can be observed. These two different behaviours can be imputed to a possible change of its mechanical properties after part of the fibres it consists of may have crushed under the mechanical pressure.

In opposite, for the cells containing the less compressible AJS, with increasing cycle number the mechanical pressure at the end of discharge increases almost linearly, reaching a kind of plateau at the end of life.

Figure 55 shows that a “process of self compression” takes place for the AJS system. From a practical point of view, it means that the plate stack can be put together tightly in the cell container by the manufacturing and that provided the case does not deform, the changes in the active material that happen with increasing cycle number will lead to the development of a mechanical pressure in the case. This is only allowed by the fact that the separator does not deform when submitted to a mechanical pressure.

The straight line interpolation of both curves relative to AJS between cycles 50 and 900 gives the results presented in Table 11.

	Equation of the strait line	Regression coefficient
AJS 30 kPa	$Y= 0.084*X+26.4$	$R^2=0.98$
AJS 80 kPa	$Y= 0.081*X+50.4$	$R^2=0.98$

Table 11: Linear interpolation of the mechanical pressure at the end of discharge versus cycle number.

The increase of the mechanical pressure for one cycle is independent from the initial external mechanical pressure. Additionally, the kind of plateau is reached for the two AJS cells after the same number of cycle, i.e. some 900 cycles.

The fact that the mechanical pressure does not recover the initial value after one cycle can be related with three possible ageing processes:

- Firstly with the sulphation i.e. the formation of lead sulphate crystals during the discharge that are not reduced during the subsequent charge. This sulphation is related with an irreversible expansion of the active material
- Secondly with the corrosion of the positive grid that happens during charge. The products of the corrosion of lead have a bigger volume than the initial alloy and since the corrosion reaction is a solid state reaction the transformation can be associated with a development of force (see section 4).
- Thirdly to an irreversible change in the structure of the active material. It was already observed that e.g. the porosity of the PAM increases during cycling life. (see next section and Figure 42)

Even the application of high initial mechanical pressure cannot hinder the ageing process that is causing the increase of mechanical pressure with increasing cycle number. This is shown by the fact that the initial external mechanical pressure applied on the AJS cell has no influence on the increase of mechanical pressure with cycle number and this increase is linearly going on, even at high cycle number.

The ageing process now has to be identified. This only can be done by post mortem analysis of the plates of cycled cells. This analysis is reported in the following section.

3.6 How does EMPA affect the performance of the lead-acid battery

3.6.1 Changes in the structure of the negative electrode

The negative electrode is affected by the application of mechanical pressure in a manner that can lead to a limitation of its capacity. In Table 12, the porosity and thickness of negative electrodes of two cycled cells and one new cell are recorded. In this case, the porosity was determined by water saturating and weighting the plates that have been washed and dried after opening.

Cell	Cycles performed	Porosity /%	Negative plate thickness /mm
New	0	55-57	1.9
Gel	472	46	1.9
AJS 60 kPa springs	464	40	1.7

Table 12: Porosity and thickness of new and cycled negative plates

The porosity decrease with increasing cycle number of the negative plate in the lead-acid batteries is a well known phenomenon. It is a normal process when associated with an expander loss (see

section 1.6.7). In the case of the AJS cell Table 12 refers to, the decrease in porosity is much more pronounced than for the gel cell cycled under lower constraint. This leads to the conclusion that the application of mechanical pressure on the walls of a lead-acid cell is responsible for a decrease of the porosity of the negative plate due to a mechanical compaction. In parallel with the porosity, the thickness of the negative plate decreases as a result of compaction and the final thickness of the negative plate is the thickness of the grid.

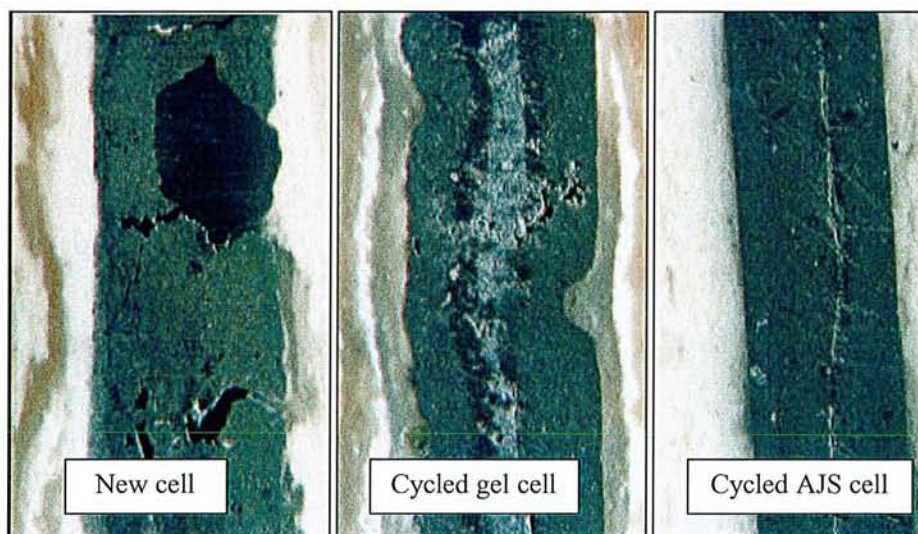


Figure 56: Cross section of the negative plates.

The pictures of the negative plates cross sections in Figure 56 show that the loss of porosity is associated with the formation, in the middle of the negative plates, of a region of higher porosity and of different aspect that seems to consist of lead sulphate while the outer layers are consisting of lead. There seems to exist a lack of recharge of the inner part of the plate that is responsible for the lead sulphate layer in the centre of the negative plate.

Surprisingly, when looking at the data of Table 13, the sulphate content of the negative plate is increasing with increasing mechanical pressure. While the sulphate repartition in the negative plate of the AGM differs between the top and the bottom, no stratification of the sulphation is observed between the top and the bottom of the plate for the AJS cells. The presence of sulphates is not related to an inhomogeneous repartition of the electrolyte. In the same time as the sulphate content increases, the thickness of the central layer decreases what speaks in favour of a more homogeneous repartition of the sulphate when mechanical pressure is applied.

Cell	negative top	negative bottom
AGM 30 kPa (1039 cycles)	10.9	15.1
AJS PA 30 kPa (1051 cycles)	10.1	10.5
AJS 60 kPa springs (467 cycles)	12.5	12.4
AJS 30 kPa (1051 cycles)	11.9	10.0
AJS 80 kPa (1024 cycles)	14.0	14.7

Table 13: Lead sulphate content of the negative plates (mass %)

In the beginning of the cycling life, a compaction of the outer part of the negative electrode takes place. From Figure 55, one deduces that until cycle 100, the irreversible increase of the mechanical pressure with cycling is partially compensated by the compaction of the negative active material. From cycle 100 on, there seems to happen no more compaction. The separator is now applying the mechanical pressure on the grid and there is no more deformation of the negative active material.

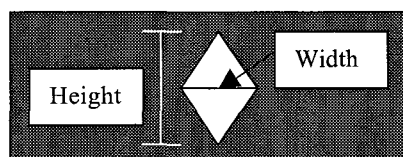
It is quite logical that the compact layer is formed on the surface of the negative electrode. The inner part of the electrode is not affected because the transfer of the pressure to the central part of the plate is hindered by the presence of the grid and by the fact that the AJS separator cannot be deformed. As can be seen on Figure 56, the negative plate has a very regular, very straight surface, showing the perfect contact between the separator and the plate. Only a kind of smooth “print” of the negative grid could be observed on the surface of the separator in Figure 27 and no concave parts were present on the surface of the negative plate thus showing that once the separator is in contact with the grid, the compaction stops.

The compaction of the negative active material could be hindered if the plate was not overpasted. The results presented here show that once the AJS separator is applying the pressure on the grid, no further compaction of the negative plate takes place that is due to mechanical pressure. Therefore, if the negative plates are not overpasted, the separator would be in contact with the grid from the beginning on and there would be no compaction due to mechanical effects but only electrochemical compaction due to the expander loss.

3.6.2 *Post mortem analysis of the positive electrode*

3.6.2.1 Analysis of the positive active material

The sulphate content of the active material that composed the electrodes was chemically analysed with the method described in section 2.4. The plate thickness and the thickness of the grid were measured under optical microscopy. The dimensions of the grids wires are explained in the following schema.



All these values are summarised in Table 14.

Cell	Lead sulphate top/bottom /wt%	Plate thickness /mm	Wire height and width /mm
New	<5/<5	2.85	2.4/1.9
AGM	11.1/13.5	3.9	2.1/1.7
AJS 30 kPa	12.8/10.5	3.65	2.1/1.7
AJS 80 kPa	9.2/13.4	3.35	2/1.6

Table 14: Sulphate content, grid and plate thickness of new and cycled positive electrodes

The positive grid corrosion was much advanced in all the cells after over 1000 cycles but no conclusion about the corrosion rates can be made. All grids were corroded to the extent that the integrity of the plate was only conserved because of the tight stack packing. Of course, the corrosion can lead to the development of forces due to the higher volume of the corrosion products but it is very improbable that

the increase of mechanical pressure is related to these mechanical effects since the small deformations at the grid/active material interface are absorbed by the near surrounding active material.

The sulphate content is quite similar in all the cells. Even if doubled in comparison with a new plate, the sulphate content in the active material is not high enough to be the reason for failure of the plates.

The point that is really emerging from these data is the expansion of the active material. In the three cells, the positive plate grew. In parallel with the growth of the plate, the active material becomes more porous, thus showing that the growth is not related to an irreversible formation of sulphates. Table 15 illustrates the parallel modification of the plate thickness and of the porosity.

Cell	Cycles performed	Porosity /%	Positive plate thickness /mm
New	0	51-57	2.85
AJS 60 kPa springs	464	58-61	3.4
Gel	472	63	4.1

Table 15: Positive plate thickness and porosity of cycled cells.

Therefore, the increase of mechanical pressure over life that is recorded in Figure 55 is explained by the expansion of the positive active material. Since the free room in the cell is limited and the thickness of the cell is kept constant, this expansion happens at the expense of the negative plate and by a reorganisation in the cell (accommodation of the small initial irregularities of the surfaces...).

3.6.2.2 Structural changes in the positive electrode

The fact that the porosity of the positive plates increases with cycling was proved in the former section. It is now of interest to see how the porosity changes, if homogeneously or not.

Figure 57 shows pictures of the positive electrodes cross sections of an AGM cell and two AJS cells under different initial mechanical pressures after over 1000 cycles.

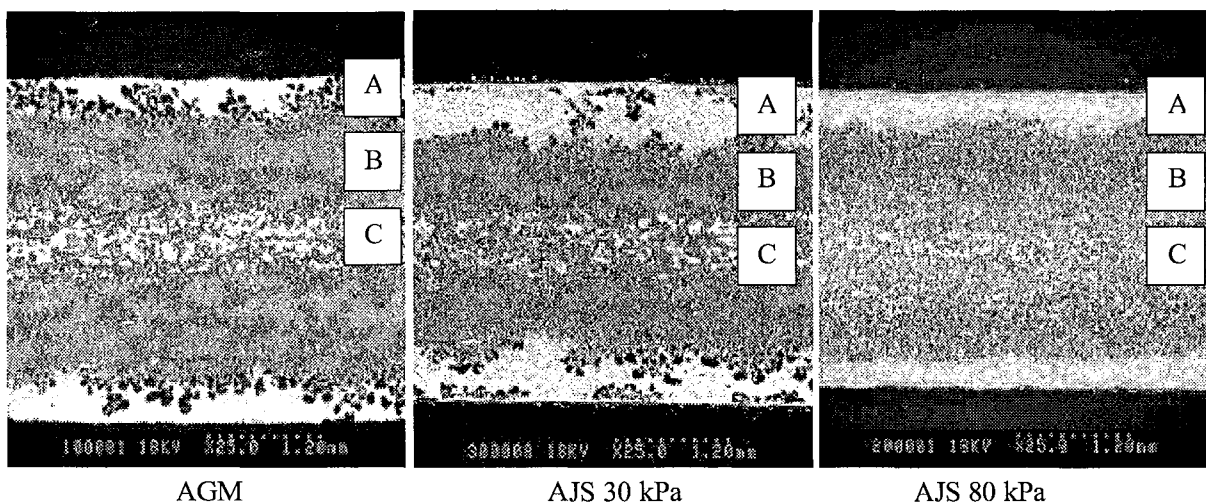


Figure 57: Pictures of the cross sections of cycled electrodes in a charged state after over 1000 cycles

Naturally, also in these cells, the higher the initial external mechanical pressure, the smaller the expansion of the positive active material.

Generally, three layers can be distinguished as schematically represented in Figure 58.

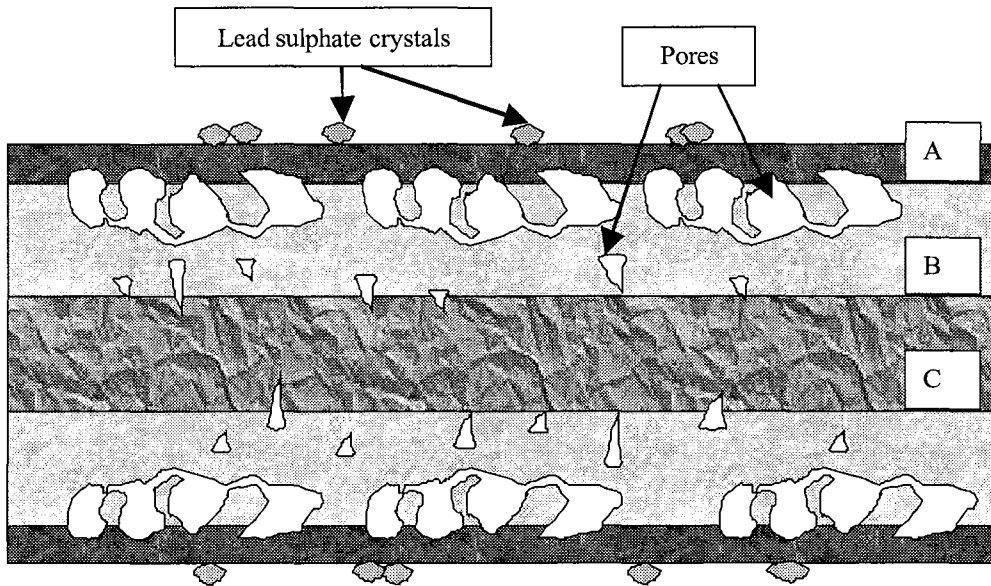


Figure 58: Schematic representation of the structure of a cycled positive electrode

Layer A. The outer layer, that is somewhat thicker and with less big pores in the AJS cells corresponds to the region of high packing density that forms nearest the electrolyte in positive electrodes cycled under compressive condition as described by Hollenkamp in [33]. It is composed of small crystals of lead dioxide with a high packing density. For Hollenkamp, these particles have lost contact with the bulk and have been transported by oxygen bubbles out of the active material at the end of charge or during overcharge. The thin lead dioxide particles come from the inside of the bulk and have been stopped at the surface of the separator when there was no room to move further. In the case of a flooded cell, these particles would have left the electrode. When the separator in contact with the positive electrode has large pores, the fine particles of material can enter the separator as is the case at some places in AGM. And when the separator has very small pores, the “would have shed” active material is retained at the interface separator/positive electrode.

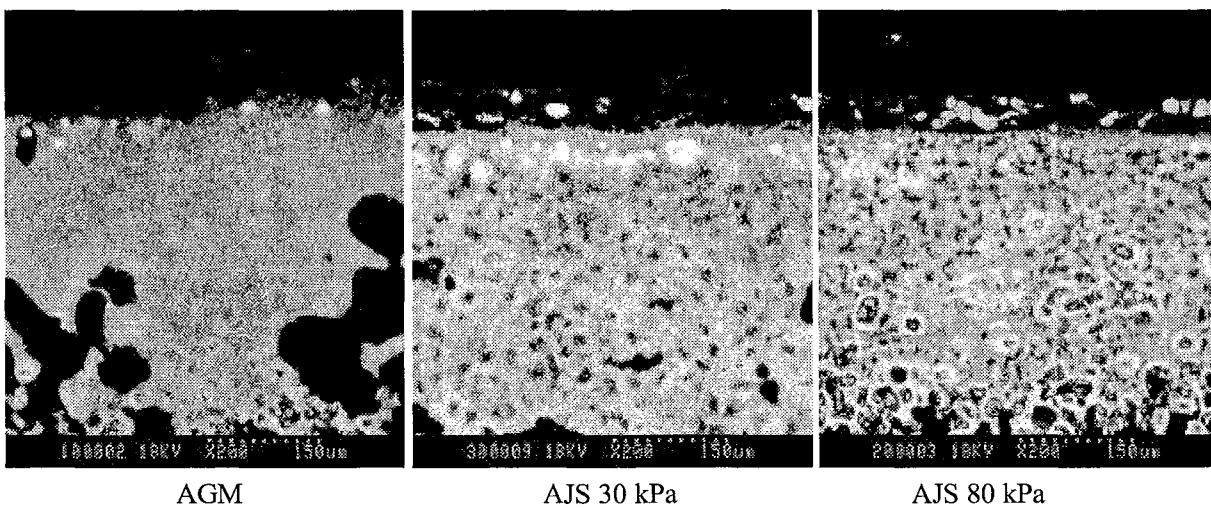


Figure 59: Pictures of the superficial layers of the positive plates after cycling in an AGM cell or in an AJS cell under two different initial mechanical pressures.

Figure 60 shows the BSE micrograph of the positive electrode external layers of two AJS cells under a different initial external mechanical pressure. The microprobe analysis shows that the layer A consists exclusively of lead dioxide which surface is partially covered with big lead sulphate crystals

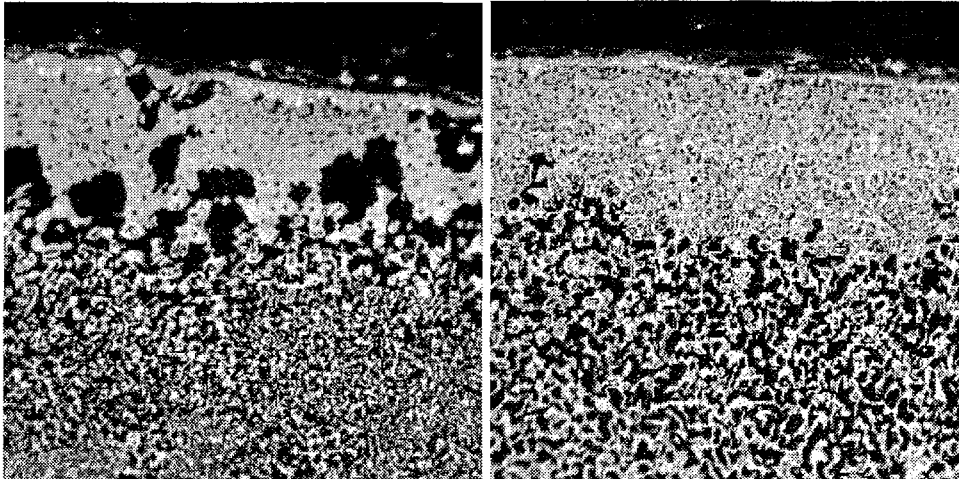


Figure 60: BSE picture of the positive plate of AJS 30 kPa (A) and AJS 80 kPa (B) (multiplication factor 60)

It seems that the external layer is not electrochemically inactive and takes part to the charge and discharge processes. Otherwise, it would not consist of pure lead dioxide but would show a strong transformation into sulphate as a result of self discharge over the long time of inactivity. But the dense layer A may have the drawback of hindering the acid diffusion between the active material pore system and the separator bulk electrolyte system.

With increasing mechanical pressure, the zone of very large porosity at the interface between the layers A and B disappears. This zone of very high porosity probably forms as a result of the free room that exists when the relaxation of the structure takes place during charge. When only little mechanical pressure is applied on the cell, some free space can develop between the separator and the positive plate as the positive plate shrinks during charge. This free room becomes partially filled with the “would have shed” material but large pores are present at the periphery of the positive active material that is filled with electrolyte and provides an electrolyte reservoir for the next discharge. This only happens if there is room for expansion, so that the positive plate is allowed to grow and undergo elastic deformation. When there is no room for the positive plate to grow, the discharge products must precipitate in the structure and irreversibly deform the structure.

It also seems possible, basing on the shape of the large round pores and of the pores in the inner layer, that some gas under pressure is responsible for the formation of the layer A and of the large pores at the frontier between layers A and B.

Layer B contains the active material with the main contribution to the charge/discharge reactions at the considered rate of discharge. It is composed of lead dioxide of high porosity. When the mechanical pressure applied on the electrode increases, this layer is more homogeneous and composed of coarser particles with larger pores between the aggregates.

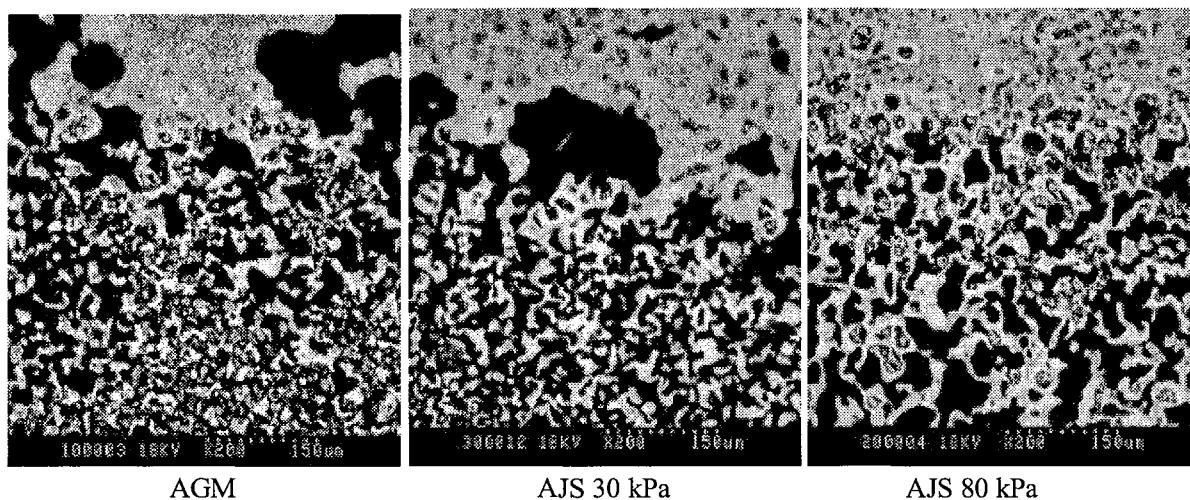


Figure 61: Intermediary layer (B layer) of positive plates in the charged state after cycling in AGM and AJS cells

In the case of the AGM cell, layer B is composed of small lead dioxide aggregates juxtaposed with lead sulphate crystals. In the case of the cells with AJS, the aggregates have a rounder shape and this layer contains fewer sulphates than in the AGM cell. For comparison, the intermediary layers B of two cells are shown in Figure 62 with a larger magnification.

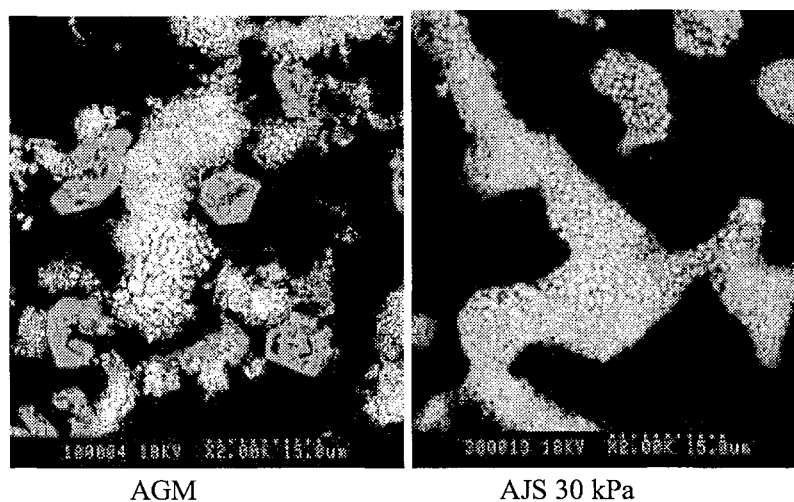


Figure 62: Intermediary layer of the positive electrode of an AGM cell and an AJS cell after over 1000 cycles

In our experiments, the cycling regime consisted of discharges at approximately the two hours rate. At this rate, the usual observation is that only the outer part of the positive active material takes part to the discharge. This was shown in [82] by analysing the sulphate content versus the position in the electrode after discharge of a positive plate and is illustrated in Figure 63.

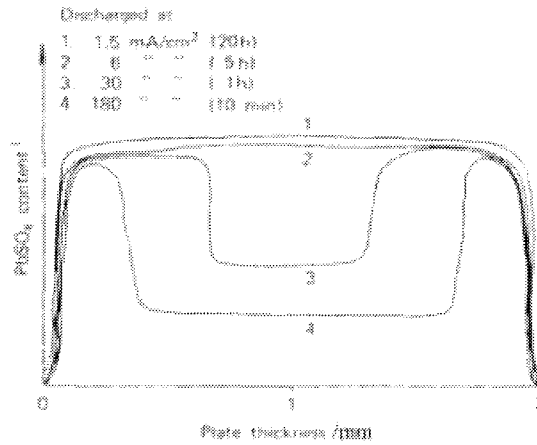


Figure 63: Lead sulphate distribution across the thickness of discharged positive plates as a function of current density [82]

The reason for the inhomogeneous mass utilisation is the limitation of the acid supply. At high discharge rates, the inner acid contributes more to the discharge and the contribution from the outer acid is limited to the zone near the edge of the electrode. The diffusion of sulphuric acid is even more limited in positive electrodes with a compact layer on the surface, what explains the presence of the third layer of medium porosity in the inside of the plates.

Layer C is much more observable in the cells submitted to low initial mechanical pressure. This layer is composed of the active material that did almost not participate to the charge discharge cycles because of the high discharge rate and the subsequent limitation of the discharge capacity through limited acid supply in the inside of the electrode. When the mechanical pressure applied on the electrode increases, layers B and C tend to form one unique layer.

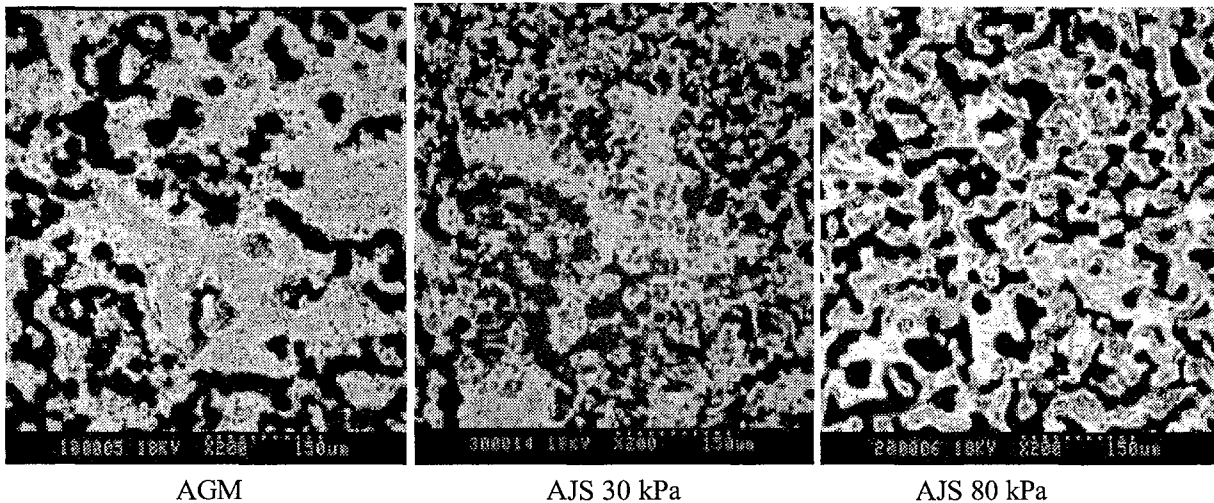


Figure 64: SEM pictures of the internal layers of the positive plates after cycling in an AGM cell or in an AJS cell under two different initial mechanical pressures.

Layer C has different structures depending on the cell concerned as can be observed on Figure 64. For the cells under low compression, the structure of the internal layer is similar to the one of the new active material, thus demonstrating that layer C effectively consists of active material that did not fully

participate to the charge and discharge reactions. The active material particles have a shape with angles as if consisting of particles from the original active material from which a part did dissolve.

Surprisingly, with increasing external mechanical pressure on the positive electrode, the thickness of layer C decreases or more precisely, the shapes of particles from layer B and C are very similar and the porosity as well. The active material consists of agglomerates of rounder shape. Clearly, the structure of layer C in the AJS cell under 30 kPa is the intermediary between the structure of this layer in the cell cycled under low mechanical pressure (AGM) and the cell cycled under high mechanical pressure (AJS 80 kPa). The pictures of the four structures of layer C are presented in Figure 65.

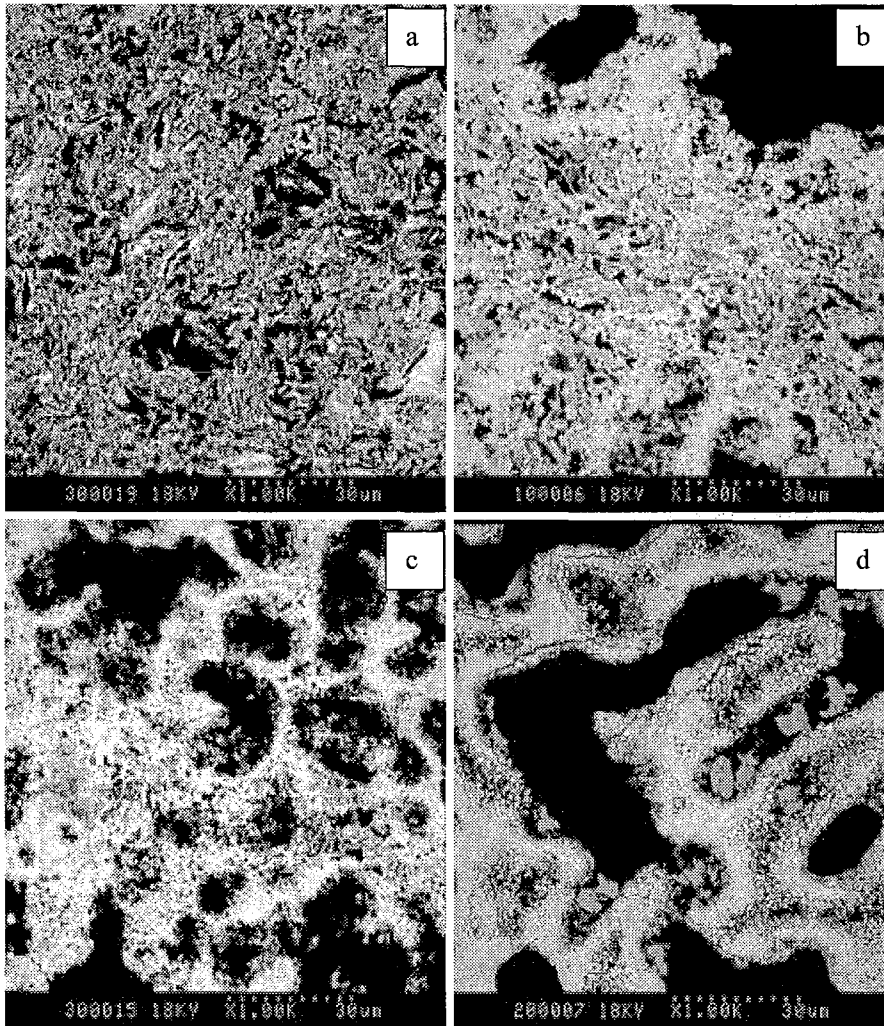


Figure 65: SEM pictures of layer C for a new cell (a) and cells after cycling: AGM (b), AJS 30 kPa (c) and AJS 80 kPa (c)

With increasing mechanical pressure, there is a displacement of the charge/discharge reactions to the inside of the positive plate. The reason for this displacement is the diminution of the free room related to the mechanical pressure application.

When during discharge the lead sulphate crystal has reached such a size that its faces press on the walls of the pore in which it grows, the further crystallisation is delayed because the supersaturation does not provide a sufficient driving force to break the structure. As a consequence, the reaction is displaced to the inside of the plate because the acid had a bit time to diffuse to a place where less supersaturation was

UNIVERSITY OF ALBERTA
LIBRARY
EDMONTON, ALBERTA
T6G 2G4
CANADA

required for the growth of the lead sulphate. When the relaxation takes place during charge, a void is left that can be filled with acid and can act as an acid reservoir for the next discharge.

When only little mechanical pressure is applied on the cell and there is free room for the expansion of the active material, the reduction reaction is limited to the external part of the positive plate since there is no driving force for a displacement of the reaction towards the inside of the plate. Namely, the deformation of the structure is easy and the expansion can take place in the free room. Thus, no large porosity forms in the inside of the plate that would itself allow the utilisation of the active material inside of the plate.

That way, the displacement of the discharge reaction towards the inside of the positive plate results from the application of mechanical pressure. This displacement create more favourable conditions for a higher active material utilisation in the zones where the active material already underwent a discharge/charge cycle and the propagation goes progressively on.

Some of the agglomerates of layers B and C in the AJS cell under high initial mechanical pressure can be considered as “islands with a beach of lead dioxide around a heart of lead sulphate”. Figure 66 illustrates this idea and both “beach” and “island” were analysed with the microprobe analyser.

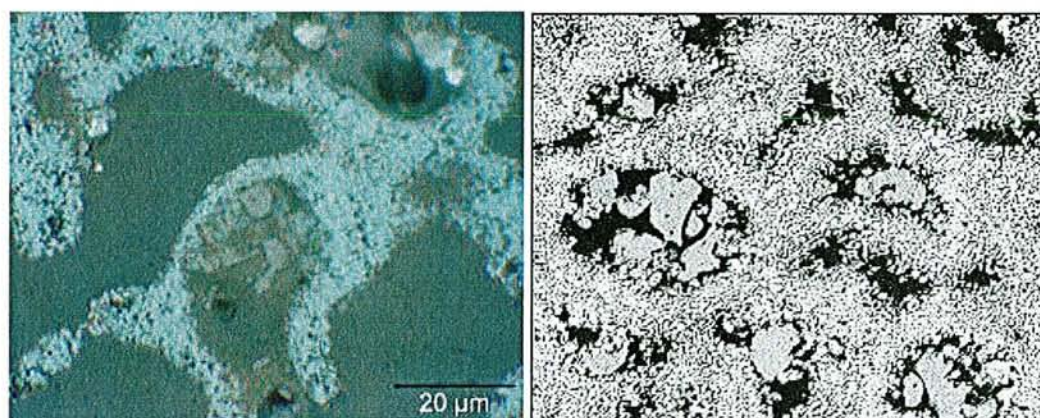


Figure 66: Agglomerates in the active material of the AJS 80 kPa cell after over 1000 cycles [optical micrograph *500, BSE micrograph *700]

The formation of these “sulphate islands” in the plates submitted to high mechanical pressure proves a limitation of the mass transfer through the lead dioxide formed under high mechanical pressure. During charge, the surface of the lead sulphate crystals dissolves to form lead dioxide and the sulphate ions have to diffuse away from the reaction site. The fact that the recharge cannot fully proceed is proving that the lead dioxide formed during charge under mechanical pressure is more compact and slows down the mass transfer. The process of formation of these compact belts of lead dioxide is easily understandable. When the lead sulphate crystal grows, it pushes the small lead dioxide particles and aggregates around it that do not take part to the discharge. Since there is only few free room due to the applied mechanical pressure, the lead dioxide particles and aggregates are pushed against each other.

During discharge, the lead sulphate dissolves but the belt of compact lead dioxide slows down the diffusion of sulphuric acid outside of the cavity the lead sulphate crystal created. The higher the mechanical pressure applied on the cell, the smaller the free room. Thus, the more compact the lead dioxide belts. For this reason, the sulphate islands are more observable in the cell under higher compression even if the forms typical for the process of alveole formation are also observable in the AJS cell under low mechanical pressure.

This process of “alveole” formation is also the base for the formation of a skeleton of compact lead dioxide that can be observed on the second picture in Figure 62. When a lot of free room is available as is the case in the AGM cell, the density of lead dioxide aggregates is not so high so that they do not agglomerate to form the skeleton.

3.6.3 Models describing the positive active material

As described in section 1.6.6.2, the premature loss of capacity of the positive electrode, that is the cause of failure for many of the batteries, is proved to be a consequence of the decrease in the conductivity of the positive plate or more precisely, of some regions of the positive plate [33].

3.6.3.1 Conductivity and mechanical pressure

The conductivity of the powder of an electronic conductive material can be related to the mechanical pressure to which is submitted [83] and the lead dioxide of the batteries positive active mass can be approximately described as a sintered powder. But it was proved that in the case of the lead dioxide positive active material of the lead-acid battery, both the resistance of the interface active material/current collector and the active mass resistance measured in cells on which walls a mechanical pressure is applied “are independent of compression” [84]. It means that the electrical conductivity of the lead dioxide material itself is not improved by the pressure applied on it in the range considered (between 0 and 200 kPa). Therefore, the improvement of the performance of the lead-acid battery, when submitted to mechanical pressure, cannot be imputed to the direct effect of mechanical pressure on the conductivity of lead dioxide.

3.6.3.2 PbO₂ as an agglomerate of sphere

Following the work of Euler on the conductivity of powders (e.g. [83], [85]), the agglomerate of sphere model was first applied to the lead dioxide electrode in 1989 [87] (AOS, in German “Kugelhaufen”). In order to explain the variation of the PAM conductivity over discharge. Meissner wrote a very useful review on the AOS theory in [30] and a further development of the AOS theory is made in the excellent paper of Edwards and Schmitz [17]. In the next lines, we try to summarise the idea and the main results of the AOS.

The fully charged positive electrode of the lead-acid battery is considered as consisting of spheres of lead dioxide. These spheres are contacted by so called necks. A schematic representation of the structure of the active material is represented in Figure 67. With such a representation, in a given volume of active material, the conductivity is governed by the number and shape of inter-particles.

As was described in section 3.4.2.2, “a small crystal experiences compressive stress as a result of its surface energy” [79]. The Laplace pressure for the neck and the sphere are also given in Figure 67 as well as the potentials associated to these pressures.

The Laplace pressure on the necks is negative therefore, under equilibrium conditions, material will flow from the spheres to the necks in order to decrease the absolute value of the Laplace pressure on the necks until $|P_N|$ equals the yield stress (ϵ_0) of the material. Therefore, there is a fixed relation between R and h. (with the geometric relation $R^2 + (h+r)^2 = (R+r)^2$ and if $h \ll R$, $|P_N| \approx 2\gamma R/h^2 = \epsilon_0$)

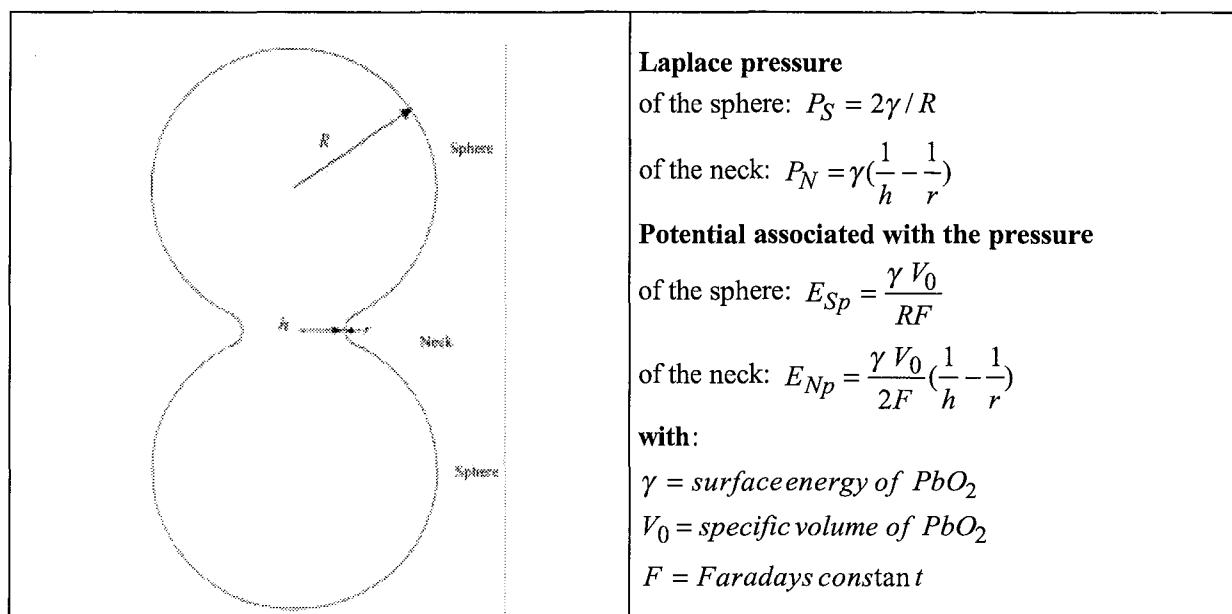


Figure 67: Geometry of the AOS model [17]

Accordingly to the equations in Figure 67, the potential of the sphere associated with the Laplace pressure is higher than the potential of the necks.

For Meissner, the difference of potential between the necks and the spheres leads to very important conclusions concerning the lead-acid battery. During rest, the material of the spheres will tend to dissolve and move to the necks, thus stabilising the structure of the agglomerate of spheres. And during discharge, the reaction will preferentially happen on the spheres, thus leaving the necks intact. As a consequence, the conductivity of the active material is not affected until discharge is quite advanced.

The difference in potential between the necks and the spheres can be related to a variation of the stoichiometry of the lead dioxide. In fact, the “The deviation from stoichiometry δ of $\text{PbO}_{2.8}$ decreases with increasing $\text{PbO}_{2.8}$ electrode potential” [30]. Therefore, the active material composing the necks deviates more from the stoichiometry than the active material composing the spheres. Since the deviation δ has lower and upper limits ($0.003 \leq \delta \leq 0.016$), the potential difference between the necks and the spheres has also an upper limit.

$$\Delta E = E_{Sp} - E_{Np} = \frac{\gamma V_0}{2F} \left(\frac{2}{R} - \frac{1}{h} + \frac{1}{r} \right) = -0.124 \log(\delta_R / \delta_h) \leq 0.09 \text{ V} \quad \text{Equation 14}$$

Therefore, with the geometric relation $R^2 + (h+r)^2 = (R+r)^2$ between R , r and h , the relative values of R and h are limited by the critical value that equalises both terms in Equation 14.

Edwards and Schmitz come to the critical ratio by another way. For them, the lead dioxide electrode is also an oxygen electrode since the stoichiometry of lead dioxide depends on the oxygen partial pressure. Therefore, the potential of the lead dioxide electrode at the necks and at the spheres is a summation of the term associated with the Laplace pressure and the term related with the oxygen partial pressure. It can be noted $E = E_{Laplace} + 0.991 - 0.124 \log \delta + 0.0592 \text{ pH}$

Consequently, the difference in potential between the two locations on the lead dioxide electrode can be calculated.

$$\Delta E = E_{Sp} - E_{Np} - 0.124 \log(\delta_R / \delta_N)$$

The difference in potential related to the Laplace pressure can be accommodated by the stoichiometry of the necks and spheres. For this purpose, contrary to the idea of Winsel et al. [86] and [87], δ will increase on the spheres while it will decrease on the necks. With the same limits of deviation from the stoichiometry, they find the same critical ratio for R/h that can be accommodated by the stoichiometry. If the critical ratio of R/h is exceeded, the difference in potential between the necks and the spheres due to the Laplace pressure can no longer be accommodated by the stoichiometry and the oxygen evolution is favoured over the charge reaction in the necks regions. Therefore, the necks dissolve and shedding happens. For these authors, the application of mechanical pressure increases the critical R/h ratio from which on the oxygen evolution is favoured on the necks zones.

3.6.3.3 Coarse structure and micro-structure

While the AOS theory explains the micro-structural changes in the positive plate of a lead-acid battery, the changes in the coarse structure stay unexplained. Pavlov and Bashtavelova [88] were the first to develop the idea of the positive plate consisting of a skeleton that is responsible for the mechanical stability and the conductivity and that is covered by thin active material that is the energy part of the plate and takes part to the charge discharge process.

3.6.4 *Why mechanical pressure application increases the life of the positive active material*

Figure 60 shows that the aspect of layer A is not much influenced by the increase of the initial external mechanical pressure even if in the AGM cell, the layer can be discontinuous and present some large pores. Therefore, the decreased production of oxygen and decreased transport of particles that lost contact to the bulk does not seem to be the reason for the improvement of the positive plate performance by mechanical pressure application. Additionally, the theory of Edwards and Schmitz that implies that the necks dissolve during charge is difficult to accommodate with the fact that capacity loss is observed in cases of insufficient charge and when low current is used at the beginning of charge.

It is clearly understood that the loss of capacity is related to a loss of conductivity of the positive active material or more precisely, of some parts of the active material [33]. This conductivity loss is associated with an increase of the porosity and therefore, we will conclude that the loss of mechanical integrity is responsible for the loss of conductivity.

The results presented induce the conclusion that the application of mechanical pressure is responsible for less expansion of the positive plate, a decrease of the porous interface between layers A and B, a more homogeneous structure of the layer B and a more homogeneous active material utilisation. The observation of cycled positive plates shows that at high external mechanical pressure, the internal layer of the positive plate also takes part to the electrochemical reactions.

Therefore, the application of mechanical pressure has an effect on the skeleton that influences itself the microstructure.

- In first line, the application of a mechanical pressure affects the coarse structure of the positive active material. The growth of the lead sulphate crystals pushes the lead dioxide aggregates that do not take part to the discharge and since the application of external mechanical pressure reduces the free room, the aggregates are pushed against each other and form a skeleton looking like a coral. This process is associated with the formation alveoles in the charged state as a result of the dissolution of the lead sulphate crystals and allows a more homogeneous utilisation of the active material since the alveoles are filled with acid that allows the surrounding active material to take part to the next discharge process. The progression of the alveole-skeleton formation process towards the inside of the positive plate is favoured by the external mechanical pressure in the fact that the mechanical pressure application reduces the room for expansion. Since the room is limited, when the lead sulphate crystal

grew until filling the pores of the outer part of the positive electrode where electrolyte is available, a higher over-saturation is needed to allow the further growth of the lead sulphates that would have to deform the structure to further grow. This "crystallisation delay" allows the sulphuric acid to diffuse farther towards the inside of the positive electrode and react there where lower crystallisation pressures are required.

- The microstructure of the PbO_2 forming the skeleton is indirectly affected by the external mechanical pressure. It is in fact the mechanical pressure that is developed by the growth of the lead sulphates that leads to the formation of the lead dioxide with wider necks as a result of the reduction of room for expansion the external mechanical pressure is responsible for.

When the "alveole-skeleton" formation process proceeds, the active material around the alveoles is pressed together and becomes more dense. This development of mechanical pressure helps forming a highly stable structure by widening the connecting zones between the lead dioxide particles. In our view, basing on the AOS model, the pressure at the neck surface is the sum of the mechanical pressure that is transferred to the surface of the neck and of the Laplace pressure. Since the limit value of the pressure on the necks is the yield stress ($\epsilon_0 = P_{\text{mechanical}} + P_{\text{Laplace}}$), any increase of the mechanical pressure transferred to the neck will lead, for compensation, to a decrease of the Laplace pressure and thus, to an increase of the neck radius. Therefore, at equilibrium, in the places to which a mechanical pressure is transferred, the active material of the positive plates has a structure that is much more stable since the wider necks resist longer before they are desegregated during discharge.

That way, the skeleton consists of active material that is more robust against discharge but this "improved microstructure" of the positive active material is only the indirect result of the external mechanical pressure application.

As a summary, one can say that external mechanical pressure application decreases the free room for expansion. That way, a secondary mechanical pressure develops in the positive electrode as a result of the lead sulphate crystal growth that leads to the formation of an alveoles-skeleton structure. This indirect mechanical pressure is the one that is responsible for the improved microstructure of the positive active material that keeps a high conductivity while discharge proceeds as a result of wider necks according to the AOS theory. This explains why the application of a mechanical pressure does not directly affect the performance of a positive plate but increases its life.

3.7 Conclusion about mechanical pressure application on the lead-acid cell

Once again, we could measure that the application of a mechanical pressure on the walls of a lead-acid cell improves its cycling life. Moreover, the new separation system AJS was tested in lead-acid cells and batteries. Near the fact that the cells/batteries show good performance both in parameter tests and in cycling life tests, AJS proved to allow the application and the conservation over life of mechanical pressure.

3.7.1 Mechanical pressure variation on the cell walls

Independently from the separation system used and from the number of cells connected in series, in the course of one cycle, the mechanical pressure that is transferred to the walls of one cell that is **kept at a constant thickness** increases during discharge and decreases during charge.

The increase of the mechanical pressure during discharge is a result of the bigger volume of the reaction products. Even if the double sulphate reaction is a dissolution/precipitation reaction, the localised growth of crystals in the pores of the active material can lead to the development of a force sufficient to explain the development of mechanical pressure on the cell walls. The maximum of this force is related with the supersaturation of lead II species during the discharge process.

Over life, the mechanical pressure transferred to the walls progressively increases on all cells, independently of the level of initial constraint. It is the sign of the structural modification of the positive active material and it reaches a saturation around 900 cycles.

3.7.2 *Structural changes in the negative electrode*

The application of mechanical pressure has a negative effect on the negative electrode by leading to a compaction of the active material on the external sides of the electrode. This compaction can lead to a capacity loss and even worst, to a lower charge acceptance of the negative plate. This drawback could be overcome in AJS cells by not over-pasting the negative plates. That way, the separator applies the pressure on the only grid and no compaction of the active material due to mechanical effects takes place.

3.7.3 *Structural changes in the positive electrode*

A layering in the structure of the positive active material could be demonstrated.

- **A:** layer of compact lead dioxide formed on the surface of the positive electrode at the interface with the separator. The thickness and the regularity of this layer depends on the porosity of the separation system and of the intensity of the initial external mechanical pressure. The fine particles constituting this layer lost mechanical contact with the bulk of the positive active material and were transported to the outside of the bulk by oxygen bubbles. The material that composes this layer would have shed in flooded cells or entered the separator if it would have had large pores.
- **B:** intermediary layer of very porous material that consists of the active material that took part to the charge discharge reactions. For an AGM cell, this layer also contains many lead sulphate crystals. For the AJS cells, the intermediary layer consists of aggregates of lead dioxide of round shape. Part of these aggregates contain lead sulphate crystals in their centre.
- **C:** internal layer consisting of active material that did not take part to the electrochemical reactions.

3.7.4 *How does mechanical pressure application improve the life of the lead-acid battery*

The application of mechanical pressure leads to less expansion of the positive electrode because the free room is limited. Therefore, e.g. the porous interface between the superficial and the intermediary layer of the positive electrode disappears. This limitation of the expansion room has two major consequences.

- A compaction of the lead dioxide happens as a consequence of the growth of the lead sulphates and the compacted lead dioxide forms the skeleton of the positive active material. In parallel, the dissolution of the lead sulphates during charge leaves alveoles that act as sulphuric acid reservoirs in the inside of the bulk.
- A displacement of the discharge reaction towards the inside of the positive electrode takes place and therefore a better material utilisation. At high external mechanical pressure, even the most internal layer also participates to the charge/discharge reactions.

These results are proved by both the evolution of the mechanical pressure during one cycle and over life and by the observation of cycled electrodes cross sections.

3.7.5 *Importance of the separator*

The mechanical properties of the separator have a large influence on the transmission of the mechanical pressure to the active material or more correctly, on the development of a mechanical pressure in the cell. It could be clearly observed from the evolution of the mechanical pressure over one cycle where the increase of pressure during discharge related to the formation of lead sulphate was smoothed when the separation system was compressible.

But additionally to the good mechanical properties, the structure of the separator has a large influence on the evolution of the PAM structure. Comparing AJS and AGM, one can conclude that the material that

would have shed in a flooded battery or that would have entered the pores of a separator with large pore size is blocked at the interface electrode/separator when the separator has small pores. Therefore, no loss of mechanical pressure can happen through the loss of material in lead-acid cells with a separator that is hard to deform and that has small pores.

3.7.6 Perspectives

With the positive effect of the application of compression clearly defined, the question is open of “how to apply it”. A patent of 1995 [89] describes a pre-compressed AGM that would expand at the addition of electrolyte, thus setting the plate stack under a certain degree of mechanical pressure. Many ideas were also proposed by CSIRO, from the compression plate to the pneumatic plastic bag [64] and [90].

The first limitation to the application of mechanical pressure on the plate stack from the inside of the battery container is that nowadays, the polymer used for battery casing undergo deformations. One can often observe the convex form of the battery walls after some cycles as schematically represented in Figure 68.

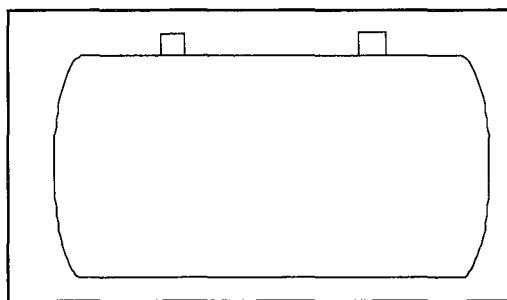


Figure 68: Schematic representation of a battery after some cycles.

In fact, the application of an external mechanical pressure would be already partially practised if the battery cases would undergo only little deformation. That way, the irreversible expansion of the positive active material would lead to a “self compression”. But the poor mechanical properties of the separation systems used at the present time hinder a “full scale self compression effect”. Therefore, a separator with better mechanical properties is also necessary for sustaining the mechanical pressure over the cycling life. Our work showed that a new separation system (AJS) allows a mechanical pressure to build up progressively in the battery that leads to an improved cycling life with no cost for the electrical performances. Thus the utilisation of a hard battery case in association with the AJS separator, plates with high paste density and a regular surface may be a solution to the premature capacity loss of the current batteries. The high density paste would be allowed to expand a bit to fill the small free room that is related to the irregular plate thickness and the “self compression mechanism” could enter in action. Additionally, the negative plate must not be overpasted so that no compaction of the negative plate takes place that would both limit the capacity and hinder "a full scale self compression effect".

In our view, it is not the intensity of the applied mechanical pressure that is important, it is the restriction of the free room for expansion. Thus, with respect to the "self compression effect" we observed, the recipe for an easy production of a "compression battery" would be.

- A separator with good mechanical properties like AJS
- A battery case of strong polymer or a stiff geometry of the case
- Negatives plates pasted on the only grid thickness
- Positive plates of high density material
- Plates with a regular surface and constant dimensions

With such components, there should be no necessity to apply an additional external mechanical pressure as the positive active material contention would already be performed.

Résumé et conclusion du chapitre concernant l'application d'une pression mécanique sur les parois d'une batterie au plomb.

Dans ce chapitre, après une description de l'état de l'art en matière de pression mécanique appliquée sur une cellule plomb/acide, les caractéristiques des différents systèmes de séparation existant pour les batteries fermées ont été comparées avec celles d'un nouveau système de séparation (AJS) mis au point par l'entreprise Daramic. Nous avons montré que des cellules et batteries produites avec le nouvel AJS présentent des performances électriques et des durées de vie extrêmement satisfaisantes. En outre, il a été prouvé que l'application d'une pression mécanique durable est rendue possible par l'utilisation du nouveau séparateur et qu'elle a pour effet, ainsi qu'il est reporté dans la littérature, d'augmenter la durée de vie d'une cellule ou batterie.

Les mécanismes par lesquels l'application d'une pression mécanique permet une amélioration des performances d'une cellule/batterie au plomb ont été identifiés.

Tout d'abord, l'amélioration des performances est le fait d'une modification structurelle de la matière active positive alors que cette même pression mécanique a un effet néfaste sur la matière active négative, conduisant à une compaction de cette dernière jusqu'à ce que le séparateur repose sur la grille de plomb.

L'application d'une pression mécanique limite l'espace libre laissé à la matière active positive pour son expansion lors de la décharge. Cette limitation de l'espace libre a pour conséquence d'une part de permettre la formation d'une structure coralloïde de la matière active positive et d'autre part, de permettre à cette structure en alvéoles de progresser vers l'intérieur de la plaque positive, conduisant ainsi à une utilisation plus homogène de la matière active.

- La structure coralloïde résulte de la formation d'îlots de sulfates de plomb pendant la décharge. Ces cristaux, en grossissant, poussent les agrégats de dioxyde de plomb les uns contre les autres et lorsque l'espace pour la croissance des cristaux est restreint, ces agrégats forment des agrégats plus gros avec des zones particulièrement compactes là où la pression des cristaux s'est exercée. De cette façon, un squelette de dioxyde de plomb est formé où les particules de dioxyde de plomb sont connectées entre elles par de plus grosses surfaces et sont ainsi plus résistantes pendant la décharge, ce qui stabilise la structure du squelette. Lors de la recharge suivante, les cristaux de sulfate de plomb se dissolvent et laissent à leur place des alvéoles contenant de l'acide sulfurique et servant ainsi de réserve d'acide pour la décharge suivante.
- La progression de cette structure coralloïde vers l'intérieur de l'électrode positive résulte elle aussi de la limitation de l'espace d'expansion. Lors d'une décharge à fort courant, seule la partie extérieure de l'électrode participe à la décharge du fait de la diffusion limitée de l'acide vers l'intérieur de l'électrode. Lorsque les sulfates de plomb se forment dans cette zone périphérique de l'électrode et ont rempli tout l'espace libre, leur croissance peut se poursuivre s'ils déforment la structure existante et pour ce faire, une pression de cristallisation plus élevée est nécessaire c'est à dire une plus grande sursaturation en ions plomb II. Ce retardement de la cristallisation laisse la possibilité à l'acide de migrer vers des zones plus internes de l'électrode où une sursaturation moins élevée est nécessaire pour la précipitation des sulfates de plomb. Ainsi, au fur et à mesure des cycles de charge et décharge, les réactions électrochimiques peuvent se produire sur une plus grande épaisseur de l'électrode puisque la formation de sulfates dans une zone interne de l'électrode permet pendant la recharge la création d'une réserve d'acide et ainsi, une utilisation immédiate de cette zone pendant la prochaine décharge.

L'évolution de pression mécanique sur les parois d'une cellule pendant un cycle et sa variation avec le nombre croissant de cycles subis supportent cette hypothèse au même titre que l'observation de sections de la matière active à l'issue du cyclage.

- Pendant un cycle, la pression mécanique sur les parois d'une cellule augmente pendant la décharge et diminue pendant la charge. Ceci résulte de la croissance pendant la décharge de cristaux de sulfate de plomb dont le volume est supérieur à celui des matières premières. Cette croissance exerce une contrainte sur la structure des électrodes pendant la décharge et la relaxation de cette contrainte est observée pendant la charge lorsque les cristaux se dissolvent et reforment les matières actives de plus faible volume.
- Lorsque le nombre de cycles subis par une cellule augmente, pour un même état de charge, la pression mécanique exercée par le bloc d'électrodes sur les parois augmente. Ceci résulte de la formation irréversible de la structure coralloïde.

Par conséquent, l'intensité de la pression mécanique exercée initialement n'est pas le critère décisif pour l'accroissement de la durée de vie. Le point important est de restreindre l'espace que la matière active positive pourrait utiliser pour son expansion pendant la charge. Pour ce faire, il faut remplir certains critères qui permettraient une production et un assemblage aisés de la "batterie en compression".

- **Choix du séparateur.** Seule l'utilisation d'un système de séparation non compressible assurera une résistance aux contraintes qui se développent dans la matière active positive. Si, comme c'est le cas du gel ou du matelas de fibres de verre, le séparateur a de faibles propriétés mécaniques, la restriction du volume de l'électrode positive n'est pas assurée. Ceci empêche la formation de la structure coralloïde et la progression des réactions électrochimiques vers les parties internes de l'électrodes à taux de décharge élevés, limitant ainsi la durée de vie.
- **Electrode négative.** Dans la mesure où la matière active supportée par la grille négative est un plomb spongiforme, celle-ci a de faibles propriétés mécaniques et se compacte sous l'effet des contraintes développées par la matière active positive pendant la décharge. Cette compaction se poursuit au fur et à mesure du cyclage jusqu'à ce que le séparateur repose sur la grille de plomb dans le cas d'un séparateur ayant de bonnes propriétés mécanique. Il est même envisageable que la compaction se poursuive dans les alvéoles de la grille si le séparateur est déformable. Outre donc un séparateur à bonnes propriétés mécaniques, des plaques négatives empâtées sur la seule épaisseur de la grille sont nécessaires pour conserver la porosité de la matière active négative lors du cyclage.
- **Régularité des composants.** Dans la mesure où le séparateur ne peut accommoder que de petites déformations, il est nécessaire de veiller à la planéité des composants et particulièrement des plaques positives et négatives. Une grande régularité de l'empâtage sera ainsi utile afin d'assurer un minimum d'espace vide dans le bloc d'électrodes.
- **Matériau du bac.** Il n'est pas rare de voir lors du cyclage les parois des bacs de batteries prendre une forme convexe sous l'effet de la pression de gaz et des contraintes liées à l'expansion de la matière active. Dans une telle configuration, la restriction de l'espace d'expansion n'est bien entendu pas assurée. Pour la production d'une "batterie en compression", un polymère relativement rigide doit être utilisé pour la production du bac.
- **Densité de la pâte positive.** L'utilisation d'une pâte positive à relativement faible densité pourrait permettre une fabrication aisée des batteries sans nécessité d'appliquer une pression mécanique excessive à l'assemblage. Nos mesures ont montré que dans des conditions d'espace d'expansion limité, un effet d'auto-compression se produit dans la cellule au plomb. Si une pâte à haute densité est utilisée, son expansion va combler le faible espace laissé libre lors de la production et la porosité de la matière active croît dans la même proportion. Une fois l'espace libre ainsi comblé, la formation de la structure coralloïde peut se produire.

4 Corrosion

4.1 Generals about corrosion of lead and lead alloys

4.1.1 Definition

The term corrosion comes from the Latin word “corrodere” or more precisely “rodere” that means “to gnaw” [91]. Corrosion describes the “reaction of a metallic material with its environment” [92]. With such a definition, some characteristics of corrosion are left behind. For example the fact that the reaction that is defined as corrosion is a reaction that is mostly a drawback and therefore not desired. The term corrosion is replaced by “oxidation” or “surface passivation” when the process is favourable. For another author, “corrosion is defined as a gradual wearing away or alteration ...[of a metal]... by a chemical or electrochemical oxidising process” [93].

The positive or the negative grid -that acts as a current collector and a carrier for the active material- is damaged by reacting with its environment. This happens because lead is not thermodynamically stable in an environment of concentrated sulphuric acid as shown on the Pourbaix diagram (Figure 7). In many cases, the irremediable corrosion is the life limiting factor of the lead-acid battery. It happens when the grid is that much corroded that it is not able any more to conduct the reaction current from the active material to the outside of the battery, when the contact between the active material and the current collector is lost or when the active material is not mechanically stabilised any more.

A growth of the positive grid is associated with its corrosion. When the positive grid grows and the rest of the stack keeps the same size, the potentiality of short circuits building across the edges of the separator is high. Figure 69 illustrates this phenomenon.

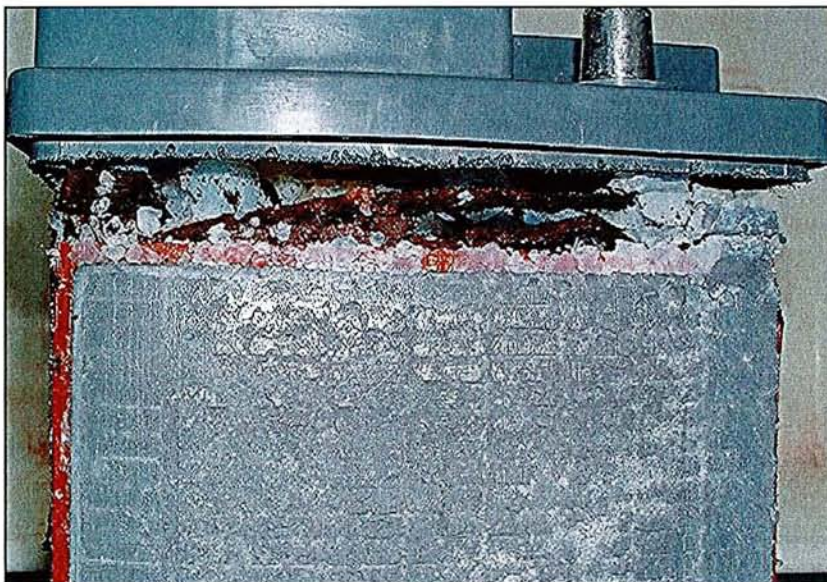


Figure 69: Picture of a gel battery that failed by corrosion of the positive grid (grid growth leading to short circuits around the top edges of the stack)

There is an additional effect of corrosion that has to be taken into account. When corrosion occurs, the oxygen ions that are reacting with the lead grid are taken from the water and the corrosion causes a dramatic water loss. While this water loss is compensated in flooded cell, in VRLA batteries, no refilling

takes place. In 1994 [94], Brecht calculates that corrosion of 25% of the grid lead in a lead-acid battery leads to a loss of 10% water. In systems, like AGM, that are very sensitive to saturation, a decrease of as much as 20% of the capacity can be observed if 10% of the water is bound in the corrosion layer.

4.1.2 When does corrosion occur

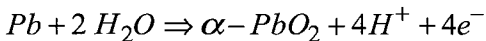
Just in the same way as for each chemical or electrochemical reaction, a corrosion reaction occurs when the value of the free energy change between the reactants and the products is negative.

$$\Delta G = [G(\text{products}) - G(\text{reactants})] < 0$$

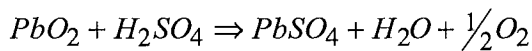
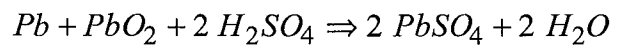
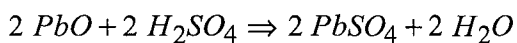
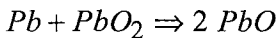
In most of the cases, one speaks of corrosion when a metal reacts with its environment and forms oxides. In this case, the reaction is necessarily thermodynamically favoured since the metal production is based on the reduction of the oxide ores. Even if this argument is not exactly valid for lead since its ore is PbS and called galena, lead reacts in the air (formation of lead oxide in presence of oxygen) and also in the electrolyte of the lead-acid battery. This reaction consumes the lead of the positive grid.

Thermodynamically favourable conditions for the corrosion of the positive lead grid are met during charge/overcharge or during rest. The corrosion reactions on the positive grid are listed below.

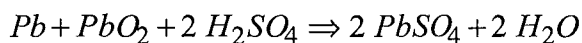
During polarisation (formation, charge and overcharge)



During rest



Self discharge reaction



Direct reaction of Pb with the electrolyte

The negative grid corrosion was described in section 1.6.7. In the present section, only positive grid corrosion will be discussed. It is in fact the one that is of most concern because leading to many of the batteries failures.

4.1.3 The corrosion layer on the positive lead grid

The nature of the developing corrosion layer is very sensitive to the polarisation conditions [95] and [96]. The following sections suggests an explanation for this phenomenon that also means that the corrosion products and corrosion rates depend on the battery operation conditions. Additionally, depending on the application a battery is built for, a different alloy will be more suitable than another, depending on its corrosion rate under the given polarisation conditions.

4.1.3.1 Positive grid corrosion during polarisation

During charge and overcharge, the potential of the grid is forced to high values. The corrosion process is then similar to a process under constant current polarisation. This is relevant for batteries used under float conditions.

In this case, the corrosion reaction has two fronts: the one at the grid /corrosion layer interface and the second at the corrosion layer/electrolyte interface [97]. At the grid/oxide interface, a dense corrosion layer builds up consisting of t-PbO and α -PbO₂, because PbO₂ and Pb cannot thermodynamically coexist [16].

When the battery is always submitted to a high polarisation, oxygen is steadily evolved. Since the corrosion layer is dense and compact, the diffusion of the oxygen species through it is hindered and limits the growth of the corrosion layer that follows the Wagner law. It means that the variation in mass of the corrosion layer increases as the square root of the time.

At the oxide/electrolyte interface, a porous layer consisting essentially of β -PbO₂ is formed as the result of a dissolution and re-crystallisation of the α - form.

4.1.3.2 Positive grid corrosion at low potential of the electrode

During rest, the potential is not forced to high values by the application of a current. A battery that undergoes cycles also goes through as rest and discharge periods and the structure of the corrosion layer is modified thereby.

In 1964, Ruetschi and Angstadt [98] described the corrosion process of a positive lead electrode at low polarisation. At a potential below 1.3V (against mercury/mercurous sulphate electrode), a lead sulphate film forms at the surface of the electrode that is only slowly oxidised to β -PbO₂ (potential between 1.14V and 1.3V against mercury) or even not oxidised at all (potential below 1.14V). The sulphate layer built by this process can act as a semi-permeable membrane and can block the transfer of big ions (SO₄²⁻) to the reaction sites in the corrosion layer, thereby favouring a higher pH and subsequently, the formation of lead oxides species of low stoichiometry like PbO. This paper is the first reference in the literature to a semi-permeable layer that promotes higher pH conditions inside of the corrosion layer. But it has to be mentioned that the conditions for the formation of a corrosion layer in a battery are quite different from those described in the paper.

In 1967, Simon was the first to report about mechanical effects in the corrosion layer [99], related to the higher volume of the corrosion products in comparison with lead. And in 1974, Simon and Caulder [100] observed that "the corrosion product around the grid section builds up during continued cycling to a point where internal stress generated within the film is relieved by cracking which extends outwards from the grid at the points of critical stress".

In 1984, Chang [101] investigated pasted grids of Pb-Ca and Pb-Sb alloy under deep cycling and found out that the corrosion layer in both cases consisted of a dense layer in contact with the grid and a more porous layer between the dense layer and the active material. The dense inner layer proved not to be modified by discharge in both case. For the Pb-Ca grid, the outer layer was covered with small lead sulphate crystals during discharge, hindering further discharge. The accumulation of these sulphates due to incomplete re-oxidation is a cause for very premature capacity loss (PCL1)

In his book of 1993 [16], D. Berndt described that at open circuit voltage, no current forces the conversion of the thin PbO layer at the lead surface to be oxidised to α -PbO₂. But the reaction between Pb and PbO₂ goes on and the PbO layer grows. Since this oxide is not stable in sulphuric acid, the fast reaction $PbO + H_2SO_4 \Rightarrow PbSO_4 + H_2O$ takes place and severe grid corrosion can occur during rest periods because the protective corrosion layer (α -PbO₂) is destroyed (particularly in flooded batteries where electrolyte is in excess).

4.1.3.3 Formation of passive layers at high pH

The Pourbaix diagram shown in Figure 7 (section 1) gives the regions of stability of the lead compounds in solution depending on the pH of the solution and on the potential. In concentrated sulphuric acid, only lead dioxide can be encountered at the positive plate potential. But if a thin layer of high density forms on the surface of lead that hinders the diffusion of sulphate ions, the pH under the barrier layer can increase

to values where isolating species like lead oxides are stable. These species are responsible for the dramatic form of the premature capacity loss.

4.1.4 Effect of the active material on the corrosion

In 1967, Simon reported that the mechanical stress caused by the active material volume variation is not responsible for the stress corrosion in the grids of the lead-acid storage batteries. He showed that the cracks that result from intergranular corrosion in the grid metals do not extend to the outer surface of the corrosion layer. And “in those few cases where the cracks did extend through the corrosion products, they also extended for a considerable distance into the active material itself, and again the cracks narrowed at the end in the active material” [99].

In 1974, Simon and Caulder [100] investigated whether active material covering has a beneficial effect on the problem of Pb/Sb grid corrosion. They showed that “while not dependent on a definite thickness, ...any effect of over-pasting is due to mechanical support of the corrosion product at the critical stress areas which thus may delay cracking”. In fact, the table in this paper showing the dependence of the corrosion layer thickness on the location of the layer indicates that the thickest corrosion layer can be measured at the place where the active material is the thinnest (if present at all). Additionally, they found out that if two pastes with the same composition but a different density are used, the formation of the adherent and dense PbO₂ corrosion layer is delayed on the plates with a high density paste. Firstly, large lead sulphate crystals are formed that are afterwards converted to lead dioxide upon continued cycling.

In 1978 [102], Feliu et al. reported clearly that pasting reduces the constant current corrosion of lead antimony grids. They explained this effect by the fact that “the paste acting itself as an anode displaces [the] anodic reaction from the metal surface towards the external surface of the paste. Since oxygen becomes liberated far away from the metal surface, the possibilities for a direct reaction between oxygen and lead decrease a great deal”. And in 1978 also [52], Alzieu wrote that his “considerations tend to attribute for the active material a preponderant role in the protection of the positive grid from corrosion”. In this case, the observation based on flooded cells in which the places where shedding occurred suffered a dramatic corrosion.

But in 1995 [95], Garche reported that during constant polarisation of a lead rod, the presence of PAM or even electronically isolating α -Al₂O₃ around the rod decreases the corrosion rate of the rod dramatically. This measurements proved that the displacement of the oxygen production to the surface of the active material, and the therefore longer diffusion time for the oxygen species were not the main reason for the reduction of the corrosion by pasting as Feliu et al. thought it to be. The reduced corrosion was proved to be related to changes in the structure of the corrosion layer (mechanical stabilisation). Additionally, if rest periods are added during the polarisation, the corrosion rate is higher for the same total time of polarisation. In fact, during rest, the corrosion layer relaxes and self discharge/corrosion takes place both in the cracks and at the lead surface that is made reachable by the cracks. The corrosion layer has then become porous throughout its entire thickness and during the following polarisation period, the dense corrosion layer has to be built again, going through a phase of accelerated corrosion.

Later on, the mechanical relaxation and associated structural modification of the corrosion layer during rest periods was proved by ultrasound measurements. [39]

4.1.5 Conclusion of the literature study on corrosion

Under constant current polarisation or overcharge, after formation of the oxide layer of critical thickness, the corrosion rate is constant depending on time. The corrosion under polarisation is a balance between two processes. Firstly the solid state oxidation of lead to t-PbO and α -PbO₂, that is limited by the

transport of oxygen ions towards the substrate and subsequently, by the oxygen production. The second process is the formation of the porous external layer with a high concentration of β - PbO_2 . This layer appears as a result of the relaxation of the stress caused by the increase in volume of the corrosion products compared to lead. Namely, in the case of a solid state reaction, forces can develop as a result of the difference in specific volume between the reactants and the products. The relaxation takes place via cracking and the cracks fill up with corrosion products from dissolution precipitation reactions, i.e. β - PbO_2 . Once the first dense layer has reached a critical thickness, the further production of t - PbO and α - PbO_2 by a solid state corrosion reaction leads to excessive internal stress and the external porous layer begins to form. The dense layer keeps a constant critical thickness and the porous layer develops. The critical thickness of the dense layer is depending on the polarisation conditions, on the nature of the lead alloy and on the mechanical stabilisation by active material.

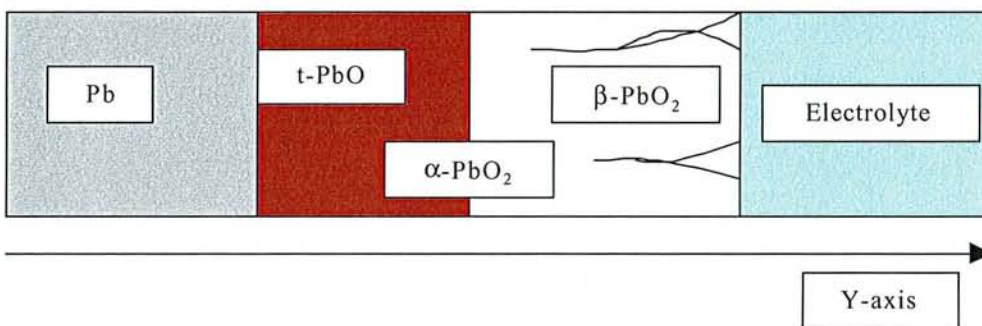


Figure 70: Structure of the corrosion layer under continuous polarisation

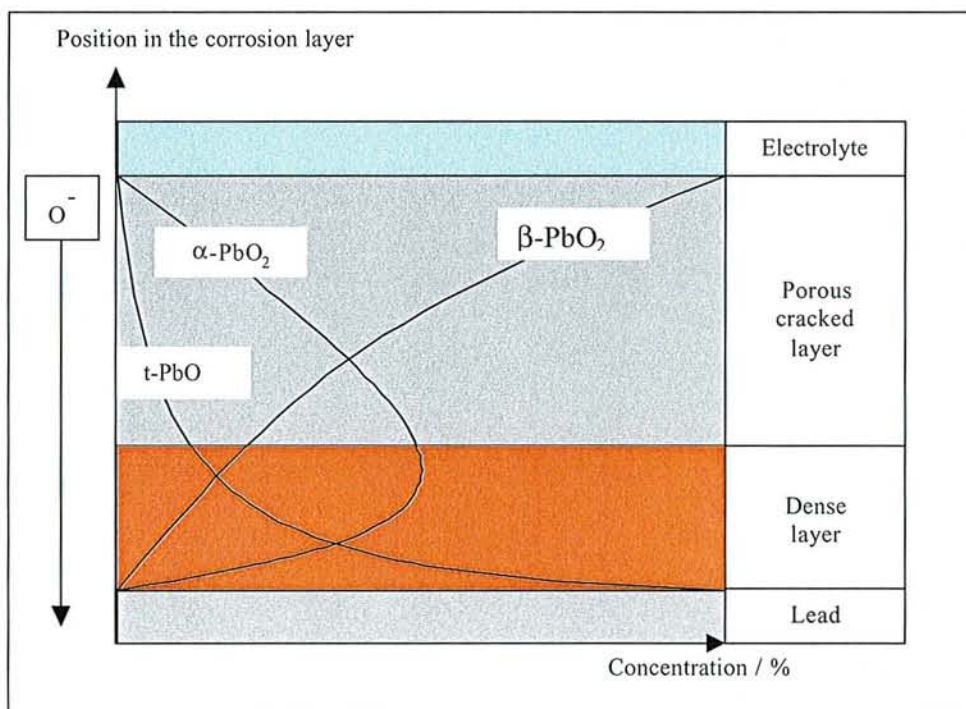


Figure 71: Schematic representation of the concentration variation for the different corrosion products in the corrosion layer

During rest, as a consequence of the mechanical reorganisation of the corrosion layer, the lead oxide of the dense layer is reached by the solution of sulphuric acid and is allowed to convert to lead sulphate. During discharge, only the external porous part of the corrosion layer is affected and converted to lead sulphate.

4.1.6 Effect of antimony

The reviewing of papers concerning the corrosion of lead alloys gave raise to many questions concerning the effect of antimony on the corrosion process. Of course, since this work deals in first line with valve regulated lead-acid batteries, the alloys that are used are generall antimony free. But the still open questions on the effect of antimony represented a small challenge and in the following section, an explanation based on the literature review is proposed for these effects.

In presence of antimony, the corrosion rate of the grid of storage batteries is lower and the corrosion product is better retained [99]. Simon explains this phenomenon by both the larger specific volume of the alloy in comparison with pure lead and the dissolution of antimony before formation of the lead dioxide corrosion product (namely, the primary corrosion product of lead antimony grids contains no antimony). These two factors lead to a “reduced volume change in the conversion from lead (alloy) to lead dioxide” and a subsequent reduction of the stress due to the bigger specific volume of the corrosion products. By opposition, under constant polarisation conditions, an alloy containing no antimony will show a better corrosion resistance than an alloy with antimony [96]. The results of Papazov et al. are summarised in Figure 72.

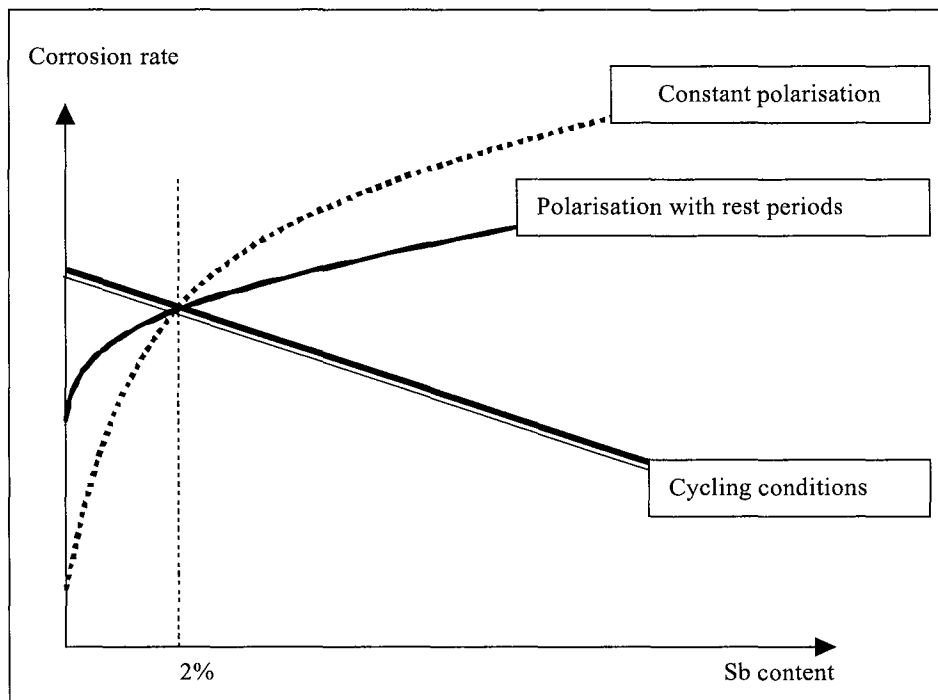


Figure 72: Dependence of the corrosion rate of a lead alloy on its antimony content for different polarisation conditions [96]

At least, Wagner [26] reports that Pb-Sb alloys suffer intergranular corrosion in a much bigger extend than Pb-Ca alloys do.

A listing of the properties of antimony in lead alloys can help understanding the processes.

- Favoured anodic dissolution of Sb in comparison to Pb.
- Increased intergranular corrosion in presence of Sb (related to the favoured dissolution).
- Higher specific volume of the Pb/Sb alloy in comparison to pure Pb.
- Smaller variation of the specific volume between the alloy and the corrosion product if Pb/Sb alloy.

Antimony seems not to influence the dense/porous structure of the corrosion layer [101]. In fact, since antimony is dissolved from the alloy and is not present in the corrosion layer, this is logical.

The importance of the mechanical effects in the corrosion layer is much increased by the rest periods, therefore the figure of Papazov et al. can be explained by the balance between the modification of the mechanical effects associated with the presence of antimony and the fact that antimony is preferentially dissolved and increases intergranular corrosion. For the same polarisation time, the more rest periods are inserted between the polarisation periods, the more the rate of corrosion related to mechanical effects increases. At constant polarisation, the effect of intergranular corrosion is predominant and the presence of antimony increases the corrosion rate. With increasing rest time inserted between the polarisation periods, the proportion of corrosion rate associated with mechanical effects increases and since the presence of antimony decreases these mechanical effects, with cycling conditions, the presence of antimony decreases the total corrosion rate.

The explanation why antimony diminishes the appearance of PCL 1 is also related to the decrease of the mechanical effects in the corrosion layer in presence of antimony. Since the difference in volume between the alloy and the corrosion product is reduced, the zone of contact between the grid and the active material is subjected to less stress in presence of antimony and the lead dioxide layer resulting from the corrosion has a low porosity and a high α -lead dioxide content. Thus the formation of a zone of high porosity, and consequently of low conductivity, is hindered by use of a lead-antimony alloy for the positive grid.

Facing this effect of antimony, it is now difficult to find an alloying element that allows the corrosion product to have a lower volume, i.e. an element that dissolves from the alloy without entering the corrosion products. But at the same time, this element should not plate the negative electrode and decrease the hydrogen overpotential. This alloying element has to have the same properties as antimony but it should not dissolve **preferentially** so that the intergranular corrosion is reduced.

4.2 Effect of mechanical pressure on corrosion

With the mechanism of corrosion explained, it was of interest to find out whether the application of mechanical pressure had an effect on the corrosion of lead. For this purpose, the grids of cycled VRLA cells were observed and investigations were carried out on pure lead electrodes outside of the battery.

4.2.1 Corrosion measurement under potentiostatic conditions

Assuming that the corrosion products do not leave the electrode and that the utilisation is independent of the thickness, the amount of lead dioxide contained in a corrosion layer can be measured by discharging this corrosion layer. The approximations are true for relatively thin corrosion layers. The mass of lead dioxide is then directly deduced from the discharge capacity using Faraday's equation.

$$Q = \int I dt \text{ (in Ah)}$$

$$Q = n_{PbO_2} * z * F$$

$$m_{PbO_2} = Q \times M_{PbO_2} / zF$$

The discharge capacity measured with the set-up described in section 2.8.2 is displayed versus cycle number in Figure 73.

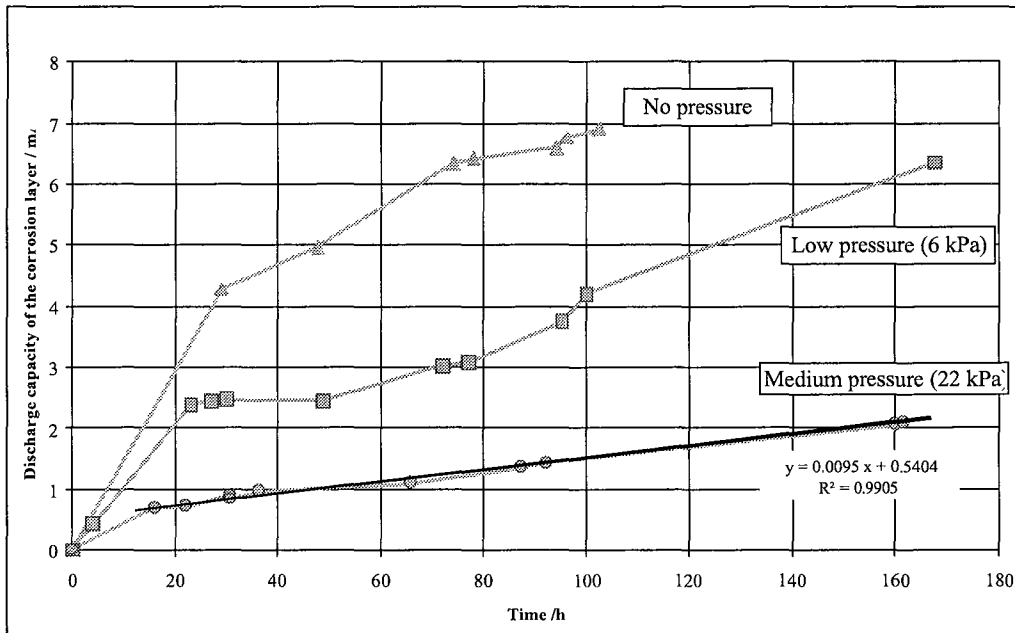
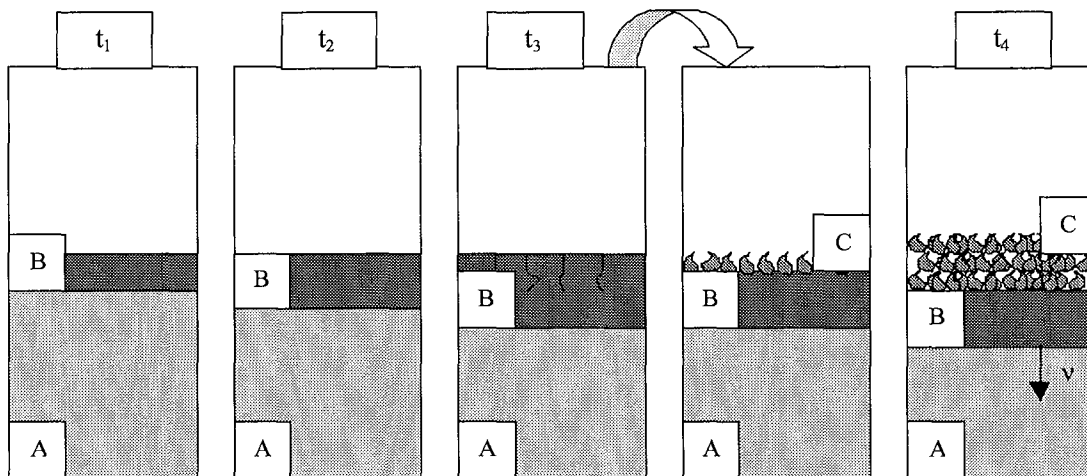


Figure 73: Discharge capacity of the corrosion layer versus cycling time.

In fact, the dense corrosion layer is almost not affected by the discharge, only the outer porous layer is participating in the discharge process. The discharge capacity of the corrosion layer increases much more rapidly, the less mechanical pressure is applied on the surface of the electrode. It means that the thickness of the porous corrosion layer decreases with increasing mechanical pressure application.

The different steps of the corrosion process are schematised in Figure 74.



A: Lead

B: Dense layer of PbO and α -PbO₂

C: Porous layer of β -PbO₂

v: Progression rate of the corrosion front

Figure 74: Schematic representation of the different steps of formation of the corrosion layer with increasing cycling time

At t_1 the corrosion process begins: a thin layer of α -PbO₂ deposits on the surface of the lead electrode and PbO forms between the lead and the lead dioxide. At t_2 , the α -PbO₂ layer grows until it reaches at t_3 the critical thickness at which cracks form to relax the mechanical stress accumulated in the layer due to the higher molar volume of the corrosion products. At this point the cracks are filled with β -PbO₂ and the porous external layer begins to form. With increasing cycling time, the internal layer does not grow any more and keeps the critical thickness. Its front just progresses towards lead with the progression rate v and the thickness of the porous layer increases. This view of the process is of course idealised since on the surface of α -PbO₂, reaction with the electrolyte takes place that transforms part of the α -PbO₂ to β -PbO₂, but the contribution of the superficial layer is believed to be negligible.

The fact that for the same number of cycles, the porous corrosion layer thickness decreases with increasing mechanical pressure is quite logical, with respect to the nature of the corrosion layer. The application of mechanical pressure is responsible for a compensation of the internal stress that appears in the dense corrosion layer. This stress appears as a result of the bigger volume of PbO₂ comparatively to Pb. Thus, by application of mechanical pressure the critical thickness at which cracking occurs is increased.

Once the internal layer has the critical thickness, the system reaches a kind of equilibrium (after some 16 cycles) in which the front of corrosion in the lead progresses linearly with the cycle number. In fact, the oxygen ions need a certain time to diffuse through the dense layer. Since the compact corrosion layer is thicker in the case of higher applied mechanical pressure, less oxygen ions reach the lead surface and the corrosion speed decreases, according to the first Ficks law.

$$J_{O^{2-}} = -D \frac{\delta C}{\delta x}$$

The flux of the O²⁻ ions thus decreases if the thickness of the PbO₂ layer is increasing.

In our experiment, since the charging time is fixed, at each cycle, the same amount of oxygen species have time to diffuse to the lead surface and thus, the same progression of the corrosion front happens, associated with a same growth of the porous layer.

As an example, the linear approximation of the variation of the corrosion thickness is represented in Figure 73 for the electrode under 22 kPa mechanical pressure ($y = 0.0095x + 0.5404$, $R^2 = 0.9905$). The capacity of the porous layer increases of 0.0095 mAs at each cycle and this approximation has a good regression factor.

For the experiments with less mechanical pressure, the approximation by a straight line fits not so good to the increase of the porous corrosion layer. This is due to the smaller critical thickness of the dense layer that can be easier cracked on its whole depth. In such a case, the dense layer is broken and has to build up again. Therefore, the linear approximation cannot be made. The evolution of the porous layer thickness would more resemble the schema of Figure 75

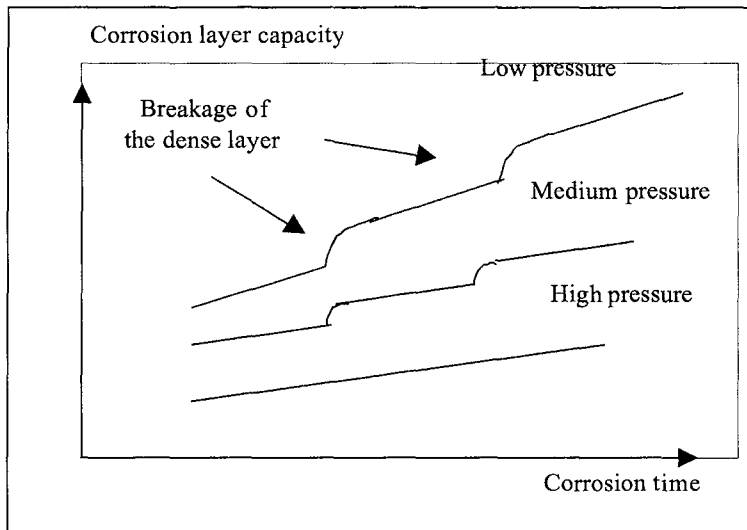


Figure 75: Schematic representation of the porous corrosion layer thickness for different mechanical pressure.

These experiments of corrosion on pure lead under mechanical pressure allowed the following conclusions.

- The corrosion layer has a structure with a dense layer and a porous layer. The critical thickness of the dense layer is constant and once it is reached, the porous layer grows linearly with time.
- The application of mechanical pressure increases the critical thickness.

The application of mechanical pressure stabilises the dense corrosion layer by increasing its critical thickness and hinders any breakage of it on its whole thickness. Therefore, at high mechanical pressure, the linear approximation of a porous layer growth with charging time is verified.

4.2.2 Mechanical stabilisation of the plate stack with the AJS separator

The direct effect of mechanical pressure on corrosion itself was proved in the former paragraph. There is an additional effect that is encountered in the AJS cells: the mechanical stabilisation of the plate stack in the plane of the electrodes. This effect is not present in cells with other separation systems, except possibly in AGM cells submitted to high external mechanical pressure.

In fact, in an AJS cell, the packing of the electrodes is so tight that the possibility for expansion of the positive grid is very much limited. Thus, even if corrosion proceeds on the positive grid, the only drawback related to corrosion that can be present in the AJS cell is the loss of conductivity of the current collector. Mechanical stability loss and appearance of short circuits as a result of grid growth are prevented by the AJS separator. A schematic representation of the process of deformation of the plate stack as a result of the positive grid corrosion is made in Figure 76.

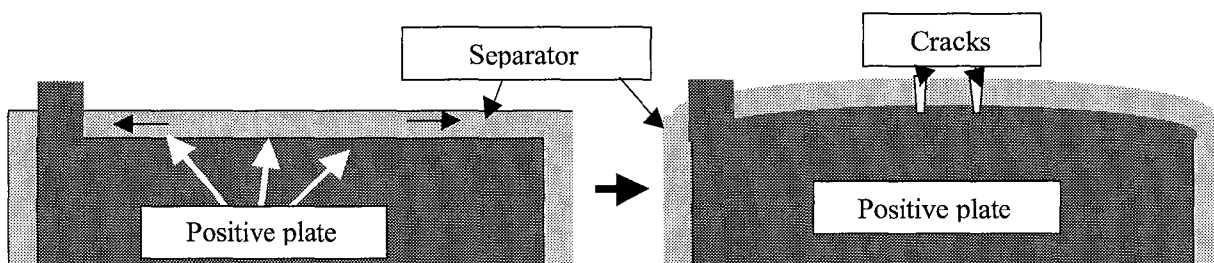


Figure 76: Schematic representation of the grid growth process in an AJS cell

The consequence of this positive grid growth is a deformation of the whole plate stack. It can be seen from Figure 77 that the negative plate did deform in a way similar to the positive and that the deformation of the whole stack leads to a cracking of the edges of the separators.

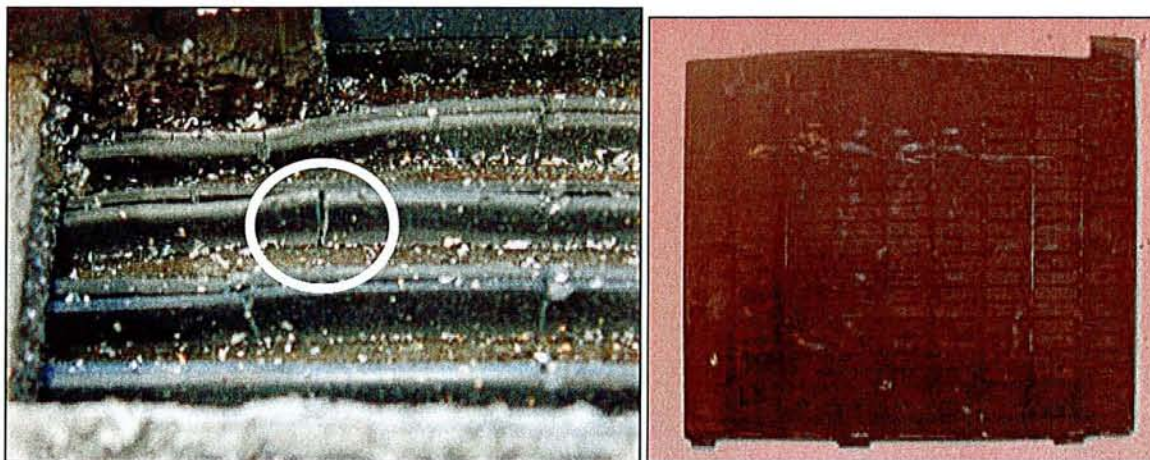


Figure 77: Pictures of the top of an AJS cell and of a negative plate after deformation of a plate stack by positive grid growth

This effect is only possible because the contact between the plates and the separator is very tight. If it is not the case, the process shown in Figure 69 happens. In this case, the gel immobilisation system in association with the separator does not provide any mechanical stabilisation of the positive electrode in the direction parallel to the plan of the electrode.

4.2.3 Observation of grids after cycling

The observation of positive plates cross sections after over 1000 cycles was a quite difficult point. In fact, all grids are quite corroded and the deduction from the only cross section of the extend to which corrosion did proceed was not possible. Only the subjective impression that the mechanical integrity of the positive plate was better when higher mechanical pressure was applied can be reported here. A dissolution of the positive active material and following weighting of the remaining lead would have been useful but was not performed.

4.2.4 Conclusion about the effect of mechanical pressure on the positive grid corrosion

- Potentiostatic measurements showed that the application of a mechanical pressure on a pure lead electrode decreases its corrosion rate. The corrosion products have a higher volume and mechanical stress builds up in the corrosion layer. The release of this stress leads to the splitting of the corrosion layer in a dense part and a porous part. Mechanical pressure application balances this stress and increases the critical thickness of the dense layer from which on the layer cracks and the porous layer begins to form.
- The use of the AJS separator allows an additional diminution of the damages associated with the corrosion. The high packing density of the plate stack allowed by the utilisation of AJS leads to less positive grid growth and thus can solve the problem of life limitation by short circuit around the edges of the plate stack or loss of mechanical integrity associated with the corrosion of the positive grid.

- The direct effect of mechanical pressure on the corrosion process was difficult to show in cells after cycling. The mechanical stabilisation through high packing density seems to be the predominant effect when using AJS separators.

Résumé et conclusion du chapitre concernant la corrosion des grilles positives de batteries au plomb.

Après une synthèse bibliographique concernant le processus de corrosion des la grille positive dans les batteries au plomb et un approfondissement de la recherche au sujet de l'effet de l'antimoine sur le processus de corrosion, l'effet de l'application d'une pression mécanique sur la corrosion de la grille de l'électrode positive a été étudié.

- Il a été montré tout d'abord par des expériences de voltampérométrie cyclique que l'application par le biais du séparateur AJS d'une pression mécanique sur une surface de plomb pur diminue de façon spectaculaire la vitesse de corrosion. Cet effet est dû à la stabilisation mécanique de la couche de corrosion interne dans laquelle des contraintes se développent en conséquence du plus grand volume des produits de corrosion par rapport au plomb. Sous l'effet de la pression mécanique, la couche de corrosion dense atteint une plus grande épaisseur avant de se fissurer. La couche dense limite la diffusion des ions oxygène vers la surface du plomb par conséquent, l'augmentation de son épaisseur conduit à une diminution de la vitesse de corrosion.
- La diminution de la corrosion des grilles positive par l'application d'une pression mécanique a été observée sur des cellules avec électrodes de type Fauré mais dans une nettement moins grande mesure que pour les tests où la pression mécanique était appliquée directement sur la surface de plomb.
- L'effet prédominant dans les cellules avec AJS est une stabilisation mécanique du bloc d'électrode qui empêche la croissance des grilles positives. En effet, dans une batterie avec un système de séparation à faibles propriétés mécaniques, le bloc d'électrode est moins compact et lorsque la grille positive est corrodée, elle tend à croître jusqu'à ce que des morceaux de grille positive dépassent du bloc d'électrodes et forment des court circuits sur les côtés du bloc. Dans le cas des cellules avec le séparateur AJS sur lesquelles une pression mécanique est exercée, le bloc d'électrodes est très compact et pour pouvoir croître, la grille positive doit déformer avec elle le séparateur et les électrodes négatives qui l'entourent. Par conséquent, la croissance des électrodes positives est extrêmement limitée dans les batteries avec AJS sous pression mécanique et le risque de court circuits par les côtés du bloc d'électrodes dus à la croissance des grilles positives est grandement diminué.

5 *Phosphoric acid*

In order to improve the performance of the lead-acid battery, phosphoric acid is the additive most commonly used for deep cycling applications in gel batteries. Surprisingly, while it seems to have a positive effect on cells where the electrolyte is truly immobilised and where the separator has a very thin porosity, its positive effect in flooded cells and in VRLA cells with AGM separator is a subject of controversy. Therefore, the effect of phosphoric acid in the lead-acid battery in general was investigated and its interaction with the new separation system also.

5.1 Bibliography of the phosphoric acid

The addition of phosphoric acid and phosphates in the electrolyte of lead-acid batteries is already current since 1900. But until now, despite the numerous research that has been performed on that topic, no clear answer was found at the question whether phosphoric acid addition is beneficial to the lead-acid battery or not. Furthermore, the mechanism by which phosphoric acid influences the reactions in the lead-acid battery stays unclear. It is proposed that the phosphate reversibly adsorbs on the PbO_2 active sites and modifies its growth from 3-dimensional to 2-dimensional [103]. The 2D- PbO_2 has a smaller surface area and is more difficult to reduce than the 3D form [104]. Lead phosphates [$\text{Pb}_3(\text{PO}_4)_2$] are claimed to be present in the lead corrosion films [105] and hinder PCL1 by impeding the reduction of the 2D-form of PbO_2 and thus preventing the formation of an isolating lead sulphate layer. In his review of 1988 [106], Voss details the earliest work on phosphoric acid and describes the formation during charge of lead (IV) species at the positive electrode.

In reference [107], Hullmeine et al. suppose the presence of $\text{Pb}(\text{HPO}_4)_2$ in the charged positive active material. They also observe an “higher electrolyte flow resistance which is observed in Eloflux experiments with Fauré electrodes after H_3PO_4 addition”.

In 1991 [108], Garche et al. interpret the action of phosphoric acid as resulting from the formation of a fine lead sulphate layer acting as a semi-permeable membrane that favours more alkaline conditions in the active mass bulk and therefore promotes the formation of $\alpha\text{-PbO}_2$. They also show that H_3PO_4 has only an effect when present during the charge of the positive electrode thus it influences the only oxidation of lead sulphate to lead dioxide and not the reverse reduction reaction (see also [109]).

In 1992 [110], Doering et al. explain the fact that the presence of phosphoric acid hinders the formation of a passivation layer between the grid and active material of the positive electrode by the fact that lead sulphate of very fine structure precipitates at discharge of the corrosion layer, thus preventing further discharge, i.e. the subsequent formation of large lead sulphate crystals and related sulphation/insulation of the corrosion layer.

While most authors observe no effect of phosphoric acid on the behaviour of the negative electrode [103], in 1993, S. Venugopalan finds out that phosphoric acid decreases the hydrogen evolution on the negative electrode of lead-acid batteries [111]. Since there is a direct relation between the hydrogen evolution on the negative electrode and the corrosion rate of the positive electrode of a VRLA battery, this increase of the hydrogen overpotential is responsible for a decrease of the corrosion of the positive grid.

In 1997[112], E. Meissner makes a useful review about phosphoric acid as an additive for lead-acid batteries in electric vehicle applications. Table 16 tries to give an overview of the effects of phosphoric acid addition.

Positive effect	Drawback
Increases cycle life[104]	Capacity loss in the initial cycles [104]
Reduces corrosion [104]	Formation of lead dendrites (mossing)[104]
Reduces the irreversible sulphation [104]	Poor low temperature performance [104]
Reduces self discharge	Increased potential of the positive electrode[107]
Reduced shedding of PAM	Passivation of the positive electrode [109]
Hinders PCL1 by antimony free grids	Increases the solubility of Pb^{4+} species, oxidative for the separators [106]
Better low temperature performance [113]	

Table 16: Summary of the advantages and drawbacks of the addition of phosphoric acid

But the effect of phosphoric acid is a subject of controversy since for example, while a decrease of the low temperature performance in presence of the additive is reported in [104], an increase is reported in [113]. Still there seem to be a lot of work to be done in order to explain the process by which phosphates and in particular phosphoric acid affect the lead-acid battery. It seems that the effect of phosphoric acid is strongly depending on the separation system used and on the application the cell/battery is used for. Additionally, the mode of action of phosphoric acid is not elucidated yet. The purpose of this work was also a contribution to a better understanding of how phosphoric acid acts in a lead-acid battery.

5.2 Results concerning the influence of phosphoric acid

In this section, our purpose was to test small additions of phosphoric acid in the electrolyte of AJS cells. In fact, the positive effect of phosphoric acid in gelled cells is already known for long. And AJS is only a few more than a “gel in slices”. Therefore, the effect of phosphoric acid was tested outside the cell and afterward, in the AJS cell in comparison to cells with the same design and no phosphoric acid.

5.2.1 Cyclic voltammetry on pure lead

In order to observe the influence of phosphoric acid on the positive and the negative electrodes, cyclic voltammetry was performed on pure lead electrodes in the positive and negative potential ranges. The potential was varied by 5 mV each second and the potential measured against a mercury/mercurous sulphate electrode.

Figure 78 shows that the presence of 0.2 mol/l (i.e. 19.59 g/l) H_3PO_4 in the electrolyte has a strong effect on the positive electrode. The oxidation peak is shifted towards more positive potentials and oxidation is almost totally impeded. As a result, the reduction peak is very small and it is also shifted to more negative potentials.

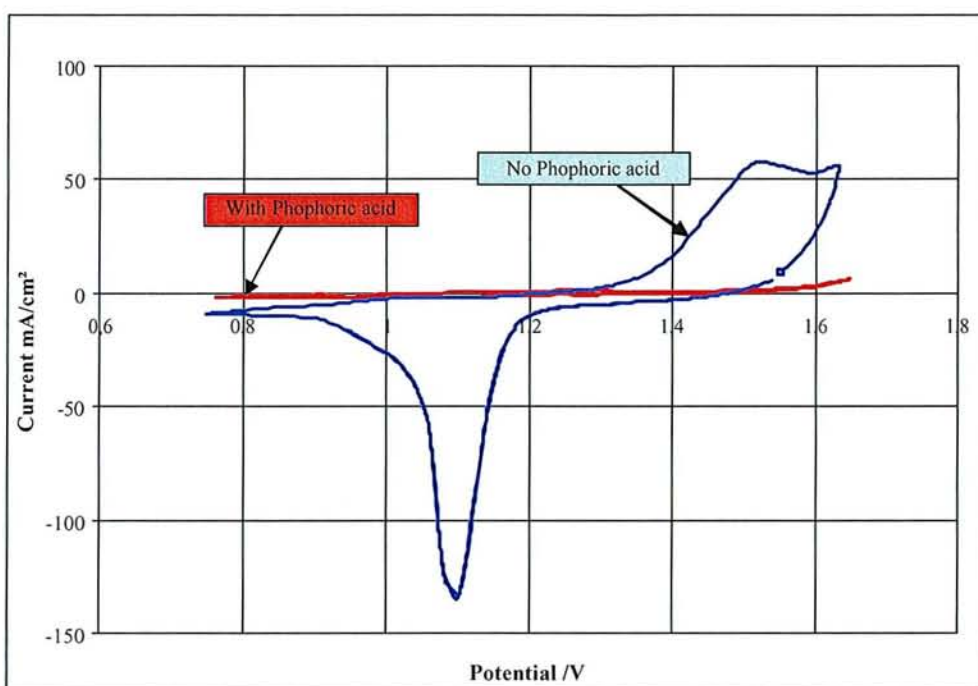


Figure 78: Cyclic voltammogram in the positive potential range with and without phosphoric acid in the electrolyte ($d = 1.28 \text{ g/cm}^3$, 5 mV/s , $[\text{H}_3\text{PO}_4] = 0.2 \text{ mol/l} = 19.59 \text{ g/l}$)

By opposition, the presence of phosphoric acid only shifts a little bit the hydrogen formation peak on the negative electrode without affecting the Pb/PbSO_4 reactions (Figure 79). This is exactly in accord with all the results reported in the literature.

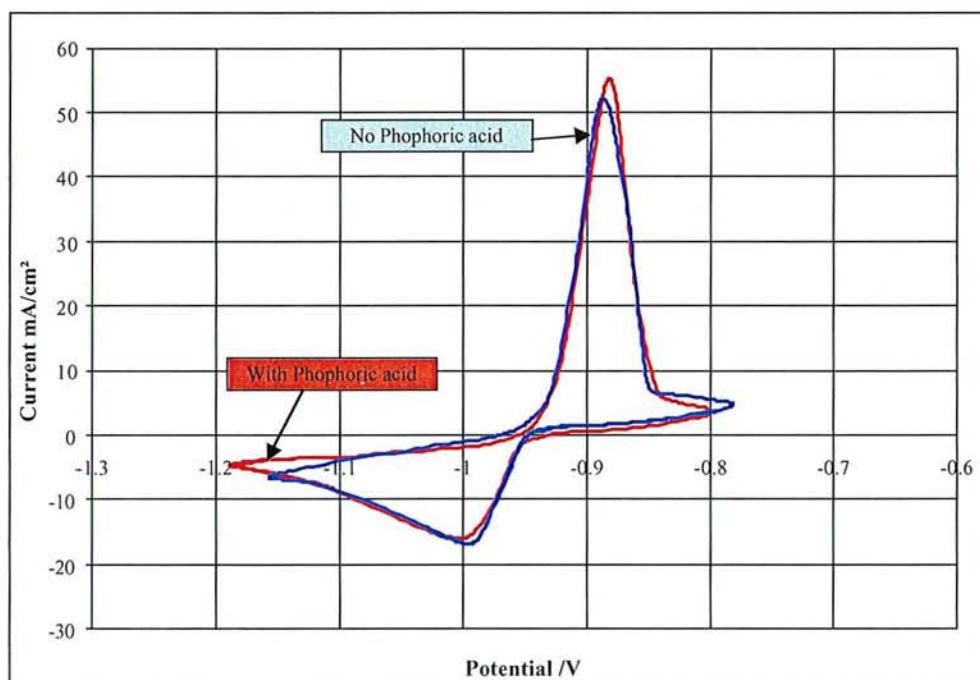
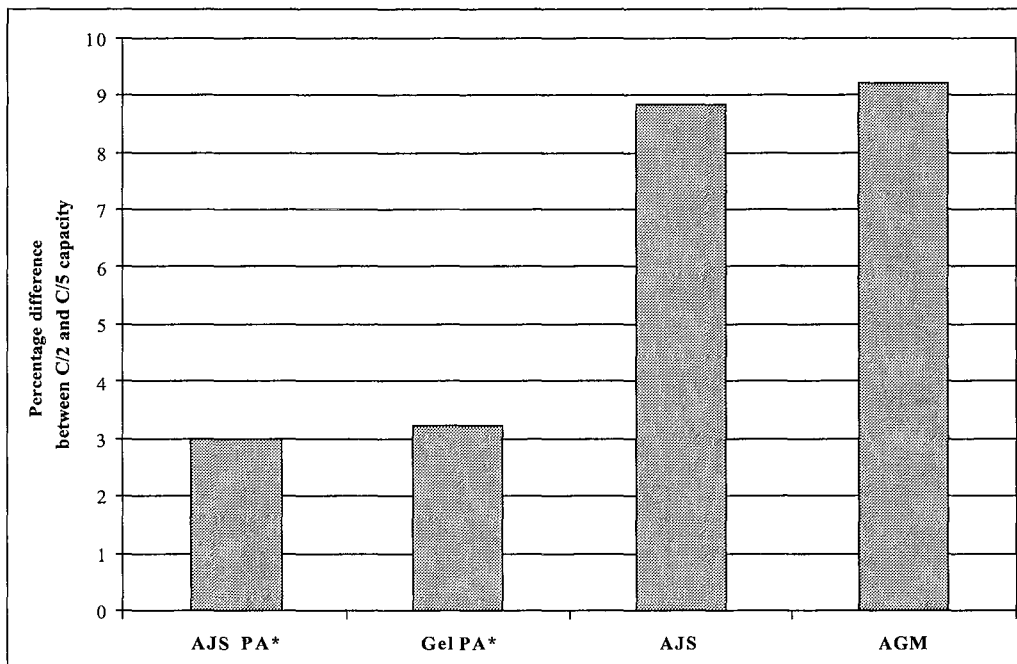


Figure 79: Cyclic voltammogram in the negative potential range with and without phosphoric acid in the electrolyte ($d = 1.28 \text{ g/cm}^3$, 5 mV/s , $[\text{H}_3\text{PO}_4] = 0.2 \text{ mol/l} = 19.59 \text{ g/l}$)

5.2.2 Phosphoric acid and electrical performance

It was often claimed that the addition of phosphoric acid in the lead-acid battery leads to a decrease of its capacity, in the beginning of its life for some authors or durably for some others.

Our different measurements showed that the presence of phosphoric acid has only a very small effect on the high rate discharge capacity after some 10 acclimatisation cycles but decreases the low rate capacity. An illustration of this is made by representing the variation in capacity between a C/2 discharge and the following C/5 discharge for different separation/immobilisation systems. These results concern the cells described in section 3.3.1.1. Figure 80 is showing the middle value of the calculation made for many consecutive C/2 and C/5 cycles all along the life of the cells. The relative variation between the C/2 and the C/5 capacity is not influenced by the age of the cell or battery. All cells presented in Figure 80 have the same plate design and are submitted to the same initial external mechanical pressure.



* PA means phosphoric acid

Figure 80: Increase in capacity between the C/2 and the C/5 discharge rate.

The low rate capacity is decreased by the addition of phosphoric acid in comparison with the same cell/battery containing no additive. The high rate capacity in presence of phosphoric acid is almost not affected and thus, the cells/batteries containing phosphoric acid are less sensitive to the discharge rate. This result is fully in accord with the results of Meissner [112].

The comparison of the cycling behaviour of AJS cells under different initial mechanical pressures with and without phosphoric acid in their electrolyte is shown in Figure 81.

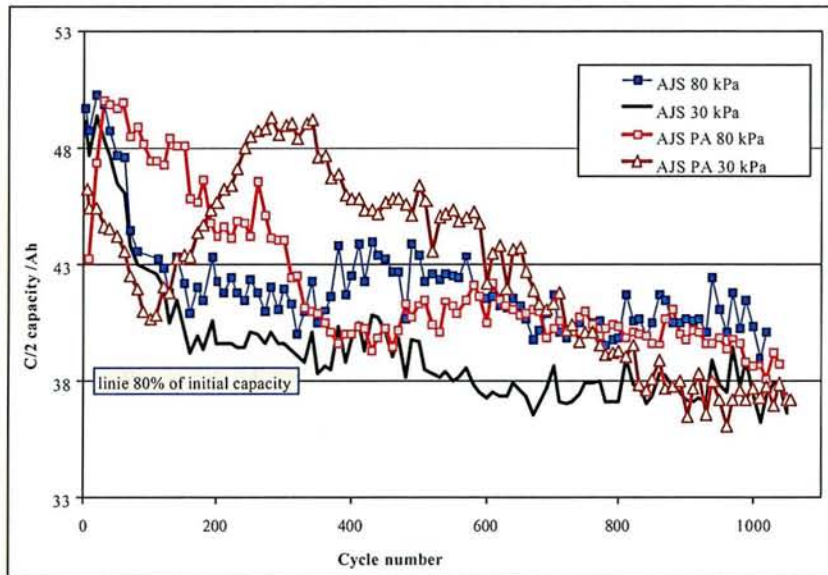


Figure 81: Evolution of the discharge capacity versus cycle number for AJS cells with and without phosphoric acid

At low pressure, the cycling life is significantly increased by adding phosphoric acid while at higher mechanical pressure, the benefit of phosphoric acid addition is more questionable. The surprising point is that at the end of life, for a same initial mechanical pressure, the cells with and without phosphoric acid have a similar behaviour, thus maybe showing that after a while, the phosphoric acid loses its effect.

5.2.3 Mechanical pressure and the effect of phosphoric acid.

The evolution of the mechanical pressure transferred to the walls of an AJS lead-acid cell with and without addition of phosphoric acid in its electrolyte is shown in Figure 82 for cycle 100.

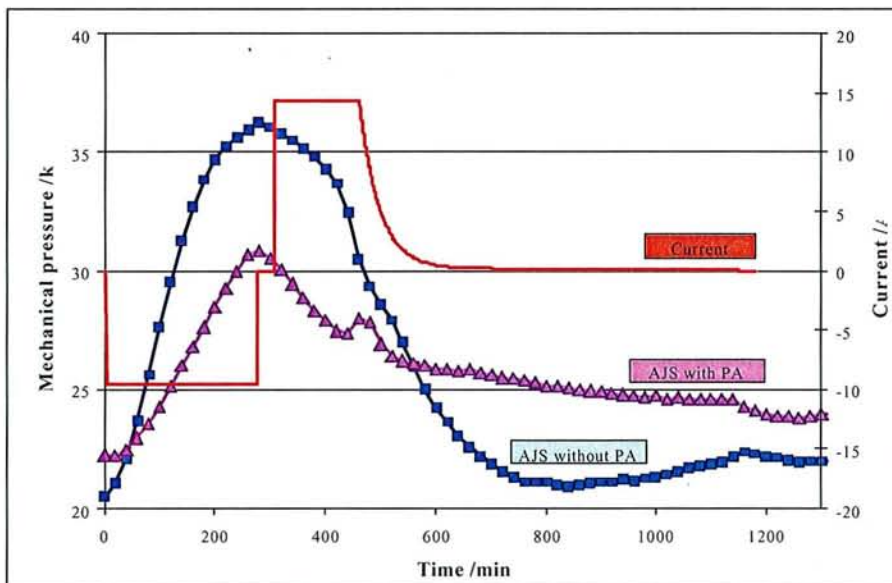


Figure 82: Evolution of the mechanical pressure during cycle 100 for AJS cells with and without phosphoric acid

During cycle 100, for two cells with the same design and initial mechanical. the mechanical pressure evolution is different if the electrolyte is added of phosphoric acid or not. Namely, the increase of the mechanical pressure during discharge is smaller in presence of phosphoric acid.

This smaller increase of the mechanical pressure during discharge in presence of phosphoric acid is observed during the beginning of life but is not marked any more after some 350 cycles as can be seen from Figure 83.

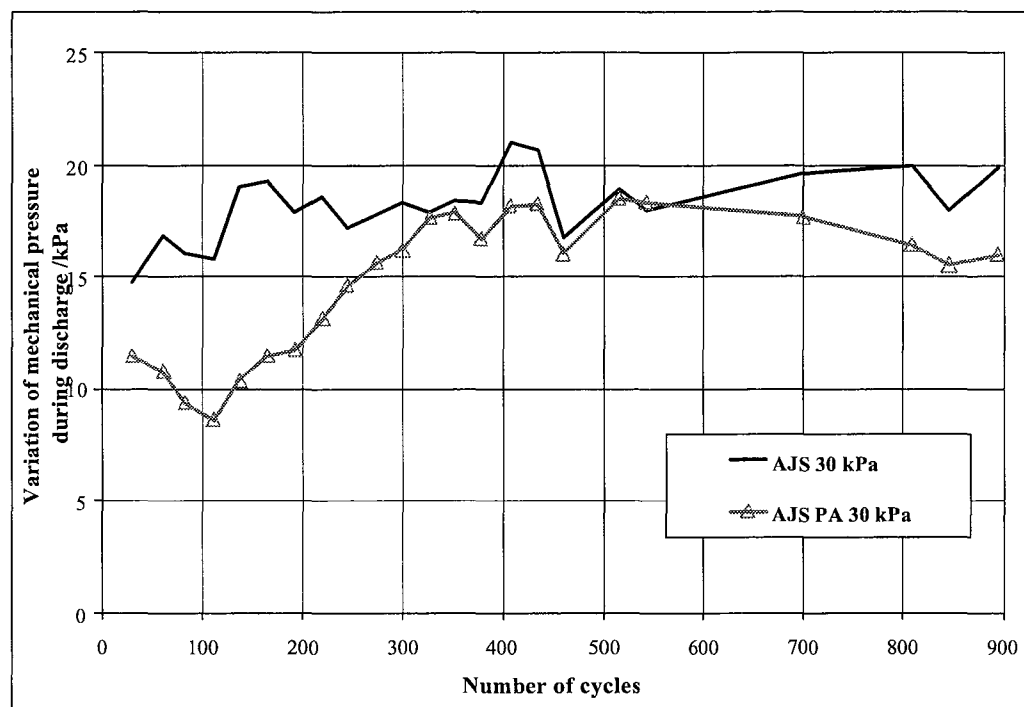


Figure 83: Mechanical pressure variation during discharge versus cycle number for two AJS cells with and without phosphoric acid.

As reported in section 3.5.1, the variation of mechanical pressure during discharge associated with the growth of the lead sulphate crystals is steady over cycling life for the cell without phosphoric acid, independently of the cell capacity. For the cell containing phosphoric acid, this variation decreases in the beginning of life until cycle 100 and increases then until reaching the level of the cell without phosphoric acid. The decrease of this variation may be associated to a progressively higher adsorption of the phosphoric acid in the first 100 cycles. After that, a process of degradation of the phosphoric acid or of “passivation” of the “phosphoric acid effect” takes place. Phosphoric acid can be lost in the formation of inactive compounds like e.g. $Pb_3(PO_4)_2$ or $PbHPO_4$. Nevertheless, it can be observed that until the end of life, for a same capacity, the increase of mechanical pressure during discharge is still higher for the cell containing no phosphoric acid (cycle 900).

In Figure 84, the comparison is made between the mechanical pressure variation during discharge and the discharge capacity of the AJS cell with phosphoric acid and low mechanical pressure. Surprisingly, in the beginning of life, a correlation can be found between these both parameters. The correlation does not exist for cells without phosphoric acid and for the cells with phosphoric acid, the dependence disappears after some 300 cycles.

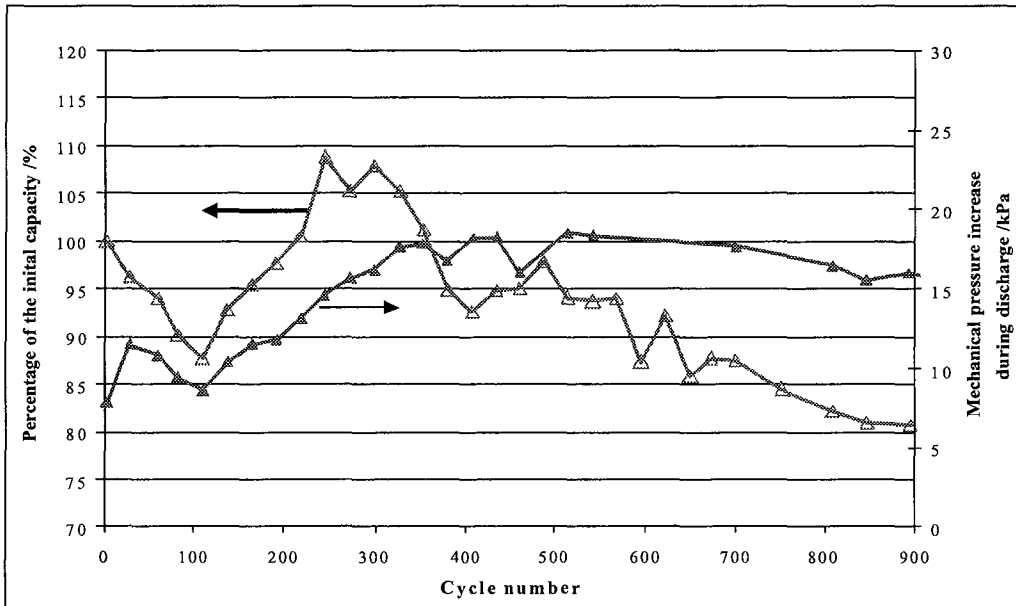


Figure 84: Comparison between the discharge capacity and the mechanical pressure increase during discharge versus cycle number for AJS PA 30 kPa

In conclusion, for a same discharge capacity, the mechanical pressure on the cell walls increases less if the cell contains phosphoric acid. Since the presence of phosphoric acid leads to a finer crystallisation of the lead sulphate, one can conclude that the growth of several small crystals exert a smaller mechanical stress on the structure of the positive active material than the growth of less crystals of bigger size. Concerning the crystallisation, phosphoric acid acts as if the electrode had been discharge at a higher rate. The effect of phosphoric acid seems to be limited in time.

5.2.4 Effect of phosphoric acid on the potential of pasted electrodes

Figure 85 shows the influence of phosphoric acid on the cells potential evolution during charge.

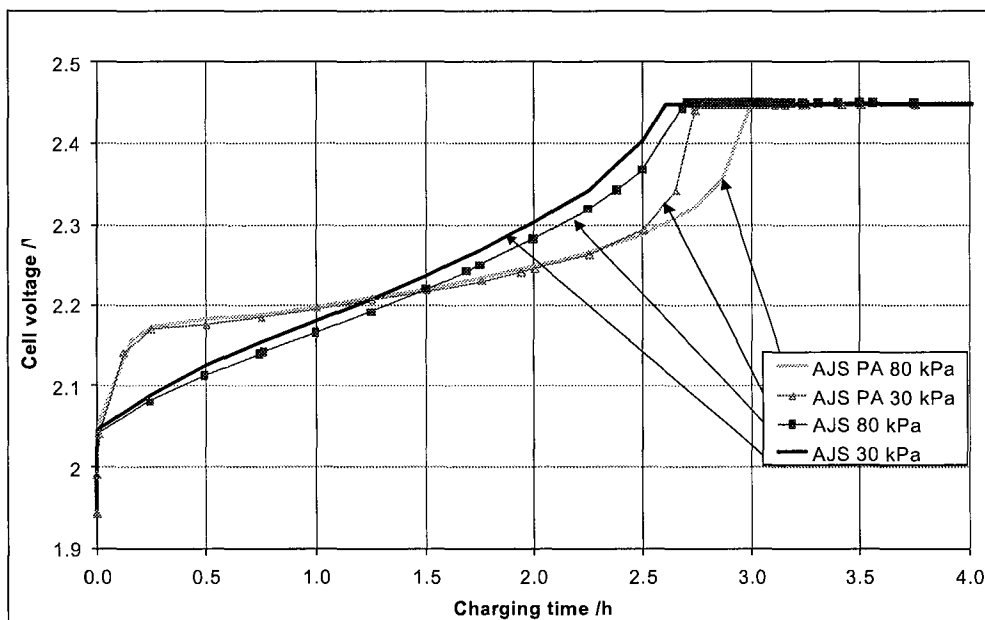


Figure 85: Evolution of the charging potential for cells with or without phosphoric acid

All cells have a similar capacity (except AJS PA 80 kPa that lies a bit higher than the others) and are in the beginning of their life (they already performed some 115 cycles). Independently from the initial external mechanical pressure, the potential of the cells containing PA increases rapidly at the beginning of charge, it reaches then a kind of plateau before it increases again steeply at the end of the constant current period of charge. By opposition, the potential of a cell containing no phosphoric acid increases constantly from the beginning to the end of the constant current charging period.

The positive electrode is responsible for these different behaviours. For the charge reaction of the positive electrode to proceed, a higher potential is needed in presence of phosphoric acid. This was shown by the displacement of the oxidation peak towards higher potential in the cyclovoltammetrical measurements. Therefore a strong overpotential builds rapidly up on the positive electrode in presence of phosphoric acid and the charge happens.

5.2.5 Phosphoric acid and gas formation

The measurement of the amount of gas emitted by the cells during the charging process is presented in Figure 86.

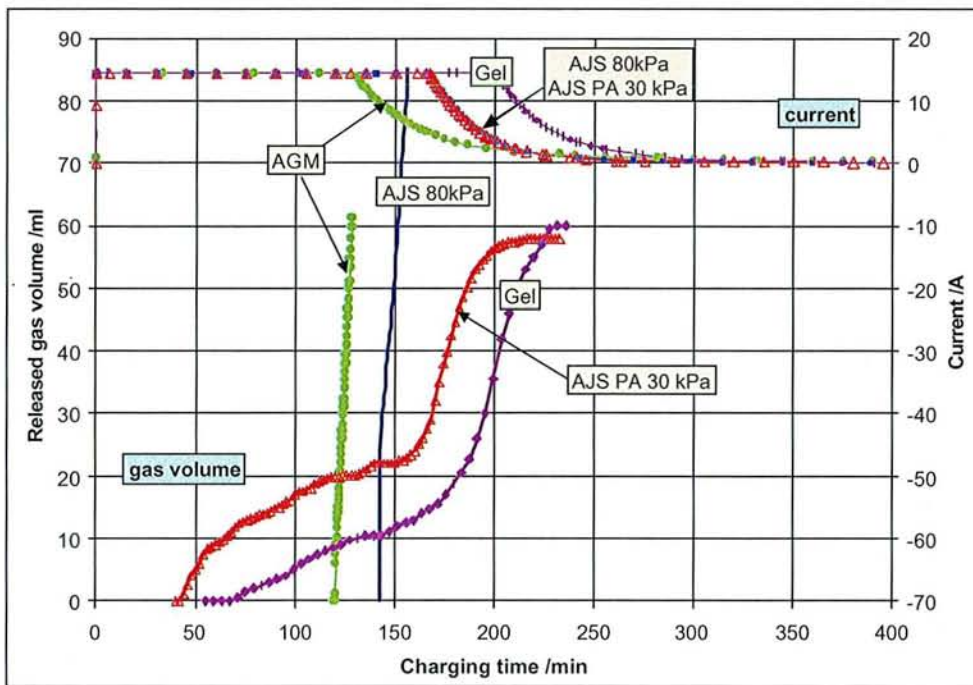


Figure 86: Evolution of the current and volume of gas released versus charging time for different cells

These results correlate perfectly with the evolution of the potential of a cell during charge. As a result of the strong polarisation of the positive electrode early in the charge, in the cells containing phosphoric acid (i.e. either the AJS cell with phosphoric acid or the gel cell) some gas is released very early in the constant current period. The cell voltage at the valve opening for the different cells is reported in Table 17.

Cell description	Average cell voltage at vent opening /V
Gel (PA)	2.18
AJS PA 30 kPa	2.18
AGM	2.35
AJS 80 kPa	2.33
AJS 60 kPa springs	2.34
AJS 30 kPa	2.36

Table 17: Average cell voltage at vent opening for different cells.

Gassing begins at a low cell voltage in the cells containing phosphoric acid. In these cells, while the negative electrode is not polarised yet, the positive electrode is strongly polarised and oxygen is already evolved at low cell voltages and at low states of charge. This correlates with the results delivered by the cycling voltammetry that showed a displacement of the potential of the oxidation reaction of lead sulphates to lead dioxide towards more positive regions. The overpotential of the oxygen evolution may be increased, but since the positive electrode is more polarised, the oxygen formation begins earlier in the charge.

5.2.6 Oxidative effect of phosphoric acid

The AJS separator performed very well in the cells and batteries and the electrical results were very satisfying both in presence and in absence of phosphoric acid. The post mortem analysis showed that the AJS separator is absolutely intact after cycling in cells without phosphoric acid. In presence of the additive, the very external surface of the AJS separator that was in contact with the positive electrode was a bit corroded.



Figure 87: Picture of the separator from the AJS 80 kPa battery with some rest positive active material on the top part and the thin corrosion layer in white

The white layer one can observe in Figure 87 was analysed by EDX and proved to consist of pure silicon (SiO_2). The silicon oxide is coming from the separator. After the matrix of polyethylene has been corroded, only the silicon oxide is left.

Later on, Daramic modified the formulation of the AJS separator in order to improve its resistance against oxidation and the new formulation proved to perform well and have better mechanical characteristics after 450 cycles. The superficial corrosion in presence of phosphoric acid is reduced.

The oxidative effect of phosphoric acid in the lead-acid batteries is well known and associated with its stabilisation of the lead IV species (see reference [106]). The high potential of the positive electrode that we demonstrated in section 5.2.4 is a part of this same process.

5.2.7 Phosphoric acid and corrosion

5.2.7.1 Negative grid corrosion

The corrosion of the negative pole seems to be increased on the top lead of the cells that contained phosphoric acid. This remark is only of quite subjective nature since it bases on the only observation of the top lead of the negative stack at the opening of cells and batteries. There seemed to be more “sulphate flowers” on the top lead as well as on the edges of the negative plates and a quite thick white layer on the top lead Figure 88. This remark is only relevant by documenting the fact that the lead sulphate may be more soluble in sulphuric acid added of phosphoric acid.



AGM cell after 1050 cycles without phosphoric acid

AJS battery after 650 with phosphoric acid

Figure 88: Pictures of the negative strap at opening after cycling with and without phosphoric acid

Additionally, it seemed to be of interest to point out the possibly increased negative top lead corrosion in presence of phosphoric acid since this result correlates with the increased “oxygen effects” that are observed in section 6.1.

As a last point, the higher solubility of the lead II ions could also explain why the development of forces is smaller during discharge in presence of phosphoric acid. Namely, a higher solubility of the lead II ions would imply a smaller over-saturation and thus, a smaller force development basing of the theory of crystal growth in pores.

These point would need further study to be demonstrated.

5.2.7.2 Positive grid corrosion

The cell containing phosphoric acid showed a better integrity of the positive grid at the end of life after some 1000 full $C/2$ cycles. In the same way as in the experiments on corrosion without phosphoric acid, this allegation was difficult to document since the positive grids of the cells that underwent over 1000 cycles were all quite badly corroded.

After 650 cycles, while the gel and AGM batteries suffered quite pronounced top grid corrosion and associated grid growth, the AJS batteries were still healthy. It means that two contributions are present in the AJS cells containing phosphoric acid that need to be differentiated: the one of the phosphoric acid itself and the mechanical effect. Both the mechanical pressure applied via the separator (see section 4.2.1) and the expansion restriction provided by the separator (see section 4.2.2) are very important facing the problem of corrosion.

In order to prove any effect of phosphoric acid on corrosion, measurements were performed on lead grids. First, since the usual industrial processes use some 30 g/l phosphoric acid in the electrolyte, we prepared 1l electrolyte solution of 1.28 g/cm³ sulphuric acid with 30 g phosphoric acid. In this solution, a positive grid consisting of lead calcium alloy was placed between two negative pasted plates of 48 Ah capacity. The positive grid was subjected to cycles basing on the same idea as the corrosion test in section 4.2.1 but the regime was galvanostatic and not potentiostatic as in section 4.2.1. The typical behaviour of a lead calcium grid in sulphuric acid at the density 1.28 g/cm³ is shown in Figure 89.

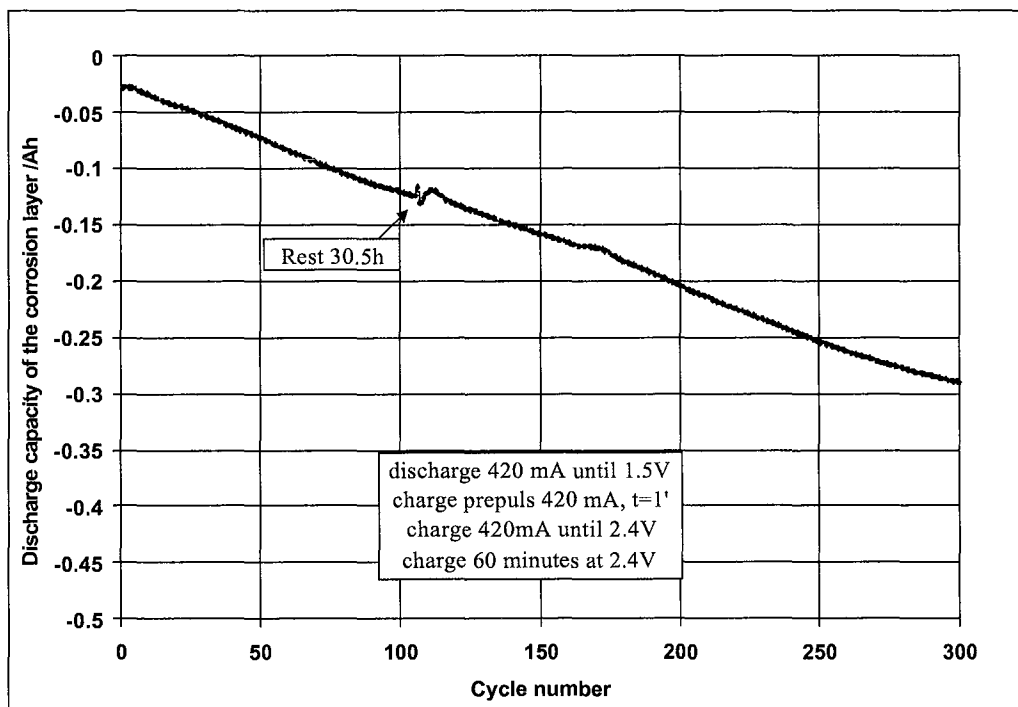


Figure 89: Discharge capacity of the corrosion layer versus cycle number in sulphuric acid ($d=1.28\text{g/cm}^3$)

The discharge capacity of the porous corrosion layer increases progressively with cycle number. After some 400 cycles, this increase is slowed down. The cycling regime of the grid is shown in the figure. It bases on galvanostatic charge and discharge.

The cycling regime in the electrolyte with phosphoric acid was a bit different. The regime and the evolution of the discharge capacity of the corrosion layer are presented in Figure 90.

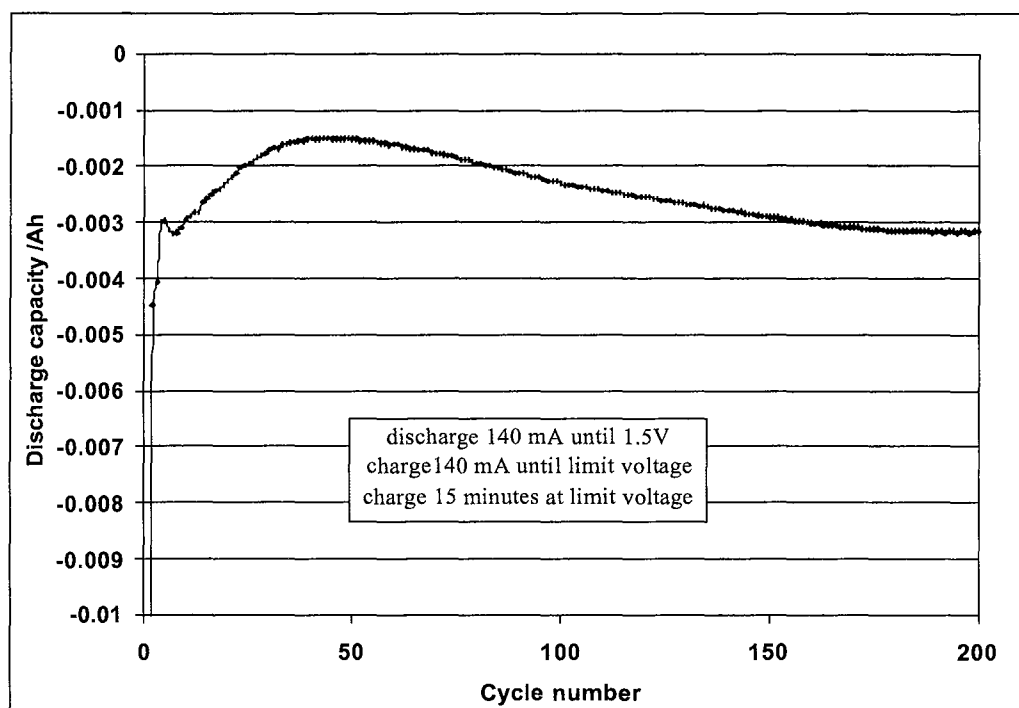


Figure 90: Discharge capacity of the corrosion layer versus cycle number in electrolyte with phosphoric acid

The presence of phosphoric acid affects drastically the grid corrosion in the usual potential region. The discharge capacity of the porous corrosion layer is extremely low and this effect is not only attributable to the lower charge/discharge intensity. For increasing the corrosion, the value of the charge limit voltage was increased but with no significant effect. The discharge capacity even decreased where we would have expected an increase.

These results show clearly that the presence of phosphoric acid dramatically decreases the corrosion rate of lead calcium grids. In ref. [114], the author describes the adsorption of perfluorinated surfactants and the mechanism of adsorption and reduction of surface tension. At high state of charge, the positive electrode surface is charged positively. If one imagines that the phosphate ions are adsorbed on the electrode surface when the surface is charged positively, it means that the adsorption happens only at high state of charge of the electrode. Even more, there seem to be a dependence between the corrosion rate and the electrode potential in presence of phosphoric acid. The higher the positive electrode potential, the lower the corrosion rate. It can mean that more phosphoric acid is adsorbed on the positive electrode hindering more and more the lead dioxide formation.

The thin layer of white material covering the surface of the positive grid at the end of the measurement after charge was analysed by X ray diffraction. The diffractogram is shown in Figure 91.

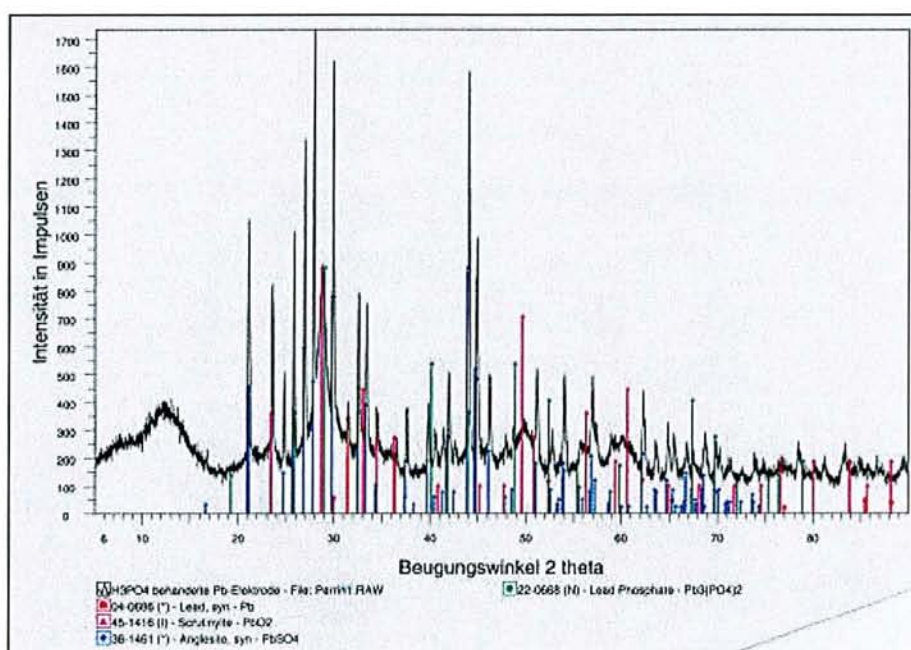


Figure 91: Diffractogram of the material covering the lead grid after cycling in electrolyte containing phosphoric acid

The external part of the corrosion layer proved to consist of lead, lead dioxide, lead sulphate and lead phosphate $[Pb_3(PO_4)_2]$. K. Bullock [105] already found such lead phosphates in the corrosion product. Additionally, a kind of white “skin” did form that deposited on the bottom of the container in which the measurement was performed. This skin was initially believed to consist also of lead phosphate. It was analysed and proved to be pure lead sulphate of the Anglesite form!

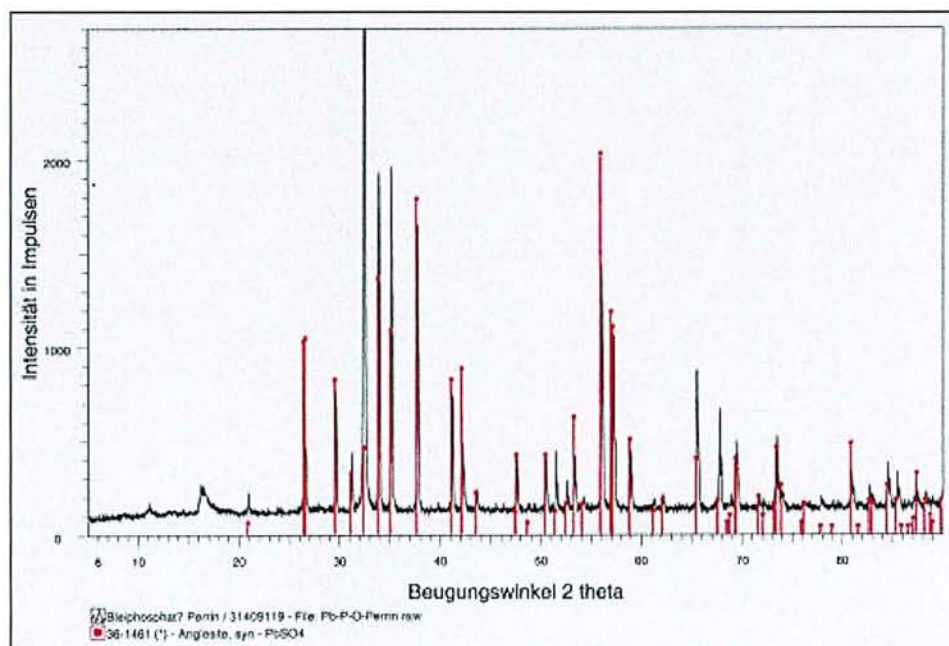


Figure 92: Diffractogram of the material composing the white “skin” present in the electrolyte after cycling of the grid lead in sulphuric acid added of phosphoric acid.

The apparition of this "white skin" must be related to the adsorption of the phosphates on the sites where either the lead dioxide or the lead sulphate would have deposited. The most probable mechanism is explained in the following lines.

During charge at high potential, the adsorbed phosphates block most of the sites where lead dioxide would precipitate. The solubility of the lead IV species is increased and lots of lead IV ions are present in solution.

At the beginning of discharge, the surface of the electrode is still positively charged and the desorption of the phosphates happens only slowly. As the potential of the electrode decreases, the lead IV species are reduced to lead II and the precipitation of the first lead sulphates happens on the few number of sites that are not blocked by the phosphates. The further lead sulphates precipitation happens then preferentially on the few germs that are present and the growth of the sulphate takes place towards the solution and not on the electrode. Thus leading to the formation of the "white skin".

A schematic representation of the different steps is presented in Figure 93.

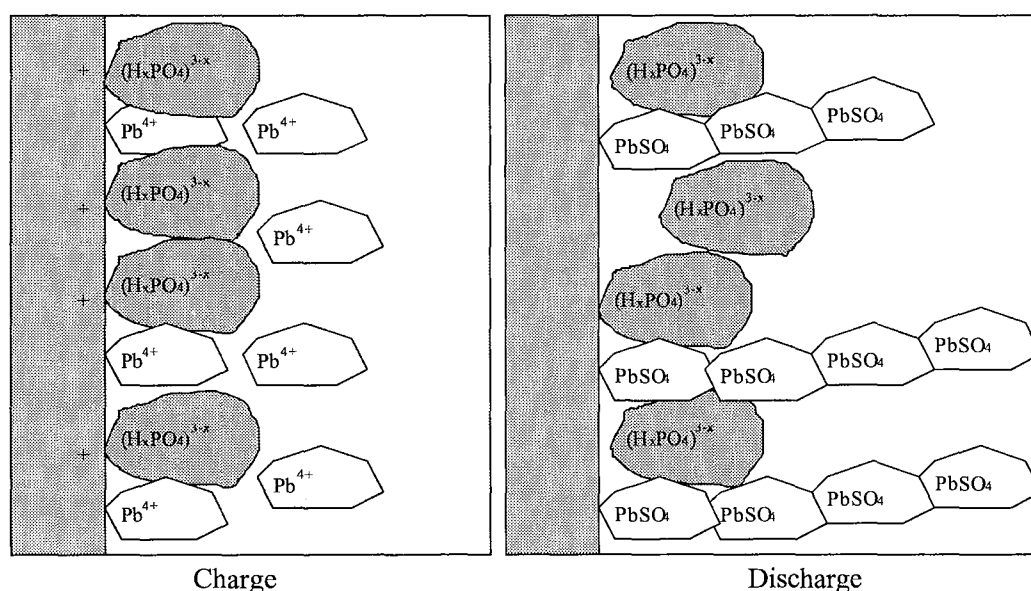


Figure 93: Schematic representation of the adsorption of the phosphates during charge and of the precipitation of the lead sulphates during discharge

Our experiment for the determination of the effect of phosphoric acid on corrosion delivered three interesting results.

- ◆ The corrosion rate of a tin calcium grid is drastically decreased in presence of phosphoric acid. This effect is due to the adsorption of phosphates on the active sites of the grid where lead dioxide would have formed. This blocking of the reaction sites for the lead dioxide is responsible for an increased solubility of lead IV species and the high oxidative effect of phosphoric acid in lead acid batteries.
- ◆ The adsorption of the phosphates seems to be driven by the potential of the positive electrode. Therefore, the higher the positive grid potential, the slower the corrosion rate. But this point needs more investigation to be clearly assessed.
- ◆ During discharge, the lead sulphate precipitate on the only few sites that are unblocked at the beginning of discharge. The growth of the sulphates then goes on the few germs thus forming a chain of small lead sulphate crystals that grows in the solution.

5.2.8 Structural changes in the positive active material due to phosphoric acid

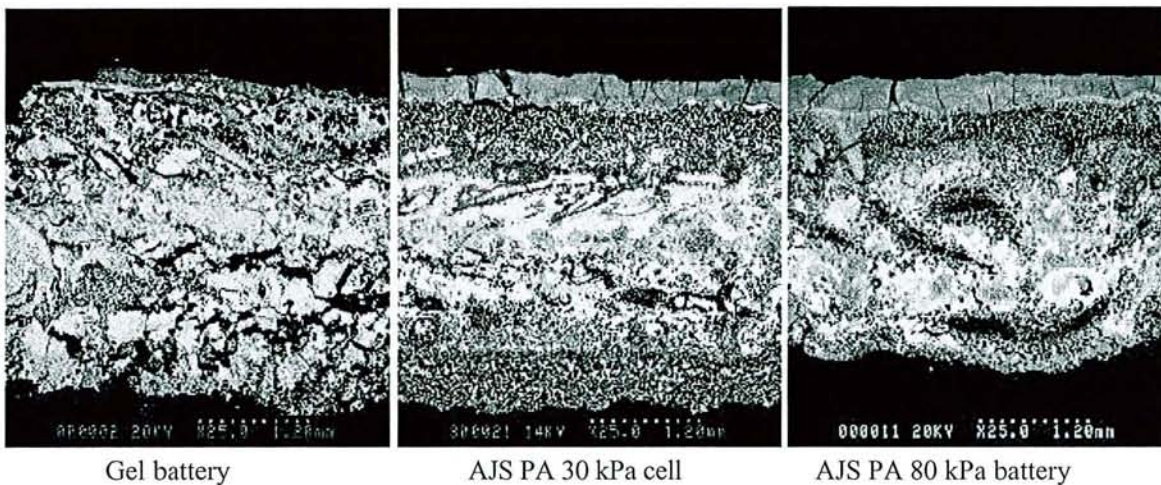
When cycled with phosphoric acid, the cells/batteries show out an unusual shape of the surface of the positive electrode. The picture of Figure 94 represents a positive plate at the battery opening. It is a plate from the AJS battery cycled under 80 kPa external mechanical pressure after it has performed some 650 cycles.



Figure 94: Surface of a positive plate at the opening of a battery after cycling with phosphoric acid

One can observe the external layer of brighter colour that is like a crust. This layer is easy to remove from the plate. The material the layer consists of is also very brittle. Therefore, it was almost impossible to cut cross sections from the positive electrodes that would still be integer.

Figure 95 show a view of the whole electrodes sections. Some pieces of the surface are failing on the bottom of the pictures because the external layer did break out. In the same way as for the cells under mechanical pressure without phosphoric acid, one observes a layering of the positive active material.



Gel battery

AJS PA 30 kPa cell

AJS PA 80 kPa battery

Figure 95: SEM pictures of the positive active electrodes from cells and batteries cycled with phosphoric acid

Layer A. The external layer at the surface of the plate corresponds to the “crust” of brighter colour that was observed at the opening of the cells cycled with phosphoric acid in Figure 94. This layer is very brittle, differing in this from the external layer of batteries cycled without phosphoric acid. When only little mechanical pressure is applied on the cell, layer A is much thinner as can be seen for the gel cell on the first picture of Figure 96.

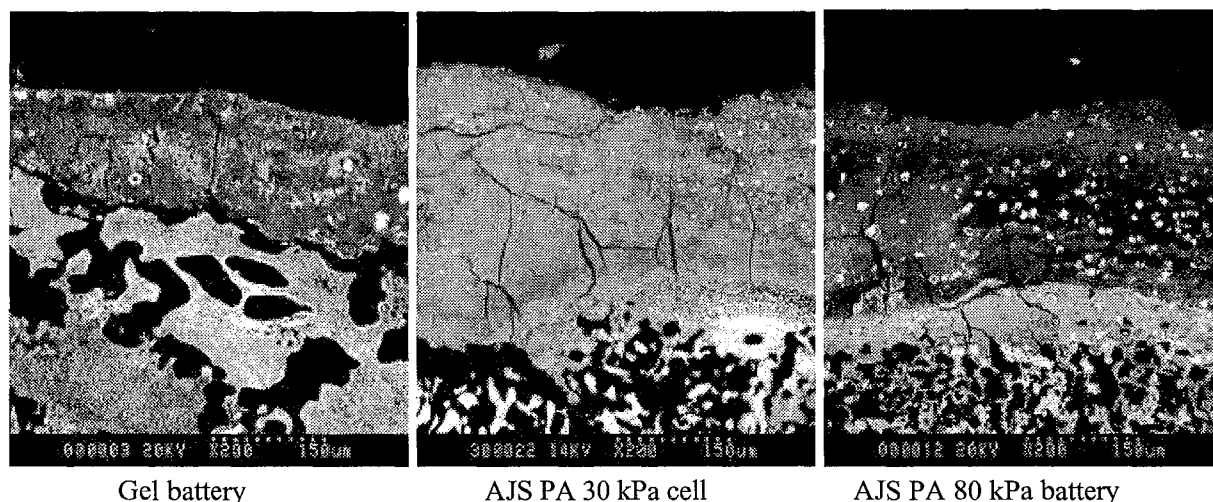


Figure 96: SEM pictures of the external layer of positive active electrodes from cells and batteries cycled with phosphoric acid

While layer A constituted a part of the positive electrode cycled without phosphoric acid, in presence of the additive, layer A has a much different aspect and is also absolutely not tightly bound to the active material. The picture shows cracks that develop in layer A perpendicularly to its surface. The cracks are orientated towards the inside of the electrode. They mostly not reach the outer surface of the electrode. They seem to come from the deformation of the active material in the internal part of the electrode.

The composition of layer A was analysed with the microprobe. It consists of lead dioxide, even the small bright crystals that can be observed particularly at high pressure.

Layer B. The inside of the electrode has a quite complicated structure. For the gel battery, the A-B-C layering cannot be observed while for the AJS cell and battery, a thin layer B is present. As can be seen on Figure 97, the lead dioxide aggregates that form the intermediary layer have a shape similar to the ones of the layer B of the AGM cell or the AJS cell after cycling under low external mechanical pressure but with a higher porosity.

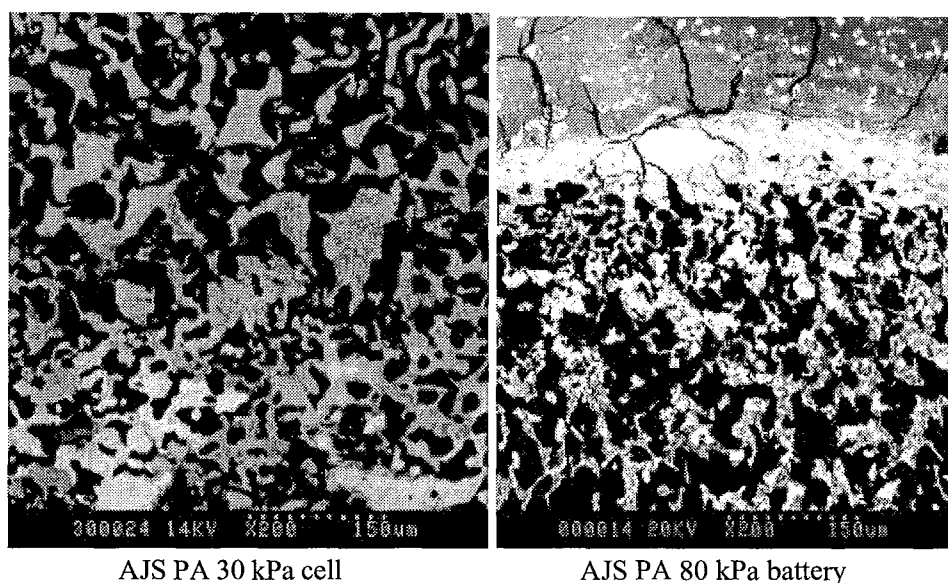


Figure 97: Layer B of and AJS cell and an AJS battery after cycling.

Layer C. The inner part of the positive plates cycled with phosphoric acid has a much unusual aspect. One observes a random disposition of aggregates of various size.

On a SEM picture, the density of the compound observed is responsible for the contrast. The denser the compound, the brighter its colour on the SEM picture. For the AJS cell/battery cycled with phosphoric acid, places can be observed that consist of a bright compound surrounded with a darker areas (see Figure 98).

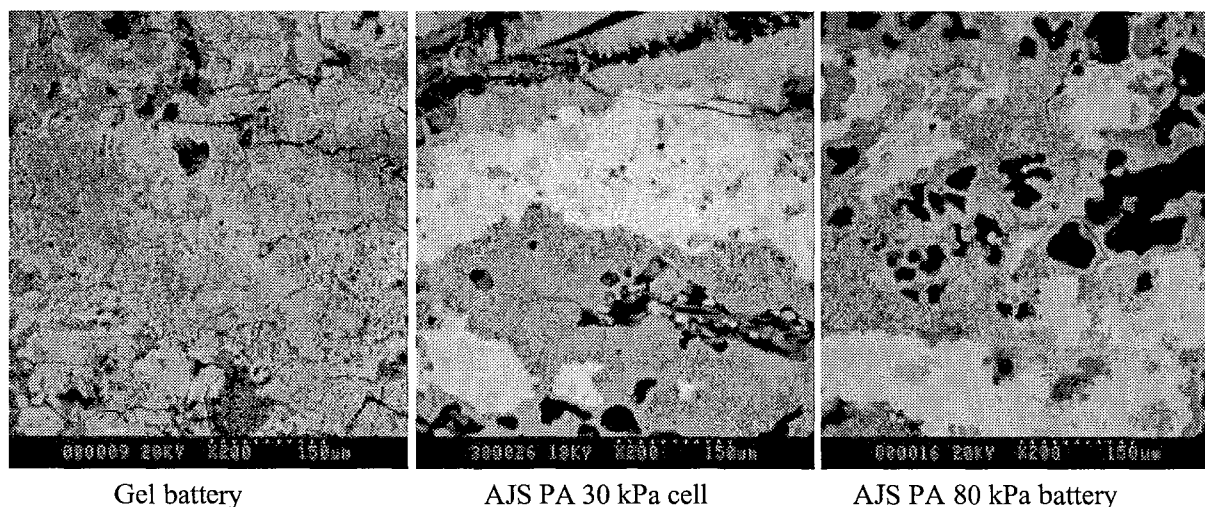


Figure 98: Internal layer of the positive electrode after cycling in a gel battery and in AJS battery and cell.

Figure 99 c shows the detail of the interface between these regions. They prove to consist of a dense material surrounded with a more porous one. The microprobe analyses demonstrated that the internal parts of these agglomerates consist of lead dioxide. The compound surrounding the bright zones contains some phosphor (in the range of 2 atom%) and the material proved not to be stable under the beam. One could observe the formation of a bubble under the carbon plating and the element analysis did not go to

100%. A deeper analysis of the compound was not realised that would show for example if one is in presence of a hydrogenated compound, what could explain the instability under the beam.

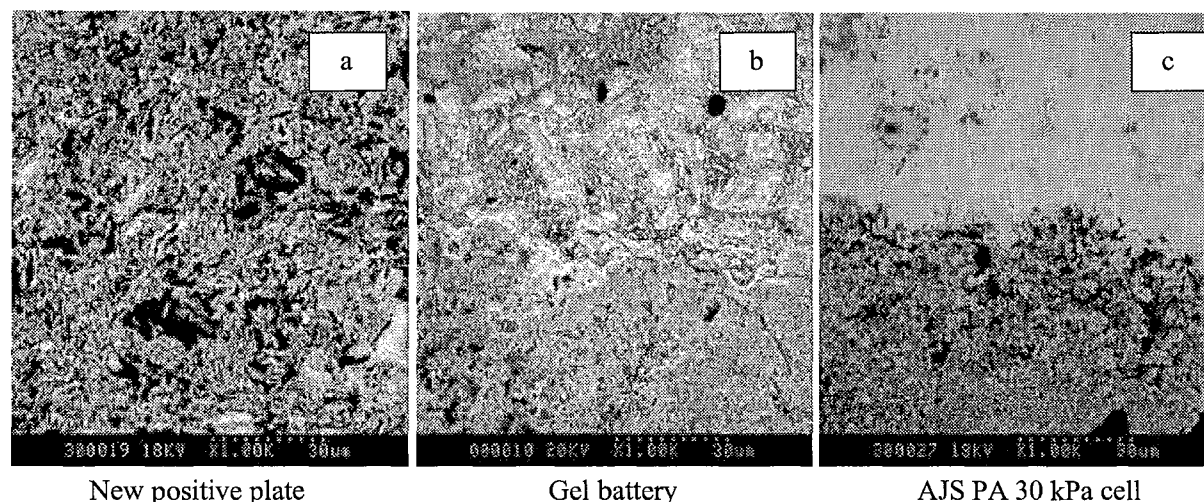


Figure 99: SEM pictures of the internal layer of a new positive plate and plates cycled with phosphoric acid in a gel battery or in an AJS cell

The positive active material from the internal layer of the cells cycled with phosphoric acid is even denser than the material from a new plate. It can be seen by comparing pictures **b** and **c** with picture **a** from Figure 99. It means that a material reorganisation takes place in which lead dioxide migrates from the external part of the plate or the outside of the aggregates towards zones that are more in the inside of the plate or in the inside of the lead dioxide aggregates and are that way less exposed to the phosphoric acid adsorption.

5.3 Conclusion about the effect of phosphoric acid

The effect of phosphoric acid is an inhibition of the charge reaction by hindering the three dimensional growth of the lead dioxide and subsequently promoting a fine crystallisation of the lead dioxide formed during charge. The subsequent discharge of the PbO_2 formed in presence of H_3PO_4 is also inhibited and allows the formation of fine lead sulphate crystals.

When phosphoric acid is adsorbed on a surface, it blocks the precipitation sites for lead dioxide. Thus, lead IV ions are present in higher concentration in the solution and this is the reason why lead dioxide precipitate more finely as a result of the higher over-saturation. These ions are also susceptible to diffuse to places where no phosphoric acid is adsorbed and precipitate there. This is the most probable mechanism to explain the aggregates of high density we observed in the positive active material after cycling with phosphoric acid.

Disappointingly, a full global explanation of the effect of phosphoric acid on the positive electrode processes could not be found.

Résumé et conclusion du chapitre concernant l'acide phosphorique.

Après une synthèse bibliographique montrant que l'effet de l'addition d'acide phosphorique sur les performances de la batteries au plomb est un sujet controversé, différentes influences de l'acide phosphoriques ont été montrées.

- D'une façon générale, il est accepté que l'acide phosphorique n'a pas d'effet sur les réactions électrochimiques de l'électrodes négative. Notre étude a montré que les potentiels et intensités des réactions dans un milieu d'acide sulfurique concentré ne sont effectivement pas modifiés. En revanche, la présence d'acide phosphorique semble accroître la corrosion des collecteurs de plomb de l'électrode négative des batteries fermées où le film d'électrolyte est mince et la réduction de l'oxygène se produit.
- L'addition d'acide phosphorique à l'électrolyte d'une batterie au plomb agit principalement sur l'électrode positive en modifiant la précipitation du dioxyde de plomb. Les sites de précipitation du dioxydes de plomb étant en partie bloqués par des espèces phosphates adsorbées, la solubilité des ions plomb IV est accrue. Le milieu devient ainsi plus oxydant pour le séparateur et les surtensions des réactions sur l'électrode positive sont accrues. En outre, la corrosion du plomb pur est très affectée par la présence d'acide phosphorique dans les expériences sur grilles même si cet effet est atténué par la présence de matière active dans les batteries avec des plaques de type Fauré. Il ressort finalement de nos expériences que l'effet de l'acide phosphoriques sur les performances de cellules ou batteries construites avec le nouveau séparateur est plutôt positif mais semble décroître au fur et à mesure du cyclage. Pour obtenir un batterie à grande durée de vie, l'application d'une pression mécanique est finalement beaucoup plus efficace que l'addition d'acide phosphorique même si cette seconde peut être bénéfique pour les performances de la batterie en début de vie dans la mesure où une charge permettant une forte polarisation de l'électrode positive a été appliquée à la cellule/batterie. L'adsorption de l'acide phosphorique et donc son efficacité est en effet dépendante du potentiel de l'électrode positive.

6 Oxygen cycle

The history of the VRLA battery and the different technologies were already reviewed in sections 1.5.2 and 3.2. The phenomenon that allows the construction of such maintenance free batteries is the oxygen cycle. The principle of the oxygen cycle is simple and schematised in Figure 100. During charge, oxygen is evolved on the positive electrode as a result of the unavoidable secondary reaction of water decomposition. With respect to the electrodes dimension and the state of charge at which oxygen and hydrogen evolution begin on each electrode respectively, oxygen is formed on the positive electrode while the negative electrode is still in the charge reaction and the hydrogen production has not begun yet. The oxygen can move from the positive to the negative electrode via gas channels in the separator or via the gas space. When oxygen reaches the negative plate, the reduction of the oxygen is predominant on the charge reaction. Thus the electrode is depolarised by oxygen reduction and no hydrogen production takes place. Half cell potential measurements undertaken by Mahato et al. [115] prove this chain of happenings in the oxygen cycle.

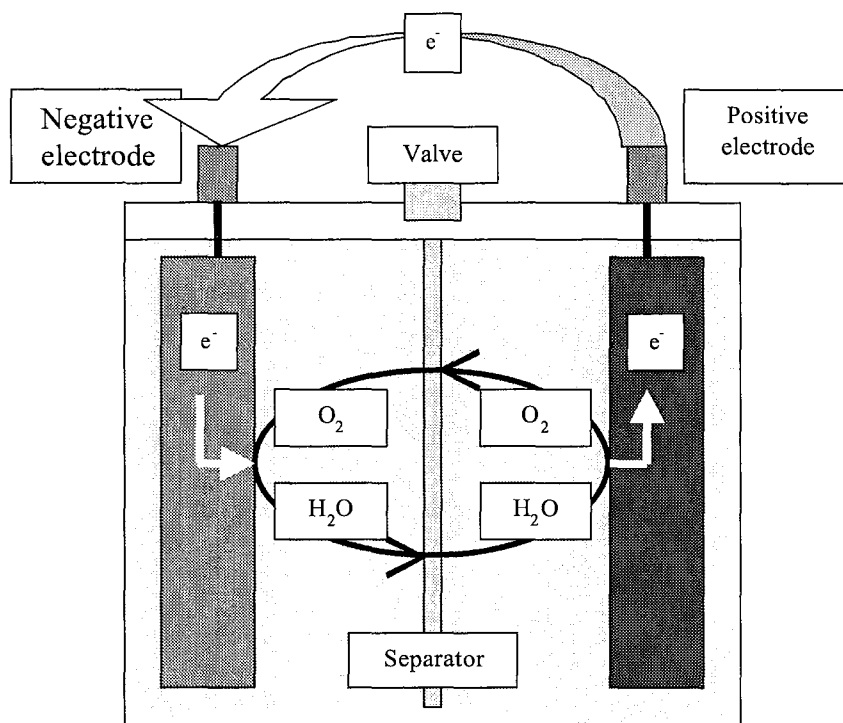


Figure 100: Schematic representation of the oxygen cycle

Of course, the full efficiency of the oxygen cycle can only be obtained for charging currents below a certain level. Above this level, the transfer of the oxygen to the negative electrode is limiting. Too much oxygen is evolved which cannot be fully “recombined” on the negative electrode and must be vented through the valve.

But even if the charge/overcharge current is low enough so that the oxygen cycle is fully efficient, the corrosion of the positive grid takes place and the part of the charging current that flows in the corrosion must be compensated by hydrogen formation on the negative plate [116]. It means that even in the best configuration, an overpressure will build up in the cell. The batteries must therefore be equipped with a vent that allows the release of gases when the pressure increases.

Depending on the separation system and on the initial electrolyte saturation, the evolution of oxygen on the positive electrode, the transfer from the positive to the negative and the reduction on the negative electrode can be different. These steps also change over the life of the cells and batteries. Therefore, it became important to look closer at the oxygen cycle in cells and batteries with the new AJS separator.

In fact, the oxygen cycle is a phenomenon with still some questions open yet. The rate at which it must proceed is a subject to controversy since a fully efficient oxygen cycle prevents extreme water loss but it is also responsible for higher heat production, leading in extreme cases to thermal runaway ([28] and [117]). Additionally, when the oxygen produced at the positive plate incessantly attains the negative plate, the electrode cannot reach a full state of charge and may become sulphated.

The way oxygen goes from the positive to the negative plate, if through the separator or across the gas space, is still under investigation [118].

As a last point, the reaction by which the oxygen is reduced on the negative plate is also subject to discussions as well as the factors affecting this "recombination".

With all these questions still open, the oxygen cycle in AJS cells was investigated.

6.1 Observation of the gas effects trough mechanical pressure recording

6.1.1 Mechanical pressure during one charge

Figure 101 displays the evolution of mechanical pressure during charge for an AGM cell in the beginning of its cycling life. The original measured curve was split between the contribution of the active material and separator, and the contribution of the gas effects.

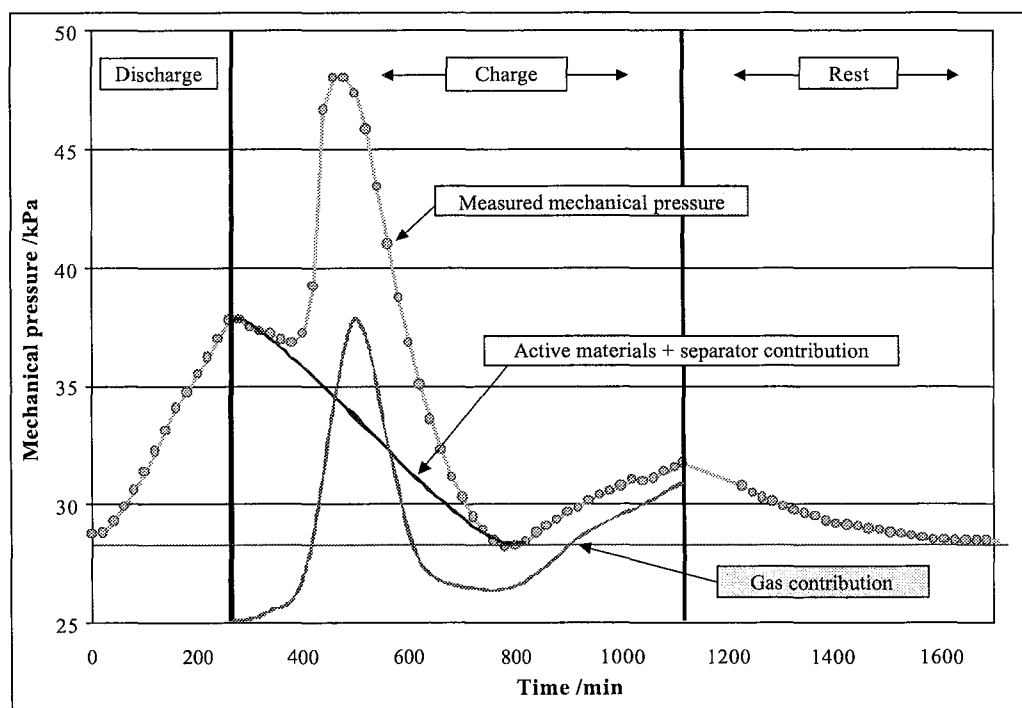


Figure 101: Evolution of the mechanical pressure on the AGM cell walls and different contributions to the mechanical pressure during one cycle in the beginning of cycle life

During charge, in the beginning, the pressure decrease is associated with the relaxation of the stress caused by the lead sulphates on the structure. Just at the end of the constant current charging period, a force peak can be observed that is caused by the oxygen formation. In the following minutes, the oxygen

evolution decreases, then the oxygen recombination takes place resulting in a quick pressure decrease. In this period of charge, the contribution of the force decrease by oxygen recombination is much higher than the shrinkage of the active material. At the end of charge, gas formation takes place again, this time with formation also of hydrogen.

The mechanical pressure reaches a minimum during the constant voltage period. This minimum is even lower than the pressure at the beginning of discharge, thus showing either a delay in the spring characteristics of the AGM separator or a partial crush of the separator. One can make the approximation that at that time, no additional hydrogen has been formed in this cycle yet and that almost all the oxygen evolved was reduced. Then, the extrapolation of the mechanical pressure relaxation curve (in blue) is not the reflection of the stress curve during discharge. This is a characteristic related to the AGM separator and much different from the behaviour of an AJS cell.

The red curve is an approximation of the gas pressure contribution to the total mechanical pressure recorded. The reduced oxygen generation during the constant voltage charge period is caused by the increasing polarisation of the negative electrode (lower available amount of PbSO_4 , starting of the hydrogen generation). As the negative electrode dominates the single electrode potentials, the increased polarisation of the negative electrode lowers the potential of the positive, causing a reduced oxygen production during constant voltage charge.

At the end of charge, the oxygen flow increases again and hydrogen formation takes place as almost all the lead sulphate has been converted to active material in the charged state (Pb and PbO_2). The cell observed here is valve regulated and oxygen reduction takes place on the negative plate. Thus hydrogen formation is minimised but we showed that even if the oxygen cycle is fully efficient, during overcharge, the corrosion of the positive plate imposes some hydrogen formation at the negative electrode. In reference [119], gas flow measurements through the valve of a VRLA corroborate the shape of the red gas curve and measurements of each electrode potential during an IU charge confirm the potential behaviour of the positive and negative electrode proposed here.

During rest, after the end of charge, the mechanical pressure decrease corresponds to the reduction of the remaining oxygen on the negative plate.

For the same cycle as shown in Figure 101, Figure 102 superimposes the mechanical pressure evolutions on the walls of AJS cells with and without phosphoric acid.

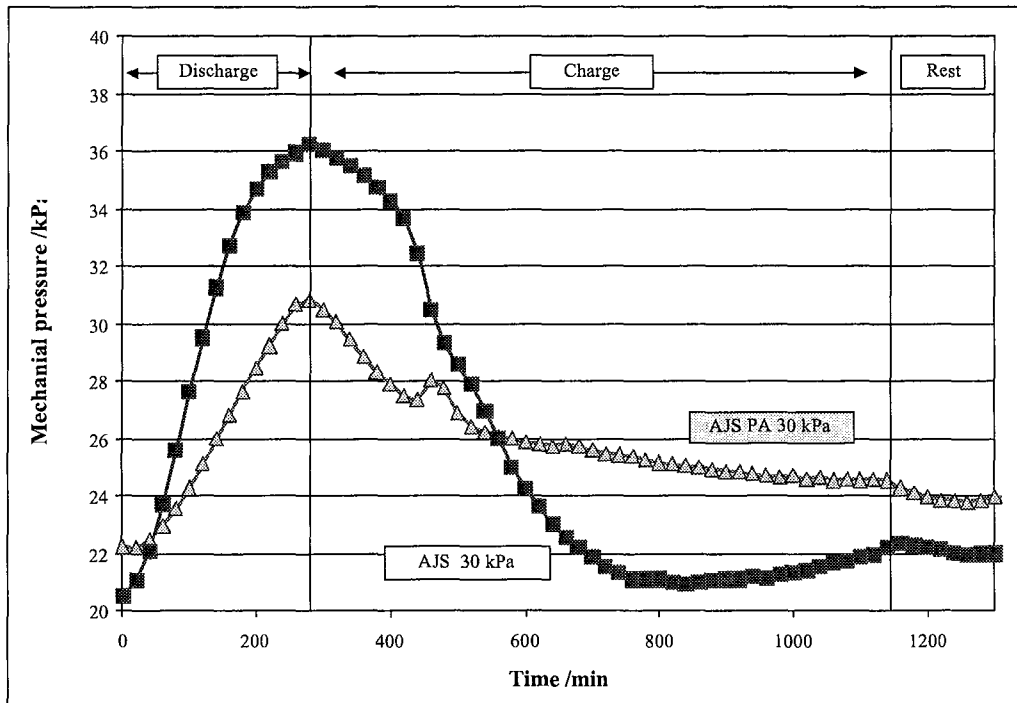


Figure 102: Evolution of the mechanical pressure during cycle 75 for AJS cells with different electrolytes at the same initial mechanical pressures

For an AJS cell, almost no oxygen peak is observable at the end of the constant current period as well as only a smooth gas peak at the end of charge. This is the result of a slow oxygen recombination. The gas space is already filled with the gases of the previous charge and under a pressure near the valve opening pressure. The further gas evolution only leads to a small increase of the mechanical pressure until the vent opens. The intensity of the initial mechanical pressure has no effect on the “gas behaviour” of the cell. We can conclude that AJS cells operate near the opening pressure of the valve just from the beginning of cycle life and the mechanical pressure curve over one cycle reflects quite exclusively the mechanical behaviour of the active material/separator system.

In presence of phosphoric acid, the peaks are more marked and the oxygen reduction during rest also. It could mean that the oxygen cycle is favoured by the presence of phosphoric acid but to confirm this affirmation, more investigations are needed with oxygen sensors registering the oxygen partial pressure during cycling and during overcharge.

6.1.2 Evolution over life of the gas effects

The shape of the mechanical pressure during charge over life suggest modifications of the cells behaviour concerning the oxygen cycle.

The first effect is the decrease with increasing cycle life of the peak associated with the oxygen production at the end of the constant current period. It can be best observed from Figure 103 that concerns the AGM cell. At the end of life, the peak is reduced to a shoulder as is the case right from the beginning in the AJS cells.

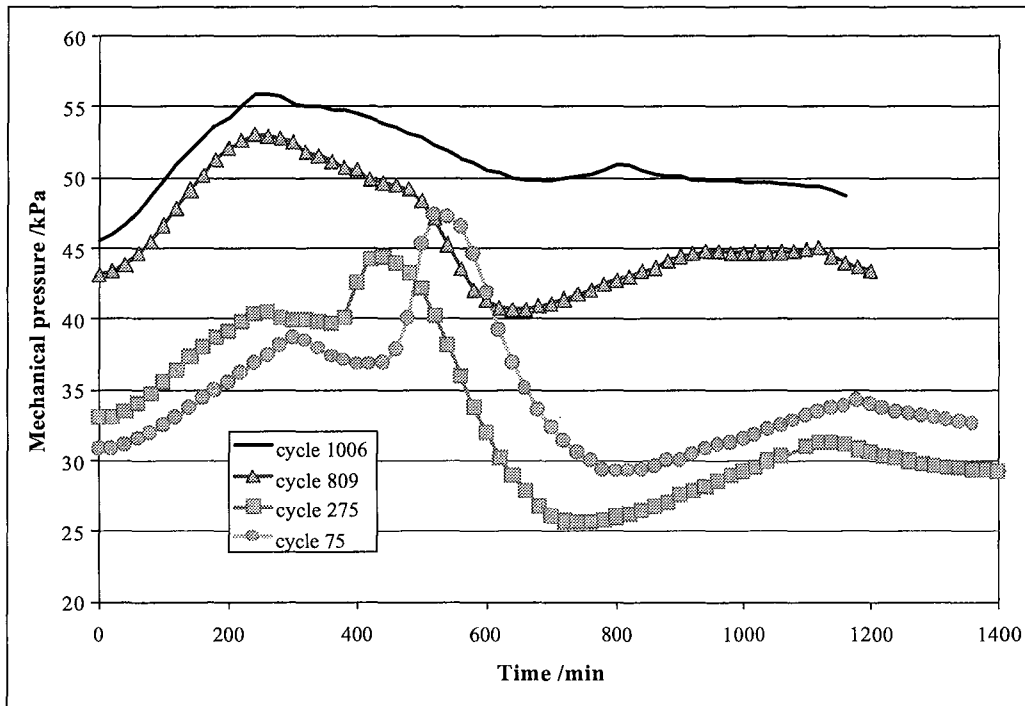


Figure 103: Mechanical pressure on the AGM cell walls at different ages of the cell

The decrease in the oxygen contribution is due to the accumulation over life of hydrogen in the cells gas space. Hydrogen is produced during charge and overcharge of the cell. And while oxygen is reduced on the negative plate, the produced hydrogen accumulates in the gas space so that the pressure at the end of rest after recharge increases progressively. Thus, the pressure increase until the vent opens is limited and the height of the peak associated with the oxygen production at the end of the constant current charging period decreases with increasing cycle number.

When the vent opens, both oxygen and hydrogen are vented. After recombination during the constant voltage period of the oxygen present in the gas space, the gas pressure can increase again at the end of charge resulting from the oxygen and hydrogen evolution.

One can suppose that the AGM separator does not crush any more after some 300 or 400 cycles. But even at cycle 809, the marked mechanical pressure decrease under the value of the discharge begin can be observed. It would mean that the hypothesis of a “AGM relaxation delay” is the correct one and that the AGM separator needs some time before it fully recovers its thickness after it has been compressed.

For an AJS cell containing no phosphoric acid, the mechanical pressure evolution during one cycle is not modified with increasing cycle life. From the beginning on, the oxygen generation peak at the end of the constant current charging period is reduced to a shoulder and there is no observable modification of the recombination behaviour over life.

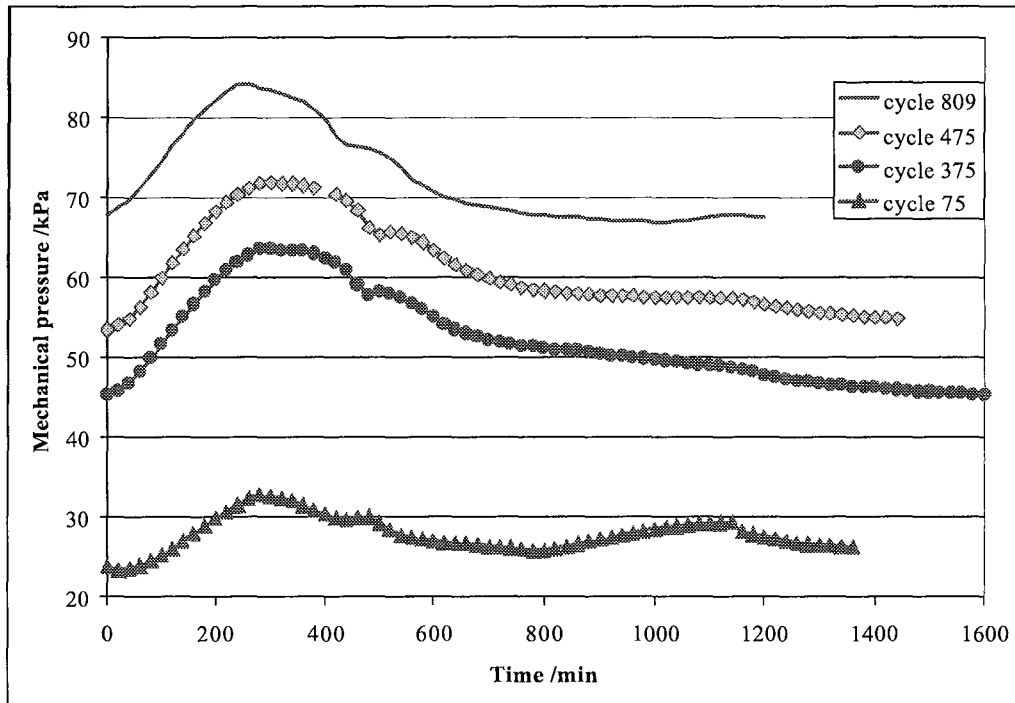


Figure 104: Mechanical pressure evolution for one cycle at different ages of the AJS PA 30 kPa cell

In presence of phosphoric acid, the mechanical pressure peaks associated to gas formation during charge are much sharper. With increasing cycling life, the gas shoulder at the end of the constant current charging period does not disappear as noted for the AGM cell.

In conclusion, while the gas effects do almost not contribute to the evolution of the mechanical pressure during one cycle in AJS cells without phosphoric acid, in AGM cells and AJS cells with phosphoric acid, at least during charge, the measured mechanical pressure curves are strongly influenced and even sometimes dominated by the gassing/recombination conditions and in addition, by the flexible separator for AGM. Both influences are lowered with increased number of cycles (gas space filled with hydrogen, AGM separator compressed) and therefore, the mechanical pressure curves get closer to the mechanical expansion shrinkage of the active material.

6.2 Recombination efficiency

6.2.1 Current repartition and recombination efficiency determination

During the charge and the overcharge of a lead-acid battery, the current at the positive electrode can be consumed by in the following reactions:

- | | |
|------------------------------------|-----|
| Normal charge reaction | (1) |
| Positive active material formation | (2) |
| Organic materials oxidation | (3) |
| Hydrogen reduction | (4) |
| Positive grid corrosion | (5) |
| Oxygen evolution | (6) |

For the determination of the oxygen recombination rate, many techniques have been developed and all of them rely on measurements during overcharge or rest. The reaction of charge of the positive active mass

(1) can then be neglected as well as the rest formation of the positive active material (2) provided some cycles have been performed before the measurement.

Symanski et al. [120] show that the oxidation of organic materials (3) can be neglected, leading to a maximal error on the oxygen recombination rate of 0.02% in the worst case. With the increasing trend of the manufacturers to add organic fibres to the active material for a better mechanical integrity of the plates, this low error may need to be reconsidered but it should not increase tremendously.

The hydrogen reduction (4) is almost not measurable, according to e.g. Ruetschi and Mahato.

The corrosion current (5) can be determined on a bare grid. As showed in section 4, the corrosion current is higher in absence of active material. Anyway, it also can be neglected as it represents a correction of less than 2% of the overcharge current [121].

As a consequence, the approximation that only oxygen evolution (6) occurs on the positive electrode during overcharge leads to a maximal error on the recombination rate of about 3%.

The earliest technique to determine the oxygen recombination rate relied on the water loss of the battery determined by gravimetric method. The hypothesis is that inefficiency in the recombination leads to a water loss. The maximal possible water loss for a given overcharge current is calculated and compared to the effective water loss measured.

But very small water losses could not be weighted even if some vented gas could be observed. It became clear that the above method did not lead to reliable results in short time experiments and the newer techniques for the evaluation of recombination rate are based on the composition measurement of the ventilated gases or of the gas in the free space after overcharge or under open circuit conditions.

One first technique for measuring the oxygen recombination efficiency (ORE) consisted in measuring the quantity of hydrogen released by the vent and comparing the deduced "hydrogen current" to the total overcharge current.

$$[ORE] = \frac{I - I_H}{I} * 100$$

Then Symanski determined the ventilated gas composition utilising gas chromatography. The currents corresponding to the measured quantity of oxygen vented for a given overcharge current and time are calculated according to the Faradays law. It results in the following oxygen recombination efficiency :

$$[ORE] = \left(1 - \frac{I_{oxygen\ vented}}{I_{overcharge}}\right) * 100$$

This technique is quite expensive and needs a gas sampling that may disturb the system. In addition, the composition of the sample depends on the sampling place if no mixing chamber is added.

In 1987, W. B. Brecht [122] proposed an easy method to evaluate the effect of diverse conditions on the recombination of oxygen. The hypothesis is the following: as long as the oxygen reduction occurs on the negative electrode, this electrode is no polarised. The dependence of the negative electrode polarisation on the charging current is plotted as well as the battery polarisation. The effect of different conditions are deduced from the way the polarisation curves are shifted. This technique can be used on a bare electrode but is difficult for measurements on pasted plates in real cells.

In 1991, Dietz and al. [123] measured the cell pressure during galvanostatic overcharging and after circuit opening. The oxygen reduction rate depends on the oxygen partial pressure while the oxygen formation depends on the overcharge current and time. Then, for each overcharge current, the pressure evolution in the battery reaches a plateau after a while, when the oxygen cycle is fully achieved. At this point, the overcharge current and the oxygen reduction current have the same value. The problem is that this plateau is never reached in a practical case. During the overcharge, the oxygen evolved on the positive electrode is either reduced on the negative or remains in the free space of the battery. If the circuit is then opened and maintained in an open state, the total pressure in the free space decreases because of a reduction of the oxygen and at the end, the only remaining pressure corresponds to the hydrogen. The part of the current corresponding to the oxygen reduction during the overcharge is then the difference between the overcharge current and the current deduced from the pressure decrease under open circuit conditions.

The above mentioned method has the advantage to be easy and to require a single pressure sensor in the free space of the battery. No gas composition analyse is needed introducing no problem of homogeneity. Further techniques reported in the literature are based on a composition analysis of the gas in the free space of the battery, either with chromatography or Raman spectroscopy. Their high cost and complexity make them difficult to use.

6.2.2 Recombination efficiency of an AJS cell

The equipment shown on Figure 105 was used for measuring the recombination efficiency of different cells.

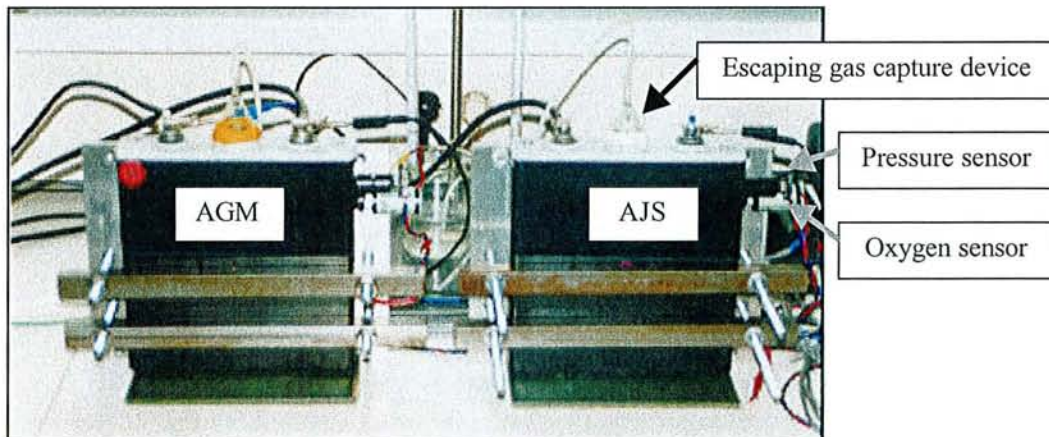


Figure 105: Picture of the recombination efficiency measurement device.

The cells were equipped with compression bars in order to prohibit a rapid degradation of the cells due to a total absence of external mechanical pressure. The escaping gas volume was measured and the pressure and oxygen partial pressure in the gas space were recorded. The measurement was performed for different overcharge currents and the curves obtained are presented in Figure 106.

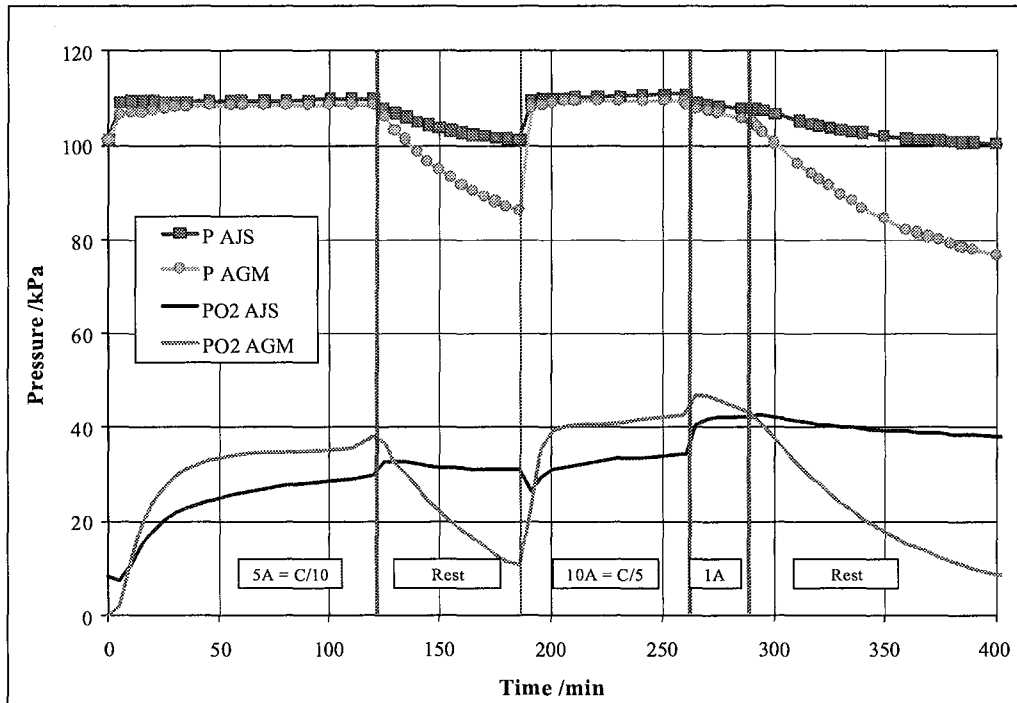


Figure 106: Evolution of the pressure and oxygen partial pressure in the gas room during overcharge at different currents and rest for an AGM cell and an AJS cell

- During overcharge, the pressure in the gas room increases rapidly for both cells until it reaches the valve opening pressure. At about 109 kPa, the valve opens and the pressure stays constant.
- During overcharge, the oxygen partial pressure in the gas space increases much slower in the AJS cell than in the AGM cell. This is a sign for a little oxygen recombination in the AJS cell. Namely, when oxygen does not reach quickly the negative electrode, hydrogen is evolved because no depolarisation of the negative electrode takes place and the gas space is filled with stoichiometric proportions of oxygen and hydrogen. It means an oxygen partial pressure of about 35 kPa.
- A surprising phenomenon takes place in the AJS cell: at the moment the current is increased, the oxygen partial pressure decreases before it increases again, as is normally expected. And when the current is decreased, e.g. at the beginning of rest, the oxygen partial pressure increases shortly before it decreases. It would speak for the AJS system in favour of a phenomenon of oxygen adsorption or more probably, a certain pressure of oxygen builds up on the positive electrode. This “oxygen delay” is specific to AJS.
- During rest, the oxygen partial pressure decreases much quicker in the AGM cell as a sign of the better oxygen recombination. Figure 107 shows this point more in detail.

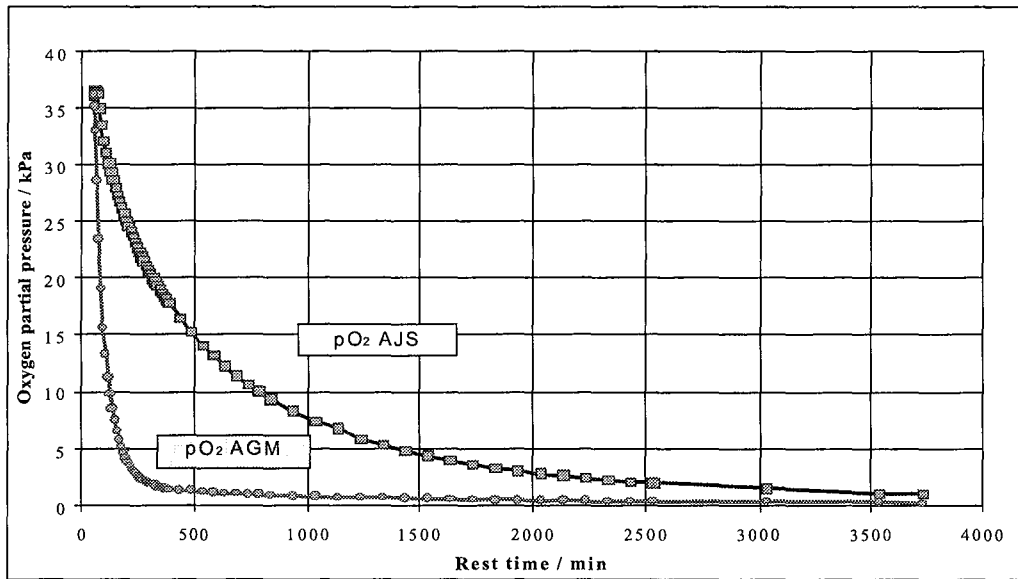


Figure 107: Evolution of the oxygen partial pressure during rest after overcharge for an AGM cell and an AJS cell

The recombination takes place in both cells until the oxygen partial pressure reaches zero kPa. It is a sign for the good tightness of our cells. But the recombination is much slower in the AJS cell than in the AGM cell. If one represents the logarithm of the pressure depending on the time, the first portion of the curve is a straight line whose slope is over 5 times higher for the AGM cell than for the AJS cell. It means that $\ln(P) = At$ and as a consequence that $dP/dt = -AP$. The recombination rate depends on the oxygen partial pressure and for a same pressure, it is 5 times quicker in the AGM cell.

In Figure 108, the volume of gas escaping from the cell during overcharge at different currents as well as the theoretical maximum volume of gas that could have escaped are represented assuming stoichiometric proportion of 1/3 oxygen and 2/3 hydrogen.

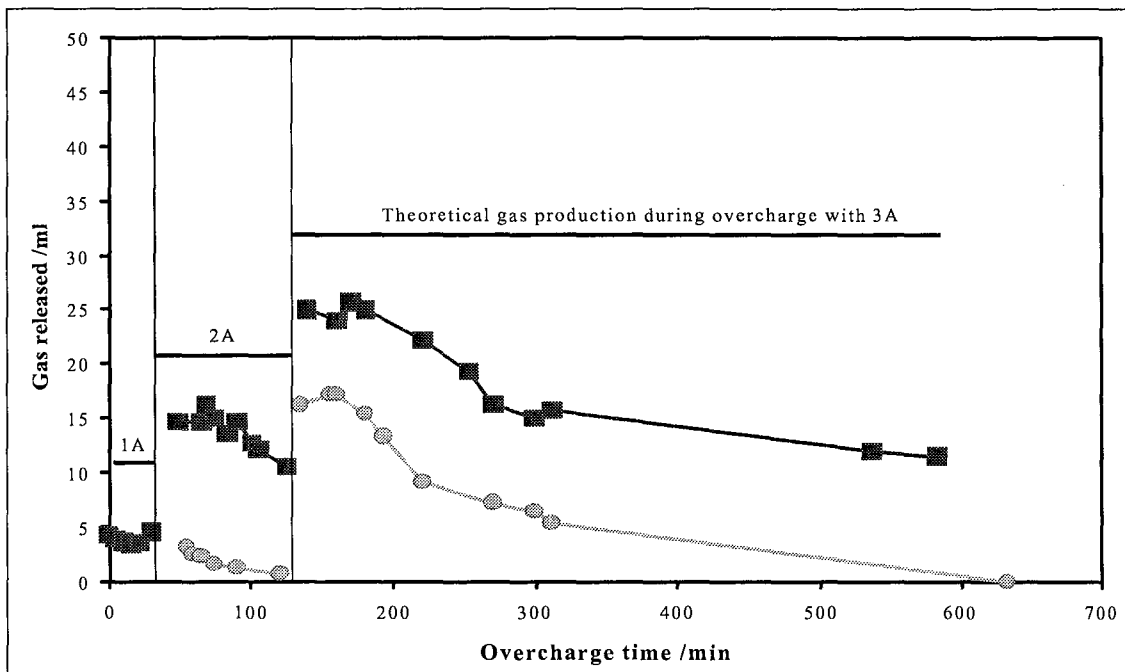


Figure 108: Volume of gas escaped during overcharge and theoretical maximal gas volume.

At 1A overcharge (about C/50 rate), the oxygen is fully recombined in the AGM cell from the beginning of overcharge on while in the AJS cell, half of the gas that could theoretically escape can be measured. With increasing overcharge current, even in the AGM cell the oxygen cycle is not fully efficient. With increasing overcharge time, the cells recombine better and better. This can be associated with the increased number of free channels that are appearing in the separators as a result of drying out or liquid expelling but also to heat effects that catalyse the oxygen cycle. The oxygen recombination efficiency (ORE) calculated from this measurement is shown in Table 18

Overcharge current /A	AGM ORE /%	AJS ORE /%
1	100	62
2	91	34
3 (beginning)	49.33	25
3 (after 8h)	82	56.66

Table 18: Oxygen recombination efficiency during overcharge of an AJS cell and an AGM cell

In conclusion, the AGM cell has a much more efficient oxygen cycle than the AJS cell but during overcharge, a certain amount of oxygen is recombined, even in AJS cells.

6.3 Transfer of oxygen from the positive electrode to the negative electrode

6.3.1 IR pictures for the determination of the recombination sites

The oxygen reduction reaction is highly exothermic. Therefore, it may be possible to look at the places where the oxygen reduction takes predominantly place with help of an infra red camera. The places where the recombination takes place are the places where oxygen is predominantly available and it may thus be possible to differentiate between a transfer of the oxygen that takes place predominantly trough the gas space and a transfer that takes predominantly place through the separator. Basing of this idea, cells with different separation systems were observed in different positions with the IR camera while they underwent overcharge. These cells were at the beginning of their life and therefore not at their optimum of recombination efficiency. The idea of an IR picturing of VRLA cells was already used by Giess [124] who could investigate thermal phenomena in VRLA AGM batteries. He was able to see the inhomogeneities between the different cells of one battery monobloc during discharge and charge. The electrolyte drainage in tall cells could also be observed.

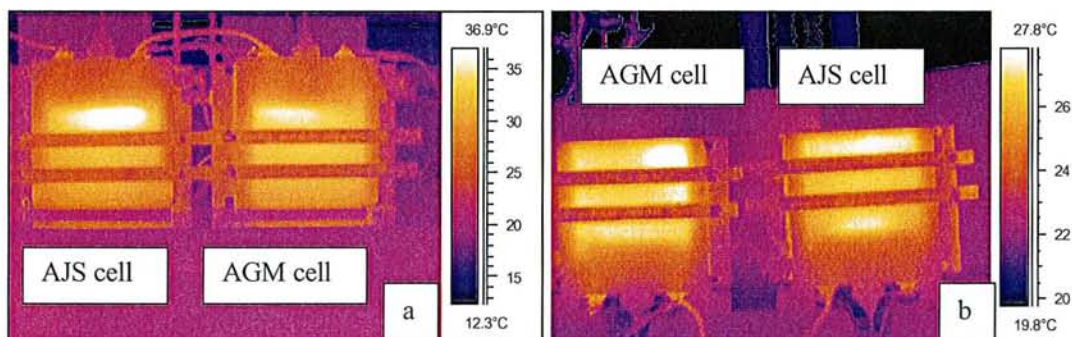


Figure 109: IR pictures during overcharge of an AJS cell and an AGM cell at the beginning of their life

It was difficult to conclude about the recombination behaviour of the cells on the base of these only pictures. The different effects of the electrolyte repartition, of the voltage drop on the current collector and of the oxygen recombination itself were not possible to dissociate. The only conclusion that can be made is that even in the AJS cell, where there is free room at the sides as well as at the top, it was not possible to see a localisation of the heat generation at the periphery of the negative plate. This observation speaks a lot in favour of a transfer way that goes through the separator.

The cells were tilted and left in this position for 2 weeks. The overcharge measurements were then repeated and it could be observed that once again, the warm place was the highest point of the cell. It means that either a drainage took place that liberated gas channels in the separators in the highest third of the cell or that the oxygen is going up by convection. The second explanation is the most probable since for cells tilted to 90° and immediately overcharged, the hot spot moves also to the highest place of the cell even if there was not enough time for a new repartition of the electrolyte.

6.3.2 Oxygen transfer trough the AJS separator

In order to quantify the amount of oxygen that is able to go through the separator depending on its saturation in electrolyte, measurements were undertaken in a gas cell which principle is shown in Figure 110.

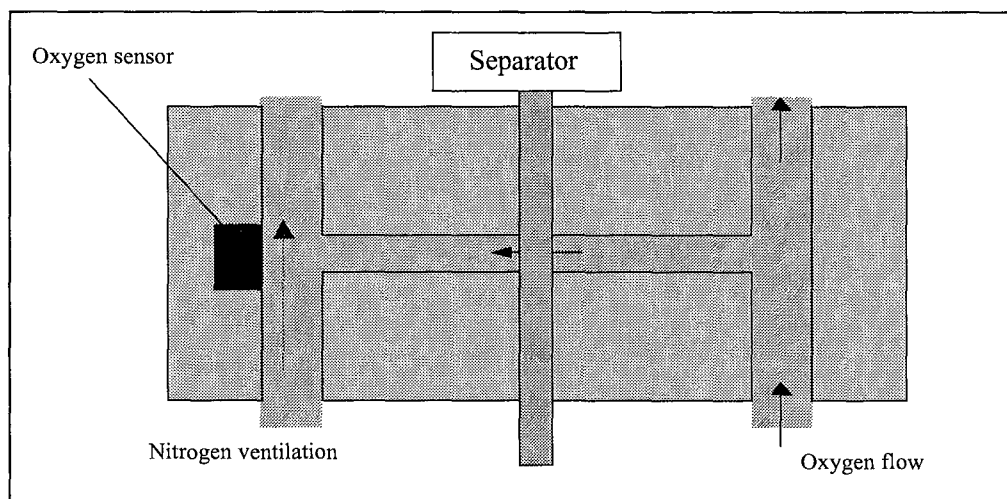


Figure 110: Schematic representation of the oxygen transfer measurement device

A piece of separator is first fully saturated in water and inserted between two plates of Plexiglas. Both half cells are initially purged with nitrogen. The first half cell is then flooded with oxygen. In the second half cell, nitrogen is sent with a regulated flow rate so that the pressure difference between the two half cells is controlled. On the “nitrogen side” of the equipment, an oxygen sensor is fixed that measures the partial pressure of oxygen in the nitrogen flow. Once the oxygen flow is turned on, the sensor records the oxygen partial pressure evolution in the nitrogen flow.

After a while, the oxygen flow through the separator has partially dried it out. For different values of the corresponding oxygen partial pressure in the nitrogen flow, all flows are interrupted, the separator is promptly removed and the piece of it that allowed the oxygen transfer is cut and weighed. The separator piece is then dried and the dry weight is recorded. The volume of the separator piece is determined and its saturation at the end of the measurement is calculated.

The oxygen diffusion coefficient is calculated on the base of the Ficks law as shown in the following equations.

$$\Phi_{O_2} = D \frac{\delta C}{\delta x} = D * \frac{1-C}{E}$$

$$\Phi_{O_2} = C * (F + \Phi_{O_2}) = \frac{C * F}{1-C}$$

$$D = \frac{F * E * C}{A * (1-C)^2}$$

Φ_{O_2} = oxygen flow through the separator / m³/s

D = oxygen diffusion coefficient / m²/s

C = fraction of oxygen in the nitrogen flow

E = separator thickness / m = 1.45 * 10⁻³

F = nitrogen flow / m³/s = 8.33 * 10⁻⁷

A = diffusion surface / m² = 0.7854 * 10⁻⁴

With these data, the dependence of the oxygen transfer coefficient on the saturation of the separator can be drawn. The data concerning the AGM separator in Figure 111 is taken from reference [23] and was not measured in our laboratory.

In this measurement, the difference of pressure between the two half cells was set between 20 and 40 mm water (0.2 to 0.4 kPa) and the result proved not to be modified by the variation of the pressure in this range.

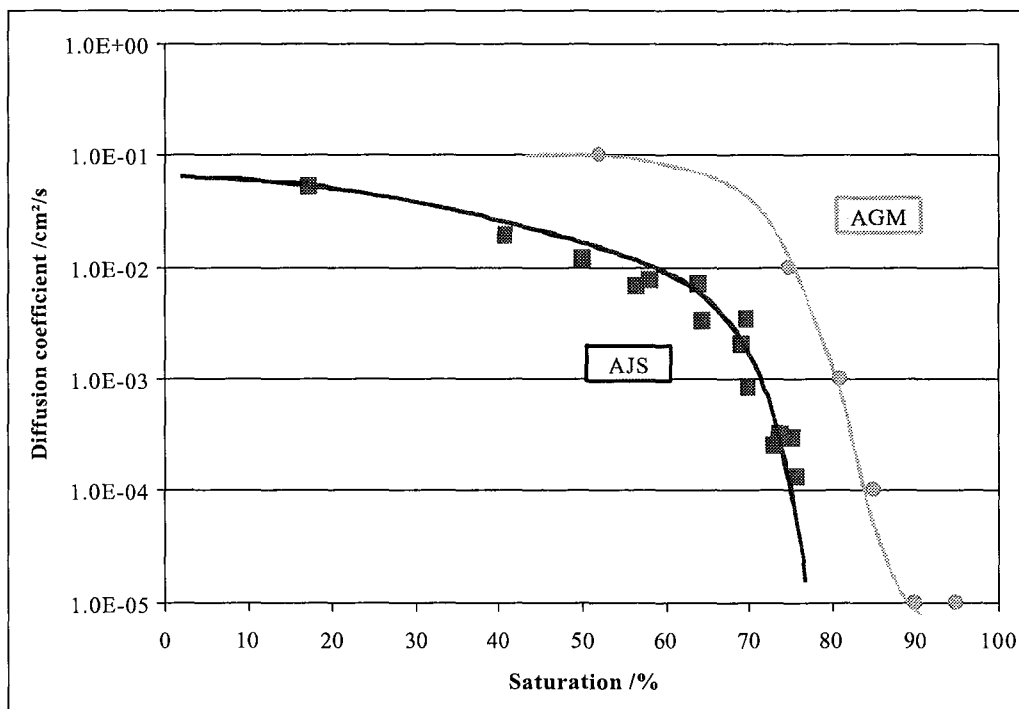


Figure 111: Diffusion coefficient of oxygen through a separator versus separator saturation.

For a same saturation of the separator, the oxygen diffusion coefficient is about 10 to 100 times smaller in AJS than in AGM. It would mean that for a saturation of the AJS separator higher than 70%, practically no oxygen transfer would take place through the separator. For example, the diffusion coefficient at about 75% saturation ($D=2 \cdot 10^{-4} \text{ cm}^2/\text{s}$) would correspond to an oxygen recombination current of 242 mA (for a cell with 6 negative plates and a diffusion surface of 182 cm² if the oxygen diffusion is the limiting factor for the reduction).

But we measured oxygen recombination currents of over 0.5 A during overcharge at a saturation of over 95% of the AJS cell. Therefore, the transfer must take place via another way.

The oxygen transfer was proved not to take place preferentially via the gas space by IR picturing but the transfer coefficient of oxygen through the AJS separator measured at low pressure differences between the two sides of the separator are too low to explain the high oxygen recombination currents observed. Basing on the shape of the oxygen partial pressure curves obtained during overcharge measurements, the idea of the formation of an oxygen pressure on the positive electrode appeared to be coherent. This theory would also explain the shape of the active material in the AJS cell cycled under mechanical pressure. Namely, as shown again in Figure 112, the corralloid structure of the active material looks like a network of caves produced by a fluid under pressure.

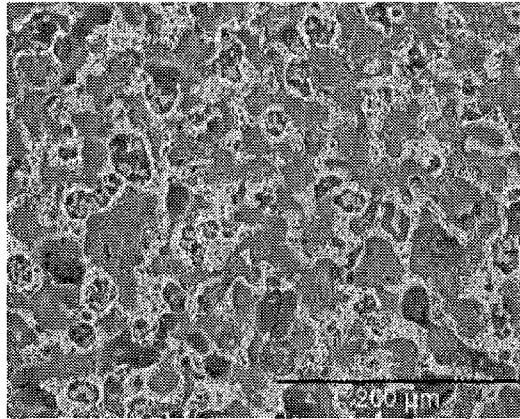


Figure 112: Intermediary layer of the positive electrode of an AJS cell after cycling

The AJS separator has an average pore size of $0.19 \mu\text{m}$ but the total porosity consists in volume of 10% pores of $1.59 \mu\text{m}$ diameter and 90% pores of $0.012 \mu\text{m}$ diameter. The pore size distribution of an AJS sample is shown in Figure 113.

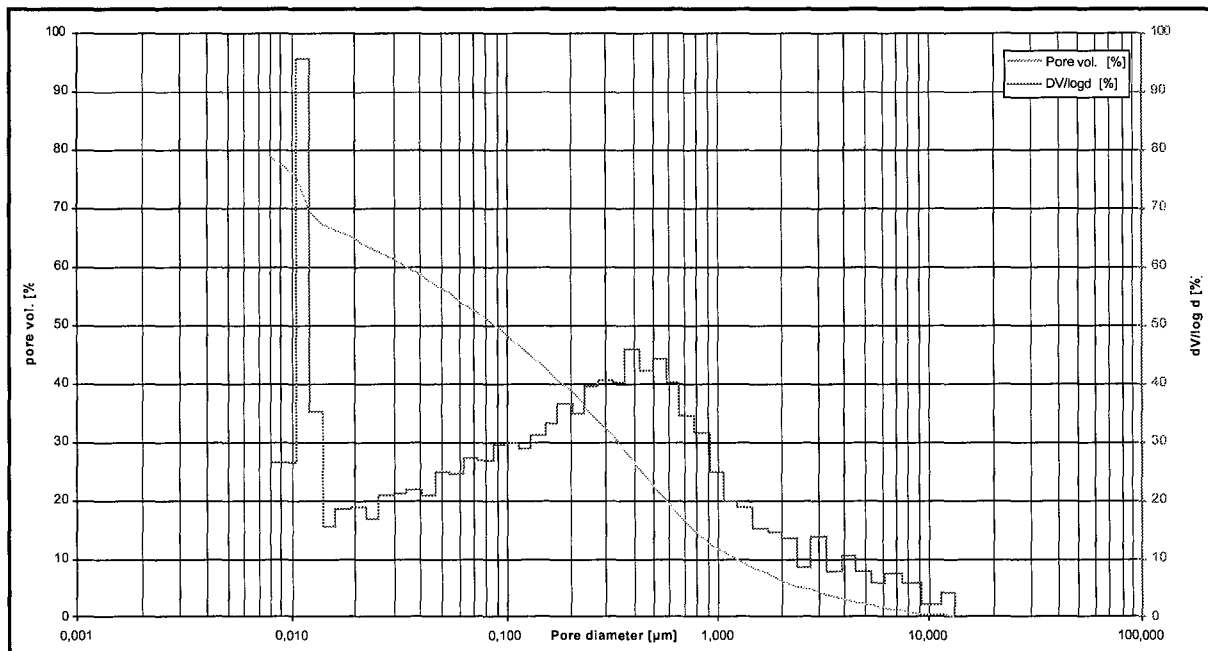


Figure 113: Pore size distribution in AJS separator

A gas pressure higher than the capillary pressure in the pore is needed to expel liquid from a pore. Thus the required gas pressure is inversely proportional to the pore size. It means that large pores can be easily freed of their electrolyte while small pores stay filled.

The Laplace pressure was given in section 3.4.2.2 as $P_L=2\gamma/r_p$ for a round pores of radius r_p . With the estimation that the surface tension of the AJS separator is in the range of the surface tension of unmodified polyethylene [125], i.e. $\gamma \approx 34 \text{ mJ/m}^2$, the Laplace pressure in the pores is represented in Table 19.

Pore diameter /m	Laplace pressure /kPa
$1.59 \cdot 10^{-6}$	85.5
$0.19 \cdot 10^{-6}$	715.8
$0.012 \cdot 10^{-6}$	11333.3

Table 19: Laplace pressure in the pore depending on the pore diameter basing on a surface tension of AJS of 34 mJ/m^2

It means that the oxygen partial pressure that can build up on the positive electrode is possibly sufficient to free the largest pores of the AJS separator of their electrolyte. The transfer of oxygen is then possible via the gas channels with a diffusion coefficient corresponding to the diffusion of oxygen in the gas phase. The measurement of this “pneumatic effect” in the oxygen transfer was not undertaken in the set-up for transfer coefficient determination but it can explain the fact that the oxygen recombination efficiency is better in practice than the one that can be deduced from the diffusion coefficient.

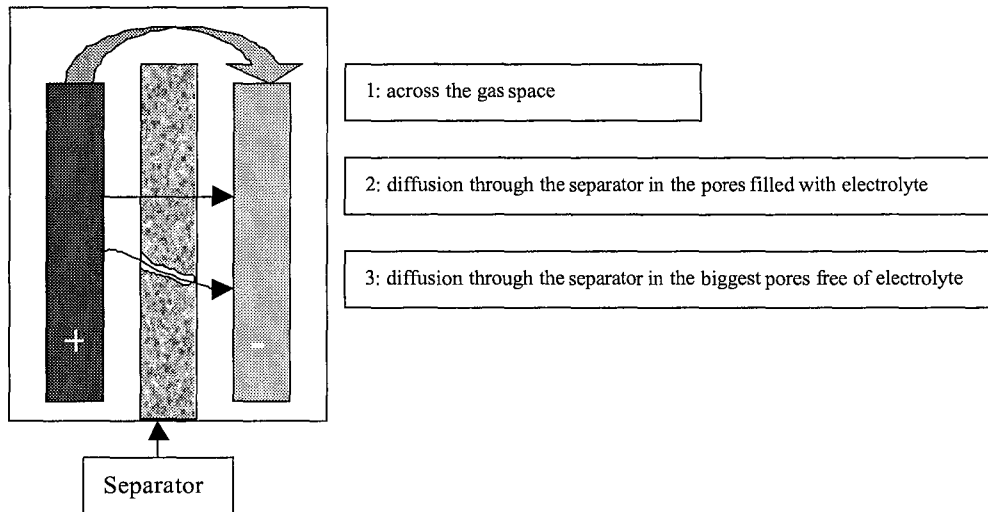
The last mechanism by which oxygen transfer can take place from the positive to the negative electrode is “a preferential adsorption and exchange mechanism on the surface of amorphous silica chains” described by Brecht [126]. In this mechanism, “a flip-flopping of bonded species” takes place at the surface of the silica “wherein oxygen and hydroxyl groups exchange places with respect to surface silicon atoms”.

Since the AJS separator also consists for the biggest part of silicon dioxide, this mechanism is also susceptible to take place in VRLA AJS cells. A real quantification of the oxygen transfer rate associated with this “silica effect” was never undertaken and we could find no precise description of this mechanism. Brecht only observed that in all the VRLA batteries with separation/immobilisation systems consisting of silica, the oxygen transfer rates were higher than those corresponding to the only transfer through the gas channels. When separators containing no silica were tested, much lower transfer rates could be observed.

6.4 Conclusion about the oxygen cycle

The oxygen recombination was shown to take place much slower in AJS cells than in AGM cells as a result of the higher electrolyte saturation and of the smaller size of the pores in the AJS separator.

Even if slower in the AJS cells, the oxygen cycle proceeds at a measurable rate during overcharge in AJS lead-acid cells. There are three ways how the transfer of oxygen can take place from the positive electrode to the negative electrode. They are recapitulated in the following schema.



Way 1. The transfer of oxygen from the positive to the negative plate was shown by IR pictures not to take place preferentially via the gas space surrounding the electrodes.

Way 2. A measurement of the oxygen diffusion coefficient through the separator depending on the separator saturation was undertaken that also proved that the oxygen transfer happens via another way than through simple diffusion through the saturated separator.

Way 3. It is well probable that a diffusion via gas channels takes place when an oxygen overpressure builds up on the positive plate that expels the electrolyte from the largest pores of the separator.

Way 4. The last transfer mechanism that is susceptible to take place in an AJS cell is a mechanism associated with the presence of silica. This mechanism was not proved yet but can well also take place in AJS cells where the AJS separator consists principally of silica.

But the oxygen cycle is not a target by nature. It is only an expedient to avoid a limitation of the lead-acid cell/battery life by drying out in maintenance free designs. The electrical tests showed that the AJS cells/batteries have a longer cycle life than cells/batteries with another separation system and a better recombination efficiency. It means that the quantity of electrolyte present in the AJS cell from the beginning is sufficient to allow the cell to perform over 1000 full cycles and the point of the slow oxygen recombination is therefore not critical for the AJS cells.

Résumé et conclusion du chapitre concernant l'effet du nouveau séparateur AJS sur le cycle de l'oxygène dans les batteries au plomb fermées.

- L'observation de l'évolution de la pression mécanique sur les parois de cellules au plomb fermées ainsi que la mesure lors d'expériences de surcharge des pression totale et pression partielle d'oxygène ont permis de démontrer que le phénomène de recombinaison de l'oxygène se produit beaucoup plus lentement dans les cellules contenant le nouveau séparateur AJS. Cet effet est lié à la porosité plus faible du séparateur AJS et aux plus petites dimensions de ses pores ainsi qu'à la saturation en électrolyte plus importante des cellules avec AJS.
- Mais si le cycle de l'oxygène est moins performant dans les cellules avec AJS que dans des cellules avec un séparateur en fibre de verre, il a tout de même lieu. Des mesures par caméra infrarouges ont prouvé que le transfert de l'oxygène de l'électrode positive à l'électrode négative ne se produit pas de façon prédominante par l'espace gazeux qui entoure le bloc d'électrodes. La détermination du coefficient de diffusion de l'oxygène à travers le séparateur en fonction de la saturation en eau de ce dernier a en outre délivré des valeurs très basses du coefficient de diffusion pour les saturations rencontrées dans les batteries quand la différence de pression entre les deux côtés du séparateur est faible. Ces faibles valeurs ne suffisent pas à expliquer les courants de recombinaison de l'oxygène mesurés lors d'expériences de surcharge. Par conséquent, le transfert de l'oxygène se produit probablement en phase gazeuse par le biais de canaux qui sont libérés de leur électrolyte par l'accumulation d'oxygène sur l'électrode positive. Un calcul de la pression nécessaire à libérer les plus gros pores du séparateur confirme la plausibilité de cette hypothèse au même titre que l'observation de la variation de la pression partielle d'oxygène dans l'espace gazeux de la batterie lorsque le régime de surcharge est modifié.
- En dernier lieu, il est important de remarquer que le cycle de l'oxygène n'est pas une fin en soi mais un moyen pour éviter la limitation de la durée de vie d'une batterie fermée par son dessèchement. Nous avons prouvé que les cellules et batteries contenant le nouveau séparateur peuvent délivrer de l'ordre de 1000 cycles profonds sans souffrir de pénurie d'électrolyte.

En conclusion, un cycle de l'oxygène se produit dans les cellules/batteries avec AJS et même s'il est moins efficace que pour d'autres systèmes de séparation, il ne représente pas une limitation pour le système AJS. La quantité initiale d'électrolyte présente dans les cellules est suffisante pour assurer une durée de vie très satisfaisante.

General conclusion

Achievements of this Ph.D. work

The suitability for VRLA application of a new separation system called AJS and its ability to improve the cycle life of lead-acid batteries via durable mechanical pressure application was demonstrated.

The application of mechanical pressure is not able to fully hinder the expansion of the positive plate but leads to a more homogeneous positive active material utilisation provided only very few free room is left for the active material expansion. Additionally to the better utilisation of the positive active mass, the application of mechanical pressure is also responsible for a lower corrosion rate of pure lead grids and the association of the new separation system with a tight electrode packing provides a mechanical stabilisation of the plate stack, thus hindering the positive grid growth process and the diseases that are associated with it. The application of mechanical pressure has the drawback to cause a compaction of the negative active material if the negative grids are overpasted. The use of a non-compressible separator allows the development in the lead-acid battery of a self compression effect that promises a technically easy manufacture of “pressure batteries” provided the battery case is hard, the plate surface is regular and the negative plates are not overpasted.

Phosphoric acid was added in AJS cells and proved to decrease the corrosion of the positive grid, possibly increase the negative top lead corrosion in VRLA batteries and improve the oxygen recombination. The positive effect of the phosphoric acid on the discharge capacity at high discharge rates could be observed in the beginning of life provided sufficient high positive plate voltages are achieved during charge but this effect proved to progressively disappear with increasing cycle number.

The utilisation of the new separation system leads to a lower recombination of the oxygen in the cells where it is used. But the AJS cells are not sensitive to the initial saturation in electrolyte in the beginning of life and our measurements showed that the cells and batteries can last for 1000 full cycles at a C/2 discharge rate. Therefore, the level of recombination of the AJS cells can be considered as sufficient because recombination is only an expedient not to have the life limited by drying out.

Perspectives

While this work gave answers to open questions concerning the lead-acid battery, each answer was associated with two new questions as is usual in research.

In first line, it was not possible to find a satisfying global explanation for the different effects the addition of phosphoric acid has on the lead-acid accumulator and for the disappearance of its influence with increasing cycle number. For this reason it would be interesting to further investigate the effect phosphoric acid can have on the oxygen cycle in lead-acid batteries as well as on the positive and negative grid corrosion and to measure the dependence between phosphoric acid adsorption and positive plate potential.

Secondly, the effect of mechanical pressure on the corrosion of positive grids should be observed as well as the influence of the active material on it in terms of thickness and density.

Thirdly, this Ph.D. work proposes a “recipe” for the elaboration of an improved battery. It would be interesting to produce such a battery and verify the results found in this work.

As a last point, many different ways exist for improving the lead-acid battery for cycling applications. One particularly interesting way that was not followed here could be the improvement of the specific energy by varying the characteristics of the active materials and adopting a thin plate design.

Towards sustainable development

It is possible to develop a lead-acid battery that has sufficient performance to be suitable for electric vehicle application. But even if such a battery is produced, the user will have to adapt its driving behaviour because it will take a long time before a zero emission vehicle is built that has the same driving characteristics as a car with a combustion engine in term of driving range and of power. Therefore, the short term future of the hybrid vehicle is more promising than for the zero emission vehicle for what concerns the private car because the hybrid vehicle is characterised by a small diminution of the emissions without affecting the qualities of power and driving range. ZEV have a chance to get some parts of the market only in the case of fleets in which the driving range is not primordial and where the fast charging is possible.

Additionally, it is heart breaking to admit that on a global point of view, a ZEV vehicle is just as much polluting as a car with combustion engine that consumes 3 litres of oil for 100 km. This is due to the global energy mix that is used for electrical energy production (see Figure 1 in the introduction). In fact, the production of electricity for loading the batteries generates as much greenhouse gases as a combustion engine of low consumption. Of course, this is only true as long as electricity is not produced on the base of renewable energy (i.e. PV, bio-mass, water, wind...) or nuclear energy. Therefore, while developing an accumulator suitable for the ZEV, the problem of the energy mix and of the minimal part of the renewable energies in it has also to be solved.

Naturally, on a local level, the limitation of the emission by using ZEV is very important. In most of the cases, pollution is only a question of concentration and the nature is able to absorb large quantities of polluting agents when they are diluted. By using ZEV, the disease associated with high concentration of greenhouse gases can be reduced in the cities and the quality of life can be dramatically improved.

Near the greenhouse gases, a car is also a source of "noise pollution" and in this field, the electric vehicle is unbeatable.

As a last point, one has to take the problems one after the other. The extended use of electric vehicles will present many advantages from an environmental point of view and the question of the energy mix for the production of electrical energy is already the subject of a lot of research. The work presented in this Ph.D. thesis is a contribution towards a better understanding of the lead-acid battery and an improvement of this battery system for "environment friendly" applications. It inserts itself in the global research work that puts science on service of sustainable development.

Conclusion de ce travail de thèse

Les résultats obtenus

L'utilisation d'un nouveau séparateur a permis d'améliorer les performances mais surtout la durée de vie de batteries au plomb fermées. Cette amélioration est liée aux bonnes propriétés mécaniques du séparateur qui est capable de transférer au bloc d'électrodes une pression mécanique et de la soutenir tout au long de la vie de la batterie.

L'application d'une pression mécanique sur les parois d'une cellule au plomb permet de restreindre l'espace vide que la matière active positive peut occuper lorsque sa structure devient plus poreuse au fur et à mesure des cycles. Lorsque l'espace d'expansion est limité, d'une part un squelette de particules de dioxyde de plomb densément agglomérées se forme qui rend la matière active positive plus robuste à la décharge. D'autre part, à forts taux de décharge, une utilisation plus homogène de la matière active sur toute l'épaisseur de l'électrode est autorisée. Ainsi, la restriction de l'espace d'expansion est un élément primordial du design d'une batterie qui peut être contrôlé par l'intensité de la pression mécanique extérieure exercée.

L'utilisation du séparateur AJS permet en outre de diminuer la corrosion des grilles positives et les effets qui lui sont associés. Tout d'abord, la pression mécanique transférée aux grilles positives diminue la vitesse à laquelle elles se corrodent. Ensuite, le séparateur AJS stabilise le bloc d'électrodes en lui donnant une grande compacité. La croissance de la grille positive liée à la corrosion est ainsi limitée et ainsi les risques de formation de court circuit par le dessus du bloc d'électrodes.

L'addition d'acide phosphorique dans une cellule au plomb fermée contenant le nouveau séparateur peut améliorer encore ses performances à fort courant de décharge en début de vie dans la mesure où un régime de charge approprié permettant une forte polarisation des électrodes positives est appliqué. Dans un tel cas, l'adsorption de l'acide phosphorique sur les électrodes positives permet une fine cristallisation du dioxyde de plomb liée une haute solubilité des espèces plomb IV qui ont tendance à précipiter là où l'acide phosphorique n'est pas adsorbé et à augmenter la compacité des agrégats de dioxyde de plomb dans l'électrode positive. L'influence de l'acide phosphorique perd toutefois en intensité au fur et à mesure que le nombre de cycles subis par la batterie augmente.

Enfin, une cellule au plomb/AJS fermée se caractérise par un cycle de l'oxygène moins efficace. Ce cycle a tout de même lieu dans une certaine mesure grâce au transfert en voie gazeuse de l'oxygène de l'électrode positive vers l'électrode négative par le biais des plus gros pores du séparateur. L'accumulation d'oxygène sur l'électrode positive qui conduit à une différence de pression entre les deux côtés du séparateur permet de libérer ces pores de leur électrolyte. Ainsi, une recombinaison de l'oxygène a lieu qui, même si elle est plus lente que dans des cellules avec d'autres systèmes de séparation, suffit à ne pas limiter la durée de vie de l'accumulateur au plomb/AJS fermé par le dessèchement.

Ainsi la production d'une batterie à performances améliorées en cyclage peut être réalisée sans application de pression mécanique extérieure par l'utilisation du phénomène d'expansion de la matière active positive. Les « ingrédients » optimaux pour cette batterie seraient:

- Un matériau rigide pour les bacs
- Un séparateur présentant de bonnes propriétés mécaniques tel AJS
- Des plaques négatives empâtées sur la seule épaisseur de la grille
- Des plaques positive avec une pâte de densité assez élevée
- Des constituants de grande régularité afin d'avoir un espace vide minimal dans chaque cellule
- Un électrolyte contenant 30 g/l d'acide phosphorique
- Une saturation initiale en électrolyte de 100% ou légèrement supérieure

Un régime de charge adéquat est aussi nécessaire pour assurer ses pleines performances à cette batterie.

Perspectives

Ce travail a apporté un nouvel éclairage sur certaines zones d'ombre de l'accumulateur au plomb. Cependant, chaque nouvelle réponse posait elle-même de nouvelles questions et de très nombreuses pistes de recherches restent ouvertes à l'issue de cette thèse.

En premier lieu, un mécanisme qui explique les divers effets de l'aide phosphorique ainsi que sa perte d'activité au cours de la vie de la batterie de façon satisfaisante doit être trouvé. Ainsi, des investigations plus poussées seraient nécessaires dans cette direction avec une détermination précise de l'effet de l'acide phosphorique sur le cycle de l'oxygène de même qu'une observation de l'effet du potentiel de l'électrode positive sur l'adsorption de l'acide phosphorique et enfin, une quantification plus poussée de l'effet de cet additif sur la corrosion des électrodes positive et négative.

En second lieu, la corrosion des grilles positives d'une batterie au plomb soumise à une pression mécanique devrait être mesurée précisément et le rôle de la matière active évalué (épaisseur, densité...).

En troisième lieu, ce travail propose une méthode pour l'élaboration d'une batterie améliorée qui pourrait être testée dans un processus industriel.

Enfin, il existe de nombreuses autres possibilités pour améliorer la batterie au plomb pour les utilisations en cyclage. En particulier, le problème de la densité d'énergie pourrait être abordé en modifiant les caractéristiques de la matière active.

Vers un développement durable

Il est donc possible de développer une batterie plomb/acide mieux adaptée pour l'utilisation dans un véhicule électrique. Mais même dans cette hypothèse, l'utilisateur sera contraint d'adapter son style de conduite. En effet, de nombreuses années s'écouleront encore avant qu'un véhicule non polluant apparaisse sur le marché qui ait les mêmes caractéristiques en matière de puissance et d'autonomie qu'un véhicule avec moteur à combustion. C'est pourquoi l'avenir proche du véhicule hybride, qui présente des caractéristiques de conduite semblables au véhicule traditionnel avec une petite réduction des émissions, est plus radieux que celui du véhicule totalement électrique si ce n'est dans le cadre de flottes où une autonomie réduite est acceptable et où des équipements de charge rapide peuvent être installés aisément.

Il est un point supplémentaire que même le plus fervent défenseur du véhicule électrique doit concéder, c'est que globalement, les émissions produites pour parcourir 100 km avec un véhicule électrique sont équivalentes à celles produites par un véhicule à combustion qui consommerait 3 litres de carburant pour 100 km. Ce bilan s'appuie sur le fait que l'électricité produite pour charger les accumulateurs du véhicule électrique est pour la plus grande part issue de la combustion de matières premières fossiles (voir Figure 1 dans l'introduction). Ainsi, pour réduire à l'échelle globale les émissions de gaz à effet de serre, le développement des énergies renouvelables ou nucléaire doit être poursuivi conjointement avec le développement d'un accumulateur pour le véhicule électrique. Toutefois, d'un point de vue local, le bénéfice associé à l'utilisation du véhicule électrique est énorme. La forte concentration de gaz à effet de serre dans les villes est responsable de nombreux problèmes de santé et la pollution sonore nuit grandement à la qualité de vie. Au regard de ces deux points, l'utilisation du véhicule électrique représente un progrès indiscutable.

Finalement, chaque problème doit être résolu en son temps. L'utilisation du véhicule électrique représenterait déjà un grand bénéfice du point de vue de l'environnement et la question de la part d'énergie renouvelable dans la production d'électricité est un domaine sur lequel les progrès vont aussi bon train. Le travail présenté dans cette thèse contribue à une meilleure compréhension du système plomb/acide et à une amélioration de celui-ci pour des utilisations «écologiques». Il s'inscrit dans le processus général qui tend à mettre la recherche au service du développement durable.

References

- [1] <http://www.iaea.or.at>
- [2] <http://royal.okanagan.bc.ca>
- [3] <http://www.soton.ac.uk>
- [4] Herald Tribune, *Deadly pollution*, 18th of June 1999
- [5] <http://europa.eu.int> Economic evaluation of sectoral emission reduction objective for climate change, Top-down analysis of the greenhouse gas emission reduction possibilities on the EU
- [6] GEO-2000, Earthscan Publications Ltd, London, UK
- [7] B. Eliasson, M Robertson, *The global environmental issue and the power industry*, Intelec 99
- [8] K. R. Bullock, *Journal of Power Sources*, 51 (1994) 1-17
- [9] X. Muneret, P. Lenain, colloque Gaston Planté 2000
- [10] J. Garche, Otti Enerige-Kolleg, Wiederauflabare Systeme, ZSW 15-16th May 2001
- [11] D. R. Battlebury, *Journal of Power Sources* 80 (1999) 7-11
- [12] P. Moseley, *Journal of Power Sources*, 80 (1999) 1
- [13] K. Peters, *Journal of Power Sources* 59 (1996) 9
- [14] Paul Ruetschi, *Journal of Power Sources*, 2 (1977/78) 3
- [15] J. Garche, *Journal of Power Sources*, 31 (1990) 401
- [16] D. Berndt, *Maintenance-Free Batteries, A handbook of battery technology*, Reseach Studies Press LTD., England
- [17] D. B. Edwards, C. Schmitz, *Journal of Power Sources* 85 (2000) 63-71
- [18] R. F. Nelson, *Power Sources* 13 (1991) 13
- [19] <http://www.varta.com>
- [20] W. Fischer, Blei-Fibel, Hoppecke 1994
- [21] B. Culpin, D. A. J. Rand, *Journal of Power Sources* 36 (1991) 415-438
- [22] D. Berndt, 7th ELBC, Pre Conference Seminar, Oxygen Cycle Meeting, 19 September 2000
- [23] B. Culpin, J. A. Hayman, *Power Sources* 11 (1986) 45
- [24] <http://www.acq.osd.mil/bmdo/bmdolink/html/bipolar.htm>
- [25] <http://electrosource.com>
- [26] R. Wagner, *Journal of Power Sources*, 53 (1995) 153-162
- [27] J. Alzieu, G. Schweitz, P. Izzo, S. Reymann, Colloque Gaston Planté, October 2000, France
- [28] D. Pavlov, *Journal of Power Sources* 64 (1997) 131-137
- [29] V. Svoboda et al., *Proceeding of the 2nd ABA*, Brno 2001 June 17th to 21st, paper 36
- [30] E. Meissner, *Journal of Power Sources*, 78 (1999) 99-114
- [31] A. C. Simon, S. M. Caulder, *Power Sources* 4 (1974) 109-122; D. H. Collins ed., Academic Press London
- [32] J. Bouet, J. P. Pompon, *Electrochemica Acta*, 26/10 (1981) 1477
- [33] A. F. Hollenkamp, *Journal of Power Sources* 59 (1996) 87
- [34] A. F. Hollenkamp, *Journal of Power Sources* 36 (1991) 567-585
- [35] N. Anastasijevic, J. Garche, K. Wiesener, I. Doroslovacki, P. Rakin, *Journal of Power Sources*, 14/4 (1985) 277-284
- [36] R. F. Nelson, D. M. Wisdom, *Journal of Power Sources* 33 (1990) 165-185
- [37] S. Atlung, B. Zachau-Christiansen, *Journal of Power Sources* 30 (1990) 131
- [38] S. Atlung, B. Zachau-Christiansen, *Journal of Power Sources* 52 (1994) 201-209
- [39] J. Garche, *Phys. Chem. Chem. Phys.*, 3 (2001) 356-367
- [40] P. Faber, *Power Sources* 4, D. H. Collins ed., Oriel Press, Newcastle-upon-Tyne, 1973, p. 525

- [41] F. Zaninotto, These de doctorat de l'université Pierre et Marie Curie, Paris, 1998
- [42] S. Laruelle et al., Colloque Gaston Planté, October 2000, France
- [43] A. J. Ritchie, A literature review, Internal documents, St. JOE mineral corporation
- [44] J. Garche, H. Doering, M. Perrin, Forschungsverbund Sonnenenergie Workshop, Fortschrittliche Back-up- und Speichersysteme für regenerative Energieversorgungsanlagen, 23/24 September 1996
- [45] EV Battery Test Procedure, EUCAR Traction Battery Group, December 1996
- [46] JRC, Traction Battery Working Group, Specification of Test Procedures for Traction Batteries for Electric Vehicles, October 1993
- [47] ZSW ISO procedure, Arbeitsanweisung 3A03AA01
- [48] ZSW ISO procedure, Arbeitsanweisung 3A03AA02
- [49] ZSW ISO procedure, Arbeitsanweisung 3A03AA03
- [50] ZSW ISO procedure, Arbeitsanweisung 3A03AA05
- [51] J. J. Lander, Journal of the Electrochemical Society 103/1 (1956) 1
- [52] J. Alzieu, B. Geoffrion, N. Lecaude, J. Robert, 5th International Electric Vehicle Symposium, Philadelphia, October 1978
- [53] J. Alzieu, J. Robert, Journal of Power Sources, 13 (1984) p.93
- [54] J. Alzieu, N. Koechlin, J. Robert, Journal of the Electrochemical Society, 134 (1987) p. 1881
- [55] G. Terzaghi, Journal of Power Sources 73 (1998) 78-85
- [56] W. Boehnstedt, Journal of Power Sources 59 (1996) 45-50
- [57] K. Takahashi, M. Tsubota, K. Yonezu, K. Ando, Journal of the Electrochemical Society 130 (1983) 2144
- [58] T. G. Chang, Journal of the Electrochemical Society, 131/8 (1984) 1755
- [59] E. M. L. Valeriotte, A. Heim, M. S. Ho, Journal of Power Sources 33 (1991) 187
- [60] M. Tsubota, S. Osumi, M. Kosai, Journal of Power Sources 33 (1991) 105
- [61] P. Rüetschi, Journal of the Electrochemical Society 139 (1992) 1347
- [62] J. Landfors, Journal of Power Sources 52 (1994) 99
- [63] K. K. Constanti, A. F. Hollenkamp, Journal of Power Sources 55 (1995) 269
- [64] A. F. Hollenkamp, R. H. Newnham, Journal of Power Sources 67 (1997) 27
- [65] E. Bashtavelova, A. Winsel, Journal of Power Sources 53 (1995) 175-183
- [66] T. V. Nguyen, R. E. White, H. Gu, Journal of the Electrochemical Society, 137/10 (1990) 2998
- [67] Rulac Zwerg, A. Rudolf, German Patent 609184, French Patent 857601
- [68] John Devitt, Journal of Power Sources 64 (1997) 153-156
- [69] G. Zguris, The Battery Man, march 1997
- [70] G. Zguris, The Battery Man, august 1997
- [71] K. McGregor et al., Journal of Power Sources 73 (1998) 65-73
- [72] W. Boehnstedt, Journal of Power Sources 78 (1999) 35-40
- [73] W. Boehnstedt, J. Deiters, K. Ihmels, J. Ruhoff, German Patent 19702757
- [74] Zen-Ichiro Takehara, Journal of Power Sources 85 (2000) 29-37
- [75] K. Harris, R. J. Hill, D. A. J. Rand, Journal of Power Sources 8 (1982) 175-196
- [76] D. Pavlov, E. Bashtavelova, Journal of the Electrochemical Society 133/2 (1986) 241
- [77] Zen-ichiro Takehara, Journal of Power Sources 85 (2000) 29-37
- [78] Z. Al-Saad, M. A. H. Abdel-Halim, Engineering Structures 23/8 (2001) 926-933
- [79] G. W. Scherer, Cement and Concrete Research 29 (1999) 1347-1358
- [80] E. Hameenojy, T. Laitinen, G. Sundholm, Electrochimica Acta 32/1 (1987) 187-189
- [81] R. C. Weast, Handbook of chemistry and physics, The Chemical Rubber CO., Cleveland
- [82] H. Bode, Lead-acid batteries, John Wiley & Sons, London
- [83] K. J. Euler, Bulletin de l'association Suisse des Electriciens, 63/ 25 (1972) 1498-1507

- [84] M. Calabek et al., *Journal of Power Sources* 67 (1997) 85-91
- [85] K. J. Euler, R. Kirchhof, H. Metzendorf, *Journal of Power Sources* 5 (1980) 255-262
- [86] A. Winsel, E. Voss, U. Hullmeine, *Journal of Power Sources* 30 (1990) 209-226
- [87] U. Hullmeine, A. Winsel, E. Voss, *Journal of Power Sources* 25 (1989) 27-47
- [88] D. Pavlov, E. Bashtavelova, *Journal of the Electrochemical Society*, 131-7 (1984) 1468
- [89] G. C. Zguris, F. C. Harmon, US patent US5468572, 1995-11-22
- [90] A. F. Hollenkamp, R. H. Newnham, Patent WO9730486-A1; AU9717123-A
- [91] Paul Robert, *Dictionnaire Le Petit Robert*
- [92] J. C. Scully, *The fundamentals of corrosion* (3rd edition, 1990), Pergamon Press
- [93] D. M. Berger, *Corrosion and corrosion protection handbook*, Philip A. Schweitzer ed., Marcel Dekker inc., New York
- [94] B. Brecht, *Batteries International*, July 1994
- [95] J. Garche, *Journal of Power Sources* 53 (1995) 85-92
- [96] G. Papazov et al., *Journal of Power Sources* 6 (1981) 15-24
- [97] D. Pavlov, T. Rogatchev, *Electrochimica Acta*, 23 (1978) 1237
- [98] P. Ruetschi, R. T. Angstadt, *Journal of the Electrochemical Society*, 111/12 (1964) 1323
- [99] A. C. Simon, *Journal of the Electrochemical Society*, 114/ 1 (1967) 1
- [100] A. C. Simon, S. M. Caulder, *Journal of the Electrochemical Society*, 121/4 (1974) 531
- [101] T. G. Chang, *Advances in lead-acid batteries*, D. Pavlov, K. Bullock ed., 1984
- [102] S. Feliu, E. Otero, J. A. Gonzalez, *Journal of Power Sources* 3 (1978) 145-153
- [103] H. Doering, Ph.D. Thesis, University of Dresden
- [104] K. R. Bullock, D. H. McClelland, *Journal of the Electrochemical Society*, 124/10 (1977) 1478
- [105] K. R. Bullock, *Journal of the Electrochemical Society*, 126 (1979) 1848
- [106] E. Voss, *Journal of Power Sources* 24 (1988) 171-184
- [107] U. Hullmeine, E. Voss, A. Winsel, *Journal of Power Sources* 30 (1990) 99-105
- [108] J. Garche, H. Doering, K. Wiesener, *Journal of Power Sources* 33 (1991) 213-220
- [109] M. Maja et al., colloque Gaston Planté 2000
- [110] H. Doering et al., *Journal of Power Sources* 38 (1992) 261-272
- [111] S. Venugopalan, *Journal of Power Sources* 46 (1993) 1-15
- [112] E. Meissner, *Journal of Power Sources* 67 (1997) 135-150
- [113] V. Branzoi et al., *Revue Roumaine de Chimie* 40/3 (1995) 225-233
- [114] Z. Shi, Y. H. Zhou, C. S. Cha, *Journal of Power Sources* 70 (1998) 205-213
- [115] B. K. Mahato, E. Y. Weissman, E. C. Laird, *Journal of the Electrochemical Society* 121/1 (1974) 13
- [116] D. Berndt, U. Teutsch, *Journal of the Electrochemical Society*, 143/3 (1996) 790
- [117] D. Pavlov, B. Mohanov, *Journal of the Electrochemical Society* 145/1 (1998) 70
- [118] Y. Guo, M. Perrin et al. , *Journal of the Electrochemical Society*, in press
- [119] M. K. Carpenter, D. M. Bernardi, J. A. Wertz, *Journal of Power Sources* 63 (1996) 15-22
- [120] J. S. Symanski, B. K. Mahato, K. R. Bullock, *Journal of the Electrochemical Society* 135/3 (1988) 548
- [121] L. T. Lam, ALABC 2000 project N 3.1, Annual report July 2000-June 2001
- [122] W. B. Brecht, *Intelec'90*
- [123] H. Dietz et al., *Journal of Applied Electrochemistry*, 21 (1991) 221
- [124] H. Giess, *Journal of Power Sources* 67 (1997) 49-59
- [125] I. Krupa, A. S. Luyt, *Polymer* 42 (2001) 7285-7289
- [126] W. B. Brecht, N. F. O'Leary, *Intelec'88*, 35-42

Glossary

AGM: Adsorptive glass mat. Separator consisting of glass fibres that retain the electrolyte by capillary forces.

AJS: Acid jellying separator. New separation system consisting of silicon dioxide of very high surface area contained in a polyethylene matrix.

AMU: Active material utilisation. Percentage of the active material that did take part to a discharge process.

BTS: Battery testing system, software edited by Digatron for the Digatron testing equipment.

C/X: Rate at which a cell/battery is discharged. Discharge current = Nominal capacity/X

CSIRO: Commonwealth Scientific and Industrial Research Organisation, Division of Minerals, Melbourne, Australia

DOD: Depth of discharge.

ECE 15: Electrical test simulating the power requirement the battery has to fulfil during the driving of an electric vehicle.

EV: Electric vehicle

H&V: Hollingsworth and Vose, company producing separators, in particular AGM.

IR-OCV-P: Electrical test allowing the determination at different depth of discharge of the high discharge current internal resistance, the open circuit voltage and the peak power.

NAM: Negative active material. Spongeous lead in the charged state.

PA: Phosphoric acid = H_3PO_4

PAM: Positive active material. Lead dioxide of high porosity in the charged state.

PV: Photovoltaic.

SEM: Scanning electron microscopy.

SHE: Standard Hydrogen Electrode. Electrode against which the potential of the electrochemical pairs is measured.

VRLA: Valve Regulated Lead-Acid Battery

ZEV: Zero emission vehicle.

ZSW: Center for Solar Energy and Hydrogen Research in Ulm (Germany).

Index of Figures

Figure 1: Energy mix for production of the commercial primary energy	14
Figure 2: Schematic representation of the mechanism of the greenhouse effect [2].....	15
Figure 3: The consequences of a global warming by 1°C [3].....	15
Figure 4: All types of batteries [10].....	24
Figure 5: Electrode reactions of the lead-acid battery	26
Figure 6: Schematic repartition on the voltage scale of the reactions in a lead-acid battery.....	27
Figure 7: Pourbaix diagram of the lead/water system [17] (0,-2,-4,-6 lines indicate Pb^{2+} concentrations of 1, 10^{-2} , 10^{-4} , 10^{-6} mol/dm ³ respectively)	28
Figure 8: Cyclic voltammogram of Pb in H ₂ SO ₄ , cycle 100	29
Figure 9: Extrapolated current/potential curve of the PbO ₂ /PbSO ₄ pair	30
Figure 10: Mixed potential of the positive electrode during self discharge	31
Figure 11: Tafel lines of the hydrogen and oxygen evolutions on lead [16].....	32
Figure 12: Schematic representation of a flooded lead-acid battery [19]	33
Figure 13: Picture of a tubular plate and its components [20]	34
Figure 15: Reactions in a valve regulated lead-acid battery [22].....	35
Figure 16: VRLA battery in spiral wound design. Yellow Top by Optima	36
Figure 17: Two cells in monopolar and in bipolar design.	37
Figure 18: Schematic representation of the current flow in a stratified cell.....	40
Figure 19: Premature positive electrode failure modes[30].....	41
Figure 20: Premature negative electrode failure modes.....	42
Figure 21: Specific energy loss in a flooded the lead-acid battery at high discharge rate (about 1h)	44
Figure 22: Active material utilisation depending on average distance to the current collector [40]	45
Figure 23: Elaboration process of the plates for a lead-acid battery [41]	46
Figure 24: Summary of the IROCVP procedure for one SOC	49
Figure 25: Set-up for the cyclic voltammetry.....	52
Figure 26: Principle scheme for the measurement of the effect of mechanical pressure.....	53
Figure 27: Picture and properties of an AJS separator with 1.45 mm thickness.....	59
Figure 28: Relative deformation versus applied pressure for AJS and AGM	60
Figure 29: Picture illustrating how the bottom fleece is placed in the gel and AJS cells and batteries. (Here an AJS battery after some 650 cycle).....	62
Figure 30: Principle scheme and picture of the realisation of an online mechanical pressure recording device.....	63
Figure 31: Design for the application of a constant mechanical pressure on a lead-acid cell.	64
Figure 32: Discharge capacity versus current of discharge for cells with AGM and AJS.....	65
Figure 33: Discharge capacity and driving range for one ECE 15 cycle	66
Figure 34: Open circuit voltage versus depth of discharge for different cells.	66
Figure 35: Internal resistance at high current of discharge versus depth of discharge for different cells. .	67
Figure 36: Specific high current peak power versus depth of discharge for different cells.	68
Figure 37: Evolution of relative C/2 capacity versus cycle number.....	69
Figure 38: Cycle life of the cells of Figure 37	69
Figure 39: C/2 discharge capacity versus cycle number for batteries with different separation systems and under different initial mechanical pressures.....	70
Figure 40: Evolution of the mechanical pressure on the walls of an AJS cell during one cycle	71
Figure 41: Porosity versus active material utilisation for new electrodes.....	72

Figure 42: Maximum active material utilisation achievable if the room for expansion is limited to the only porosity.	73
Figure 43: Expression of the radial stress on the pore wall	76
Figure 44: Solubility of lead sulphate in sulphuric acid of different concentrations	77
Figure 45: Dependence of the ampere hours discharged on the mass fraction of sulphuric acid in the electrolyte for an AJS cell without phosphoric acid	77
Figure 46: Solubility of lead sulphate versus discharged capacity of an AJS cell	78
Figure 47: Evolution of the mechanical pressure versus discharged Ah at two different discharge rates for a same cell	79
Figure 48: Evolution of the mechanical pressure during one cycle for an AJS and an AGM cell after some 200 C/2 cycles	81
Figure 49: Evaluated thickness of the positive plate in an AGM cell during discharge	82
Figure 50: Evolution of released gas amount and mechanical pressure during charging of an AGM cell	82
Figure 51: Evolution of the mechanical pressure during one cycle for a Gel cell and an AGM cell	83
Figure 52: Evolution of the mechanical pressure during one cycle for two identical cells set at different initial external mechanical pressures	84
Figure 53: Evolution of the mechanical pressure during one C/2 cycle for a cell and a battery with AJS and phosphoric acid in the electrolyte	85
Figure 54: Increase of mechanical pressure during discharge versus cycle number	86
Figure 55: Evolution of mechanical pressure at the end of discharge	87
Figure 56: Cross section of the negative plates	89
Figure 57: Pictures of the cross sections of cycled electrodes in a charged state after over 1000 cycles	91
Figure 58: Schematic representation of the structure of a cycled positive electrode	92
Figure 59: Pictures of the superficial layers of the positive plates after cycling in an AGM cell or in an AJS cell under two different initial mechanical pressures	92
Figure 60: BSE picture of the positive plate of AJS 30 kPa (A) and AJS 80 kPa (B) (multiplication factor 60)	93
Figure 61: Intermediary layer (B layer) of positive plates in the charged state after cycling in AGM and AJS cells	94
Figure 62: Intermediary layer of the positive electrode of an AGM cell and an AJS cell after over 1000 cycles	94
Figure 63: Lead sulphate distribution across the thickness of discharged positive plates as a function of current density [82]	95
Figure 64: SEM pictures of the internal layers of the positive plates after cycling in an AGM cell or in an AJS cell under two different initial mechanical pressures	95
Figure 65: SEM pictures of layer C for a new cell (a) and cells after cycling: AGM (b), AJS 30 kPa (c) and AJS 80 kPa (c)	96
Figure 66: Agglomerates in the active material of the AJS 80 kPa cell after over 1000 cycles [optical micrograph *500, BSE micrograph *700]	97
Figure 67: Geometry of the AOS model [17]	99
Figure 68: Schematic representation of a battery after some cycles	103
Figure 69: Picture of a gel battery that failed by corrosion of the positive grid	106
Figure 70: Structure of the corrosion layer under continuous polarisation	110
Figure 71: Schematic representation of the concentration variation for the different corrosion products in the corrosion layer	110
Figure 72: Dependence of the corrosion rate of a lead alloy on its antimony content for different polarisation conditions [96]	111

Figure 73: Discharge capacity of the corrosion layer versus cycling time.....	113
Figure 74: Schematic representation of the different steps of formation of the corrosion layer with increasing cycling time	113
Figure 75: Schematic representation of the porous corrosion layer thickness for different mechanical pressure.....	115
Figure 76: Schematic representation of the grid growth process in an AJS cell.....	115
Figure 77: Pictures of the top of an AJS cell and of a negative plate after deformation of a plate stack by positive grid growth.....	116
Figure 78: Cyclic voltammogram in the positive potential range with and without phosphoric acid in the electrolyte ($d= 1.28\text{g/cm}^3$, 5 mV/s , $[\text{H}_3\text{PO}_4] = 0.2\text{ mol/l} = 19.59\text{ g/l}$)	120
Figure 79: Cyclic voltammogram in the negative potential range with and without phosphoric acid in the electrolyte ($d=1.28\text{ g/cm}^3$, 5 mV/s , $[\text{H}_3\text{PO}_4] = 0.2\text{ mol/l} = 19.59\text{ g/l}$)	120
Figure 80: Increase in capacity between the C/2 and the C/5 discharge rate.....	121
Figure 81: Evolution of the discharge capacity versus cycle number for AJS cells with and without phosphoric acid	122
Figure 82: Evolution of the mechanical pressure during cycle 100 for AJS cells with and without phosphoric acid	122
Figure 83: Mechanical pressure variation during discharge versus cycle number for two AJS cells with and without phosphoric acid	123
Figure 84: Comparison between the discharge capacity and the mechanical pressure increase during discharge versus cycle number for AJS PA 30 kPa.....	124
Figure 85: Evolution of the charging potential for cells with or without phosphoric acid.....	124
Figure 86: Evolution of the current and volume of gas released versus charging time for different cells	125
Figure 87: Picture of the separator from the AJS 80 kPa battery with some rest positive active material on the top part and the thin corrosion layer in white.....	126
Figure 88: Pictures of the negative strap at opening after cycling with and without phosphoric acid	127
Figure 89: Discharge capacity of the corrosion layer versus cycle number in sulphuric acid ($d=1.28\text{g/cm}^3$)	128
Figure 90: Discharge capacity of the corrosion layer versus cycle number in electrolyte with phosphoric acid	129
Figure 91: Diffractogram of the material covering the lead grid after cycling in electrolyte containing phosphoric acid	130
Figure 92: Diffractogram of the material composing the white “skin” present in the electrolyte after cycling of the grid lead in sulphuric acid added of phosphoric acid.	130
Figure 93: Schematic representation of the adsorption of the phosphates during charge and of the precipitation of the lead sulphates during discharge	131
Figure 94: Surface of a positive plate at the opening of a battery after cycling with phosphoric acid	132
Figure 95: SEM pictures of the positive active electrodes from cells and batteries cycled with phosphoric acid	132
Figure 96: SEM pictures of the external layer of positive active electrodes from cells and batteries cycled with phosphoric acid.....	133
Figure 97: Layer B of and AJS cell and an AJS battery after cycling.	134
Figure 98: Internal layer of the positive electrode after cycling.....	134
Figure 99: SEM pictures of the internal layer of a new positive plate and plates cycled with phosphoric acid in a gel battery or in an AJS cell	135
Figure 100: Schematic representation of the oxygen cycle	137

Mademoiselle PERRIN Marion

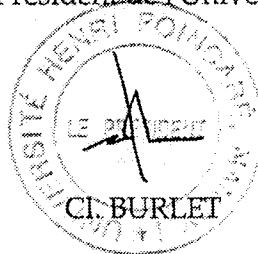
DOCTORAT de l'UNIVERSITÉ HENRI POINCARÉ, NANCY-I

en PHYSIQUE & CHIMIE DE LA MATIÈRE & DES MATÉRIAUX

VU, APPROUVÉ ET PERMIS D'IMPRIMER

Nancy, le 17 novembre 2001 n° 611

Le Président de l'Université



Abstract

The performances and life of the VRLA battery for cycling application were improved by applying a mechanical pressure on the electrode stack with help of a new separator (AJS).

The mechanical properties of AJS allow the transfer of a mechanical pressure to the electrodes throughout the cell life that limits the free space. Thus, while the negative active material is compacted, the positive active material develops a structure with a skeleton robust against discharge and large voids allowing a better utilisation over the whole plate thickness. The positive grid corrosion decreases and the mechanical stack stabilisation allowed by AJS reduces dramatically the effects associated with positive grid growth.

The association of phosphoric acid with AJS improves the cell performance at high discharge currents for a while provided the cells are adequately charged. With cycling, the effect of phosphoric acid disappears.

The oxygen recombination in AJS cells is slow but sufficient for cycling life over 1000 cycles. The oxygen transfer takes place across the gas space and through gas channels in the separator that are freed of their electrolyte by an oxygen overpressure.

Résumé condensé

La durée de vie et les performances de batteries fermées au plomb pour l'application au véhicule électrique ont été améliorées grâce à l'application par le biais d'un nouveau séparateur (AJS) d'une pression mécanique sur les blocs d'électrodes.

AJS peut soutenir une pression élevée pendant toute la vie de la cellule. Ainsi, l'espace libre pour l'expansion des matériaux actifs est limité. La matière active négative est alors compactée mais l'électrode positive développe une structure avec un squelette robuste face à la décharge et de larges pores qui permettent une utilisation homogène de la matière active sur toute son épaisseur. Sur la grille positive, la corrosion diminue ainsi que les effets associés à sa croissance car AJS stabilise mécaniquement le bloc d'électrodes.

L'utilisation d'acide phosphorique augmente les performances des cellules à fort courant de décharge si elles sont chargées avec le régime adéquat. Cet effet disparaît au cours du cyclage.

La recombinaison de l'oxygène est lente dans les cellules avec AJS mais suffit pour une vie supérieure à 1000 cycles profonds. L'oxygène passe de l'électrode positive à la négative par l'espace libre autour des électrodes et par des canaux dans le séparateur libérés de leur électrolyte par une surpression d'oxygène.